Absorptive Effects In Single Particle Inclusive (High energy) Reactions And An Application For Charge Exchange Pseudo Scalar Meson Production

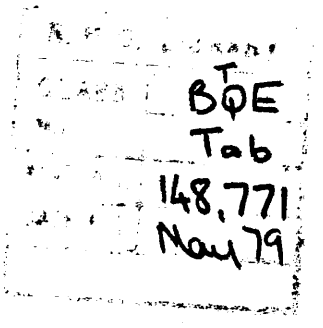

In Remembrance

Of My Father

ABSTRACT

We present a computer program tailored to the calculation of single particle inclusive reaction observables and two models for the incorporation of absorptive type corrections in the triple Regge region which do not require the inclusion of free parameters.

We conclude that the first model we present is not sufficiently realistic and so requires the derivation of the second, more sophisticated model in the Regge-eikonal approximation. Both models were used to examine the observables for pseudo-scalar meson production via charge exchange.

PREFACE

The work described in this thesis was carried out under the supervision of Dr K J M Moriarty in the Department of Mathematics, Royal Holloway College, London University of London between October 1973 and October 1976. Except where stated, the work described is original and has not been submitted to this or any other university for any degree.

I am indebted to several people and organisations for aid and assistance rendered during the course of this degree. The Science Research Council (U.K.) provided the finance in the shape of a Research Studentship. Dr Kevin Moriarty acted as my supervisor. His energy and enthusiasm for the subject and capacity for encouragement have been of much use to me. I have also learned a great deal from Dr Neil Craigie with whom my supervisor and I have collaborated. John Anderson, of the Computer Science Department at R.H.C. has been very helpful in pointing out some of my more devious errors in computer programming. I must also acknowledge the Mathematics Department at R.H.C. for its collective efforts on my behalf over more than six years, both as undergraduate and postgraduate, and the Physics Department of Imperial College where I attended the D.I.C. Lectures in 1973-4. I extend my thanks to all those at R.H.C. who made my postgraduate years a thoroughly pleasant experience, and particularly fellow postgraduates Provob Choudhury, Peter Koehler, Jalal Pashaie-Rad, Tim Scott, Hilary Thompson and Ahpisit Ung-Kitchanukit and Mr and Mrs Widdowfield who provided very amenable lodgings during my first postgraduate year.

The final preparation of this thesis has been accomplished only with the considerable assistance of the Mathematics Departmental secretaries at R.H.C. to whom part of the typing is due; of Christine Erwin and Alison Allen who have performed the remainder, and of Mrs Hill who has prepared the majority of the diagrams. Rolls-Royce and Associates Limited, my present employers have also been of considerable help during the preparation of this thesis.

Finally I am of course, heavily indebted to my mother for many years of support and encouragement, and to my wife Sally, for a very high level of understanding and for providing some fairly pointed impetus at times, when work on this thesis began to slow down; without her it might well not have been completed.

CONTENTS

CHAPTER I

General Introduction

I INTRODUCTION

This thesis is primarily concerned with the introduction of absorptive type corrections to a pure Regge pole model for single particle inclusive reactions in the triple Regge regions. Accordingly, in this introductory chapter we will briefly mention the theoretical and experimental stimulae that have led to the effort expended on single particle inclusive reactions which must include a slightly more extended mention of Mueller's Generalised Optical Theorem and the various multi-Regge scaling limits. We conclude this chapter with brief descriptions of various of the other models that have been put forward to introduce absorptive type corrections to inclusive reactions.

In chapter II a computer program is presented which was written in order to make the organisation, calculation and presentation of results for the class of reaction we consider a much easier process.

Chapter III presents the derivation of a parameter free model for the normal Regge limit (see section VI, Multi-Regge Limits and scaling) which has a natural extension to the triple-Regge limit. We also present a fairly naive model for absorptive corrections but are forced to conclude that it is not sufficiently realistic.

In Chapter IV we derive a more reasonable model which is based on the eikonal approximation to multiple Reggeon exchange and Chapter V contains a calculation of the differential cross section and target asymmetries for various charge exchange reactions. The main conclusion to this calculation being that, in contrast to the exclusive counterpart, the reaction $\pi^- p \to \pi^0 X$ should show no signature dip at around $|t|=0.5$ [GeV/c]^2 and that

the target asymmetries that we find by this method will be small. Chapter VI gives a brief recapitulation of the conclusions we can draw and also a consideration of various questions that remain unanswered.

II INCLUSIVE PROCESSES

The production of many body final states accounts for 75 - 80% of the total cross section at presently available energies [1]. However, it is almost impossible to analyse a multiparticle production event experimentally because of the complexities involved in being certain that the final observed particles attributed to a single event are in fact all that resulted from it. This would normally be done for a small number of final particles via four momentum reconstruction and quantum number conservation arguments and the extreme difficulty of detecting all the neutral produced particles must invalidate this approach for higher final multiplicities.

Similarly multiparticle final states are hard to analyse theoretically simply because of the proliferation of independant variables with particle number. Accordingly some selection of the available information has to be made. The method that has received much attention is that of the inclusive process whereby the presence of a particular particle (or set of particles) is detected in a final state, but no information is retained concerning the remainder of the produced particles. We concentrate for the remainder of this thesis on single particle inclusive processes of the form

$$1 + 2 \rightarrow 3 + X \qquad 1.1$$

which is depicted in figure 1.1. Here the particles 1 and 2 are obviously specified by the particular beam and target used in the experiment and particle 3 is of a particular type, say π^- or Δ^{++}. X symbolises the sum of all final states that can occur with 3, in order to conserve four-momentum and all the relevant quantum numbers embodied in the initial state. Thus

$$p_X = p_1 + p_2 - p_3, \quad N_X = N_1 + N_2 - N_3 \qquad 1.2$$

where p denotes four-momentum and N denotes one of the set of conserved quantum numbers, which will certainly include

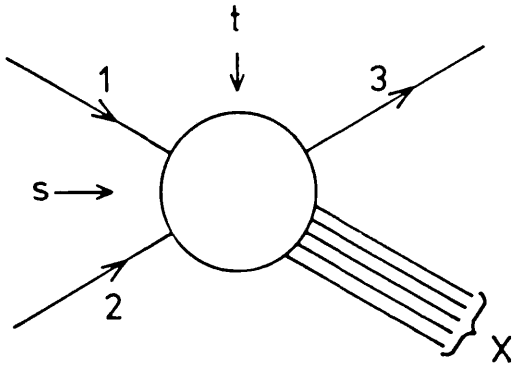

Figure 1.1. The single particle inclusive reaction 1 + 2 → 3 + X.

These processes have the advantage that they are extremely easy (comparatively) to measure experimentally, since the measurement of the momentum of a single final particle, and the knowledge of its particle type are sufficient to determine the event completely.

Theoretically these processes also appear fairly simple when viewed via a generalisation of the optical theorem due to Mueller [2] which will be considered in greater detail later. Thus the combination of ease (relative) of acquisition of data, of which there is a developing fund [3] and the amenability of these processes to theoretical analysis has greatly contributed to the interest and effort devoted to them.

Interesting reviews on the subject can be found in Ref.4.

III KINEMATICS FOR INCLUSIVE PROCESSES

We wish to analyse the process of equation 1.1 and figure 1.1 kinematically. For this purpose we choose the 1 - 2 centre of mass frame in which the four momenta appear as

$$p_1 = (E_1, 0, 0, p)$$

$$p_2 = (E_2, 0, 0, -p)$$

$$p_3 = (E_3, p_{3\perp 1}, p_{3\perp 2}, p_{3L})$$

with $p_1^2 = E_1^2 - p^2 = m_1^2$

$$p_2^2 = E_2^2 - p^2 = m_2^2$$

$$p_3^2 = E_3^2 - p_{\perp 1}^2 - p_{\perp 2}^2 - p_L^2 = m_3^2 \qquad 1.3$$

We see from the above equations that there are at most four independant variables for this process. In the case where no polarisation data is recorded this number reduces to three since an arbitrary rotation about the Z-axis will be permitted. Even if this is not the case, rotation about the Z-axis introduces at most a kinematical phase factor, and so there are only three independant dynamical variables. We will introduce some of the more widely used sets in order to show the relationship between them.

If we define

$$s = (p_1 + p_2)^2 \qquad 1.4$$

then simple manipulations of equations 1.3 tell us that

$$p^2 = \frac{1}{4s}\,[s-(m_1 + m_2)^2]\,[s-(m_1 - m_2)^2]$$

$$E_1 = \frac{1}{2\sqrt{s}}\,(s + m_1^2 - m_2^2) \qquad 1.5$$

$$E_2 = \frac{1}{2\sqrt{s}}\,(s + m_2^2 - m_1^2)$$

We can introduce the triangle function

$$\Delta(x,y,z) \equiv x^2 + y^2 + z^2 - 2xy - 2yz - 2xz \qquad 1.6$$

and then

$$p^2 = \frac{1}{4s}\,\Delta\,(s, m_1^2, m_2^2) \qquad 1.7$$

We can also introduce

$$p_{3\perp} = (p_{3_1}^2 + p_{3_2}^2)^{\frac{1}{2}} \qquad 1.8$$

then one set of variables that could be chosen is $s, p_{3L}, p_{3\perp}$. Of course not all these variables are relativistically invariant, but they are certainly experimentally reasonable since p_{3L} ranges between $\pm p$ depending on the dynamical mechanism for the production of particle 3 while $p_{3\perp}$ remains, in by far the majority of cases, below 0.5 GeV/C. [5]

We next define the missing mass, M_x^2 via

$$M_x^2 = (p_1 + p_2 - p_3)^2 \qquad 1.9$$
$$= s + m_3^2 - 2E_3\sqrt{s}$$

This variable will have a lower threshold determined by quantum number conservation and an upper threshold when particle 3 is produced at rest in the 1 - 2 C.M. frame given by

$$M_x^2 = (\sqrt{s} - m_3)^2 \qquad 1.10$$

Clearly from equation 1.5 we can say

$$q^2 = p_{3_1}^2 + p_{3_L}^2 = \frac{1}{4s}\,(s-(m_3+M_x)^2)(s-(m_3-M_x)^2) \qquad 1.11$$

and $E_3^2 = \frac{1}{2\sqrt{s}}\,(s + m_3^2 - M^2)$

With the approximations $s, M_x^2 \to \infty, p_{3\perp}^2$ small, we can say

$$p_{3L}^2 \simeq \frac{(s-M^2)^2}{4s},\ \frac{M_x^2}{s} \simeq 1 - \frac{2|p_{3L}|}{\sqrt{s}} \qquad 1.12$$

Another independant variable is defined by

$$t = (p_1 - p_3)^2 = m_1^2 + m_3^2 - 2E_1E_3 + 2pp_{3L} \qquad 1.13$$

this variable has thresholds reached as p_{3L} reaches $\pm$ its maximum value for particular values of s and M_x^2. In terms of these variables these thresholds are given by

$$|t|_{\min}^{\max} = \left\{ \sqrt{\frac{(s + m_3^2 - M_X^2)^2 - m_3^2}{4s}} \pm \sqrt{\frac{(s + m_1^2 - m_2^2)^2 - m_1^2}{4s}} \right\}^2$$

$$- \frac{1}{4s} \left[(m_3^2 - m_1^2) - (M_X^2 - m_2^2) \right]^2 \qquad 1.14$$

We can also define

$$u = (p_2 - p_3)^2 = m_2^2 + m_3^2 - 2E_2E_3 - 2pp_{3L} \qquad 1.15$$

and in a manner analogous to the relation in two body scattering we find that

$$s + t + u = m_1^2 + m_2^2 + m_3^2 + M_X^2 \qquad 1.16$$

So s, t and M_X^2 form a set of three independant dynamical variables, and it is this set that we make free use of in the remainder of this thesis.

There are however, two other variables in common use. The first is the Feynman variable or reduced longitudinal momentum [6] defined by

$$x = \frac{p_{3L}}{p_{3L\,\max}} \qquad 1.17$$

Using equation 1.12, since $p_{3L\,\max}$ will occur for the smallest admissible value of M_X^2, we can write

$$|x| \simeq \frac{2|p_{3L}|}{\sqrt{s}} \simeq 1 - \frac{M_X^2}{s} \qquad 1.18$$

Equation 1.18 is sometimes used as the definition of x but the two definitions can only be equivalent when m_1, m_2, m_3 and p_{3L} can be neglected compared to s and M_X^2. The concept of "fragmentation" can be introduced briefly here. If $x \simeq +1$ particle 3 is moving close to the original speed and direction of particle 1 and it is therefore logical to assume that it is a fragment of that particle. Similarly for $x \simeq -1$ and particle 2.

On the other hand if $x \simeq 0$ then the produced particle is almost stationary in the 1-2 C.M. frame and so cannot be associated with either particle 1 or particle 2. So the use of s, x and $p_{3\perp}^2$ provides another commonly used set of variables. We can relate t and $p_{3\perp}^2$ via equations 1.11 and 1.13 for $x \simeq +1$. If $p_{3\perp} = q\text{Cos}\theta$ then θ is the 1-2 C.M. frame scattering angle, and

$$t = t_{min} - 2pq(1-\text{Cos}\theta) \qquad 1.19$$

For small θ this can be approximated by

$$t \simeq t_{min} - \frac{p}{q} p_{3\perp}^2 \simeq t_{min} - \frac{p_{3\perp}^2}{x}$$

Since $p \simeq p_{3\perp\,max}$ and $q \simeq p_{3\perp}$.

The second widespread variable is the rapidity y defined by [7]

$$y = \tfrac{1}{2} \log \frac{E_3 + p_{3\perp}}{E_3 - p_{3\perp}} \qquad 1.20$$

If we also define the "longitudinal mass"

$$\mu^2 = (m_3^2 + p_{3\perp}^2)$$

so that $E_3^2 = \mu^2 + p_{3\perp}^2$

Then $\frac{p_{3\perp}}{\mu} = \text{Sinh } y$

$$\frac{E_3}{\mu} = \text{Cosh } y \qquad 1.21$$

The main property of the rapidity y is its easy transformation under a Lorentz boost by velocity v along the Z-axis. Since

$$p_3 = (\mu\text{Cosh } y,\ p_{3\perp 1},\ p_{3\perp 2},\ \mu \text{ Sinh } y) \qquad 1.22$$

then applying the transformation equations

$$E_3 \to \gamma(E_3 + vp_{3\perp})$$

$$p_3 \to \gamma(p_{3\perp} + vE_3)$$

Where $c = 1$ and $\gamma = (1-v^2)^{-\frac{1}{2}}$

then $y \to y + \tfrac{1}{2}\log \frac{1+v}{1-v}$ 1.23

Thus the three variables s, y and $p_{3\perp}^2$ also form an independant set.

In order to relate y to the original set of s, t and M_x^2 we must return to equations 1.13 and 1.15, which show, as $s \to \infty$ that

$$t = -\sqrt{s}\,(E_3 - p_{3L})$$

$$u = -\sqrt{s}\,(E_3 + p_{3L})$$

where we neglect m_1^2, m_2^2 and m_3^2 with respect to s. In conjunction with equation 1.16 and also neglecting $m_1^2+m_2^2+m_3^2$ we have

$$y_3 \simeq \tfrac{1}{2} \log\left(\frac{u}{t}\right) \simeq \tfrac{1}{2} \log\left(\frac{M_x^2 - s - t}{t}\right) \qquad 1.24$$

IV SINGLE PARTICLE INCLUSIVE CROSS SECTIONS

We will use the multi-particle state normalisation, which we give for spinless identical particles for simplicity,

$$\langle q_1..q_n|p_1..p_n\rangle = \sum_{\text{perms}} \prod_{i=1}^{n} \{\delta^3(\underline{q}_1-\underline{p}_{pi})(2\pi)^3 2E(q_i)\} \qquad 1.25$$

Of course only one term of this sum can be non zero, at most. Use is also made of the resolution of the identity

$$\hat{1} = \sum_{n=2}^{\infty} \frac{1}{n!} \int \prod_{i=1}^{n} \frac{d^3p_i}{2E_i(2\pi)^3} |p_1..p_n\rangle\langle p_1..p_n| \qquad 1.26$$

We also note that, since we insist upon conservation of four momentum we can write

$$\langle q_1..q_m|R|p_1..p_n\rangle = (2\pi)^4\delta^4\left(\sum_{i=1}^{m} q_i - \sum_{j=1}^{n} p_j\right) T(q_1..q_m;p_1..p_n)$$

$$= (2\pi)^4\delta^4\left(\sum_{i=1}^{m} q_i - \sum_{j=1}^{n} p_j\right) T_{n\to m} \qquad 1.27$$

Now we can write down the cross-section for two particles → n particles as

$$F\sigma_{2\to n} = \int \frac{1}{n!} \prod_{i=1}^{n} \frac{d^3r_i}{(2\pi)^3 2E_i} (2\pi)^4\delta^4\left(p_1+p_2-\sum_{i=1}^{n} r_i\right) |T_{2\to n}|^2 \qquad 1.28$$

Where F is a two particle flux factor which is equal to [5] $2\Delta^{\frac{1}{2}}(s, m_1^2, m_2^2)$. Clearly

$$\sigma_{\text{total}} = \sum_{n=1}^{\infty} \sigma_{2\to n} \qquad 1.29$$

Almost in passing we can write down the two particle unitarity equation using the unitarity of the S - matrix i.e.

$$S^\dagger S = SS^\dagger = \hat{1} \qquad 1.30$$

and writing the S-matrix in the form $\hat{1} + iR$ we have

$$\langle q_1 q_2 | p_1 p_2 \rangle = \langle q_1 q_2 | S^\dagger S | p_1 p_2 \rangle$$

$$= \langle q_1 q_2 | \hat{1} | p_1 p_2 \rangle + \langle q_1 q_2 | R^\dagger R | p_1 p_2 \rangle$$

$$- i\langle q_1 q_2 | R^\dagger | p_1 p_2 \rangle + i\langle q_1 q_2 | R | p_1 p_2 \rangle$$

Inserting the resolution of the identity between the $R^\dagger$ and R we have

$$- i(\langle q_1 q_2 | R | p_1 p_2 \rangle - \langle q_1 q_2 | R^\dagger | p_1 p_2 \rangle) =$$

$$\sum_{n=2}^{\infty} \frac{1}{n!} \int \prod_{i=1}^{n} \frac{d^3 r_i}{2Ei(2\pi)^3} \langle q_1 q_2 | R^\dagger | r_1 .. r_n \rangle \langle r_1 .. r_n | R | p_1 p_2 \rangle \qquad 1.32$$

If we make use of the time reversal invariance property of the amplitudes and of the hermitian analyticity property i.e.

$$T(s-i\varepsilon,...) = T^*(s+i\varepsilon,...) \qquad 1.33$$

and also making use of equations 1.27, 1.28, 1.29 we will have

$$2\ \mathrm{Im}(T_{2\to 2}(s+i\varepsilon, t=0)) = F\sigma_{\text{total}} \qquad 1.33$$

The complete derivation is of course not quite this simple, but this sketch proof will be useful to indicate the manner in which Mueller's Generalised Optical Theorem can be motivated. The complete proof is found in Ref.8.

We can now define the single particle inclusive cross section from equations 1.28 and 1.29 by inserting the correct delta functions. Thus

$$16\pi^3 E_3 \frac{d^3\sigma}{d^3 p_3} = \frac{1}{F} \sum_{n=1}^{\infty} \frac{1}{n!} \int \prod_{i=1}^{n} \frac{d^3 r_i}{(2\pi)^3 2E_i} (2\pi)^4 \delta^4 (p_1 + p_2 - \sum_{i=1}^{n} r_i)$$

$$(2\pi)^3 2E_3 \sum_{\ell=1}^{n} \delta^3 (\underline{p}_3 - \underline{r}_\ell) |T_{2\to n}|^2 \qquad 1.34$$

Clearly, the delta function can be used to perform one of the momentum integrations and since the final particles are identical the sum from $\ell = 1$ to n produces only a factor of n.

Thus we can say

$$16\pi^3 E_3 \frac{d^3\sigma}{d^3\underline{p}_3} = \frac{1}{F} \sum_{n=1}^{\infty} \frac{1}{(n-1)!} \int \prod_{i=1}^{n-1} \frac{d^3\underline{r}_i}{(2\pi)^3 2E_i} (2\pi)^4 \delta^4 (p_1 + p_2 - \sum_{i=1}^{n} r_i)$$

$$|T_{2\to n}|^2 \qquad 1.35$$

This is not the only form for the cross-section that is used. In Appendix 3 we derive the normalisation that is used for the next form of cross-sections we give in a similar manner to that given above.

We thus find

$$16\pi^3 E_3 \frac{d^3\sigma}{d^3\underline{p}_3} = 16\pi^3 \left\{ \frac{2p_z\sqrt{s}}{\pi} \frac{d^2\sigma}{dtdM_x^2} \right\} \simeq 16\pi^3 \left\{ \frac{s}{\pi} \frac{d^2\sigma}{dtdM_x^2} \right\} \qquad 1.36$$

where the variables are defined in section III.

If we write $d^3\underline{p}_3 = \pi |p_3| d|p_3|^2 d(\text{Cos}\theta)$ which we can do because of rotational invariance about (with our kinematics) the Z-axis, then we can give the differential cross-section in terms of the other sets of complete variables described in section III namely

$$16\pi^3 E_3 \frac{d^3\sigma}{d\underline{p}_3^3} = 16\pi^2 \frac{d^2\sigma}{d(p_{3\perp}^2)dy} \simeq 16\pi^2 x \frac{d^2\sigma}{d(p_{3\perp}^2)dx} \qquad 1.37$$

The last parts of equations 1.37 and 1.36 are really valid only as $s\to\infty$.

A further point to note is that if we integrate equation 1.35 with respect to $\frac{d^3p}{16\pi^3 E_3}$ we do not return to equation 1.28 since we have cancelled an n from the n factorial. Thus

$$\int 16\pi^3 E_3 \frac{d^3\sigma}{d^3p_3} \frac{d^3p_3}{16\pi^3 E_3} = \frac{1}{F} \sum_{n=1}^{\infty} n\, \sigma_{2\to n} \qquad 1.38$$

This gives us a method of defining an average particle multiplicity via

$$\langle n \rangle = \frac{\sum_{n=1}^{\infty} n\sigma_{2\to n}}{\sum_{n=1}^{\infty} \sigma_{2\to n}} = \frac{\sum_{n=1}^{\infty} n\sigma_{2\to n}}{\sigma_{total}} \qquad 1.39$$

This value for $\langle n \rangle$ can be seen to behave like $\langle n(s) \rangle = A+B \log s$ [9]. This shows that as interaction energy increases a decreasing fraction is used to produce new particles, the remainder staying as kinetic energy of those that are produced. This feature can be used to distinguish between various multiparticle production theories.

V MUELLER's GENERALISED OPTICAL THEOREM

Mueller [2] has indicated that there is a very strong heuristic correspondance between single particle inclusive cross-sections and the discontinuity in an unphysical three body amplitude. A diagrammatic derivation is given in figure 1.2.

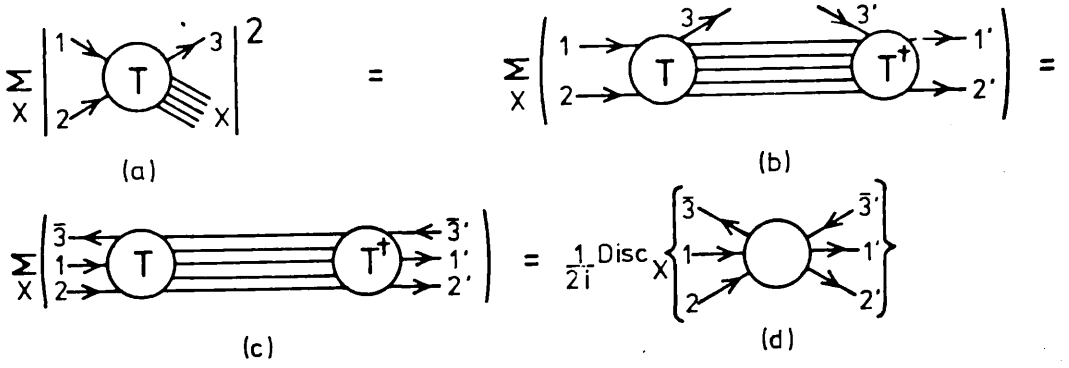

Figure 1.2. A diagrammatic representation of the derivation of Müeller's Generalised Optical Theorem.

The derivation proceeds is the same spirit as that sketched out in section IV for the two body case. We first use the completeness relation 1.26 to relate the actual inclusive cross-section of figure 1.2a to the unit sum of 1.2b. This is precisely as in the two body case. However we now make use of an analytic continuation from the case with particle 3 outgoing and particle 3' incoming to anti particle of 3 (i.e. $\bar{3}$) incoming and $\bar{3}'$ outgoing. This takes us from figure 1.2b to 1.2c. It is then possible to make use of the unitarity relation used in section IV, but with a three particle initial state, in order to pass from figure 1.2c to 1.2d. The discontinuity in this case is of course not in the variable $s = (p_1+p_2)^2$ but in the energy variable of the three body amplitude, that is $M_X^2=(p_1+p_2-p_3)^2$.

This last expression shows that this diagrammatic derivation has, in fact, glossed over some of the trickier aspects since the amplitude of figure 1.2d is clearly unphysical since particle $\bar{3}$ is constrained to have a negative energy, due to the analytic continuation. This can be expressed more clearly by realising that

$$\text{Disc}_x\{T(12\bar{3};M_x^2,s,t)\} = \{T(12\bar{3};M_x^2+i\varepsilon,s,t)-T(12\bar{3};M_x^2-i\varepsilon,s,t)\} \quad 1.40$$

i.e. we should stay on the same side of the cuts in the sub-energies s and t for the physical 3-3 amplitude. However, figure 1.2b makes it clear that for the inclusive cross-section we will be above the threshold cut in s in T but below it it $T^\dagger$. Thus for us to be certain that this result holds we require that taking the discontinuity in one variable will not affect the discontinuity taken in another. While this has not been conclusively shown there are arguments that lead us to expect it in this case [lo].

We have thus managed to relate the single particle inclusive cross-section to the discontinuity of a three body amplitude in an unphysical region of one of its momenta; measurements of this three body cross-section in its physical region are in any case unlikely to be forthcoming. The exercise is however, not in the least pointless since we can also write down the expected Regge-pole forms for this amplitude which then gives us the expected Regge-behaviour of the single particle inclusive cross-section. More detail of these forms will be given in the next section.

All the discussion of the optical theorem has so far been without any mention of spin dependance of any kind. It is however possible to write down a wider form for the optical theorem [11] where three body helicity amplitudes are used which can have different helicities for the initial and final particles. Thus

$$\sum_x \int \prod_{i=1}^{n} \frac{d^3q_i}{(2\pi)^3 2E_i} (2\pi)^4 \delta^4 \left(\sum_{i=1}^{n} q_i + p_3 - p_1 - p_2\right)$$

$$\sum_{\lambda_x} \langle \lambda_1' \lambda_2' | T^\dagger | \lambda_3' \lambda_x \rangle \langle \lambda_3 \lambda_x | T | \lambda_1 \lambda_2 \rangle$$

$$= \frac{1}{2i} \text{Disc}\, M_x^2 \langle \lambda_1' \lambda_2' \lambda_3' | T | \lambda_1 \lambda_2 \lambda_3 \rangle \qquad 1.41$$

is an expression of the full Mueller generalised optical theorem.

If we write all the symbols concerning the summations and integrations as $\oint$ and making an obvious notation for the amplitudes this expression looks simpler as

$$\oint \{f_{\lambda_3 \lambda_x}; \lambda_1 \lambda_2 \, f^*_{\lambda_3' \lambda_x}; \lambda_1' \lambda_2'\} = \frac{1}{2i} \text{Disc}\, M_x^2 \{f_{\lambda_1' \lambda_2' \lambda_3'}; \lambda_1 \lambda_2 \lambda_3\} \qquad 1.42$$

We could go on to discuss the various time-reversal, parity and hermiticity relations which will impose various constraints on the Mueller amplitudes from two directions. Either from that of the three body amplitude [12,13] or by using the fact that the inclusive cross-sections can be viewed as a sum of non-interfering quasi-two body cross-sections, with the missing mass state viewed simply as the second final body.

We choose the latter approach [14] except in the case of time reversal, because the arguments can be given in the more familiar two body helicity relations [15].

We consider time reversal first and simply remark that because of the special continuations performed, a time reversed Mueller amplitude no longer satisfies the s±iε prescription necessary as shown in figure 1.3, and so time reversal gives no relations between the different helicity amplitudes.

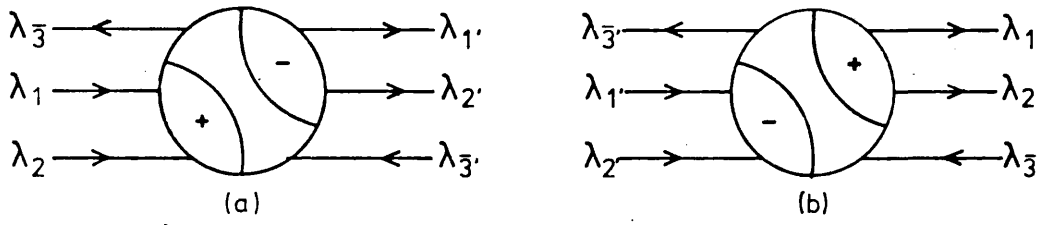

Figure 1.3. The Müeller amplitude and its time-reversed counterpart. The lambdas denote quantum numbers such as helicity.

The hermiticity property is easiest seen by taking the complex conjugate of both sides of equation 1.42. This yields

$$\frac{-1}{2i}\left(\mathrm{Disc}_{M_x^2} f_{\lambda_1\lambda_2\lambda_3;\lambda_1'\lambda_2'\lambda_3'}\right)^* = \frac{1}{2i}\,\mathrm{Disc}_{M_x^2} f_{\lambda_1'\lambda_2'\lambda_3';\lambda_1\lambda_2\lambda_3} \qquad 1.43$$

which immediately indicates that for $\lambda_i = \lambda_i'$, $i = 1,3$ the discontinuity will be pure imaginary, as in the corresponding case for two body.

To derive the parity reversal property we must consider the relation for the quasi-two body amplitudes. We use the Jacob and Wick phase convention [15] and since we will be principally interested in $0^-\tfrac{1}{2}^+ \to 0^- X$ scattering in this thesis we will consider the spin ½ proton, which will be the target particle and "type 2" in the phase convention, as particle 2.

The parity relation can then be written as

$$f_{-\lambda_3-\lambda_X;-\lambda_1-\lambda_2}(-\phi_i) = \frac{\eta_3\eta_X}{\eta_1\eta_2}\,(-1)^{s_3+s_X-s_1-s_1+\lambda_X-\lambda_3-\lambda_1-\lambda_2} \cdot f_{\lambda_3\lambda_X;\lambda_1\lambda_2}(\phi_i) \qquad 1.44$$

where s_i denotes the spin of a particle or conglomerate and the angles ϕ_i are all those internal to the particles comprising the state X. We will be integrating over all these angles and so the fact that they are reversed is no problem. Performing this integration then we have

$$\oint f_{\lambda_3\lambda_X;\lambda_1\lambda_2} f^*_{\lambda_3'\lambda_X;\lambda_1'\lambda_2'} = (-1)^{(\lambda_1-\lambda_1')+(\lambda_2-\lambda_2')+(\lambda_3-\lambda_3')} \oint f_{-\lambda_3\lambda_X;-\lambda_1-\lambda_2} f^*_{-\lambda_3'\lambda_X;-\lambda_1'-\lambda_2'} \qquad 1.45$$

or

$$\frac{1}{2i}\,\mathrm{Disc}_{M_X^2}\, f_{\lambda_1'\lambda_2'\lambda_3';\lambda_1\lambda_2\lambda_3} = (-1)^{(\lambda_1-\lambda_1')+(\lambda_2-\lambda_2')+(\lambda_3-\lambda_3')} \frac{1}{2i}\mathrm{Disc}_{M_X^2} f_{-\lambda_1'-\lambda_2'-\lambda_3';-\lambda_1-\lambda_2-\lambda_3} \qquad 1.46$$

So, since there will be $N_1^2\ N_2^2\ N_3^2$ distinct helicity amplitudes, if $N_i = 2s_i+1$ - i.e. the number of possible helicities, and so $2N_1^2N_2^2N_3^2$ different numbers to measure, the hermiticity condition reduces this by a factor of 2, as does the parity relation. There are therefore $\frac{1}{2}N_1^2N_2^2N_3^2$ different measurements to make. If we specialise to the case of interest for this thesis, namely $0^-\tfrac{1}{2}^+ \to 0^-X$, we see that there are only two possible measurements to determine the reaction completely.

These two measurements are usually taken to be the unpolarised cross-section, and the polarised target asymmetry. The former quantity is defined in section IV, but the latter needs some further investigation to cast it into the language of s-channel helicity amplitudes.

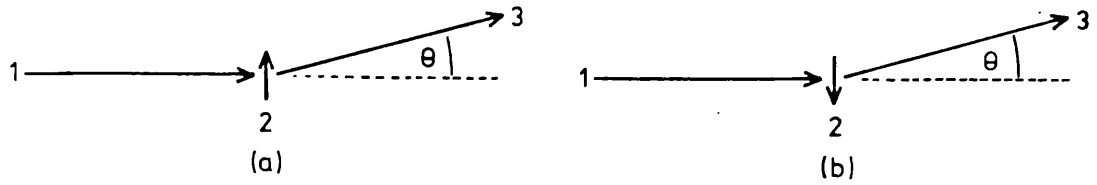

Figure 1.4. The two cross-section measurements necessary for target asymettry calculations.

The target asymmetry for a reaction is defined as the difference between the two cross-sections depicted in figure 1.4 i.e. a) - b) where the target particle is polarised at right angles to the incoming beam. This quantity is then scaled to the unpolarised cross-section. If we define the target asymmetry as Σ_2 we will have

$$\Sigma_2 = \frac{\lambda_1 \Sigma_{\lambda_3} \oint \{ | f_{\lambda_3 \lambda_x ; \lambda_1 \uparrow} |^2 - | f_{\lambda_3 \lambda_x ; \lambda_1 \downarrow} |^2 \}}{\lambda_1 \Sigma_{\lambda_3} \oint \{ | f_{\lambda_3 \lambda_x ; \lambda_1 \uparrow} |^2 + | f_{\lambda_3 \lambda_x ; \lambda_1 \downarrow} |^2 \}} \qquad 1.47$$

where we have

$$\frac{s}{\pi} \frac{d^2\sigma}{dt dM_x^2} = \frac{1}{16\pi^2 s (2\lambda_1+1)(2\lambda_2+1) \Sigma_{\lambda_1 \lambda_2 \lambda_3}} \oint | f_{\lambda_3 \lambda_x ; \lambda_1 \lambda_2} |^2 \qquad 1.48$$

which is given in Appendix 3.A.

We now convert to the helicity frame using [16]

$$\begin{aligned} |\uparrow\rangle &= \frac{1}{\sqrt{2}} (-i|+\rangle + |-\rangle) \\ |\downarrow\rangle &= \frac{1}{\sqrt{2}} (-|+\rangle + i|-\rangle) \end{aligned} \qquad 1.49$$

Defining $\tilde{\sigma} = \Sigma_{\lambda_1 \lambda_2 \lambda_3} \oint | f_{\lambda_3 \lambda_x ; \lambda_1 \lambda_2} |^2$ we then obtain

$$\Sigma_2 \tilde{\sigma} = \Sigma_{\lambda_1 \lambda_3} \oint -i \{ (f_{\lambda_3 \lambda_x ; \lambda_1 +} f^*_{\lambda_3 \lambda_x ; \lambda_1 -}) - (f_{\lambda_3 \lambda_x \lambda_1 -} f^*_{\lambda_3 \lambda_x ; \lambda_1 +}) \} \qquad 1.50$$

Using equations 1.42 and 1.46 we can rewrite this in terms of discontinuities as

$$\Sigma_2\tilde{\sigma} = \mathrm{Disc}_{M_x^2} f_{\lambda_1-\lambda_3;\lambda_1+\lambda_3} \qquad 1.51$$

Consideration of equation 1.43 with equation 1.46 assures us that this discontinuity is pure real, as, of course it must be.

The target asymmetry Σ_2 also has certain kinematical properties, but since they are based on angular momentium considerations, and are not direct results of the optical theorem we leave their derivation until chapter V where use is made of them.

VI MUELLER REGGE LIMITS AND SCALING

In the last section we have demonstrated a strong link between a discontinuity in a three body reaction and the single particle inclusive cross section. Therefore we can postulate models for the three body reaction which do not involve labarynthine integrals and sums over phase space. The class of models that seem to have benefited most are perhaps the Regge models, and single particle inclusive reactions have provided an extensive testing ground for Regge ideas.

While it is much more complicated than the corresponding partial wave decomposition of two body reactions, and their subsequent Regge-ization, it is possible to at least strongly motivate this process in the case of the six-point amplitude [17, 18]. However, because of the multiplicity of sub-energies in this case over that in the two body case there are several different Regge limits and it turns out to be convenient to distinguish between three major regions of phase space. These are the beam and target fragmentation regions, which are further divided into three sub-sections,and the central region.

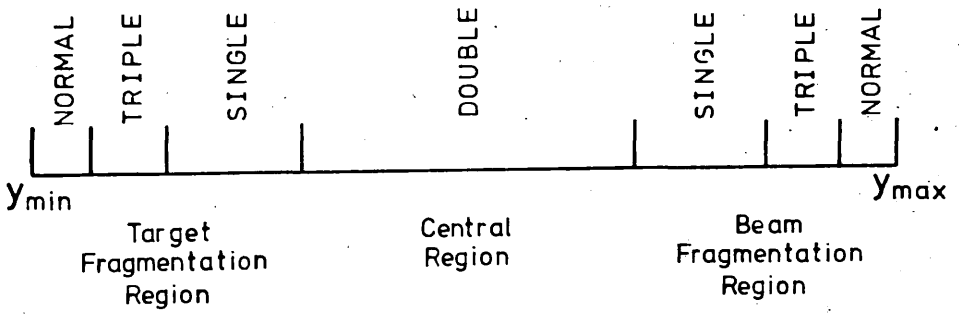

Figure 1.5. Phase space regions in rapidity for $1+2 \to 3+X$ showing the relevant Regge limits.

i) The Beam Fragmentation Region

We normally take particle 1 to be the beam particle and in this case, if particle 3 is only moving slowly in the rest frame of particle 1, we would expect particle 3 to be associated with particle 1, and indeed to be a fragment of it. In this region clearly $x \simeq 1$ and $y \simeq y_{max}$. Dealing with the sub-regions in order as x departs from 1 (x strictly equals 1 is of course elastic scattering) we have.

a) The fixed M_x^2 limit with t and M_x^2 fixed and small and $s/M_x^2 \to \infty$. This is also called the normal Regge limit since we expect the 1-3 channel to Reggerize in a similar faslion to two body scattering. This limit is illustrated in figure 1.6 and the scattering amplitude then takes on the form

$$f(1^2 \to 3) \sim \frac{1}{s} \sum_{ij} \beta_i^{1\bar{3}}(t)\xi_i(t)(s)^{\alpha_i(t)+\alpha_j(t)} \cdot \beta_j^{1\bar{3}}(t)\xi_j^*(t)f(M_x^2,t) \qquad 1.52$$

where $f^{i2\to j2}$ is the forward Reggeon particle scattering discontinuity, β_i the Reggeon-particle particle coupling, ξ_i the Reggeon signature factor and α the pole trajectory function.

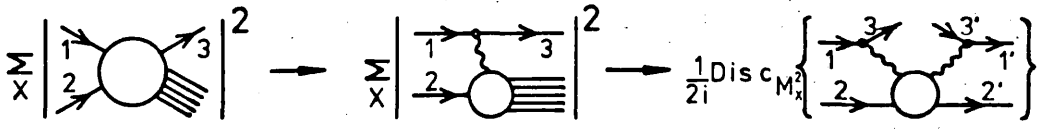

Figure 1.6. The transition to the normal Regge limit.

b) As M_X^2 increases, for large enough values of s then there is a region of phase space where both the customary 1-3 channel is capable of Regge-ization, but also the 2-2 channel of the corresponding 3 body reaction. This limit is the famous triple Regge limit which arises as t remains small and fixed and $s/M_X^2 \to \infty, M_X^2 \to \infty$. This limit is illustrated in figure 1.7. In this region the cross section retains the expression of equation 1.52, but we can now give a form for the forward Reggeon particle discontinuity, namely

$$f^{i2\to j2}(M^2 t) \underset{M_X^2\to\infty}{\sim} \sum_k^{22} \beta_k(0)\,\mathrm{Im}(\xi_k(0))\,g_{ijk}(t,t,0)\,(M_X^2)^{\alpha_k(0)-\alpha_i(t)-\alpha_j(t)} \qquad 1.53$$

The imaginary part of the signature factor appears because we have taken the discontinuity. g_{ijk} denotes the triple-Regge coupling and the other sumbols have been explained. The M_X^2 behaviour of this quantity can be understood by realising that large overlapping subenergies combine in a simple multiplicative manner [19], thus the energy of the "normal" Reggeon is proportional to s/M_X^2 and that of the other simply to M_X^2.

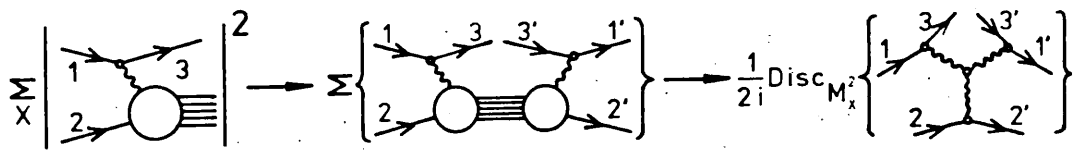

Figure 1.7. The transition to the triple-Regge limit.

c) As M_x^2 increases further we come to the situation where though the 22 channel can still Regge-ize , the 13 can no longer. This is known as the single-Regge limit and corresponds to t and s/M_x^2 fixed and finite but $M_x^2 \to \infty$. This limit is denoted in figure 1.8. Note in the literature the term "fragmentation region" refers specifically to the single-Regge limit.

The form of the cross-section can be given as

$$f(1^2 \to 3) \sim \frac{1}{s} \sum_k \beta_k^{22}(0) (M_x^2)^{\alpha_k(0)} F_k^{1\to 3}\left(\frac{M_x^2}{s}, t\right) \qquad 1.54$$

where $F_k^{1\to 3}\left(\frac{M_x^2}{s}, t\right)$ takes into account the five point upper bubble.

ii) The Target Fragmentation Region

The target fragmentation is the counterpart of the beam fragmentation region at the other end of phase space, where $(p_2-p_3)^2 = u$ is fixed and finite. The discussion of the previous section applies with the obvious changes.

iii) The Central Region

This region is in effect what is left between the two fragmentation regions. At energies above about $s = 60 GeV/c^2$ the two fragmentation regions become well separated [5] to leave a well defined central region, which, as is shown by figure 1.5, does lie in the middle of phase space where both x and y are close to zero. Figure 1.9 depicts the possible Regge limit for this region, where we see that both subenergies $(p_1-p_3)^2 = t$ and

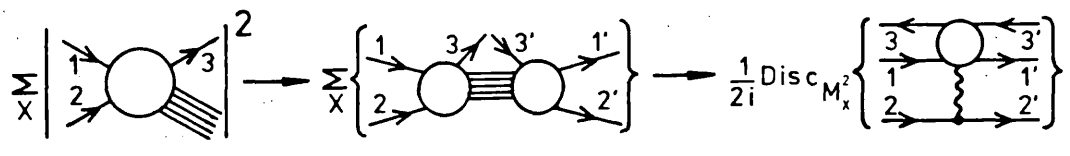

Figure 1.8. The transition to the single Regge limit.

$(p_2-p_3)^2 = u$ should be large. To see how this arises we take the $s\to\infty$ limit of equations 1.13 and 1.15 to yield

$$t = -\sqrt{s}(E_3-p_{3L}),\quad u = -\sqrt{s}(E_3+p_{3L}) \qquad 1.55$$

This gives $\frac{tu}{S} = \mu^2$ where μ is the "longitudinal mass" defined for use with the rapidity variable y (equation 1.20). Since p_{3t}^2 is generally small, for small m_3^2, μ^2 will be about 1.0GeV/c^2 at best. This shows where the figure of s = 60 GeV/c^2 before the onset of Regge behaviour occurs. We can then write down the asymptotic cross-section as

$$f(1,3,2)\ \frac{1}{s}\sum_{i,j}\beta_i^{11'}(0)\left|\frac{t}{s_o}\right|^{\alpha_i(0)} G_{ij}^{33}(\mu^2)\left|\frac{u}{s_o}\right|^{\alpha_j(0)}\beta_j^{22'}(0) \qquad 1.56$$

If we write

$$\chi_{ij}(\mu^2) = \beta_i^{11'}(0)\beta_j^{22'}(0)G_{ij}^{33}(\mu^2)\frac{s_o^2}{\mu^2}$$

then

$$f(1,3,2)\sim\sum_{ij}\chi_{ij}(\mu^2)\left|\frac{t}{s_o}\right|^{\alpha_i(0)-1}\left|\frac{u}{s_o}\right|^{\alpha_j(0)-1} \qquad 1.57$$

Here s_o is the usual energy scale normally taken to be 1.0 GeV/c^2.

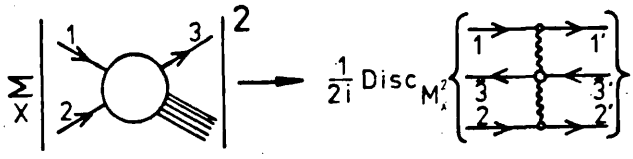

Figure 1.9 The transition to the double Regge limit.

We are now in a position to discuss the asymptotic energy dependance of the various kinematic regions. We begin with the single-Regge limit or "fragmentation region". Equation 1.54 gives this cross section and clearly we would be entitled to exchange the Pomeron with trajectory intercept = 1 at t = 0 as well as other trajectories with lower intercept. In this case $\alpha_k(0) = 1$ and

$$f(1^2 \to 3) \sim \gamma\left(\frac{M_x^2}{s}, t\right) \qquad 1.58$$

Thus the cross section depends (at fixed t) only on the ratio of two energies and is thus independant of the energy units used i.e. it "scales". The Mueller-Regge model then predicts scaling in the fragmentation region, and since the non-scaling terms due the exchange of Reggeons of intercept approximately $\alpha_k(0) = .5$, the model also predicts the speed of approach to scaling behaviour - namely as $s^{-\frac{1}{2}}$. We also note that this form of scaling extends with no alterations into the triple-Regge region, but does not extend to the normal-Regge region, which in any case occupies an increasingly small region of phase space as s increases.

This scaling result was predicted previously by Amati et al [20], Yang and co-workers [21] and Feynman [6]. Yang's views were based on a model of Lorentz contracted discs co-exciting each other and decaying. Since both σ_{el} and σ_{tot} were observed to be approximately constants, the modes of exitation should become independant of s, and the disc-decay reach a limiting distribution in its own rest frame.

The views of Amati et al. and Feynman were based on multi-peripheral models whose philosophy is that production reactions should look like that of figure 1.10 with each particle produced at small momentum transfer to those on either side of it.

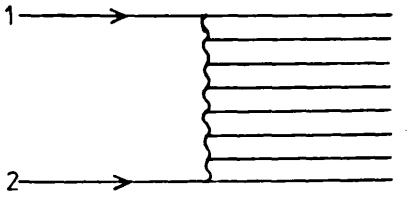

Figure 1.10 A production amplitude where the particles are produced multi-peripherally

In the models considered the distribution of particle 3 in both x and $p_{3\perp}$ became independant of s as $s\to\infty$. The result also extends into the central region as can be explained from equation 1.57. Here, if both exchanges are Pomerons we see that

$$f(1,3,2) \sim \chi_{pp}(\mu^2) \qquad 1.59$$

again independant of s.

The scaling hypothesis seems to work very well in the fragmentation region [9], but somwhat less well in the central region [22]. This is perhaps not surprising since the approach to scaling in this case is as $s^{-\frac{1}{4}}$ which comes from the exchange of a Pomeron and one secondary Reggeon. The effects which cause the deviation of the σ_{tot} from a constant are also clearly playing some part.

VII THE MUELLER-REGGE MODEL AND MULTIPLE SCATTERING

In the case of two body interactions it was rapidly found that the Regge-pole picture was capable of giving a reasonably good explanation of the experimental data. The effective trajectory of elastic data can be found by assuming

$$\frac{d\sigma}{dt} = F(t)\left(\frac{s}{so}\right)^{2\alpha(t)-2} \qquad 1.60$$

Plotting log $\frac{d\sigma}{dt}$ against log(s) at fixed t will give us a value for $\alpha eff(t)$ - the effective trajectory for that process. For charge exchange reactions at least these trajectories seem consistent between reactions and also seem to be linear [5]. However, the Regge-pole only model can be shown to be inadequate from the direction of theory [23] where it is seen that "Regge cuts" or multiple exchange of Reggeons must contribute to the asymptotic amplitude, and from phenomenology where several detailed features rule out the use of pure Regge poles alone. The simplest to see being the polarisation in the reaction $\pi^- p \to \pi^o n$. A pure pole model would predict zero polarization while a substantial value is observed [24].

The same is true for single particle inclusive reactions in the triple-Regge Limit. Much effort has been expended, and with no small success on pure pole tripleRegge analyses [25]. However, there are again theoretical arguments [26] for the inclusion of multiple-Regge exchange in this region. The problem of Pomeron de-coupling [27] arises because of an anomaly in the inclusive cross-section in the triple-Regge region. This anomaly has been examined in the light of the inclusion of multiple-Reggeon exchange [28] which removes the anomaly for this case.

On a phenomenological level, the pure-Regge pole model will predict a zero target asymmetry both from the standpoint of a factorisable Reggeon-particle-particle coupling [29] and also from that of a pure naturality exchange [30]. There seems to be some evidence that this asymmetry is non-zero [31, 32], although the data exists at too low an energy for strong conclusions to be drawn. There is also the case of the reaction $\gamma+p\rightarrow\pi^{\pm}_{0}+X$ with a virtual photon. Naturality arguments for a pure pole exchange would dictate a forward dip [33] where experimental data seem to predict a forward peak [34] though this prediction is based on the position of only one data point. There has also been much work done where a triple Regge-model incorporating poles only has been improved by the inclusion of an absorption or cut model [35].

For these reasons several groups of people have attempted to construct an absorption or Regge-cut model for single-particle inclusive reactions. This thesis sets out one such attempt and to conclude this introductory chapter we give brief summaries of some of the other models.

a) N S Craigie and G Kramer [36] constructed a model in order to cure the disease found in Ref.33 in the hope that absorption would turn the pure pole dip into the peak required by the data. The model takes the form of a partial wave analysis of the quasi two body amplitude with integrals over the internal variables of the missing mass state. The type of re-scattering corrections envisaged are depicted in figure 1.11. The transition to impact parameter space is made using the usual two-body assumptions

and it turns out to be possible to arrive at a closed form for the sum over the helicities of the missing mass state in order to arrive at the formula

$$H^{\lambda'\lambda}(\tau,\tau') = \int \frac{d^2\tau_1'}{2\pi} \int \frac{d^2\tau_1}{2\pi} S^*(\underline{\tau}'-\underline{\tau}_1') H_R^{\lambda'\lambda}(\underline{\tau}_1', \underline{\tau}_1) S(\underline{\tau}-\underline{\tau}_1)$$

where $S(\underline{\tau}-\underline{\tau}_1) = 2\pi\delta^2(\underline{\tau}-\underline{\tau}_1) - cae^{-a(\underline{\tau}-\underline{\tau}_1)^2}$ 1.61

where $t = t_{min} - \tau^2 x$ defines τ as a scalar. The vector $\underline{\tau}' = (\tau'\cos\phi, \tau'\sin\phi)$ indicate that the internal triple-Regge scattering need no longer take place in the $\phi = 0$ plane and C and a are defined via

$$\mathrm{Im}F(s,t) = \sigma_{tot}\, s\, e^{at}$$

$$C = \sigma_{tot}/(8\pi a)$$

where σ_{tot} is the $\rho^o p$ total cross-section and $F(s,t)$ the $\rho^o p$ elastic amplitude. The lambdas refer to the helicity of

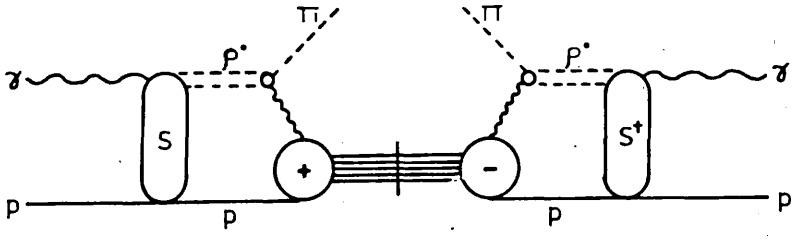

Figure 1.11. Re-scattering corrections to the Müeller-Regge expansion of the reaction $\gamma + p \rightarrow \pi + X$. (see Ref. 36)

In fact because of the form of the approximation used for the d^J functions this derivation implicitly assumes that the flip of helicity into the missing mass state will be small. See appendix 3C for a more detailed discussion of this problem and as to why this approximation is reasonable and Ref. 37 for a derivation of the two body d^J approximation.

Also, in the calculation the multiple of 2π of the delta functions in the definition of the S-factor (equation 1.61) was missed off, so while a good fit to the data was obtained it required an inordinately large value for C. The parameters fitted in this paper have been used in the estimation of the polarised target asymmetry for this reaction by K Ahmed, J G Körner, G Kramer and N S Craigie [32]

b) F E Paige and T L Trueman [38] and F E Paige and D P Sidhu [39]. In their interesting paper, Paige and Trueman give an extended review of the way in which the two body cut can be related to a diagram in single particle inclusive reactions. These two diagrams are shown in figure 1.12.

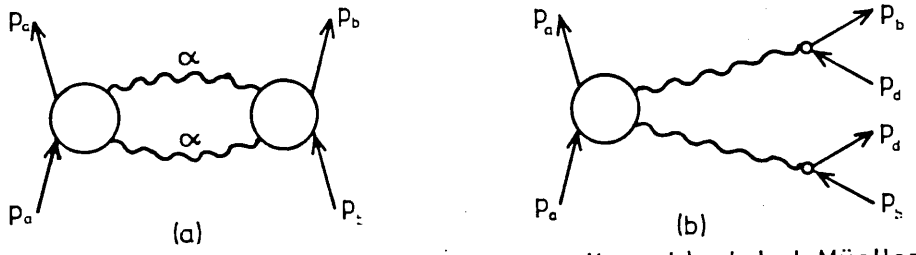

Figure 1.12 a) Regge-cut graph for total cross-sections. b) related Müeller graph. (see Ref. 38)

Their calculation is cast in the form of the Reggeon Calculus and it is possible to write down a simple closed expression for the contribution of the cut to the total cross-section, namely

$$\sigma^{cut}_{total}(s) = \int \frac{d^2q_\perp}{(2\pi)^2} \frac{\cos\pi\alpha(q_\perp^2)}{\sin^2\pi\alpha(q_\perp^2)} \begin{Bmatrix} \cos^2[\tfrac{1}{2}\pi\alpha(q_\perp^2)] \\ \\ -\sin^2[\tfrac{1}{2}\pi\alpha(q_\perp^2)] \end{Bmatrix}$$

$$s^{2\alpha(q_\perp^2)-2}\ N_a^+(q_\perp^2)\ N_b^+(q_\perp^2) \qquad 1.62$$

where the choice of term in the curved brackets is made according to the signature of the exchanged Reggeons and the cut-coupling functions Na^+ and Nb^+ are just those functions one would expect after factoring the unwanted terms in the diagram of figure 1.12b. Unfortunately when a similar procedure is attempted with the single particle inclusive cut graph and the double particle inclusive cross-section (see figure 1.13) the attempt is frustrated partly because the amplitudes in the single particle inclusive cut have differing boundary conditions from those in the double particle inclusive graph (this problem could perhaps be overcome as was a similar in the generalised optical theorem), but also because the distortion of contours required to obtain the closed form is not possible in this case due to cuts occuring in the other subenergies available in this case, though not in the two body case.

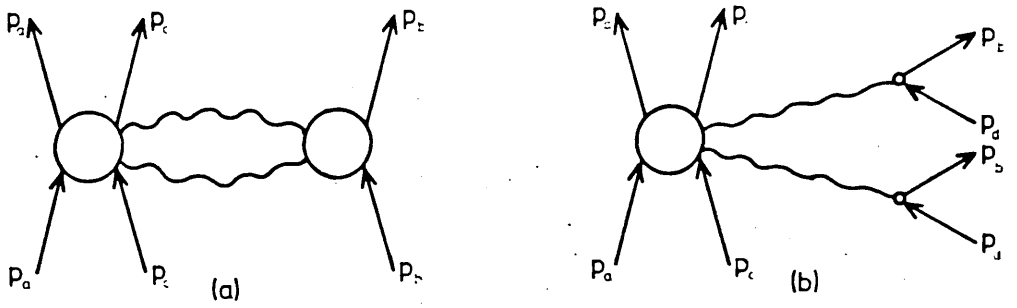

Figure 1.13. a) Müeller -Regge cut graph. b) Müeller graph for the two particle cross-section in Regge limit. (see ref. 38)

It does however, turn out to be possible to make estimates of the cut corrections in certain specialised sub-regions, the main of which is the triple-Regge region. A cut graph in this region is shown in figure 1.14 and form for the discontinuity is given by

$$\frac{1}{2i}\mathrm{Disc}_{M^2}F_{\lambda'\lambda}(s,M^2,q^2) = \frac{1}{16\pi^2}\int d^2k_\perp N_{\alpha_5\alpha_2}(q_\perp+k_\perp,k_\perp)$$

$$g_{\alpha_3\alpha_5;\alpha_4}(q_\perp,q_\perp+k_\perp)N_{\alpha_4\lambda';\alpha_2\lambda}(k_\perp)[-2\mathrm{Im}(\xi_2\xi_5\xi_3^*)]$$

$$\left(\frac{s}{M^2}\right)^{\alpha_2+\alpha_3+\alpha_5-1}(M^2)^{\alpha_2+\alpha_4-1} \qquad 1.63$$

where the Ns are again two particle, two Reggeon coupling functions, the g is a three-Reggeon coupling and the ξ's are the usual signature factors.

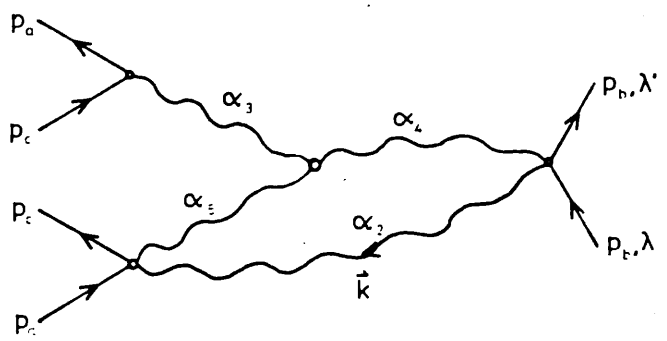

Figure 1.14 A Regge cut graph for the triple-Regge region.(see ref.38)

It is this formula that Paige and Sidhu apply in order to make estimates of the relative importance of cuts in the triple-Regge region. They make the assumptions that the cut-coupling function will be simply the product of appropriate Regge residues and make an exponential approximation for these and for the three-Reggeons coupling. They then make estimates of the ratio of σcut/σpole for the reactions $\pi^-p\to\pi^0x$, $\pi^-p\to\eta x$ and $K^-p\to\overline{K}^0x$. In all cases this ratio is greater than -1 so no large dips are predicted, and the average contributions are around 30%, increasing with $|t|$.

Paige and Sidhu also calculate Λ polarizations from various initial states. Where data exists their results which are in all cases of the order of 1% or 2%, are not inconsistent, but the data does possess large error bars.

c) J Pumplin [40]. Pumplin adopts a different view point to most of the other models for absorption in single particle inclusive reactions.

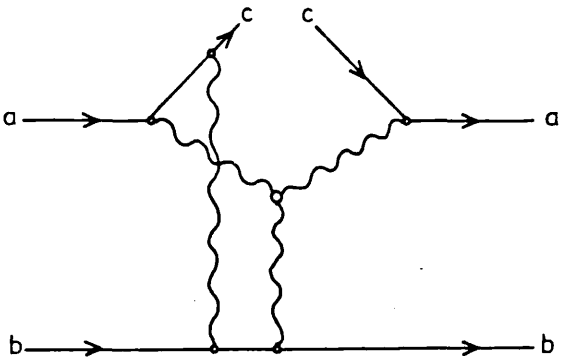

Figure 1.15 A re-scattering correction to the triple-Regge graph between particle b and particle c. (see ref. 40)

He argues that since, away from $x = 1$, the dissociation reaction $a \to c+R$ takes place over a long time, that it will be the re-scattering between particle c and particle b that is important (see figure 1.15), and by means of a fourier decomposition produces the formula

$$M(\vec{p}_\perp, \vec{p}_\perp, M^2, s) = \int d^2\vec{q} d^2\vec{q}', M_o(\vec{q}', \vec{q}, M^2, s)$$
$$[\delta^{(2)}(\vec{p}_\perp - \vec{q}') - iM^*_{cb}(\vec{p}_\perp - \vec{q}', xs)]$$
$$[\delta^{(2)}(\vec{p}_\perp - \vec{q}) + iM_{cb}(\vec{p}_\perp - \vec{q}, xs)] \qquad 1.64$$

which he specialises, using various gaussian or exponential approximations before applying it to the reactions

$\gamma + p \to \pi + x$ and $\pi^- + p \to \pi^0 + x$

in the form

$$M(p_1^2) = iM^2\sigma_{Rb}\int dq' F^*(q')\int dq F(q)$$
$$e^{-(\frac{1}{2})A(\vec{q}'-\vec{q})^2} S^*(\vec{q}'-\vec{p}_1)S(\vec{q}-\vec{p}_1) \qquad 1.65$$

where the S factors are given by

$$S(\vec{q}) = \delta^2(\vec{q}) - \frac{\eta C}{2\pi} e^{-(\frac{1}{2})C\vec{q}^2} \qquad 1.66$$

and

$$F(\vec{p}) = \beta(t)(s/M^2)^{\alpha(t)}$$

Pumplin also makes the argument, using elementary particle propagators, that these c-b scatterings are the only ones that contribute and that a-b rescatterings do not. The use of elementary propagators instead of Regge propagators however, seems slightly suspect. In the first paper Pumplin then calculates $\gamma+p\rightarrow\pi\pm x$ and indicates that this model cannot generate a forward peak with any reasonable absorption parameters and the second paper is devoted to the reaction $\pi^-p\rightarrow\pi^0x$, the main predictions being no dips seen at around $t = -0.5$ GeV/c^2, unlike the reaction $\pi^-p\rightarrow\pi^0n$ and a raising of the effective trajectory for the exchanged ρ-Reggeon.

d) A Capella, J Kaplan and J TranThanh Van [41]. These authors utilise a simplified approach to the Reggeon Calculus previously developed by them [42] for two body reactions. They make contact with the single particle inclusive process by allowing one triple-Pomeron coupling to split the simply exchanged Pomerons . This arrangement is illustrated in figure 1.16.

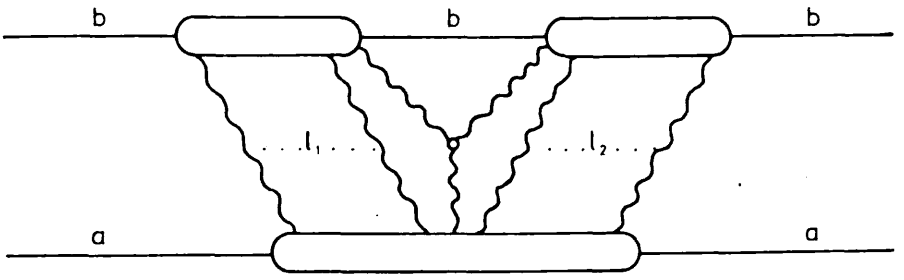

Figure 1.16. A diagram in two-body scattering related to the single-particle inclusive distribution. (see ref. 42)

It is a combinatorial re-arrangment of the discontinuities formed by cutting such diagrams through particle b and the "third leg" of the triple-Pomeron cluster that form the basis for this model of absorptive corrections. They arrive at a diagram of the form of figure 1.17. For various reasons it is clear that this formulation will hold only for x very close to one. This is clearly demonstrated in that the form for t used is $t = -p_{c_1}^{\ 2}$ rather than the more usual $t = -p_{c_1}^2/x$.

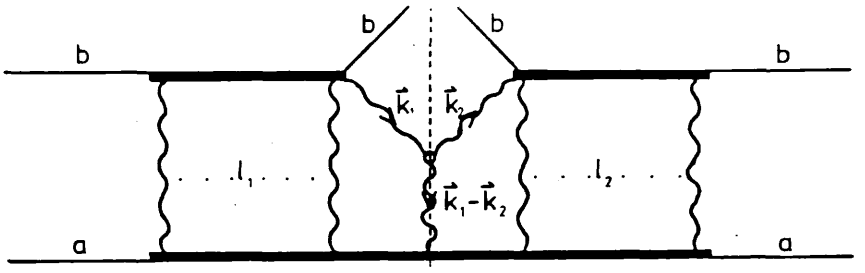

Figure 1.17. The discontinuity related to the single-particle inclusive distribution. (see ref. 42)

The detailed form of the absorptive correction is not transparent. It can be shown to be of the general form of all these models briefly described, but with a particular choice for the $S(\vec{q},s)$ factors (see equations 1.66 or 1.61) to give an eikonal type form, but also to take account of some inelastic intermediate states. For this reason the form is not given.

The main conclusion of this paper is that the absorptive corrections calculated are very large, due mainly to the combinatorics as opposed to those in the two body case. They make an estimate of the triple-Pomeron coupling, which they find to be significantly different from the pole only case, but also find that even with large absorptive corrections, the Pomeron factorisation property still seems to hold at a 10% level.

e) A Garcia Azcarate [43] studies the reaction p+p→n+x in the triple-Regge region in both the framework of a peturbative approach to Reggeon calculus, as in the previous model and a system comprising small absorption corrections of a similar type to those proposed in Ref.36. Azcarate uses a Regge-ised one pion exchange mechanism with only the Pomeron included in the π^+p elastic scattering. Since the resultant intermediate pion are so close to the mass-shell it is reasonable to use the physical values for cross-sections and coupling constants.

The model for O.P.E.R. without absorption shows reasonable behaviour, but does overestimate the normalisation (see Ref.44 for an alternative approach to this reaction in both the O.P.E.R. and weakly absorbed model). The two sorts of absorption now reduce this normalisation. However, the model of Capella et. al. produces a curve which is significantly below the data while the weakly absorbing model interpolates the data fairly well.

f) J Bartels and G Kramer [45] . These authors again approach the subject from the standpoint of the Reggeon Calculus, and, although making various numerical approximations, they consider the diagrams of figure 1.18. They achieve a cross-section for s = 20GeV/c^2 of only $^1/_3$ the pole value, and because the cuts die away very slowly as s rises (This of course comes as a consequence of the M_x^2/s scaling of the pole amplitude), this value has only increased to .44 of the original pole expression by s = 3000 GeV/c^2.

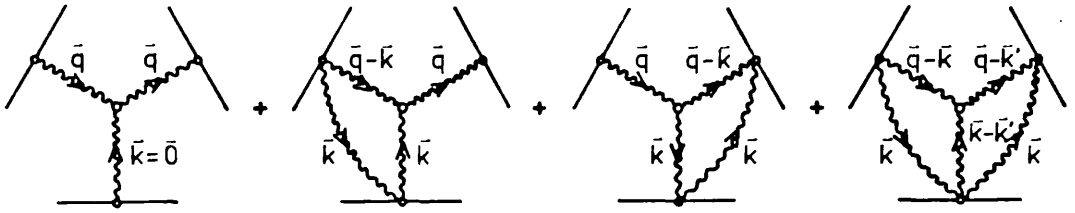

Figure1.18.The pole-only diagram and three lowest order Reggeon Calculus cut corrections.(see ref.45)

From this we see that the Reggeon calculus much stronger cuts for one additional pomeron as indicated by Ref.41 and also that these cuts persist to very high energy. The size of these cuts indicate to the authors that the investigation of both "enhanced" graphs where more than one triple Poneron vertex occurs, or perhaps higher order Po meron vertices (see figure 1.19 for representations of these graphs) and multiple Pomeron exchange in non-enhanced graphs could well be important.

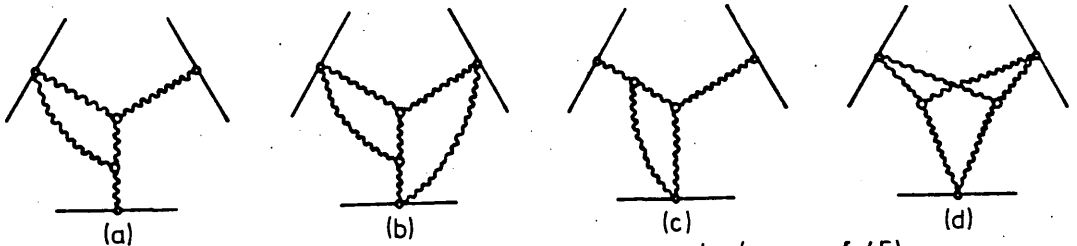

Figure1.19.Several "Enhanced" multi-Pomeron graphs.(see ref.45)

They calculate the enhanced contributions of figure 1.19 and find that from a few percent at $s = 20 GeV/c^2$, some of these graphs, particularly those of parts a) and c) have risen in importance to about 20% of the pole graph by $s = 3000\ GeV/c^2$. They also derive the multi-Pomeron exchange for Reggeon calculus in the eikonal approximations and remark that at low energies the convergence of the resulting series expansion will be slow, though this will improve as energies increase.

Bartels and Kramer therefore conclude that at low energies enhanced graphs are not yet important, but several terms in the eikonal series will need to be accounted for and as energies increase, this series will truncate sooner, but enhanced graphs become important, and at energies higher than those achievable today enhanced will begin to dominate. All in all a much more complicated area than cuts in two body reactions.

g) G R Goldstein and J F Owens [46]. These authors provide us with another impact parameter/Fourier decomposition method. They define their impact parameter as that variable conjugate to the two dimensional $p_{c\perp}$ and give references [47] to support its choice.

The analysis is easily performed and with the choice of $S_{eff}(b) = 1 - Ce^{-b^2/4a}$ the final formula is given as

$$D_{ga'b'c',abc}(p_\perp) = \int\frac{d^2k_\perp}{2\pi}\int\frac{d^2k_\perp'}{2\pi}\ {}^{R}D_{ga'b'c',abc}(k_\perp,k_\perp')$$

$$\{2\pi\delta^2(p_\perp-k_\perp)-2aCe^{-a(p_\perp-k_\perp)^2}\}\{2\pi\delta^2(p_\perp-k_\perp')-2a^*Ce^{*-a^*(p_\perp-k_\perp')^2}\} \quad 1.67$$

This form is similar to that derived in Ref 36. The impact parameter in this reference is defined as the variable conjugate to p_{c_1}/x, however, any phenomenological differences arising from this choice should be slight.

The reaction $p+p \to \Delta^{++} + X$ is chosen for study. The motivation for this is fairly clear. The reaction should be dominated by pion exchange and due to the proximity of the pion pole to the physical, it is possible to give a good estimate of the relevant triple-Regge coupling. When this is done, the existance of good quality data allows us to say that the pole only model yields a normalisation approximately a factor of two too large (see ref.48 for an alternative calculation for this reaction both in the pole only and absorbed form. These papers also give references to the data of this reaction). This discrepancy can be remedied by absorption.

Of course this reaction is also interesting since it provides, fairly easily, a measurement of the decay density matrix elements of the Δ^{++}. Predictions of these quantities should be very model sensitive.

The authors find that a good fit can be obtained to a set of data with reasonable absorption parameters and with the agreed value for the $G_{\pi N\Delta}$. A pole only fit results in an unreasonable value for $G_{\pi N\Delta}$, which is, after all, well attested to.

It is therefore possible to conclude from this analysis that the absorptive corrections do have a definite role to play.

CHAPTER II

A Computer Program for the Calculation And Display of High Energy Single Particle Inclusive Production Reaction Observables

INTRODUCTION

There are many different types of single particle inclusive production reactions of phenomenological interest. This, coupled to the need to present much more information than in the corresponding exclusive reaction case, make it desirable to be able to experiment both with the dynamic model, and the presentation of the calculated observables with as little computer reprogramming as possible. To make this possible we felt it necessary to write a computer program that would accept a standardized data deck for any of the relevant reactions, or set of reactions, and that could then perform calculations of almost all the relevant observables. The dynamic model used for these calculations is added on as a new written function, as indicated in fig 3, and which particular quantities are calculated and which presented can be completely governed by the specification of integer flags read in with the data deck.

We also felt that the manner in which the results are presented is extremely important, and to this end the program provided a line-printed output which contains all the relevant information. Parts or all of this output can be switched off using relevant flag values. We also provide the facility of plotting every set of results calculated, both for lucidity in that the user is immediately aware of effects in a suitable graph that are easily hidden in a long column of figures, and also for sheer convenience when plotted results are required for publication. This plotting facility requires the attachment of a plotting package which is freely available from Computer Physics Communications.

The program was also written to conform to the requirements of the standard minimisation package MINUIT and has been successfully used with this package to perform χ^2 minimisation for theory-data comparison.

Several people have successfully used the program (named ONCPLT) over a wide variety of inclusive reactions, and ONCPLT has, I hope, for

them provided a short cut to the adequate presentation of their calculated results.

What follows this introduction is a Program Summary giving the relevant technical details in a short form and a Long Write Up which elaborates on the conventions and techniques used within the program.

PROGRAM SUMMARY

Title of program: ONCPLT

Catalogue number: AAUR

Computer: CDC 6600, CDC 7600; Installation: University of London Computer Centre

Operating system: CDC SCOPE

Programming language used: FORTRAN IV

High speed core required: 25K words

No. of bits in a word: 60

Overlay structure: None

No. of magnetic tapes required: None

Other peripherals used: Card reader, Printer, Calcomp plotter with Calcomp compatible software

No. of cards in combined program and test deck: 4,020

Card punching code: CDC

CPC Library subprograms used: AAUN, Title APLOT, Ref 49.

Keywords: Nuclear, High Energy, Single-Particle-Inclusive Cross Section, s-Channel Helicity States, Spin Density Matrix, Effective Trajectories, χ^2-Minimization, Graph Plotting

Nature of the physical problem

This program is concerned with the phenomenological analysis and the display via both the printer and graph plotter of high-energy single-particle-inclusive production reaction observables.

Method of solution

The program can be run under either the fixed t or the fixed M^2 modes when calculating differential cross sections with that for fixed t being integrated over the t-bin by 8-point Gaussian quadrature. Total cross sections can be calculated using repeated 48-point Gaussian quadrature. In addition, effective trajectories and density matrix elements can be calculated. The results of all these types of calculation can be plotted with the inclusion

of the graph plotting package APLOT [49]. The program is compatible with MINUIT [50] and this combination has been used to perform minimization [51].

Restrictions on the complexity of the program

The number of data points considered cannot exceed 500 in general. In the case where density matrix data or effective trajectory data is to be read in the number of data points cannot exceed 100. This is purely a dimensional requirement and can be altered. If density matrices are to be calculated the final detecting particle must have spin less than 5/2.

Typical running time

The test run took 72.2 sec. (of which 32.7 sec was compilation time on the CDC 6600.) A recent minimization calculation [51] in which the program was used, 400 passes minimizing 3 parameters on 28 data points took 184 seconds.

LONG WRITE-UP

1. INTRODUCTION

The computer program described here is designed to handle calculations for single-particle-inclusive reactions in the region s/M^2 large and to compare the theoretical predictions with the experimental data both by means of line printer and graph plotter output.

The matrix elementsof interest are calculated in the TRACE function subroutine and, according to various flags in the program, the program will calculate differential cross sections in either a fixed t or a fixed M^2 mode, total cross sections integrated over a specific region of phase space, density matrices of the observed final particle and an effective trajectory for the exchanged Reggeon.

Since theory can often only provide a functional form with several adjustable parameters the program is set up to provide a χ^2 minimization on the differential cross section data when used in conjunction with the standard minimization program MINUIT [50].

2. CONVENTIONS AND KINEMATICS

The kinematics we calculate for the process $a + b \to c + X$ are the usual relativistic invariants given by

$$s = (p_a + p_b)^2, \quad t = (p_a - p_c)^2, \quad M^2 = (p_a + p_b - p_c)^2 .$$

For single-particle-inclusive production reactions the minimum $|t|$ effect is important since it is a function of both s and M^2. t is given by

$$t = m_a^2 + m_c^2 - 2E_aE_c + 2qk\cos\theta,$$

where q and k are the three-momenta of c and a in the a-b centre-of-mass frame. Transforming this to relativistic invariants we find

$$|t|_{\substack{\max\\ \min}} = \left\{ \sqrt{\frac{(s+m_c^2-M^2)^2}{4s} - m_c^2} \pm \sqrt{\frac{(s+m_a^2-m_b^2)^2}{4s} - m_a^2} \right\}^2$$

$$- \frac{1}{4s} \left[(m_c^2 - m_a^2) - (M^2 - m_b^2) \right]^2 .$$

On neglecting all single particle masses we find

$$|t|_{\max} = s - M^2, \quad |t|_{\min} = 0.$$

This approximation does not seem valid at presently available energies and so throughout the program we have used the exact expression for $|t|_{\min}$.

The normalization is taken from the expression for the total inclusive cross section

$$\langle n \rangle \sigma = \int dM^2 \int \frac{\not{d}^3 q_c}{2E_c} \frac{\not{d}^3 q_M}{2E_M} \not{\delta}^4(q_c + q_M - p_a - p_b) \cdot \frac{1}{F} \not{\sum} |\langle c,X|T|a,b\rangle|^2,$$

where $\not{d}^3 q_c$ denotes $d^3 q_c/(2\pi)^3$ and $\not{\delta}^4(x)$ denotes $(2\pi)^4 \delta^4(x)$, F is the flux factor for the particular frame of reference chosen and $\not{\sum}$ denotes all the summation and averaging over all the helicity states, different particle states, etc. and integration over all three-momenta internal to the M^2 state. We can acquire the differential cross section from this expression by inserting appropriate delta functions, i.e.

$$\langle n \rangle \frac{d^2\sigma}{dt dM^2} = \int dM^2 \int \frac{\not{d}^3 q_c}{2E_c} \frac{\not{d}^3 q_M}{2E_M} \cdot \not{\delta}^4(q_c + q_M - p_a - p_b) \delta(M^2 - [p_a + p_b - p_c]^2)$$

$$\cdot \delta(t - [p_a - p_c]^2) \frac{1}{F} \not{\sum} |\langle c,X|T|a,b\rangle|^2,$$

which in the centre-of-mass frame of particles a and b yields

$$\langle n \rangle \frac{s}{\pi} \frac{d^2\sigma}{dt dM^2} = \frac{1}{64\pi^2 k^2} \not{\sum} |\langle c,X|T|a,b\rangle|^2 .$$

$\langle n \rangle$ is the average multiplicity of the detected particle and is a function of s only. It would normally be implicitly included in the measurement of an inclusive cross section so there is no necessity to calculate it and divide it out.

We need now to consider in more detail the generalized optical theorem [11,14] which gives us

$$\sum_X \int \prod_{i=1}^{N_X} \frac{d^3 q_i}{2E_i} \delta^4\left(\sum_{i=1}^{N_X} q_i - q_M\right) \sum_x T_{\lambda_c x;\lambda_a\lambda_b} T^*_{\lambda_c' x;\lambda_a'\lambda_b'}$$

$$= \frac{1}{2i} \text{Disc}_{M^2} T_{\lambda_c'\lambda_a'\lambda_b';\lambda_c\lambda_a\lambda_b},$$

where N_X is the number of particles in the M^2 state, λ denotes the helicity of the appropriate single particle state and x denotes the helicity of the composite M^2 state. Thus we have

$$\int |\langle c,X|T|a,b\rangle|^2 = \sum_{\lambda_c} \bar{\sum_{\lambda_a\lambda_b}} \delta^{\lambda_a\lambda_b\lambda_c}_{\lambda_a'\lambda_b'\lambda_c'} \left(\frac{1}{2i} \text{Disc}_{M^2} T_{\lambda_c'\lambda_a'\lambda_b';\lambda_c\lambda_a\lambda_b}\right).$$

We can obtain parity relations for this $3 \to 3$ amplitude by noting that for the pseudo-two-body amplitude

$$T_{-\lambda_c -x;-\lambda_a-\lambda_b}(-\chi_i)$$

$$= \frac{\eta_c\eta_X}{\eta_a\eta_b} (-1)^{S_c+S_X-S_a-S_b+(x-\lambda_c)-(\lambda_a-\lambda_b)} T_{\lambda_c x;\lambda_a\lambda_b}(\chi_i),$$

where the χ_i are labels internal to to the composite state which are flipped by the parity operation. However, once we form the required combinations and integrate we find that

$$\text{Disc}_{M^2} T_{\lambda_c'\lambda_a'\lambda_b';\lambda_c\lambda_a\lambda_b}$$

$$= (-1)^{(\lambda_a-\lambda_a')+(\lambda_b-\lambda_b')+(\lambda_c-\lambda_c')} \text{Disc}_{M^2} T_{-\lambda_c'-\lambda_a'-\lambda_b';-\lambda_c-\lambda_a-\lambda_b}.$$

This formula is used in calculating spin density matrices since in forming bilinear combinations all the dependence of the M^2 state must cancel out.

In calculating spin density matrix elements of the finally detected particle we will wish to present the results in the Gottfried-Jackson frame

for the observed final particle. This involves a rotation from the reference frame depicted in fig.2.1. For the rotation calculated in the program (see Section 4) to be the correct one the "amplitudes" must be calculated according to these kinematics.

3. EFFECTIVE TRAJECTORIES

In the regime $s \to \infty$, $s/M^2 \to \infty$, the triple-Regge ansatz for the cross section (see fig.2.2) is given by [16]

$$\frac{s}{\pi}\,\frac{d^2\sigma}{dtdM^2} = \left\{\begin{matrix}\text{Normalization}\\ \text{Factors}\end{matrix}\right\} \cdot \sum_{i,j}\ \sum_{\lambda_1\lambda_2\lambda_3} \beta_i^{\lambda_1\lambda_3}(t)\ \xi_i(t)\ \frac{s}{M^2}^{\alpha_i(t)}$$

$$\cdot\ \frac{1}{2i}\ \mathrm{Disc}_{M^2}\{A^{ibj}_{\lambda_2}(t,M^2)\}\ \beta_j^{\lambda_1\lambda_3}(t)\ \xi_j^*(t)\ \frac{s}{M^2}^{\alpha_j(t)} .$$

The behaviour of the normalization factor is typically $1/s$.

To arrive at the effective trajectory we assume that essentially only one Regge exchange is involved and the expression collapses to

$$\frac{s}{\pi}\,\frac{d^2\sigma}{dtdM^2} = \left\{\begin{matrix}\text{Normalization}\\ \text{Factors}\end{matrix}\right\} \cdot G(t,M^2)\ \frac{s}{M^2}^{2\alpha(t)} .$$

Our method for calculating the effective trajectory is to calculate differential cross sections for the same values of the invariants t and M^2 but different values of s. Then

$$\alpha(t) = \frac{\ln\left\{\dfrac{\left[\begin{matrix}\text{Normalization}\\ \text{Factor 2}\end{matrix}\right]\frac{s_2}{\pi}\frac{d^2\sigma_2}{dtdM^2}}{\left[\begin{matrix}\text{Normalization}\\ \text{Factor 1}\end{matrix}\right]\frac{s_1}{\pi}\frac{d^2\sigma_1}{dtdM^2}}\right\}}{2\ln\left\{\frac{s_2}{s_1}\right\}} .$$

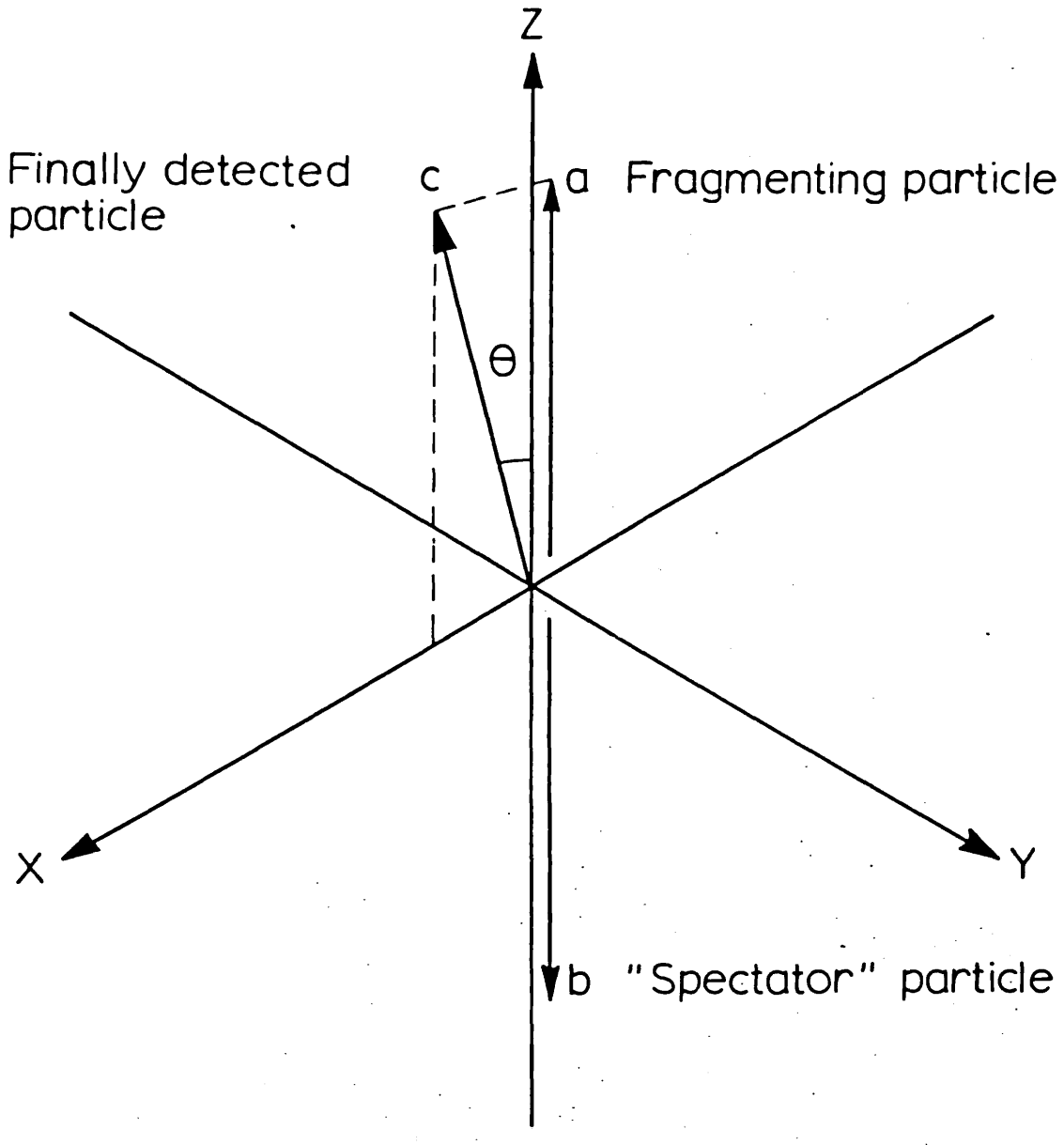

Fig.2.1. Particles a and b centre-of-mass coordinate system

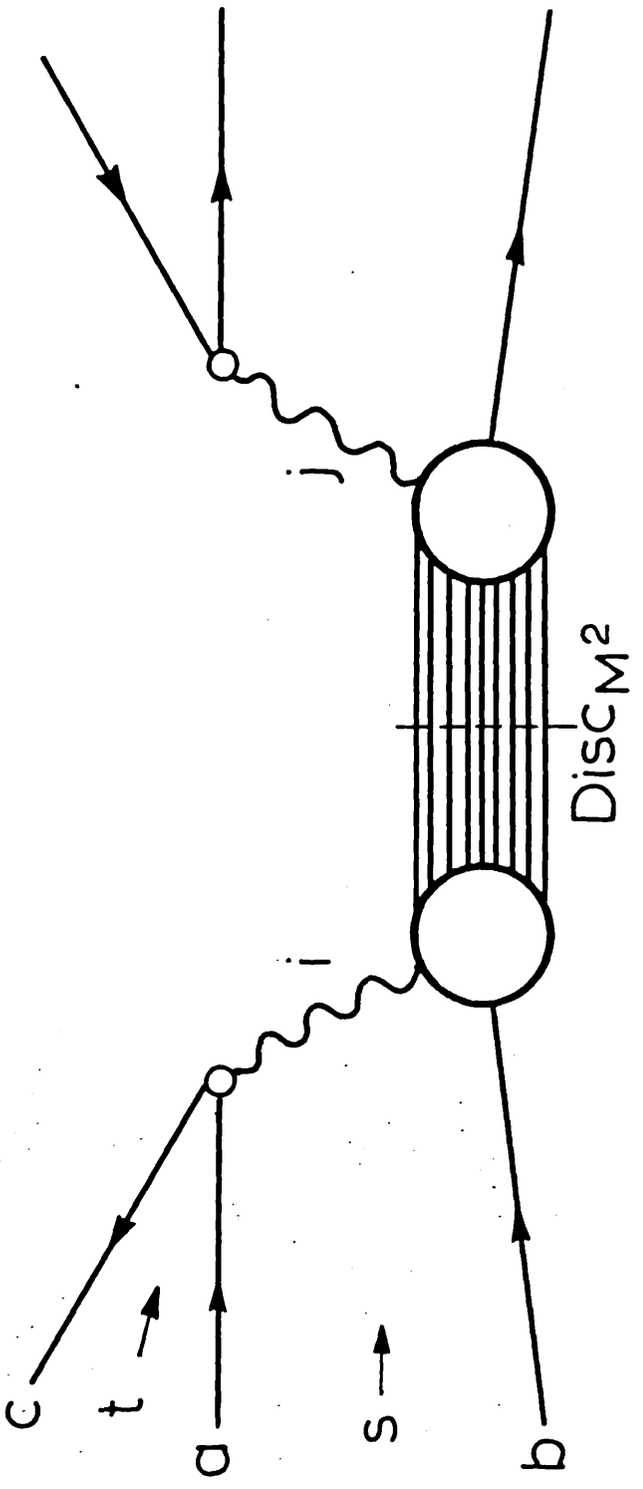

Fig.2.2. The triple-Regge diagram for the process $a + b \to c + X$

This method has the advantage that it is possible to study the dependence of the effective trajectory as M^2 varies, it is valid in both the Normal ($s/M^2 \to \infty$, M^2 fixed) and the triple-Regge ($s/M^2 \to \infty$, $M^2 \to \infty$) limits. In addition it assumes nothing about the functional form of $G(t,M^2)$.

4. SPIN DENSITY MATRIX ELEMENTS

The spin density matrix elements of the observed final particle in the reference frame of fig.2.1 are given by [11,14]

$$\rho^{CM}_{\lambda'_c\lambda_c} = \sum_{\lambda_a\lambda'_a} \sum_{\lambda_b\lambda'_b} \int_X \langle\lambda'_c x|T|\lambda'_a\lambda'_b\rangle\langle\lambda_c x|T|\lambda_a\lambda_b\rangle \rho^a_{\lambda'_a\lambda_a} \rho^b_{\lambda'_b\lambda_b} ,$$

where ρ^a and ρ^b are the density matrices of the two initial state particles. Normally these will be the unit matrices but provision is made in the program to calculate spin density matrix elements with initial polarization. Returning to the former case for clarity we have

$$\rho^{CM}_{\lambda'_c\lambda_c} = \sum_{\lambda_a\lambda_b} \text{Disc}_{M^2} \langle\lambda'_c\lambda_a\lambda_b|\ |\lambda_c\lambda_a\lambda_b\rangle .$$

This matrix is then normalized by the condition that it has unit trace. To pass from the center-of-mass to the Gottfried-Jackson frame we must apply the Wigner rotation through an angle ψ which is given by

$$\tan\psi = \frac{m_c k \sin\theta}{E_c k \sin\theta - E_a q} .$$

Thus, we have

$$\rho^{GJ}_{m'm} = \sum_{\lambda'_c\lambda_c} d^{S_c}_{m'\lambda'_c}(\psi)\, d^{S_c}_{m\lambda_c}(\psi) \rho^{CM}_{\lambda'_c\lambda_c} .$$

These matrices must be hermitian, i.e.

$$\rho_{m'm} = \rho^{*}_{mm'} \ .$$

If parity is conserved we have

$$\rho_{m'm} = (-1)^{m'-m} \rho_{-m',-m} \ .$$

These properties come from the way the matrix is constructed and the parity relations of the "amplitudes" used to construct them and, of course, we have them normalized to unit trace, i.e.

$$\sum_{m} \rho_{mm} = 1.$$

The program is dimensioned so that it is capable of calculating rotation functions up to $S_c = 5/2$.

A fairly detailed account of how ρ^{CM} is actually calculated in the program will be given in Section 8.

5. TOTAL CROSS SECTIONS

The program performs the calculation

$$\int_{M^2_{min}}^{M^2_{max}} dM^2 \int_{t_{min}(s,M^2)}^{t_{max}} dt \ \langle n \rangle \frac{d^2\sigma}{dt dM^2} \ ,$$

by repeated Gauss-Legendre quatrature [52] where M^2_{max}, M^2_{min} and t_{max} are set by the user and $t_{min}(s,M^2)$ is calculated in the program.

The program was tested for rounding errors in this aspect of its calculation by evaluating

$$\int_{0}^{10} dM^2 \int_{g(M^2)}^{2} dt \ f(t,M^2) = 13.\dot{3} \ ,$$

where $f(t,M^2) = 1$ and $g(M^2) = M^2/50$. The result was 13.333333333331.

6. MINIMIZATION

The program is written to allow it to be used in conjunction with the minimization program MINUIT [50] . Since the data on polarizations and spin density matrix elements is usually accompanied by large error bars, the program in its present state confines itself to minimizing on the χ^2 generated by the data points for the differential cross sections. The variable parameters are passed through between the minimization program and ONCPLT using a user provided routine so that the only constraint on the type and the number of parameters is that provided by MINUIT [50] . The χ^2 is defined by

$$\chi^2 = \sum_{\substack{\text{All Data} \\ \text{Points}}} \left\{ \frac{\langle n \rangle \frac{s}{\pi} \frac{d^2\sigma}{dtdM^2}_{\text{experiment}} - \langle n \rangle \frac{s}{\pi} \frac{d^2\sigma}{dtdM^2}_{\text{theory}}}{\text{Standard Deviation of } \left[\langle n \rangle \frac{s}{\pi} \frac{d^2\sigma}{dtdM^2}_{\text{experiment}} \right]} \right\}^2 .$$

For a single data point a $\chi^2 < 1$ represents a theoretical value within the statistical error. Overall normalization errors are not taken into account in this formula.

A long write-up on MINUIT [50] should be consulted before minimization is attempted.

7. PLOTTING THE RESULTS

While the program gives a comprehensive output via line printer it is often useful to have a visual comparison of the theory with experiment in the form of graphical output.

The program contains a routine which interfaces with a plotting package APLOT [49] and this routine plots the differential cross sections, the density matrices and the effective trajectories with the data points and their error bars if desired. We can have up to 20 plots in columns of four plots each on

paper 21 inches wide. It is also possible to plot total cross sections but in this mode only one plot is allowed. A multiplicative scaling of all plots is allowed by changing one card of the program.

8. THE COMPUTER PROGRAM

a) Commentation

Each routine contains within itself sufficient comment cards to make itself intelligibile. Further, in the routine FCN there is

i) a list and a description of all the COMMON variables

ii) a description of user provided routines

iii) a description of the data cards required.

b) List of subroutines

Fig.2.3 gives a list of all the subroutines of the program and also the calling sequence. The reason for inclusion of this figure is that it allows the user to easily identify portions of the program to be deleted if a particular function is not required, e.g. total cross sections. Thus, in this example, TOTX, EMMAXX, QMULT2, FUP, FLO and FN may be deleted but BLOCK DATA must remain if Gamma functions are to be calculated.

c) Flow Chart of TCHISQ

The Schematic Flow Chart, shown in fig.2.4, is included to give an easily read account of all the options open during a call to FCN (which will normally call TCHISQ). Almost all the decisions are taken according to the variables MODE and IFLAG1 - 6 a full description of which is given in the comments in subroutine DATIN.

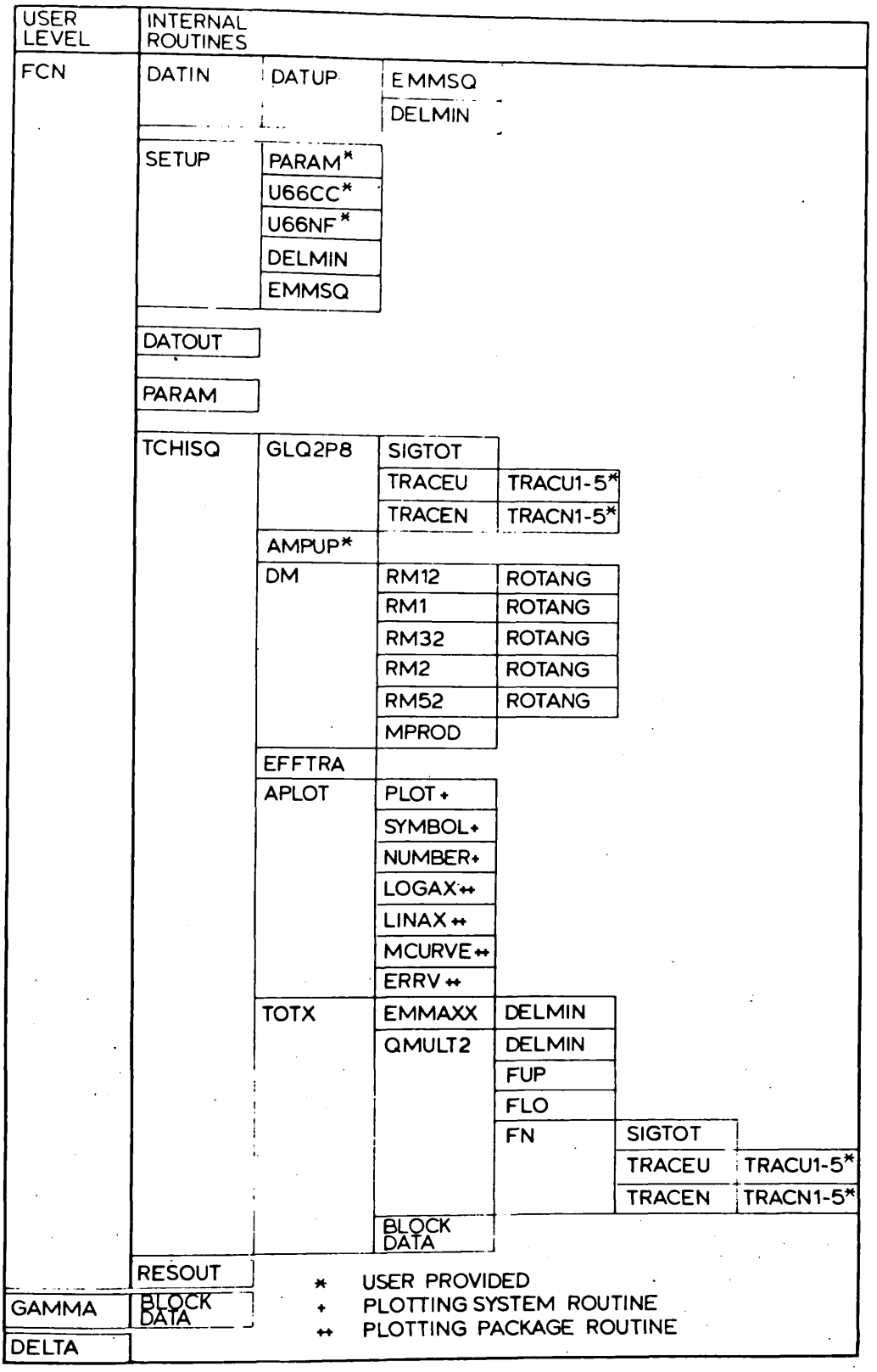

Fig.2.3. List of subroutines incorporating calling sequences

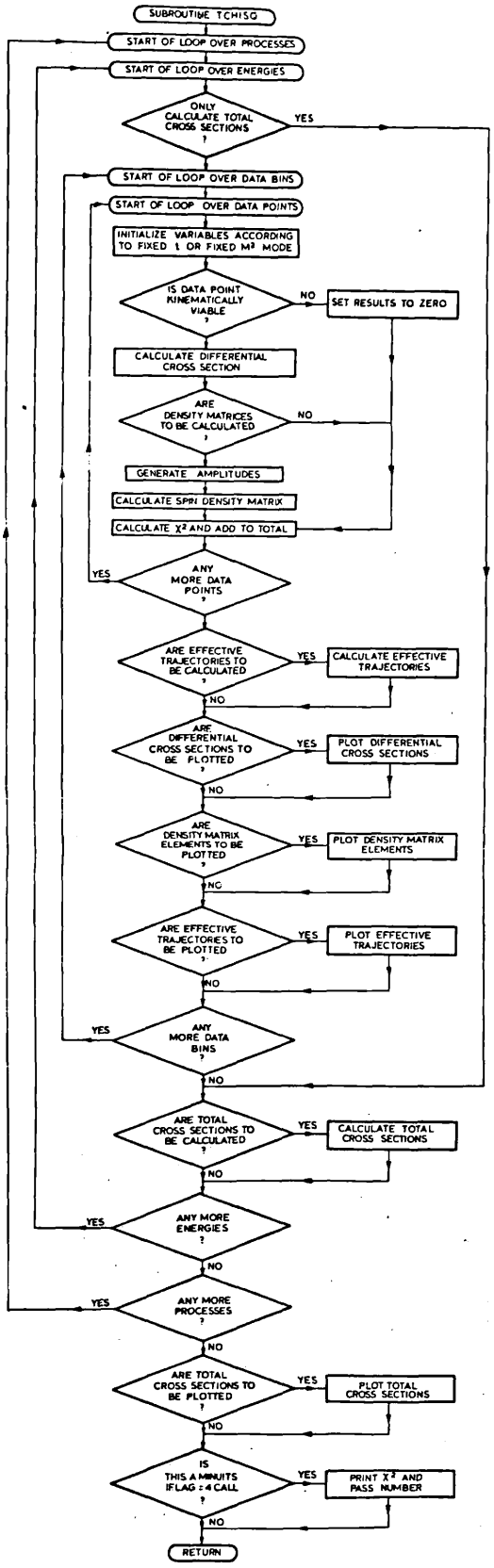

Fig.2.4. Schematic flow-chart giving the structure of subroutine TCHISQ

d) Description of the Output

Section 2 gave the kinematics in terms of the particle labels a,b and c but throughout the program the particle labels 1, 2, 3 and 4 are used. To calculate certain kinematics particle 1 is taken as the beam particle and particle 2 is the target particle. For IFLAG = 0 we make the association a = 1, b = 2 and c = 3; for IFLAG = 1 we make the association a = 2, b = 1 and c = 4. Apart from this complication the output is written so as to be self-explanatory. Any further explanation of the variables can be found either in DATIN or in the common block commentation.

e) Coded Normalization

The differential cross section is calculated as

$[ANORM(IP)/(64\pi^2k^2)]$* TRACEU (or TRACEN),

with ANORM(IP) = SPIN(IP)*(Normalization Factors), where SPIN(IP) = 1 for particle a of spin 0 and SPIN(IP) = $\frac{1}{2}$ for particle a of spin $\frac{1}{2}$ or a photon. The normalization factors will be the highest common factor of all the s-independent factors which need to be calculated for the various parts of the matrix elements. Individual differences from this value must be accounted for in the subroutines TRACU1-5 and TRACN1-5.

f) Numbers of Processes

Each call to FCN can deal with up to five processes with the type of process determining which TRACU1-5, TRACN1-5 subroutine is called and all these processes can be of differing or of the same type. Each process can have up to 5 different energies and each energy can have up to 20 different t or M^2 bins. The total limitation on the number of data points is 500 (or 100 if density matrix or effective trajectory data is read in) but this requirement could be relaxed simply by redimensioning certain arrays and changing the error statements in subroutine DATIN. This allows the parameters of a model to be determined from experimental data covering a wide range of processes and energies since the value of the χ^2 is taken cumulatively over energies and processes.

g) Note on AMPUP and DM

The quantity $\rho^{CM}_{\lambda'_c\lambda_c}$ is proportional to

$$\text{Disc}_{M^2} \langle \lambda'_c \ \lambda_a \ \lambda_b | T | \ \lambda_c \ \lambda_a \ \lambda_b \rangle \ ,$$

and it is quite feasible to perform the rotations to the Gottfried-Jackson frame using this formulation of the bilinear form. However, the program uses a factorizing technique, explained in the comment in the listing, which effectively treats

$$\text{Disc}_{M^2} \langle \lambda'_c \ \lambda_a \ \lambda_b | T | \ \lambda_c \ \lambda_a \ \lambda_b \rangle$$

$$= \sum_Y \langle \lambda' \ 0 | T_Y | \ \lambda_a \ \lambda_b \rangle \langle \lambda_c \ 0 | T_Y | \ \lambda_a \ \lambda_b \rangle^* \ ,$$

where the sum over Y allows the effects of non-interfering exchanges to be fully taken into account. The dimensioning at present is for Y = 1 to 3 and by extending this number in DM and AMPUP it would be possible to account for either more exchanges in a Regge pole framework or a regime where less factorization is possible.

h) Note on Interference Terms

In the Test Run of the program (see note (i)) we considered processes where the allowed Regge exchanges are the π, the ρ and A_2 for $K^- + p \to \Delta^{++} + X$ and the ρ and the A_2 for $K^- + p \to \bar{K}^o + X$, with absorption in the latter case. Since we have taken the ρ and the A_2 trajectories to be strongly exchange degenerate throughout there will be no interference between these two exchanges for either pure Regge poles, or, in the particular model used for the test run, absorbed Regge poles.

We also know [16] that in the regime of factorizable Regge poles, the exchange of poles with different naturality will lead to no interference, for the unpolarized cross section in the normal Regge limits ($s/M^2 \to \infty$, M^2 fixed). This property basically derives from the fact that a parity transformation on $\beta^{\lambda_1\lambda_3}$ must take into account, for the phase factor, not only the helicities and the intrinsic parities of the external particles, but also the naturality of the exchanged Reggeon i. Thus, when the sums over all external spins are performed the interferences between such exchanges cancel out. These two properties mean that in our Test Run it was not necessary to take into account any interference terms.

If, however, the condition of exchange degeneracy between the ρ and the A_2 trajectories, was removed, then all four of the diagrams of fig.2.5 would have to be considered and not just the first two, i.e., the $\rho - \rho^*$ and the $A_2 - A_2^*$ diagrams. This would be perfectly possible within the TRACEU, TRACEN framework of the program, where the appropriate TRACU1-5 function subroutines would have to be modified suitably to take these interference terms into account.

Of course, when absorption corrections take place, the absorbed exchanges can be of mixed naturality and the TRACEU and TRACEN function subroutines are merely used to hand back the necessary variables.

i) The Test Run

As a Test Run the program has been set up to calculate the two processes $K^- + p \to \bar{K}^o + X$ and $K^- + p \to \Delta^{++} + X$. The results of the Calcomp output are shown in fig.2.6. In fig.2.6 we see the invariant inelastic cross section plotted against M^2/s for fixed t and against t for fixed M^2/s for the reaction $K^- + p \to \bar{K}^o + X$. In addition the effective Regge trajectory $\alpha_{eff}(t)$ is plotted for $\bar{K}^o$ production. For the reaction $K^- + p \to \Delta^{++} + X$ we have included a plot of the decay density matrices of the Δ^{++}. Details of the

derivation of the amplitudes may be found in Moriarty and Tabor [51] and Choudhury et al. [53] for $\bar{K}^{o}$ and Δ^{++} single-particle-inclusive production, respectively.

Various other calculations of a variety of single-particle-inclusive reactions using a number of different models [35] have now been carried out using ONCPLT. In addition, the calculations of the DESY group[32,33,36], of Pumplin [40] and of Paige and Sidhu [39] are easily verified. The user is free to write his own TRACU1-5 and TRACN1-5 using whatever model he wishes.

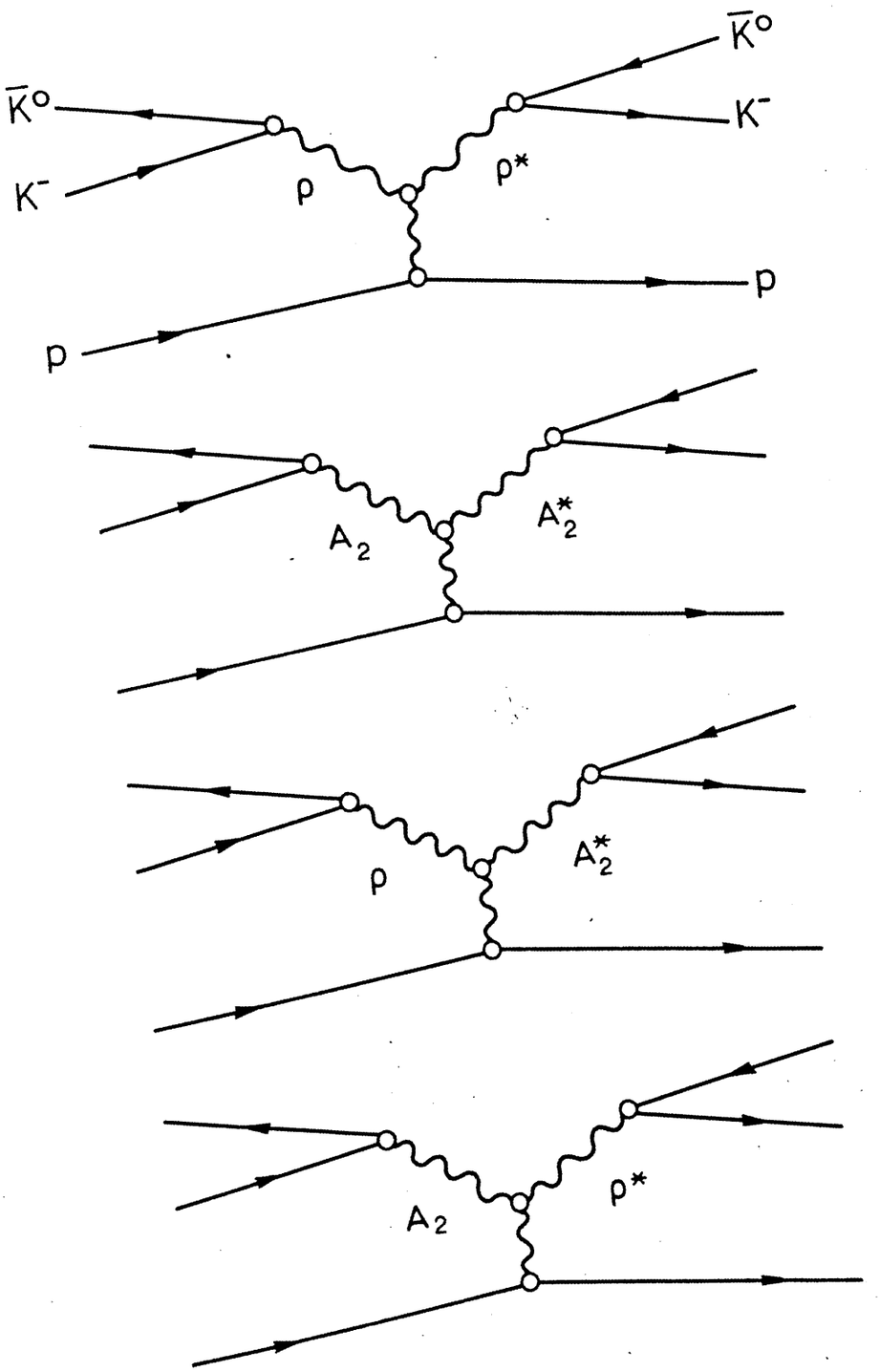

Fig.2.5. Normal and possible interference terms for the process $K^- + p - \bar{K}^o + X$

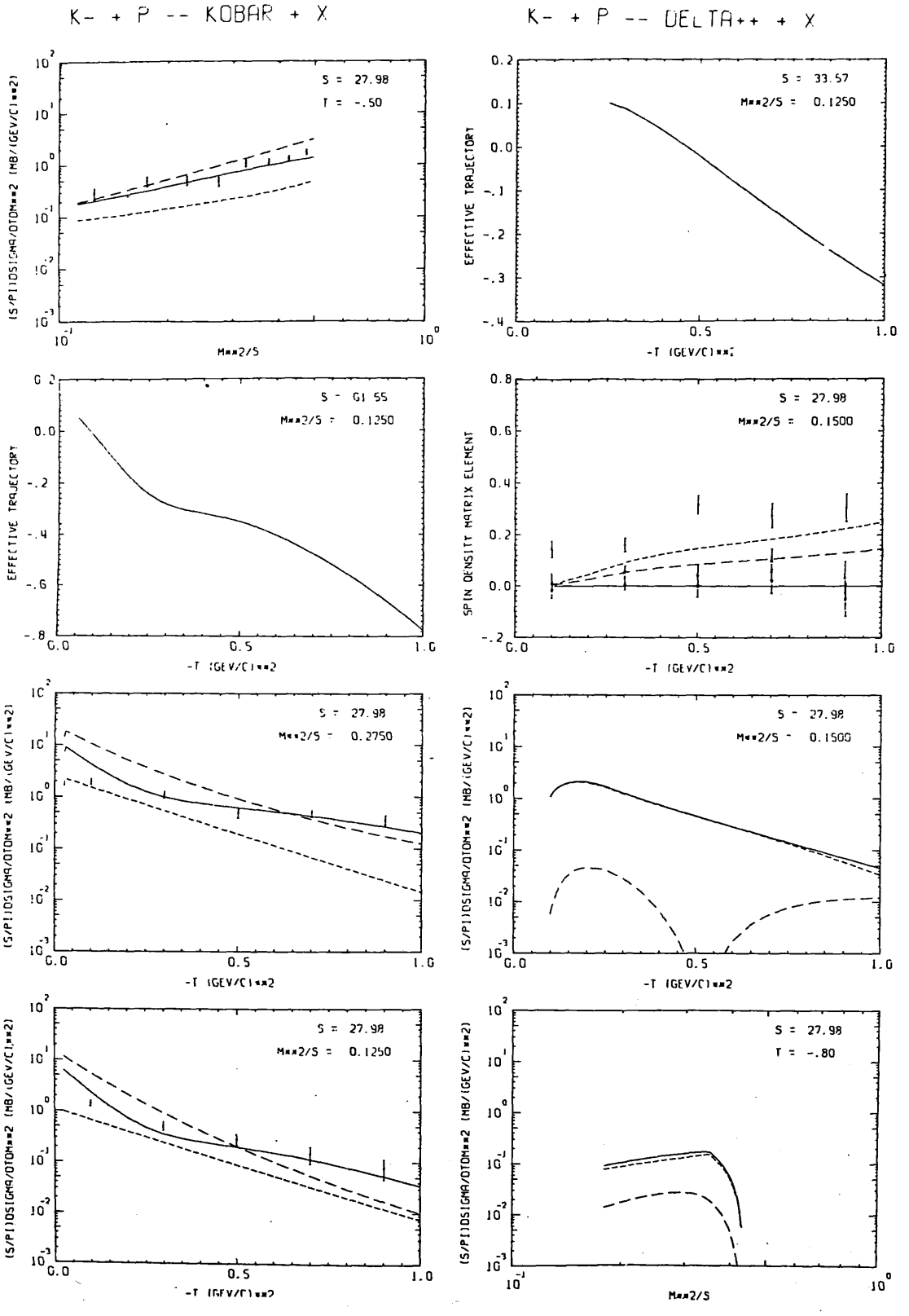

Fig.2.6. CALCOMP plotter output of the test run for the reaction $K^- + p \rightarrow \overline{K}^0 + X$ and $K^- + p \rightarrow \Delta^{++} + X$, with the results taken from the calculations of ref.35

***** RESULTS *****

K- + P -- KOBAR + X0

LABORATORY MOMENTUM = 14.300000 GEV/C

UPPER LIMIT FOR THE
MISSING MASS M**2 = 4.196349 GEV**2

LOWER LIMIT FOR THE
MISSING MASS M**2 = 2.797566 GEV**2

T	S D2S / PI DTDM2	ERROR	UNNATURAL	NATURAL	TOTAL	CHISQ
.02500	.00000032	**********	.98219471	11.75326729	6.43069017	.00000000
.05000	.00000032	**********	.86679663	9.09190957	4.59203439	.00000000
.10000	1.42144463	.19770227	.67508189	5.54691666	2.38456169	23.73202752
.15000	.00000032	**********	.52576989	3.46430076	1.29279715	.00000000
.20000	.00000032	**********	.40948215	2.20950365	.75678432	.00000000
.25000	.00000032	**********	.31891448	1.43618827	.49507530	.00000000
.30000	.53485610	.10313240	.24837823	.94978353	.36595441	2.68211695
.35000	.00000032	**********	.19344290	.63812007	.29867097	.00000000
.40000	.00000032	**********	.15065796	.43501108	.25866545	.00000000
.45000	.00000032	**********	.11733603	.30057000	.22974243	.00000000
.50000	.29402284	.07349775	.09138411	.21029293	.20486848	1.47142152
.55000	.00000032	**********	.07117214	.14885829	.18142641	.00000000
.60000	.00000032	**********	.05543057	.10652895	.15879367	.00000000
.65000	.00000032	**********	.04317065	.07702301	.13713622	.00000000
.70000	.15049691	.05509944	.03362234	.05623070	.11683533	.37322833
.75000	.00000032	**********	.02618589	.04142804	.09823873	.00000000
.80000	.00000032	**********	.02039420	.03078740	.08157315	.00000000
.85000	.00000032	**********	.01588349	.02306845	.06693260	.00000000
.90000	.08040508	.03440930	.01237045	.01742036	.05429836	.57564269
.95000	.00000032	**********	.00963440	.01325348	.04356852	.00000000
1.00000	.00000032	**********	.00750350	.01015526	.03458716	.00000000

Fig.2.7. Sample test run output

Fig.2.7. cont.

UPPER LIMIT FOR THE
MISSING MASS M**2 = 8.392699 GEV**2

LOWER LIMIT FOR THE
MISSING MASS M**2 = 6.993916 GEV**2

T	S D2S --X----- PI DTDM2	ERROR	UNNATURAL	NATURAL	TOTAL	CHISQ
.02500	.00000032	**********	1.57319292	13.57238101	6.85170468	.00000000
.03000	.00000032	**********	2.20497654	18.41488392	9.09690001	.00000000
.03500	.00000032	**********	2.14856072	17.67154796	8.60110570	.00000000
.04000	.00000032	**********	2.09358834	16.96284839	8.13474290	.00000000
.04500	.00000032	**********	2.04002247	16.28696120	7.69503511	.00000000
.05000	.00000032	**********	1.98782711	15.64216940	7.28331691	.00000000
.10000	1.96836467	.23866875	1.53396415	10.59077044	4.28529599	94.23998119
.15000	.00000032	**********	1.18372775	7.34049825	2.65145833	.00000000
.20000	.00000032	**********	.91345775	5.19563592	1.75975194	.00000000
.25000	.00000032	**********	.70489612	3.74791210	1.27133424	.00000000
.30000	1.11020122	.16186058	.54395352	2.75065861	1.00005208	.46310562
.35000	.00000032	**********	.41975752	2.05091894	.84350888	.00000000
.40000	.00000032	**********	.32391808	1.55160241	.74577681	.00000000
.45000	.00000032	**********	.24996081	1.18976118	.67684481	.00000000
.50000	.48481779	.09281916	.19288953	.92378920	.62113329	2.15682658
.55000	.00000032	**********	.14884883	.72569690	.57101866	.00000000
.60000	.00000032	**********	.11486354	.57634682	.52316960	.00000000
.65000	.00000032	**********	.08863781	.46245640	.47647985	.00000000
.70000	.50286596	.09698902	.06839995	.37467771	.43091420	.55034828
.75000	.00000032	**********	.05278283	.30634638	.38687819	.00000000
.80000	.00000032	**********	.04073141	.25265354	.34488740	.00000000
.85000	.00000032	**********	.03143159	.21008980	.30540644	.00000000
.90000	.36350989	.07715832	.02425511	.17606686	.26878212	1.50726326
.95000	.00000032	**********	.01871717	.14865667	.23522706	.00000000
1.00000	.00000032	**********	.01444365	.12640941	.20482857	.00000000

```
THE TOTAL CROSS-SECTION AT    27.975662 GEV**2 IS  1.4700532013R2 MILLE-BARNS
THE UNNATURAL PARITY CONTRIBUTION IS  6.992478680765 MILLE-BARNS
THE   NATURAL PARITY CONTRIBUTION IS  3.114232412937 MILLE-BARNS
THE TOTAL CHI-SQUARED AT THIS ENERGY   =        127.75196194
THE TOTAL CHI-SQUARED FOR THIS PROCESS =        127.75196194
*******************************************************************************

THE TOTAL CHI-SQUARED FOR THIS RUN     =        127.75196194
*******************************************************************************

THE NUMBER OF CALLS TO TCHISQ IS          1
```

Fig.2.7. cont.

CHAPTER III

Corrections to A Mueller-Regge Model Of The Reactions $0^-\frac{1}{2}^+ \rightarrow 0^- X$ Proceeding Via Charge Exchange

INTRODUCTION

In this chapter we introduce a fairly simple Regge-pole model in the "s/M^2 large" region of single particle inclusive reactions which obviates the need to introduce free parameters of any form. We then make some rather stringent assumptions which allow us to calculate, in an extremely simple manner, certain absorption type corrections to our original pole-only distribution.

To illustrate our calculations we choose certain of the reactions $0^- \tfrac{1}{2}^+ \to 0^- X$ proceeding via charge exchange, namely $\pi^- p \to \pi^0 X$, $\pi^- p \to \eta X$, $K^+ p \to K^0 X$ and $K^- p \to \bar{K}^0 X$.

We choose these reactions in particular because in the case of exclusive reactions it is reasonably clear that while the Regge-pole picture provides an almost surprisingly good explanation of high energy scattering data, there are definite reasons, both theoretical and experimental (in terms of polarizations etc.) why some kind of cut correction must be included. Investigations of the precise form of correction required are best done in the simplest possible regime, and with as few free parameters as are absolutely necessary. The exclusive reactions $\pi^- p \to \pi^0 n$ and $\pi^- p \to \eta n$ have been much used in determining both the parameters for the ρ/A_2 pole and also the sort of absorption corrections that are necessary, as well as the reactions [54] $K^- p \to \bar{K}^0 n$ and $K^+ n \to K^0 p$ which are, of course, "line reversed". These reactions have been and will continue to be so useful precisely because they are so simple in the Regge-pole picture so that any humps and dips that one pole generates cannot be masked by the contributions of others.

The reaction $\pi^- p \to \pi^0 n$ is, however, limited in its usefulness as far as Regge-cut or Absorption models are concerned, since at small momentum transfers it is dominated by a helicity flip amplitude which does not seem to require significant alteration from the simple Regge-pole with Wrong Signature Nonsense Zeros [55]. The inclusive reaction $\pi^- p \to \pi^0 X$ is not expected to be dominated by flip amplitudes; we assume dominance by the helicity non flip amplitude for the main body of the calculation. Barnes et al. [56] are

carrying out the inclusive experiment $\pi^- p \to \pi^0(\eta)X$ by detection of two photons, so there will be high energy data available for two of the four reactions in the near future.

We calculate the four reactions using strong exchange dege neracy for the ρ and A_2 Regge trajectories, and use SU(3) symmetry to relate the different particle couplings, since we feel that the introduction of any free parameters will obscure the form of the correction required, and in any case it can be argued that the measured deviations from exchange degeneracy should be precisely due to the cut correction required. We calculate all four inclusive reactions for completeness since the shape of the final absorbed curves depends not just on the size and rate of fall off of the cut corrections, of which we know a certain amount in advance, but very strongly on the relative phases of pole and cut, so that while the same poles contribute in a given reaction the final absorbed curves can look completely different.

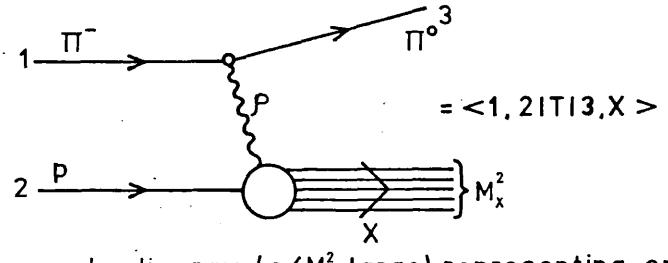

Figure 3·1a). A Regge-pole diagram (s/M_x^2 large) representing one component of a single particle inclusive distribution, with X embodying all discrete and continuous observables contained in the missing mass state.

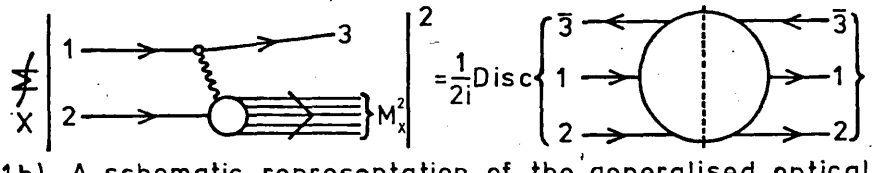

Figure 3·1b). A schematic representation of the generalised optical theorem.

FORMALISM

Our task in this section is first to produce a Regge-pole type expression for the process represented diagrammatically in Figs. 3.1(a) and (b) and then derive a prescription for performing absorptive type corrections to it.

Before we begin this it is reasonable here to exhibit the normalisation appropriate to single particle inclusive distributions.

We have, formally, for the quasi-total cross sections (we can only take events in which at least one particle of the type we desire is produced) that

$$< n > \sigma_q = \rho_f \, d\Omega_f \sum_{f.s} \overline{\Sigma}_{i.s} \{ \int_x |<1,2|T|3,x>|^2 \} \frac{1}{F} \qquad 3.1$$

Where $\rho_f d\Omega_f$ represents the final phase space, $\sum_{f.s}$ in the sum over final spin, $\overline{\Sigma}_{i.s.}$ is the average over the initial spins, F is an initial state flux factor and the symbol $\int_x$ represents all the integrations over the final phase space not accounted for in $\rho_f d\Omega_f$.

We can here make the usual definition of the appropriate relativistic invariants

$$s = (p_1 + p_2)^2, \; t = (p_1 - q_3)^2, \; M_x^2 = (p_1 + p_2 - q_3)^2 \qquad 3.2$$

and in a less formal manner we have

$$< n > \sigma_q = \int dM_x^2 \int \frac{d^3q_3}{2E_c} \frac{d^3q_{M_x}}{2E_{M_x}} \delta^4(q_3 + q_{M_x} - p_1 - p_2) \sum \overline{\Sigma} |M|^2 . \frac{1}{F} \qquad 3.3$$

This form can be converted to the differential form by inserting the appropriate δ-functions i.e.

$$< n > \frac{\partial^2 \sigma}{\partial t \partial M_x^2} = \int dM_x^2 \int \frac{d^3q_3}{2E_c} \frac{d^3q_{M_x}}{2E_{M_x}} \delta^4 (q_3 + q_{M_x} - p_1 - p_2) \delta(t-(p_1 - q_3)^2) \delta(M_x^2 - (p_1 + p_2 - q_3)^2) \sum \overline{\Sigma} |M|^2 . \frac{1}{F} \qquad 3.4$$

These integrations can be trivially performed to yield

$$< n > \frac{\partial^2 \sigma}{\partial t \partial M_x^2} = \frac{1}{64\pi s p^2} \sum \overline{\Sigma} |M|^2$$

where p in the modulus of the initial 3-momentum in the Centre of Mass Frame of particles 1 and 2.

It is conventional to include the term $< n >$ with the σ since the product is the quality measured experimentally, and a more usual form would then be

$$\frac{s}{\pi} \frac{d^2\sigma_2}{dt dM_x^2}(s, t, M_x^2) = \frac{1}{64\pi^2 p^2} \Sigma \overline{\Sigma} |M|^2. \qquad 3.5$$

This calculation can be found in greater detail in Appendix 3A.

We now return to the expression of Fig.3.1a), which can be written formally as $\langle 1,2|T|3,X\rangle$. From now on in the derivation we will specialise to the case where particle 1 is a π^-, particle 2 a proton and particle 3 a π^o. When the final expression is obtained the changes necessary to accommodate the other three reactions we will deal with will be fully outlined.

For the π^- particle dissociating into a π^o and an (off shell) elementary ρ particle we could envisage a matrix element of the form

$$J^\mu G_{\mu\nu} \Gamma_x^\nu$$

where, if we define

$$P^\mu = (p_1 + q_3)^\mu$$

$$Q^\mu + (p_1 - q_3)^\mu$$

we will have

$$G_{\mu\nu} = \frac{-g_{\mu\nu} + \frac{Q_\mu Q_\nu}{m_\rho^2}}{(Q^2 - m_\rho^2)}$$

with Γ_x^ν restricted to be a four vector only.

A suitable current for the top vertex would then be

$$J^\mu = \frac{g_{\rho\pi\pi}}{2} \left((\bar{\phi}_5)_3 (\phi_5)_1 \right)_F P^\mu - 3.6$$

which, since

$$P.Q = m_1^2 - m_3^2 \simeq 0$$

maintains the required gauge invariance.

$g_{\rho\pi\pi}$ would be given by the physical coupling constant defined by [57]

$$\frac{g^2_{\rho\pi\pi}}{4\pi} = 2.09 \ ,$$

and the expression $((\bar{\phi}_5)_2 \ (\phi_5)_1)_F$ represents an SU(3) coefficient which will assist in making the switch between reaction later on. The coefficients required for all four reactions are given in Table 3.1.

We can now expand the quantity $\int_x |< 1,2 \ |T| \ 3,x >|^2$

$$= J^\mu \ G_{\mu\nu} \ \{ \int_x \Gamma^\nu_x \ \Gamma^{\nu'\dagger}_x \} \ G_{\mu'\nu'} \ J^{\mu'} \qquad 3.7 \ .$$

The most general symmetric second order tensor capable of being constructed from the vectors available (i.e. $(p_2)^\mu$ and Q^μ) is

$$\lambda_1 \ g^{\nu\nu'} + \lambda_2 (p_2)^\nu \ (p_2)^{\nu'} +$$

$$\lambda_3 \ Q^\nu Q^{\nu'} + \lambda_4 \ ((p_2)^\nu Q^{\nu'} + Q^\nu (p_2)^{\nu'}) \qquad 3.8$$

and this must be precisely the form of the quantity $\{ \int_x \Gamma^\nu_x \ \Gamma^{\nu'\dagger}_x \}$, here the λs can at most be functions of t and M^2_x .

When we consider the form of the currents J and propagators G we arrive at the expression

$$\frac{g^2_{\rho\pi\pi}}{4} \ ((\bar{\phi}_5)_3 \ (\phi_5)_1)^2_F \quad \frac{1}{(t - m^2_\rho)^2} \ .$$

$$\{P^2 \ \lambda_1(t, M^2_x) + (P.p_2)^2 \ \lambda_2(t, M^2_x) \} \qquad 3.9$$

and since P^2 in $O(1)$ and $P.p_2$ in $O(s)$ then in the limit we will wish to take, that is, t small and fixed, $s \to \infty$, $s/M^2_x \to \infty$, the

contribution from $P^2\lambda_1(t, M_x^2)$ is dominated by $(P.p_2)^2\ \lambda_2(t,M_x^2)$ and consequently we will neglect the contribution from λ_1 to the cross-section. See Appendix 3.B for the precise reasoning for this. We can gain an insight into the normalisation and functional dependencies of $\lambda_2(t, M_x^2)$ by considering the standard optical theorem for ρp elastic scattering (for an off-shell ρ). The form we will finally adopt is

$$\lambda_2(t, M_x^2) = \frac{8m_\rho^2\ \sigma_{Tot}^{\rho p}\ (t, M_x^2)}{\Delta(M_x^2, m_\rho^2, m_p^2)} \qquad 3.10$$

where Δ has the standard form $\Delta(x,y,z) = [x^2 + y^2 + z^2 - 2xy - 2xz - 2yz]^{\frac{1}{2}}$. This form is not an exact equality. Various approximations have been made to acquire a form which can be utilised in a practical calculation. Appendix 3.B contains the full motivation for this choice.

To make contact with a process for which there is an experimentally measured total cross-section we consider the Vector Meson Dominance model [58] (See fig. 3.2) and picking out the ρ term from the sum over the available vector mesons we can say

$$\frac{\sigma_{tot}^{\rho p}}{(t - m_\rho^2)^2} = \left[98.6 + \frac{64.9}{(M_x^2)^{\frac{1}{2}}}\right] . (0.27) . \frac{.65}{(1 - {}^{t}/_{m_\rho^2})^2} .$$

This has given us a non-Reggeized form of the matrix element we require. In the kinematic limit stated before i.e. t small, $s \to \infty$, $s/M_x^2 \to \infty$ we can perform the required Reggeization via the replacement [57]

$$\frac{1}{t - m_\rho^2} \to \Gamma(1 - \alpha_\rho(t)).\ \alpha'_\rho\ \frac{(1 + \tau_\rho e^{-i\pi\alpha_\rho(t)})}{2}\ \left(\frac{s}{M_x^2}\right)^{(\alpha_\rho(t) - 1)} \qquad 3.11$$

where $\alpha_\rho(t) = 0.47 + 0.905t$. Combination of all the exhibited formulae yields for the reaction $\pi^- p \to \pi^o x$

$$\frac{s}{\pi}\frac{d^2\sigma}{dtdM_x^2} = \frac{1}{64\pi^2 p^2}\left\{\frac{g_\rho^2\pi\pi}{4}\left((\phi_5)_3\,(\phi_5)_1\right)_F^2 (P.p_2)^2 \cdot \right.$$

$$\frac{8m_\rho^2\,{}^{\rho p}_{Tot}}{\Delta(M_x^2, m_\rho^2, m_\rho^2)}\left(\Gamma(1-\alpha_\rho(t))\,\alpha_\rho'\right)^2 \left(\frac{s}{M_x^2}\right)^{2\alpha_\rho(t)-2} \frac{(1+\tau_\rho e^{-i\pi\alpha_\rho(t)})}{2} \cdot$$

$$\left.\frac{(1+\tau_\rho e^{-i\pi\alpha_\rho(t)})}{2}^{*}\right\} \qquad 3.12$$

On closer examination this form, is the limit we have described, corresponds precisely to the accepted inclusive Regge formula [16] illustrated in Fig. 3.3a i.e.

$$\frac{d^2\sigma}{dtd\,(M_x{}^2/s)} = \beta_i(t)\;\xi_i(t)\,\beta_j(t)\,\xi_j(t) \cdot$$

$$\left(\frac{s}{M_x^2}\right)^{\alpha_i(t)+\alpha_j(t)} \mathrm{Disc}_{M_x^2}\, A_{i2\to j2}(M_x^2, t) \qquad 3.13$$

In fact the form we have produced and will use henceforth is equivalent to the Triple Regge formula illustrated in Fig. 3.3b) because we have introduced a "high energy" (high M_x^2) form for the cross-section $\sigma_{Tot}^{\rho p}$, and thus the true kinematic limit we are using is $s/M_x^2 \to \infty$, $M_x^2 \to \infty$, t fixed. It would be possible, though, by using a lower energy form for $\sigma_{Tot}^{\rho p}$ to lift the condition of large M_x^2. This has been done by another author for a different reaction with some success [59] .

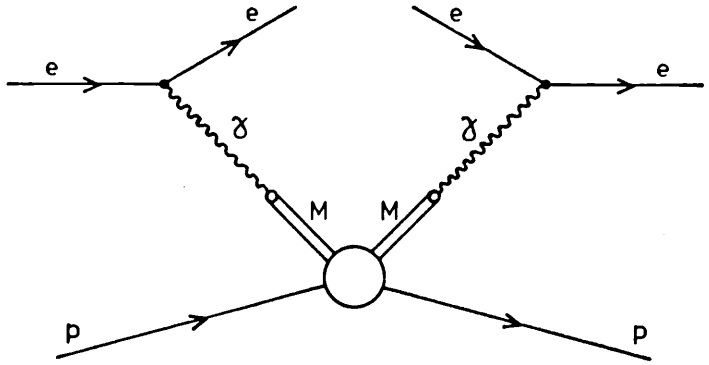

Figure 3·2.A diagram for the VMD model where the γ-p total cross-section is made up of a sum of terms such as the above where M stands for one of the 1^- mesons which can couple directly to the photon.

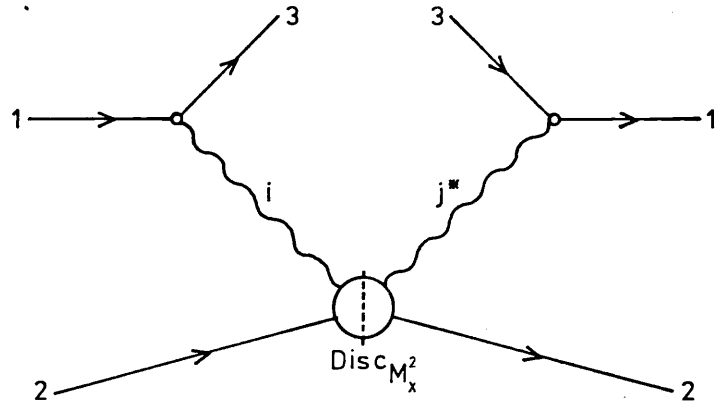

Figure 3·3a).A Regge diagram corresponding to the limit t small, s/M_x^2 large, for the exchange of Reggeons i and j.

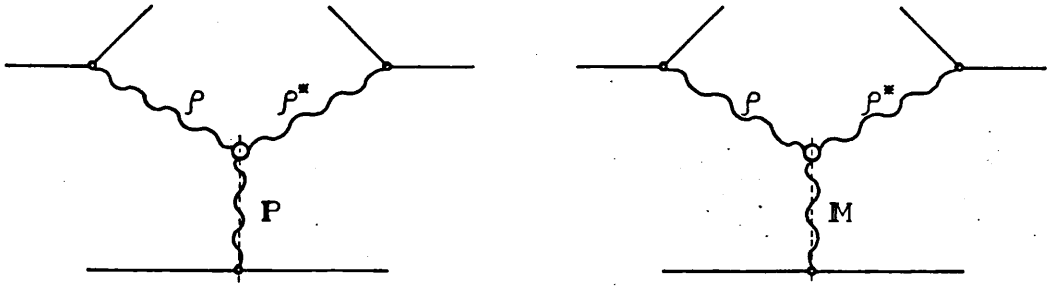

Figure 3·3b).The two triple-Reggeon discontinuities which contribute to the form of equation 3·13.

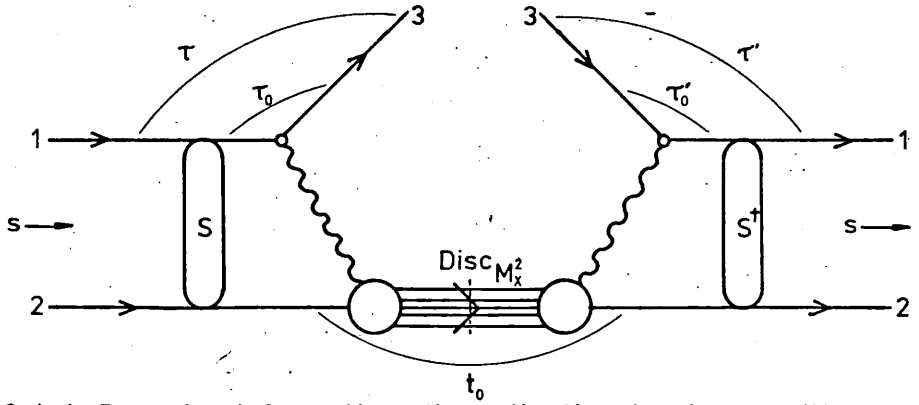

Figure 3·4.A Reggeized 3-particle discontinuity showing additional elastic scattering in the 1-2 channels.

Since we wish to incorporate the concept of strong exchange degeneracy and S U (3) symmetry in order to avoid introducing any free parameters, having gained the expression for the reaction $\pi^- p \to \pi^o X$ we can make the transition to $\pi^- p \to \eta X$ by changing the signature of the pole from τ_ρ to τ_{A_2}, and alter only the Clebsch Gordan coefficient $((\bar{\phi}_5)_3 (\phi_5)_1)_F$ to $((\bar{\phi}_5)_3 (\phi_5)_1)_D$, while leaving the coupling constant alone. Similarly when going to $K^- p \to \bar{K}^o X$ and $K^+ p \to K^o X$ we can simply add both the ρ and A_2 contributions with their appropriate signature factors and SU(3) factors. The set of SU(3) coeficients is presented in table 3.1.

We are now at the stage where we have a relatively conventional formula for the single particle inclusive matrix element which involves no free parameters.

The next stage is the implement a rather simplistic scheme of absorption type corrections. To do this we consider the full expression associated with the diagrammatic representation of fig 3.1b), namely [36]

$$
\begin{aligned}
&H^{\lambda_{\bar{1}}\ \lambda_{\bar{2}}\ \lambda_3}_{\lambda_1\ \lambda_2\ \lambda_3}\ (p_{\bar{1}}\ p_{\bar{2}}\ p_3\ ;\ p_1\ p_2\ p_{\bar{3}}) \\
&= \sum_{\chi(n,\xi)} \int \prod_{i=1}^{n} \frac{d^3k_i}{2E_i}\ \delta^4\Big(\sum_{i=1}^{n} k_i + p_3 - p_1 - p_2\Big). \\
&\quad \langle p_{\bar{3}}\ \lambda_{\bar{3}},\ k_1 \cdots k_n | T | p_1\ \lambda_1\ p_2\ \lambda_2 \rangle \\
&\quad \langle p_3\ \lambda_3,\ k_1 \cdots k_n | T | p_{\bar{1}}\ \lambda_{\bar{1}}\ p_{\bar{2}}\ \lambda_{\bar{2}} \rangle^*
\end{aligned}
\qquad 3.14
$$

Our main interest lies in the helicity behaviour of the intermediate missing mass state and to exhibit this more clearly we write

$$\sum_{\chi(n,\xi)} \int \prod_{i=1}^{n} \frac{d^3k_i}{2\varepsilon_i} \delta^4 \left(\sum_{i=1}^{n} k_i + p_3 - p_1 - p_2 \right)$$

$$\cdot \; |p_3\lambda_3; k_1 \ldots k_n\rangle\langle p_{\bar{3}}\lambda_{\bar{3}}; k_1 \ldots k_n|$$

$$= \sum_{s_x\lambda_x\eta_x} |p_3\lambda_3; p_x s_x \lambda_x \eta_x\rangle\langle p_{\bar{3}}\lambda_{\bar{3}}; p_x s_x \lambda_x \eta_x| \qquad 3.15$$

where s_x and λ_x represent the spin and helicity of the intermediate state and η_x represents all degeneracy labels not otherwise covered. This allows us to write

$$H^{\lambda_{\bar{1}}\lambda_{\bar{2}}\lambda_3}_{\lambda_1\lambda_2\lambda_{\bar{3}}} (p_{\bar{1}}p_{\bar{2}}p_3; p_1p_2p_{\bar{3}})$$

$$= \sum_{s_x\lambda_x\eta_x} \langle p_{\bar{1}}\lambda_{\bar{1}} p_{\bar{2}}\lambda_{\bar{2}} |T| p_3\lambda_3, p_x s_x \lambda_x \eta_x\rangle$$

$$\langle p_{\bar{3}}\lambda_{\bar{3}}, p_x s_x \lambda_x \eta_x |T| p_1\lambda_1 p_2\lambda_2\rangle \qquad 3.16$$

To perform a partial wave analysis on these amplitudes we choose the frame of reference where the intermediate state travels along the positive z-axis and to acquire independent expansions we only enforce

$$p_1 + p_2 - p_{\bar{3}} = p_{\bar{1}} + p_{\bar{2}} - p_3 \; -$$

and not

$$p_1 = p_{\bar{1}},\; p_2 = p_{\bar{2}},\; p_{\bar{3}} = p_2$$

The mechanics of this analysis can be seen in Appendix 3.C and we give the result after transition to an impact parameter formulation as

$$H^{\bar{\lambda}_1\bar{\lambda}_2\lambda_3}_{\lambda_1\lambda_2\bar{\lambda}_3}(p_{\bar{1}}p_{\bar{2}}p_3;p_1p_2p_{\bar{3}})$$

$$= \sum_{\lambda_x} e^{-i\phi(\bar{\mu}_2-\bar{\mu}_1)} e^{-i\phi'(\mu_1-\mu_2)} \cdot \frac{1}{4\pi^2}$$

$$\int_{b_o}^{\infty} bdb\, J_{\bar{\mu}_1-\bar{\mu}_2}(b\tau) \int_{b'_o}^{\infty} b'db' J_{\mu_1-\mu_2}(b'\tau')$$

$$h_{\lambda_x}(b,b',s,M_x^2) \qquad 3.17$$

where

$$\bar{\mu}_1 = \lambda_x - \lambda_3 \qquad \mu_1 = \lambda_x - \lambda_{\bar{3}}$$

$$\mu_2 = \lambda_2 - \lambda_1 \qquad \bar{\mu}_2 = \lambda_{\bar{2}} - \lambda_{\bar{1}}$$

$$kb_o = \max\{|\bar{\mu}_1|,|\bar{\mu}_2|\}$$

$$kb'_o = \max\{|\mu_1|,|\mu_2|\}$$

where k is the three momentum of a particle in the initial C M state.

For high energies and small helicity flips we can be confident in setting $b_o, b'_o = 0$. Otherwise account must be taken more fully of the lower limit to the b-space integration.

We must now consider the use to which equation 3.17 is to be put. Appendix 3C makes it clear that the approximate form of 3.17 can only hold for small λ_x and the further approximations that b_o and $b'_o = 0$, which make the manipulation of 3.17 relatively simple, are also only viable in a similar region. Since the formula is to be used for the reactions $0^-\tfrac{1}{2}^+ \to 0^-X$, $\lambda_{\bar{1}},\lambda_1,\lambda_{\bar{2}},\lambda_3 = 0$. The small angle behaviour of 3.17 can be seen to be

$$H^{\lambda_{\bar{2}}}_{\lambda_2} \sim \sum_{\lambda_x} \tau^{(|\bar{\mu}_1-\bar{\mu}_2|)} \tau'^{(|\mu_1-\mu_2|)} B_{\lambda_x}$$

So for the case when $\tau = \tau' = 0$ the sum in λ_x collapses down to one term, namely that for which $\lambda_2 = \lambda_x = \lambda_{\bar{2}}$ when $\bar{\mu}_1 - \bar{\mu}_2 = 0 = \mu_1 - \mu_2$, since no compensatory flip can come from the 1-3 particle vertex.

The form we will use for $H^{\lambda_{\bar{2}}}_{\lambda_2}$ posses a strong forward peak (see equation 3.12) at least for small M_x^2/s. This indicates that for the forward reaction ($\tau = \tau'$) we do not expect helicity flip into the missing mass state to dominate since if this were so, a forward turnover would be

The lack of any sign of such a turnover and the small angle character of all approximations to this point lead us to make the supposition that helicity flip into the missing mass state is negligable.

In this case equation 3.17 simplifies to

$$H_{\lambda_2}(\tau,\tau',s,M_x^2) = \int_0^\infty bdb\, J_o(b\tau) \int_0^\infty b'db'\, J_o(b'\tau') \; h(b, b', s, M_x^2) \qquad 3.18$$

where we have performed an integration over ϕ and ϕ' which removes their dependence from the L.H.S. and the factor of $\frac{1}{4\pi^2}$ on the R.H.S. Equation 3.18 is the basis of the numerical calculations we will make.

Inverting this equation we find

$$h(b,b',s,M_x^2) = \int_0^\infty d\tau\tau\, J_o(b\tau) \int_0^\infty d\tau'\tau'\, J_o(b'\tau') \; H_{\lambda_2}(\tau,\tau', s, M_2^2) \qquad 3.19$$

We introduce absorption type corrections by taking some account of elastic scattering in the 1-2 and $\bar{1}$-$\bar{2}$ channels as illustrated in Fig. 3.4. In this scheme $h(b, b', s, M_x^2)$ is modified to the form

$$S(b)h(b,b',s,M_x^2)\, S^*(b') \qquad 3.20$$

which is supposed to be the b-space decomposition of the absorbed discontinuity so

$$H^{abs}_{\lambda_2}(\tau, \tau', s, M_x^2) = \int_0^\infty db\, b\, J_o(b\tau) \int_0^\infty db' b' J_o(b'\tau')$$

$$S(b)S(b') \int_0^\infty d\tau_o \tau_o J_o(b\tau_o) \int_0^\infty d\tau'_o \tau'_o J_o(b'\tau'_o)$$

$$H_{\lambda_2}(\tau_o, \tau'_o, s, M_x^2). \qquad 3.21$$

which gives the absorbed discontinuity in terms of the pure Regge discontinuity. The parametrization used for the elastic scattering matrices will be Gaussian i.e. [60]

$$S(b) = 1 - Ce^{-\lambda b^2} \qquad 3.22$$

where $\lambda = 1/R^2$ with R the radius of the interaction and C is the opacity. Both these quantities can be calculated from experimental elastic scattering data, and the values used are given in table 3.2.

It is worth noting here that we use the full value of C calculated from the total cross section. Unitarity dictates that this value be less than, or equal to one, since a value larger than this would mean that the S-wave scattering would account for a negative particle flux. In a conventional two body inelastic absorption calculation illustrated by Fig. 3.5 the analogue of 3.20 would be

$$S_i^{\frac{1}{2}}(b)h(b,S)\, S_f^{\frac{1}{2}}(b).$$

which would then normally be approximated to

$$(1 - (\frac{C_i + C_f}{2})\, e^{-\lambda b^2})h(b,S).$$

using the power series expansion for the square root and neglecting higher order terms. Since $C_i, C_f \leq 1$ this form does not violate unitarity In our case, however, we have two separate partial wave expansions with independent impact parameters, and so we can use the full value of C without overabsorbing the S-wave.

Returning now to equation 3.21 and incorparating the form for the S matrices 3.22, we can perform immediately the two b-space integrals using the formula [61]

$$\int_0^\infty dbb\, J_n(b\tau)\, J_n(b\tau_o)\, e^{-\lambda b^2}$$

$$= \frac{1}{2\lambda}\, e^{-\frac{1}{4\lambda}(\tau^2 + \tau_o^2)}\, I_n\left(\frac{\tau\tau_o}{2\lambda}\right) \qquad 3.23$$

and equation 3.21 becomes

$$H^{abs}_{\lambda_2}(\tau,\tau', s, M_x^2) = \int_0^\infty d\tau_o \tau_o \int_0^\infty d\tau_o' \tau_o'\, H(\tau_o,\tau_o', s, M_x^2)$$

$$\left\{ \frac{1}{\tau_o}\, \delta(\tau-\tau_o) - \frac{C}{2\lambda}\, e^{-\frac{(\tau^2+\tau_o^2)}{4\lambda}}\, I_o\left(\frac{\tau\tau_o}{2\lambda}\right) \right\}$$

$$\left\{ \frac{1}{\tau_o'}\, \delta(\tau'-\tau_o') - \frac{C}{2\lambda}\, e^{-\frac{(\tau'^2+\tau_o'^2)}{4\lambda}}\, I_o\left(\frac{\tau'\tau_o'}{2\lambda}\right) \right\} \qquad 3.24$$

In order to evaluate the expression in equation 3.24 we must insert the form of equation 3.12 for $H(\tau_o,\tau_o', s, M_x^2)$. Before we can do this there are slight problems. 3.12 includes a factor $\Gamma(1-\alpha_p(t))$ which will prevent the integral from converging. This factor arises from the ghost eliminating mechanism in the Reggeizing process and is therefore valid only at small t. We make the approximation

$$\Gamma(1 - \alpha_p(t)) \sim A_1\, e^{A_2 t}$$

with

$$A_1 = 0.874886$$

$$A_2 = 0.611824$$

where A_1 and A_2 are found using a least squares technique over the range $0 < |t| < 1$ $(GeV/c)^2$.

We must also extend the form of 3.12 from the forward direction. This is easy for the τ_o and τ_o' dependence of the Regge legs (see Fig. 3.4), but for $\tau_o \neq \tau_o'$, t_o will be non-zero and we will expect

that some dependence upon t_o should manifest itself. The form of this dependence is not clear and the elastic scattering effects we have introduced will be peaked about the value $\tau_o = \tau$, $\tau_o' = \tau'$. The assumption was made therefore to disregard any t_o dependence. This assumption is the most drastic, and least easy to justify of those made to this point, since it is only fully realised if the Reggeon-particle discontinuity is isotropic. We shall see later that we must pay a certain price for accepting this simplification.

With these approximation used and with the integral [61]

$$\int_0^\infty dx\, x^n\, e^{-ax^2}\, I_\mu(kx) = \frac{k^\mu \Gamma(\frac{1}{2}\mu + \frac{1}{2}n + \frac{1}{2})}{2^{\mu+1} a^{\frac{1}{2}(\mu+n+1)} \Gamma(\mu+1)}$$

$$ {}_1F_1\left(\tfrac{1}{2}(\mu+n+1), \mu+1; k^2/4a\right)$$

and taking account of the special cases

$${}_1F_1\left(1, 1; \frac{k^2}{4a}\right) = e^{k^2/4a}$$

$${}_1F_1\left(2, 1; \frac{k^2}{4a}\right) = \left(\frac{k^2}{4a} + 1\right) e^{k^2/4a}$$

where ${}_1F_1$, is a degenerate hypergeometric function, we can perform all the integrals necessary in 3.24 analytically.

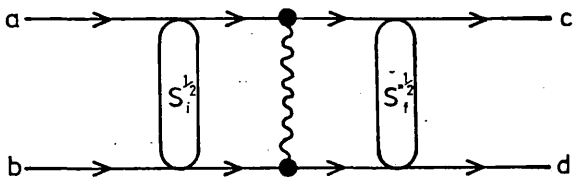

Figure 3.5.A Reggeized 2-particle amplitude showing additional elastic scattering in the initial and final channels.

RESULTS

In figures 3.7 to 3.8 we present the results of applying the preceding scheme for absorption corrections to the four reactions

$$\pi^- + p \rightarrow \pi + X^o$$
$$\pi^- + p \rightarrow n + X^o$$
$$K^+ + p \rightarrow K^o + X^{++}$$
$$K^- + p \rightarrow \bar{K}^o + X^o$$

at $s = 100\ GeV/c^2$ for both t and M_x^2/s distributionsas given on the figures. In all cases we have made allowances for the edge of phase space which is given for the different mass configurationsin figure 3.6. In the case of the η we have made no allowance for the branching ratio into $\gamma\gamma$ which would possibly be the experimental method for detecting inclusive ηs since this is also the mode for π^o detection as π^os decay almost completely in two photons.

Figures 3.9 to 3.11 give results for the reaction $K^- + p \rightarrow K^{-o} + X^o$ at an energy of $p_{lab} = 14.3\ GeV/c$ for which experimental data exists [62].

Turning to a detailed consideration of the figures, 3.6 shows that the $|tmin|$ effect leading to spurious forward turnovers should be negligible over the whole region of interest for the $\pi^- \rightarrow \pi^o$ reaction, while it should lead to very noticeable effects for $\pi^- \rightarrow \eta$. $K^+ \rightarrow K^o$ and $K^- \rightarrow K^{-o}$ present middle cases where the effect becomes noticeable only after about $M_x^2/s = 0.2$, as seen in figure 3.7b where the M_x^2/s fixed plot starts at $|t| = |tmin|$. These inclusive phase space boundaries are not strictly simply a function of M_x^2/s, and $tmin \rightarrow 0$ as $s \rightarrow \infty$ for all values of M_x^2/s, however the approach to the limit is exceedingly slow [63] and the presented figure, though valid at $s = 100\ GeV/c$ should be fairly accurate at attainable energies above this, though modification would occur at energies substantially lower.

Figure 3.7a) shows the fixed M_x^2/s plots for $\pi^- p \rightarrow \pi^o X$ and $\pi^- p \rightarrow \eta X$ in which the allowed Regge exchanges are ρ and A_2 respectively. For the

π^o plots the naturality dip which occurs for the pole only graph (represented by long dashes) at $|t| = 0.51$ GeV/c^2 is moved in to about $|t| = 0.4$ although this varies slightly with M_x^2/s. It is substantially filled in, but by no means obliterated in disagreement with the calculation of Pumplin [40] who does not introduce a naturality dip in his pole only term and acquired no dips via absorption. An experi ment by Burleson et al. [64] at the energy of $p_{lab} = 5$ GeV/c present plots for fixed M_x^2. This energy is much too low for our triple-Regge type input model but some points of note are that a pronounced dip at $t = 0.5$ GeV/c occurs for $M_x^2 < 2$ GeV/c^2. This bin is presumably dominated by the reactions $\pi^- p \to \pi^o n$ and $\pi^- p \to \pi^o \Delta^o$. For the $2 < M_x^2 < 4$ bin the dip is still noticeable, but considerably reduced. For the final bin, $4 < M_x^2 < 6$, any dip structure, if present, is obscured by the $|t \text{ min}|$ effect. The indication for larger M_x^2 that can be deduced from this experiment are that the dip at $t = -0.5$ GeV/c^2 probably does not persist.

The η plots show no great difference between pole only, and absorbed curves except for a reduction in normalization and the introduction of some very gentle dips for low M_x^2/s.

Figure 3.7b shows the fixed M_x^2/s plots for the reactions $K^+ p \to K^o X^{++}$ and $K^- p \to \bar{K}^o X^o$. The $\bar{K}^o$ reaction also has the absorbed curves not greatly different from the pole only curves with slight dips, as changes of slope for low M_x^2/s. The change in normalization again occurs. The K^o reaction, while behaving similarly for larger M_x^2/s, exhibits strong dips for low M_x^2/s. These dips arise due to a combination of ignoring the dependance for non forward diagrams and the method of treating ρ-A_2 interference terms used - i.e. they are treated as a ρ-ρ term with differing signature factors. We believe these zeros are spurious, introduced by defects in the model. Of the two mechanisms contributing, we believe the negligence of t_o dependence to be the more serious.

Considering now figure 3.8a, this shows the M_x^2/s dependance for fixed t

of the η and π^o reactions. The tail-offs for large M_x^2/s are due to the tmin effect over the t-bins which are 0.2 GeV/c^2 wide. Any seeming discrepancy over normalization between the plots of 3.7a and 3.8a is accounted for by the fact that the differential cross-section point obtained for the centre of a fixed - t bin is found using 8-point Gaussian quadrature across the t-bin.

The η plots show very little difference between the pole only curve and the absorbed curve except the change in normalization. The strange structure of the π^o plots is attributable to the dip structure of pole only, and absorbed curves, although for small $|t|$ the pole and absorbed curves are similar except for normalization changes.

Figure 3.8b gives the corresponding plots for the K^o and $\bar{K}^o$ reactions. Apart from the re-manifestation of the zero in the absorbed amplitude for $t = -0.7$ in the K^o reaction we again see little other than the now familiar normalization change. The slopes of pole only and absorbed curves for the $\bar{K}^o$ at $t = -0.70$ o differ slightly however.

In figure 3.9 we consider the reaction $K^- p \to \bar{K}^o X^o$ at the much lower energy of $p_{lab} = 14.3$ GeV/c or $s \simeq 28$ GeV/c^2. We emphasise that no fitting has been performed on the calculated curves - they are complete predictions. As can be seen the average overall normalization of the curves is not ridiculous which at least partly justifies our assumptions concerning this part of the model. Also the t-dependance of the data is fairly well accounted for, at least as well by the absorbed curve as by the pole only curve. The M_x^2/s dependance is, however, not well accounted for by either the pole only or the absorbed curve.

Since our input pole model is essentially triple-Regge in form we would expect this at least to reflect the gross M_x^2/s behaviour, and unless the differences existing in our model can account for the gross change of slope, we would be forced to consider changing Regge parameters to bring closer agreement.

The two features of our model that could have some bearing on the overall M_x^2/s shape are the inclusion of the factors $\Delta(M_x^2, m_\rho^2 m_p^2)$ which is a threshold effect, and causes the increase of all the curves for low M_x^2/s. An optimist would see justification for this in the lowest points for $t = -0.50$ and -0.70 GeV/c^2. As M_x^2 increases this factor approaches M_x^2 and so should not affect the larger M_x^2 behaviour. The other feature is the inclusion of a term proportional to $1/(M_x^2)^{\frac{1}{2}}$ in the $\sigma_{TOT}^{\rho p}$ term. This term is indicated by the V.M.D. fit and also there is no reason to exclude it upon duality grounds since the ρp channel would not be considered exotic. If this term were removed, all curves would rise more swiftly than at present; we cannot just take it out because we would like the look of the curves more without it. Being dissatisfied with the fit of our curves to the data with the predicted values to all parameters, we can change some of these parameters in order to obtain a better fit. The parameters we will free will be the overall normalization, the true Regge parameters f r the ρ-pole, and for the absorbed curve we will also free the opacity C, of the initial elastic scattering.

The motivation for this exercise is not just to see how good a fit we can obtain to the data, but also how far the parameters of the best fit are away from the predicted values, and indeed partly to make a thorough test of the minimisation facility of the program used for all the calculations, which is presented in Chapter II, and which appears as ref. 65.

The results of this minimisation are given in Table 3.3 and figures 3.10 and 3.11.

The minimisation was carried out on the 28 data points which lie in the region $0.2 < |t| < 1.0$ GeV/c^2 and $0.15 < M_x^2/s < 0.5$. We do not include the first t-bin ($0.0 < |t| < 0.2$) because this bin is affected by the $|t_{min}|$ cut off which would be extremely (computer) time-consuming to allow for in a meaningful manner. We do not include lower values of M_x^2/s since this

involves low values of M_x^2/s which our model can account for at best in an average sense. It could be argued that we should make our top M_x^2/s cut-off much lower to ensure that the top legs of the diagram (fig. 3.3 or 3.4) ar properly Reggeizing. However the data seems well behaved up to the value we use, and a substantially lower value would not yield sufficient points to make a fit meaningful.

Model A, whose plots are presented in figure 3.10a consists of a pole only model (C = 0) with the other parameters allowed to move essentially freely (note that for the minimisation we have removed the threshold effect of $\Delta(M_x^2, m_\rho^2, m_p^2)$ since it represents no physical threshold). The fitting was performed on the fixed - t plots since integration occurs over the bin which better reflects the way in which the data point was obtained. Because of the scatter of dat points, which is probably statistical rather than dynamical in nature, no fit could be expected to have a really low χ^2. The fact that model A does have a $\chi^2/(d.p)$ of less than 1 might be regarded as encouraging, but the parameter values are not. The worst parameter value found in that of α_o which has a value of around 0.1. The trajectory used in Model A seems to have little to do with the ρ particle. For Model B we constrain α_o to be greater than, or equal to 0.3. This value is still fairly well away from that expected for a ρ - trajectory, but at any rate slightly more reasonable. The $\chi^2/(d.p.)$ for Model B is however much higher.

In Model C we allow the opacity, C, to be non-zero. The fit is almost as good as that for Model A, but C is reduced almost by half its predicted value, and the Regge parameters assigned unfamiliar values, though not immediately ridiculous. A point of note is that if the data admits a slight curvature in the fixed M_x^2/s plots, this is better accounted for by Model C than by Model A.

The normalization changes in all three models are not excessive.

Figure 3.11 gives the effective trajectories for all three models.

A in short dashes, B in longer dashes and C solid. The A and B trajectories are just the input straight lines, but the trajectory for Model C is modified from that input. Its form is not too far removed from a straight line, and for a largepart of the range it lies close to that of Model A.

It is interesting to note that L.H.O'Neill et al. [66] have reported measurements for the reaction $\pi \bar{p} \rightarrow \pi^{o} X$ at 14 GeV/c and extract a fitted ρ trajectory from a triple Regge fit to their data. They have only three points and the error bars are large but the fitted trajectory is

$$\alpha_{\rho}(t) = 0.44 + 2.77t.$$

We cannot use this trajectory to make any excuses for the departure of our Regge parameters from those predicted, since our stance is that our absorption model will account for the difference between the effective trajectory and that predicted.

It does however show that the problem is not confined to one set of data, and that triple-Regge alone would not seem to account for the data without recourse to extreme Regge parameter values.

We note here also that their data does not extend to large enough values of $|t|$ to resolve any questions abot dip structures.

All of the calculations for this chapter were performed by ONCPLT [65] and originally plotted by computer using the plotting package APLOT [49].

CONCLUSIONS

We wish here to quickly draw together the implications of our model and the available data. It seems that the effective trajectory of the two sets of data we use do not correspond to the ρ trajectory found via two-body data, with exchange degeneracy, and some means must be found to account for this departure. The model we have put forward in the previous sections seems to go a short way towards doing this, phenomenologically, but by no means far enough.

That is, if we take the effective trajectory of the $\bar{K}^o$ data to be that of Model A, Model C modifies its own trajectory towards that of Model A, but only from a halfway value to the true ρ trajectory.

In addition our model has various heuristic defects which are commented upon previously. These lead, among other things, to the spurious zeros in the K^o plots, and also to setting all target asymmetries to zero, since we ignore $\sin\theta_{CM}$ dependancies to obtain our initial formula. The target asymmetry of course has a factor of $\sin\theta_{CM}$ incorporated.

Some of these defects could be corrected within the basic framework of the model, however this framework is itself so much open to question that the effort does not seem justified. We therefore conclude that the model as presented is not sufficiently realistic, and that a less restrictive model must be developed.

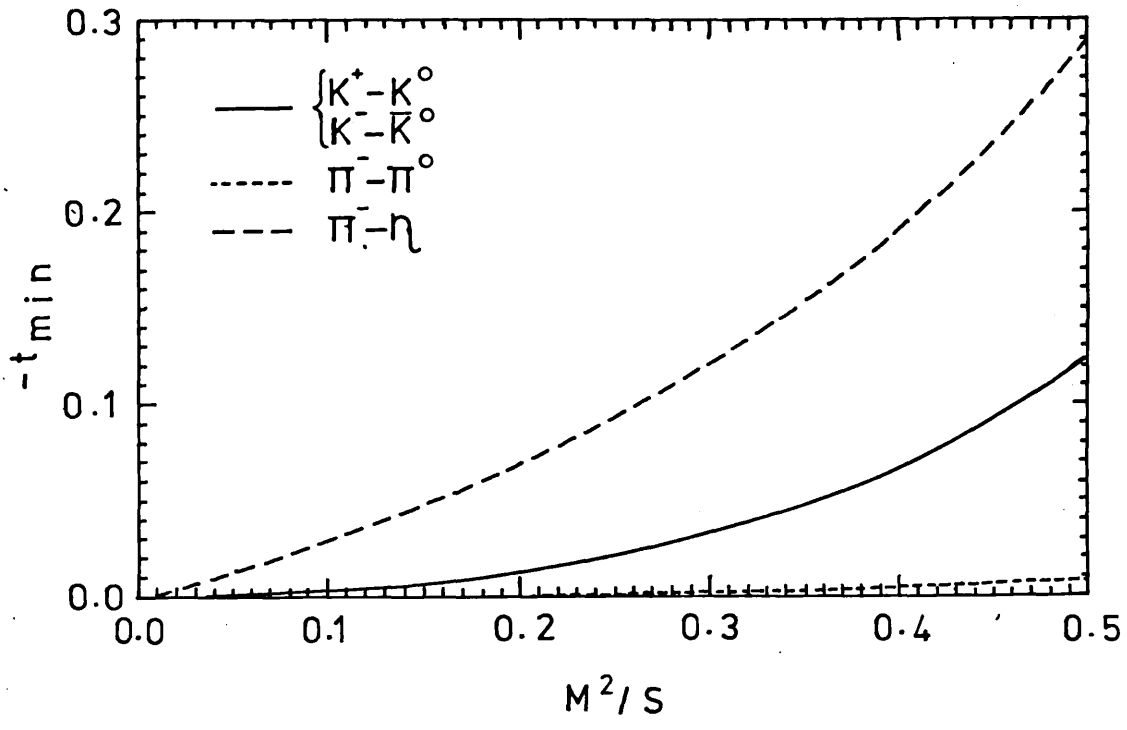

Fig.3.6. The edge of phase space for various produced particles

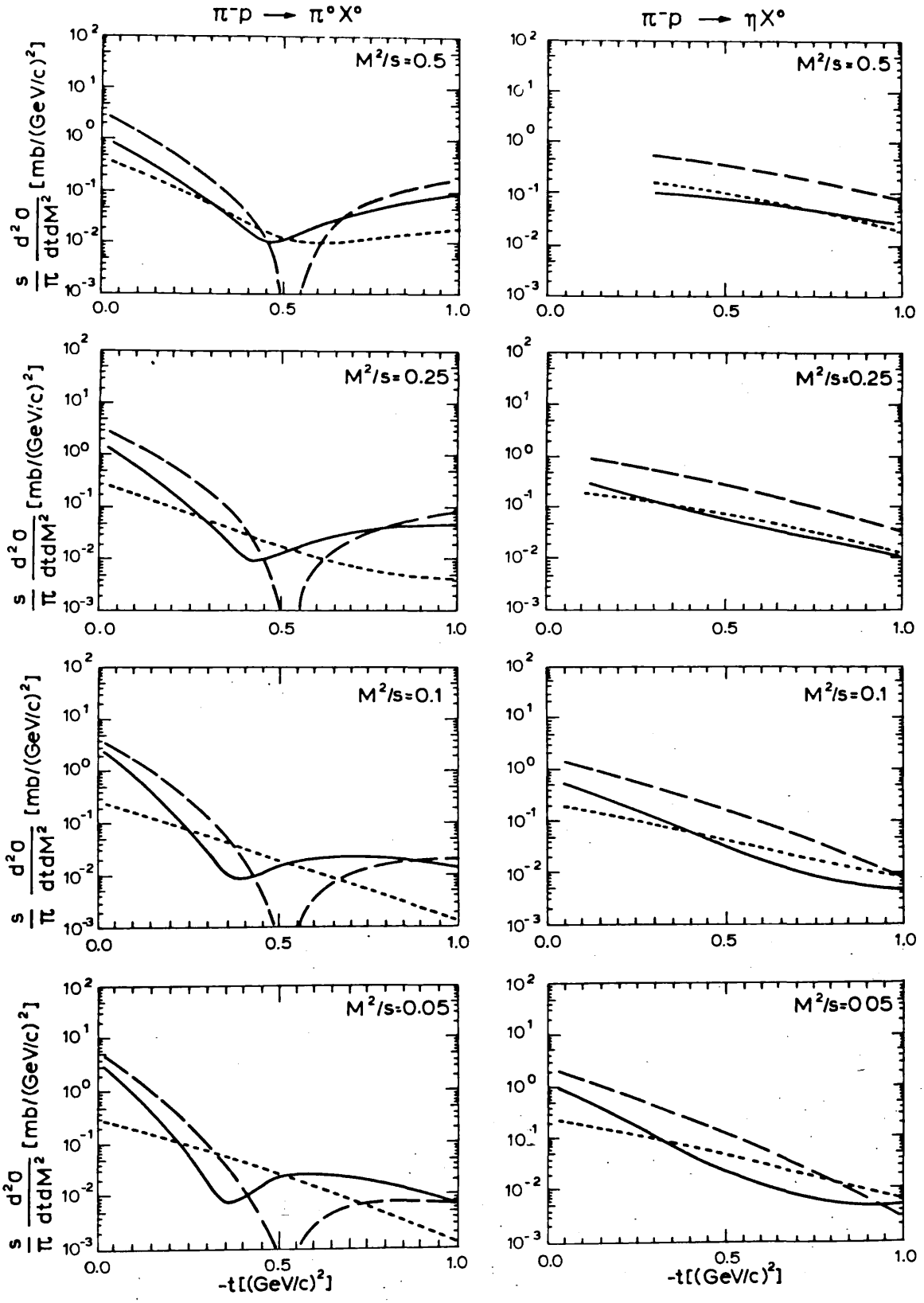

Fig.3.7a. The t distributions for the specified reactions at $s = 100(GeV^2)$ and the given value of M^2/s.

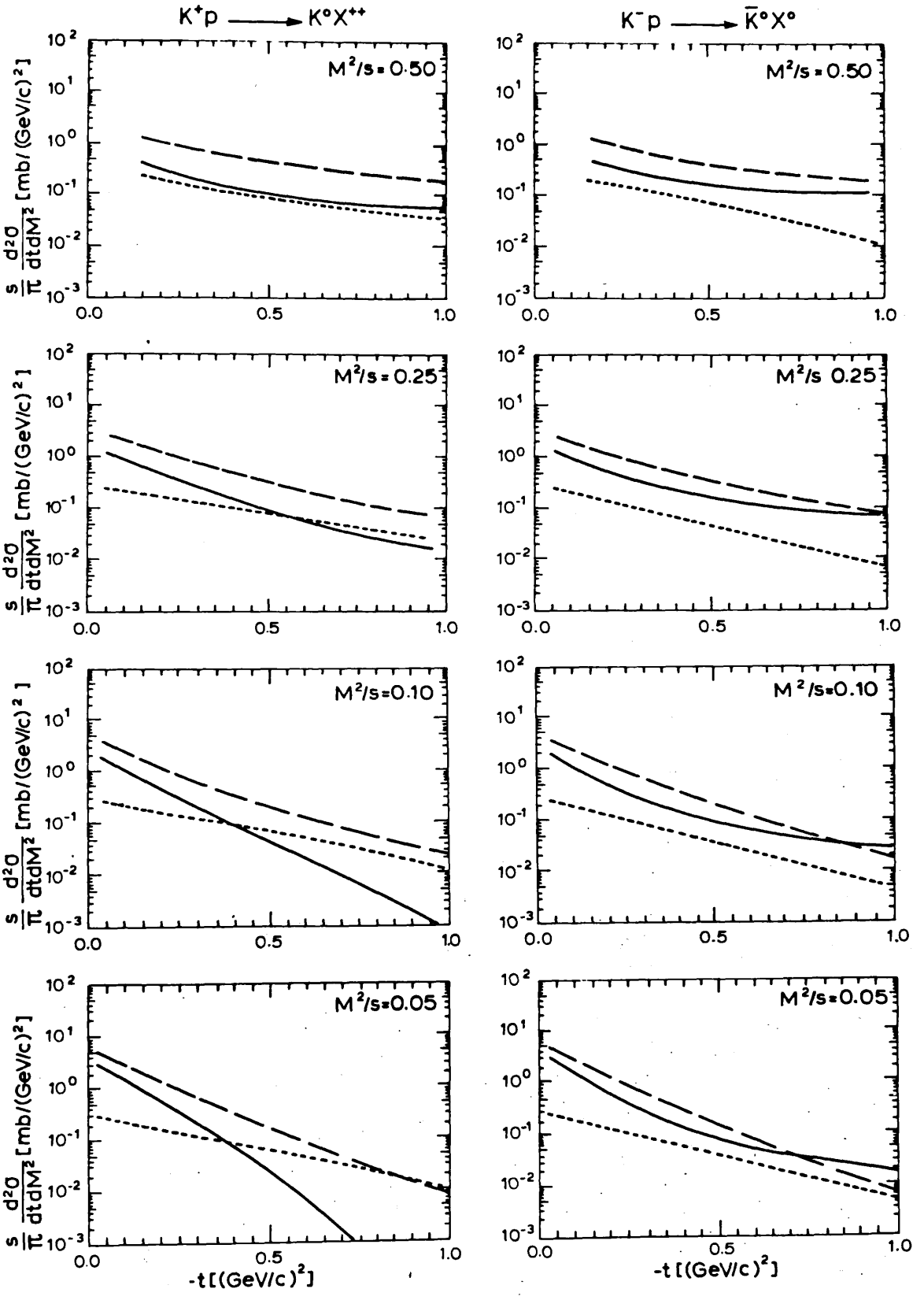
K⁺p ⟶ K°X⁺⁺
K⁻p ⟶ K̄°X°
M²/s = 0.50
M²/s = 0.25
M²/s 0.25
M²/s=0.10
M²/s=0.05
s/π d²σ/dtdM² [mb/(GeV/c)²]
-t[(GeV/c)²]

Fig.3.7b.

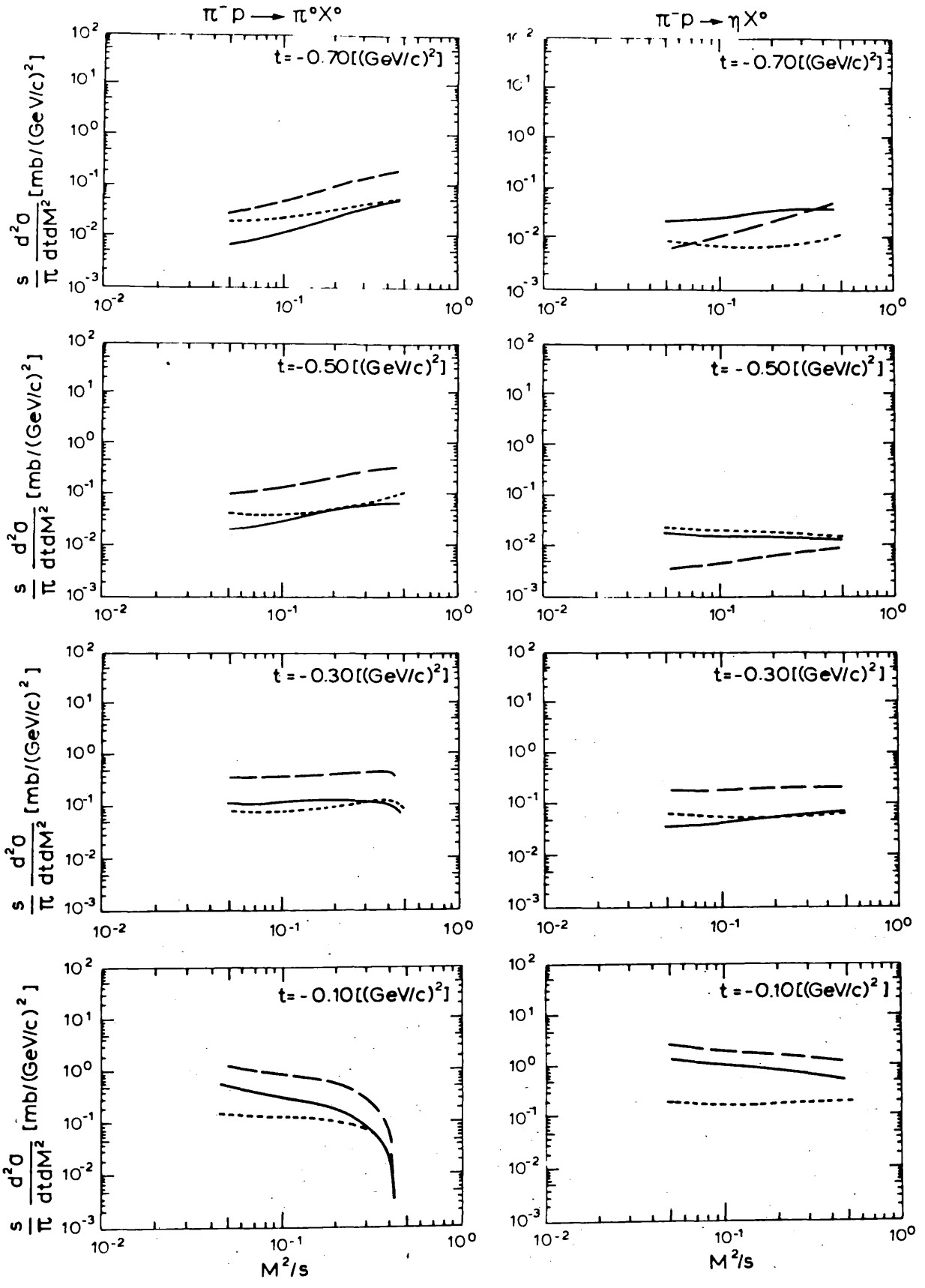

Fig.3.8a. The M^2/s distributions for the specified reactions at $s = 100(GeV^2)$. The value of t given is the mid-point of a t bin 0.2 $(GeV/c)^2$ wide and the theoretical cross sections are integrated by 8-point Gaussian-Legendre Quadrature over this bin.

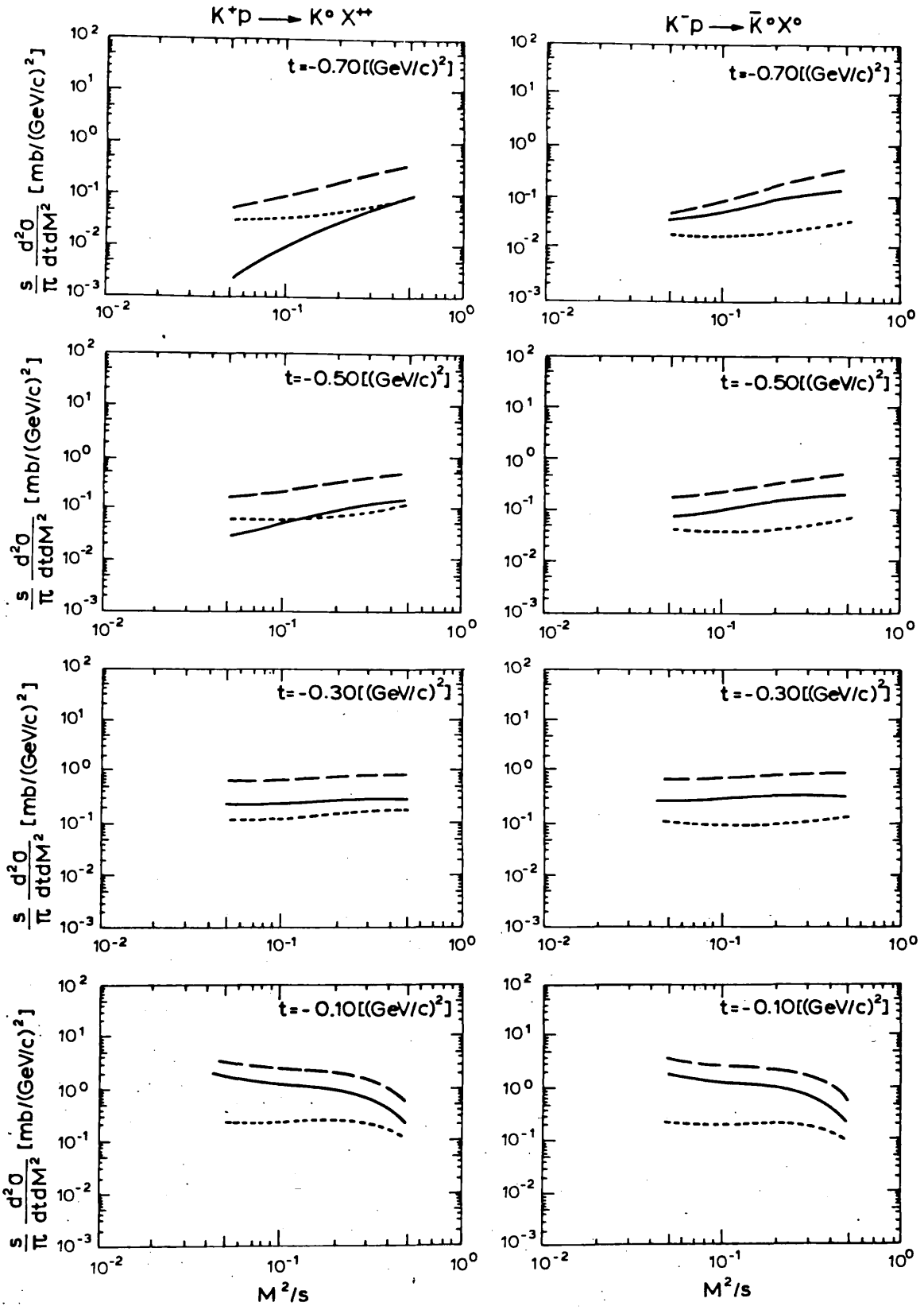
K⁺p ⟶ K° X⁺⁺
K⁻p ⟶ K̄° X°
t=-0.70[(GeV/c)²]
t=-0.50[(GeV/c)²]
t=-0.30[(GeV/c)²]
t=-0.10[(GeV/c)²]
s/π d²σ/dtdM² [mb/(GeV/c)²]
M²/s

Fig.3.8b.

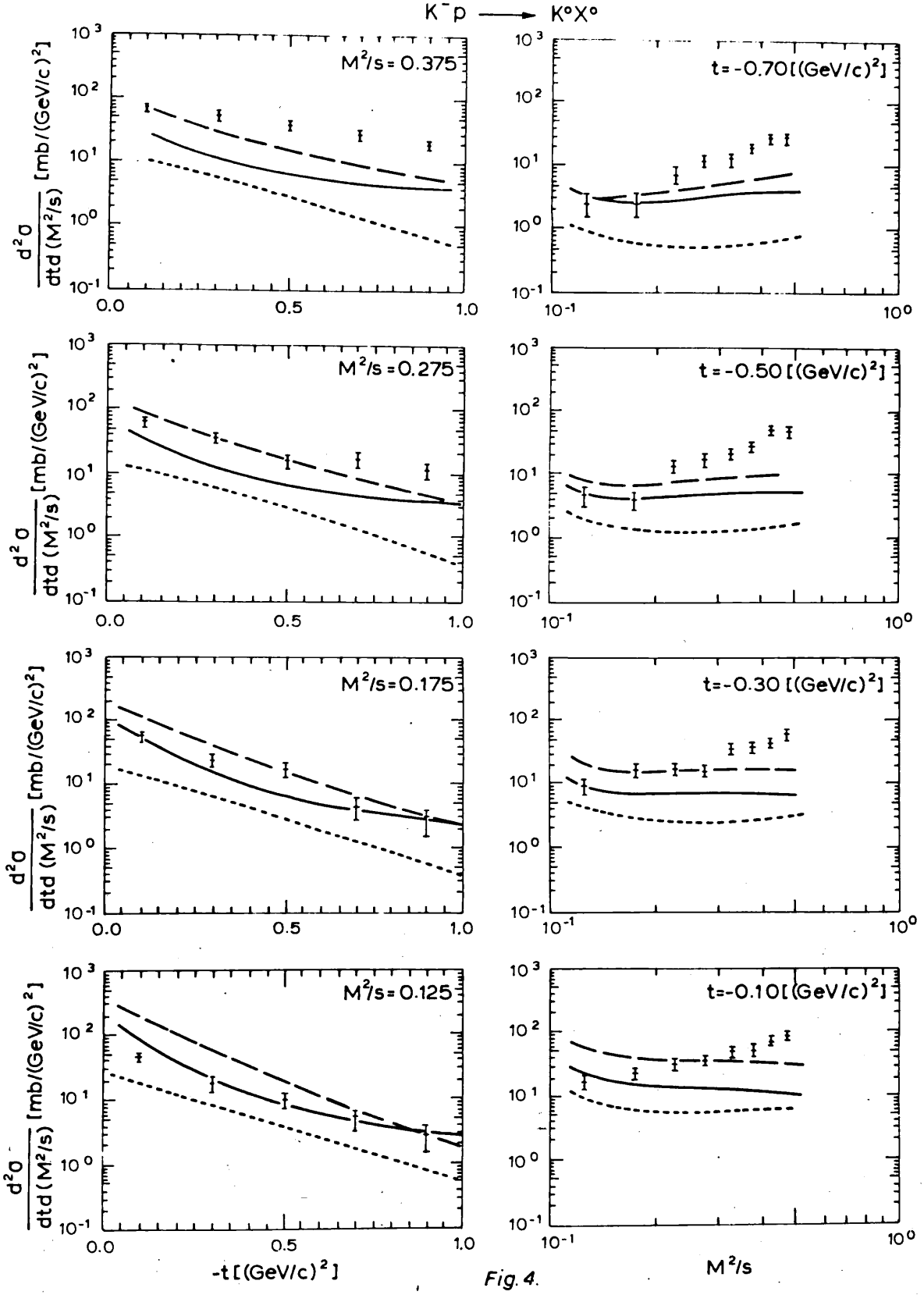

Fig. 4.

Fig.3.9. Both the t and M^2/s distributions for the reaction

$K^- + p \rightarrow \overline{K}^o + X^o$ at p_{Lab} = 14.3 GeV/c.

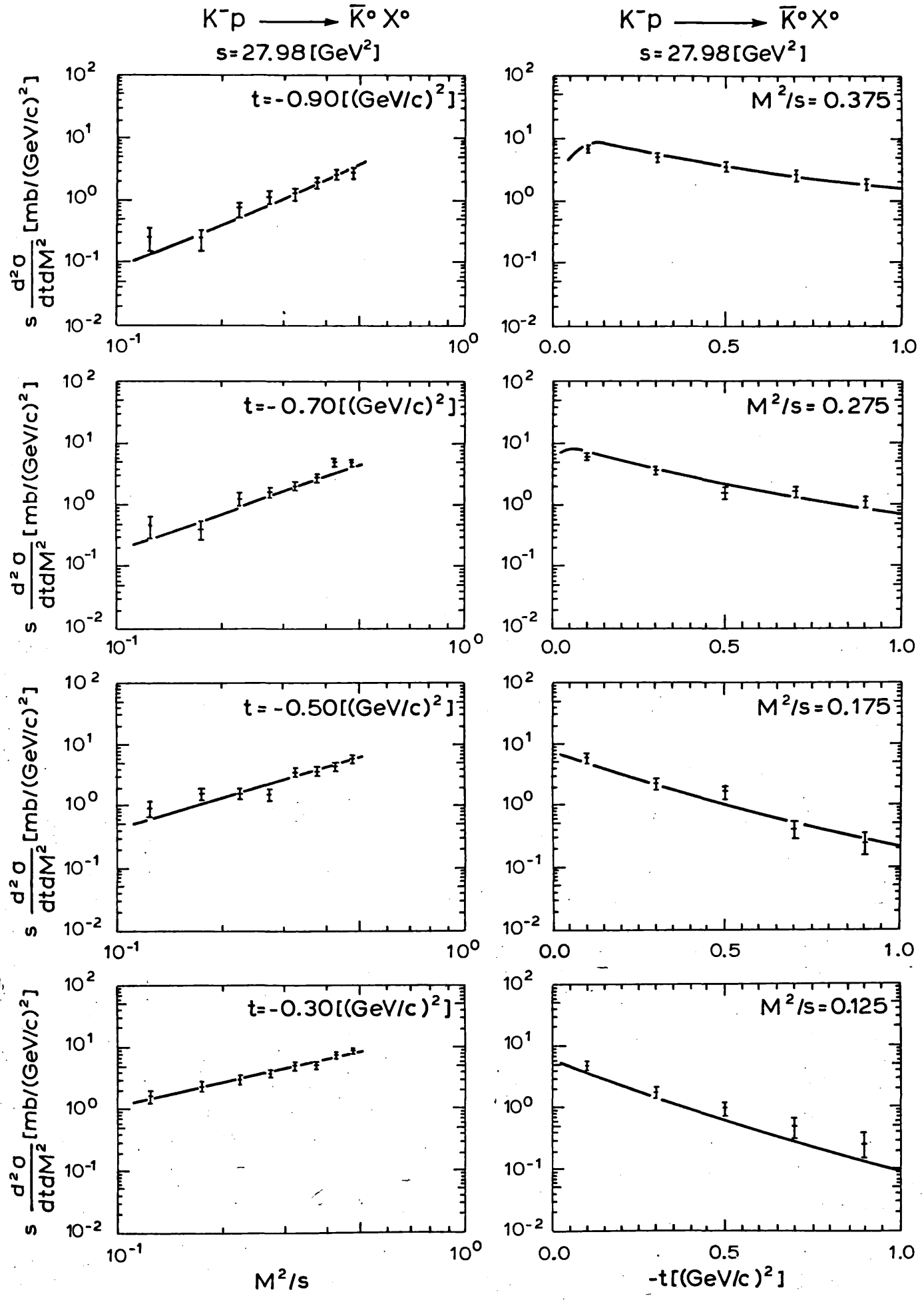
K⁻p ⟶ K̄°X°
s=27.98[GeV²]
t=-0.90[(GeV/c)²]
t=-0.70[(GeV/c)²]
t=-0.50[(GeV/c)²]
t=-0.30[(GeV/c)²]
M²/s= 0.375
M²/s= 0.275
M²/s=0.175
M²/s=0.125
s d²σ/dtdM² [mb/(GeV/c)²]
M²/s
-t[(GeV/c)²]

Fig. 3.10a.

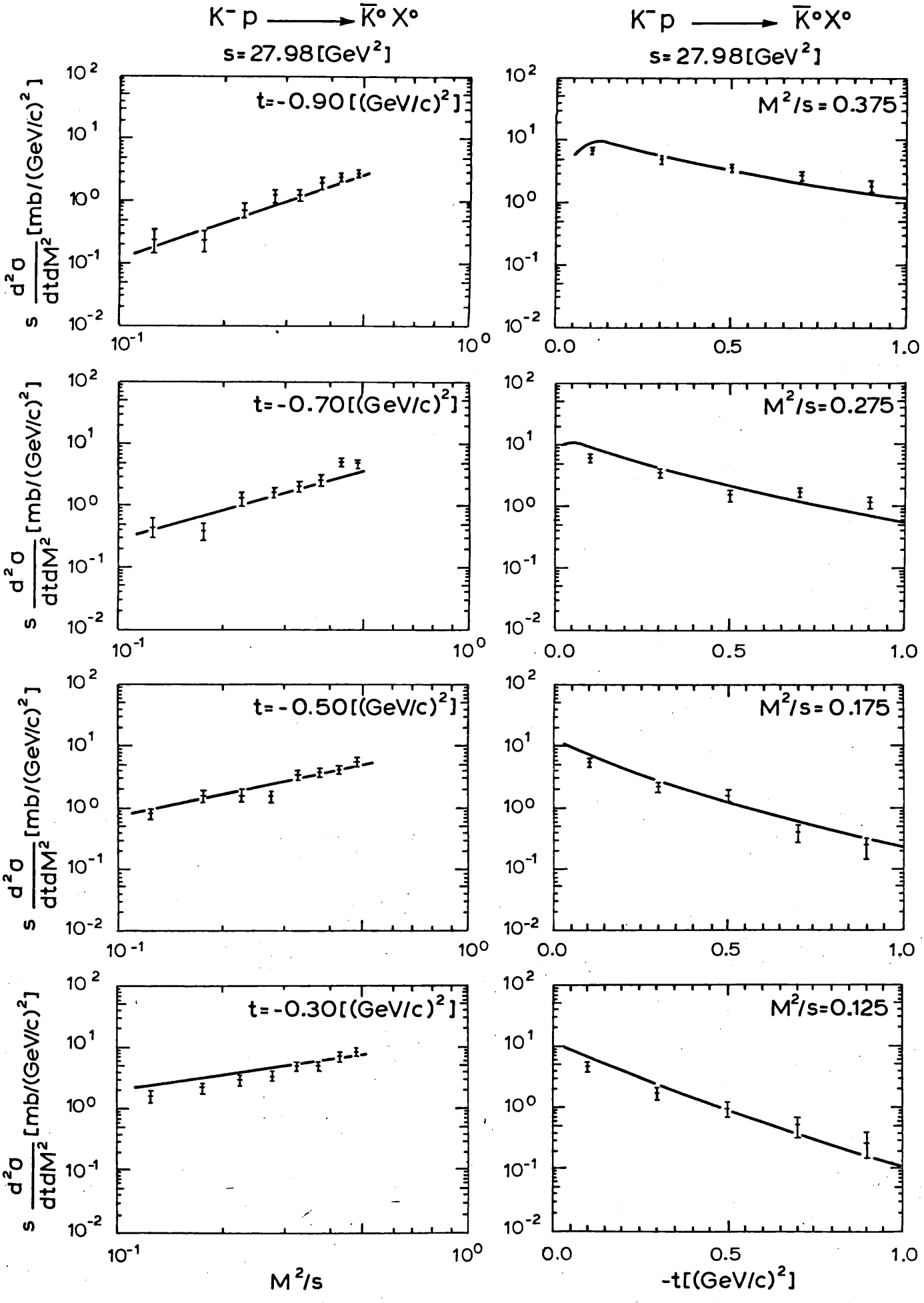
K⁻p ⟶ K̄°X°
s=27.98[GeV²]
t=-0.90[(GeV/c)²]
t=-0.70[(GeV/c)²]
t=-0.50[(GeV/c)²]
t=-0.30[(GeV/c)²]
M²/s=0.375
M²/s=0.275
M²/s=0.175
M²/s=0.125
s d²σ/dtdM² [mb/(GeV/c)²]
M²/s
-t[(GeV/c)²]

Fig. 3.10b.

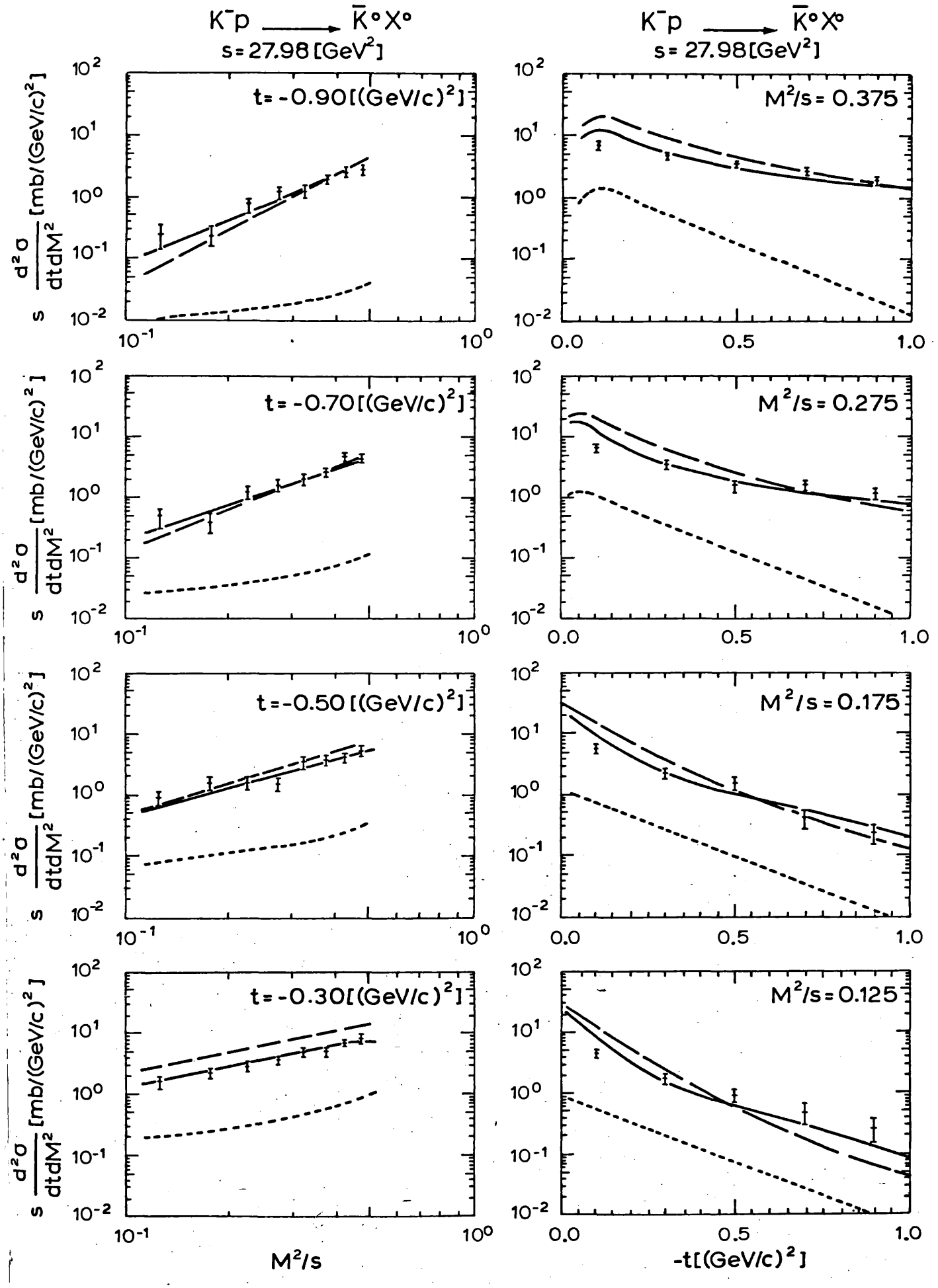

Fig. 3.10c.

——pole only; - - - - cut only; ——— pole - cut (final curve)

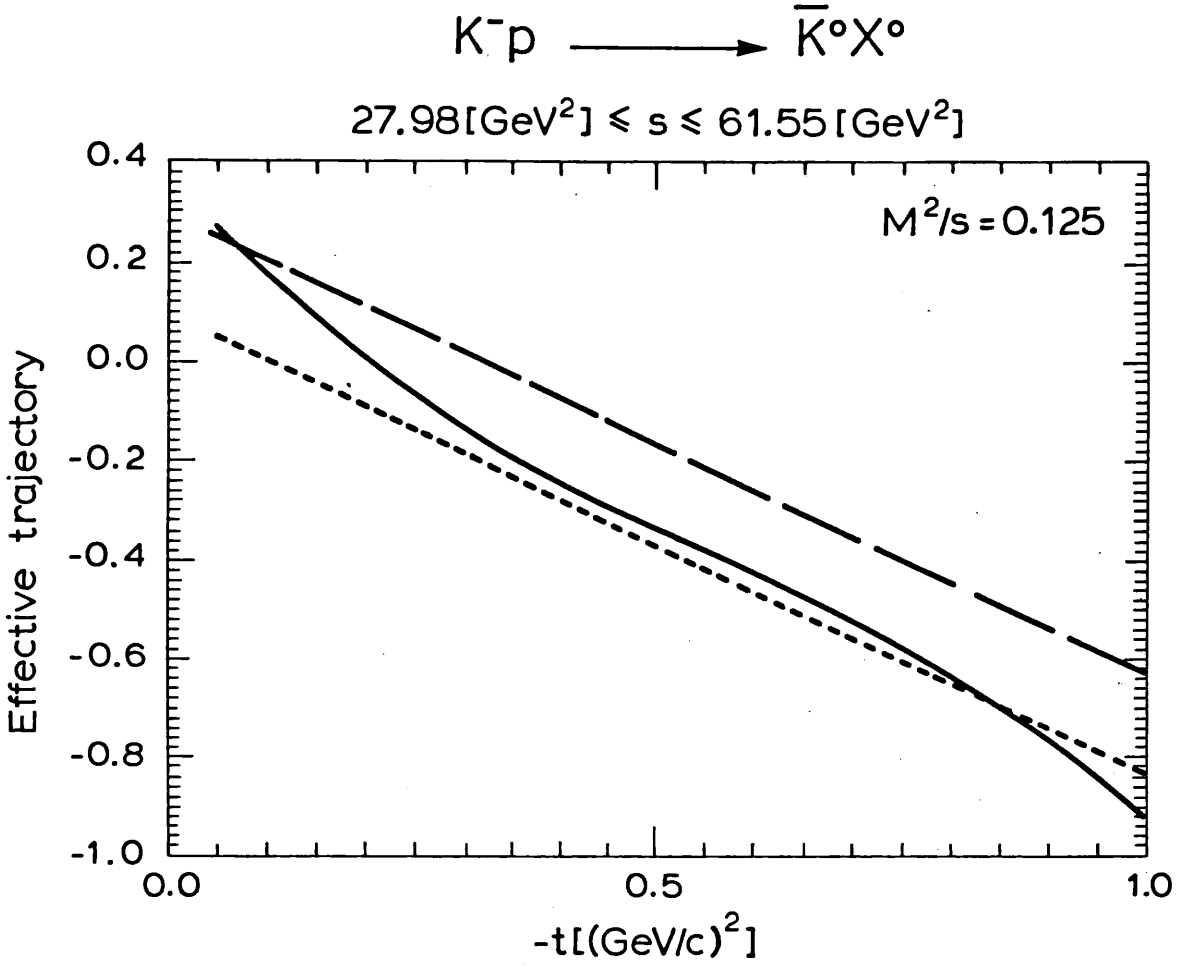

Fig.3.11.

Effective trajectories for the three models

- - - - - - - - Model A

—— —— Model B

———— Model C

TABLE 3.1

Reaction	Exchange	D-type Coupling	F-type Coupling
$\pi^- p \to \pi^o X$	ρ		2
$\pi^- p \to \eta X$	A_2	$2/\sqrt{3}$	
$K^- p \to \bar{K}^o X$	ρ		$-\sqrt{2}$
	A_2	$\sqrt{2}$	
$K^+ p \to K^o X$	ρ		$\sqrt{2}$
	A_2	$\sqrt{2}$	

SU(3) coefficients for the reactions $0^-\frac{1}{2}^+ \to 0^- X$ proceeding via charge exchange.

TABLE 3.2

Reaction	Energy $(GeV/c)^2$	C	$\lambda(GeV/c^{-2})$
$\pi^- p \to \pi^o X$	100	.663	.0676
$\pi^+ p \to \eta X$	100	.663	.0676
$K^+ p \to K^o X$	100	.536	.0729
$K^- p \to \bar{K}^o X$	100	.553	.0676
$K^- p \to \bar{K}^o X$	28	.608	.0676

Absorption Coefficients

TABLE 3.3

Parameter		Model A		Model B		Model C	
Symbol	Predicted Value	Value	Limits Enforced	Value	Limits Enforced	Value	Limits Enforced
C	0.608	0.0	fixed	0.0	fixed	0.362	0.0 1.0
N	1.0	3.644	0.0 6.0	2.113	0.0 6.0	2.080	0.0 6.0
α_o	0.470	.099	-0.5 1.0	0.3	0.3 1.0	0.313	0.3 1.0
α'	0.905	.935	0.0 2.0	.931	0.0 2.0	1.494	0.0 2.0
χ^2/data point		0.855		2.186		1.171	

Minimisation parameter values with imposed limits and a χ^2/(data point) for each of the three models.

APPENDIX 3A

We have the expression for the quasi-total cross-section σ_q

$$\langle n\rangle \sigma_q = \int dM_x^2 \int \frac{d^3q_3}{2E_3} \frac{d^3q_{M_x}}{2E_{M_x}} \delta^4(q_3 + q_{M_x} - p_1 - p_2)$$

$$\Sigma \bar{\Sigma} |M|^2 \frac{1}{F} \qquad 3A.1$$

The L.H.S. can be converted into a differential cross-section in t and M_x^2 by inserting their appropriate δ-function on the R.H.S. This ensures that integration of the differential cross-section will yield the correct form for the total cross section. We therefore have

$$\langle n\rangle \frac{\partial^2\sigma_q}{\partial t \partial M_x^2} = \int dM_x^2 \int \frac{d^3q_3}{2E_3} \frac{d^3q_{M_x}}{2E_{M_x}} \delta^4(q_3 + q_{M_x} - p_1 - p_2)$$

$$\delta(M_x^2 - (p_1 + p_2 - q_3)^2)\delta(t - (p_1 - q_3)^2)$$

$$\Sigma\bar{\Sigma}|M|^2 . \frac{1}{F} \qquad 3A.2$$

We can immediately perform the $d^3q_{M_x}$ integration to be left with

$$\langle n\rangle \frac{\partial^2\sigma_q}{\partial t \partial M_x^2} = \int dM_x^2 \int \frac{q\, dq\, d\,\mathrm{Cos}\theta\, d\phi}{(2\pi)^2\, 2E_3\, 2E_{M_x}} \delta\,(E_3 + E_{M_x} - \sqrt{s}\,)$$

$$\delta(t - (p_1 - p_3)^2)\delta(M_x^2 - (p_1 + p_2 - q_3)^2)\ \Sigma\bar{\Sigma}|M|^2\ \frac{1}{F} \ . \qquad 3A.3$$

where q is the modulus of the three momentum of particle 3, and θ,ϕ give its spatial orientation from the line of particle 1 in the 1-2 centre of mass frame. Because of rotational invariance $|M|^2$ will not depend on ϕ and so the ϕ integration can be trivially performed to yield a factor of 2π. We also perform the M_x^2 integration at this stage using the corresponding δ-function to be left with

$$\langle n \rangle \frac{\partial^2 \sigma_q}{\partial t \partial M_x^2} = \int \frac{q^2\, dq\, d\mathrm{Cos}\theta}{2\pi . 2E_3\, 2E_{M_x}} \delta\,(E_3 + E_{M_x} - \sqrt{s})\, \delta\,(t - (p_1 - p_3)^2)\ \Sigma\bar{\Sigma}|M|^2\ \frac{1}{F} \qquad 3A.4$$

We now make the transformation

$$dt\, dM_x^2 = \frac{2\sqrt{s}\, q}{E_3}\ 2pq\, dq d\mathrm{Cos}\theta \qquad 3A.5$$

which can be arrived at by considering

$$M_x^2 = (\sqrt{s} - E_3)^2 - q_3^2$$

$$t = m_1^2 + m_3^2 - \sqrt{s} . \sqrt{m_3^2 + q^2} + 2pq\mathrm{Cos}\theta$$

in the 1-2 C.M. frame, with p the modulus of the 3-momentum of particle 1, say.

It is possible to perform the t integration immediately to leave

$$\langle n \rangle \frac{\partial^2 \sigma_q}{\partial t \partial M_x^2} = \int \frac{dM_x^2}{2\pi . 2E_{M_x}} . \frac{1}{8\sqrt{s}p}\ \delta(E_3 + E_{M_x} - \sqrt{s})$$

$$\Sigma\bar{\Sigma}|M|^2 . \frac{1}{F} \qquad 3A.6$$

We now use the well known relation [67] that

$$\delta(f(x)) = \sum_a \frac{1}{|f'(a)|}\ \delta(x - a)$$

where the sum is over the zeros of $f(x)$.

Since

$$E_3 + E_{M_x} - \sqrt{s} = \sqrt{m_3^2 + q^2} + \sqrt{M_x^2 + q^2} - \sqrt{s}$$

we have

$$\delta(E_3 + E_{M_x} - \sqrt{s}) = 2E_{M_x}\, \delta(M^2 - \chi) \qquad 3A.7$$

This allows us to perform the final integration and inserting the form of the flux factor for two particles i.e. $F = 4\sqrt{s}\, p$ 3A.8

we have

$$\langle n \rangle \frac{\partial^2 \sigma}{\partial t \partial M_x^2} = \frac{1}{64\pi sp^2} \Sigma\bar{\Sigma}|M|^2 \ . \qquad 3A.9$$

A more conventional form, if symbolically incorrect for this quantity would be

$$\frac{s}{\pi} \frac{d^2\sigma}{dtdM_x^2} = \frac{1}{64\pi^2 p^2} \Sigma\bar{\Sigma}|M|^2 \qquad 3A.10$$

and it is this form that is used throughout.

APPENDIX 3B

We consider the optical theorem which give a total cross-section as the discontinuity of the elastic amplitude at $t = 0$, namely

$$2\Delta(s,m_1^2,m_2^2)\,\sigma_{TOT}(s) = \mathrm{Disc}_s\Big(\bar{\Sigma}_{\lambda_1\lambda_2} \langle p_1 j_1 \lambda_1, p_2 \lambda_2 \lambda_2 | T | p_1 j_1 \lambda_1 p_2 j_2 \lambda_2 \rangle\Big) \qquad 3.B1$$

The case we are interested in is that of $\frac{1}{2}^+ 1^-$ elastic scattering, and using an M-function decomposition we can say

$$\langle p_1\lambda_1, p_2\lambda_2 | T | p_1\lambda_1, p_2\lambda_2\rangle = \bar{u}_\alpha^{\lambda_2}(p_2)\varepsilon_\nu^{*\lambda_1}(p_1)\, M_\beta^{\alpha\nu\mu}\varepsilon_\mu^{\lambda}(p_1)\, u^{\beta\lambda_2}(p_2). \qquad 3.B2.$$

If we perform the helicity sum over λ_2 and consider the available tensorial forms for M we have

$$2\Delta(s, m_1^2, m_2^2)\,\sigma_{TOT}(s) = \Big(\Sigma_{\lambda_1} \varepsilon_\nu^{*\lambda}(p_1)\{\lambda_1 g^{\mu\nu} + \lambda_2 (p_2)^\mu (p_2)^\nu\}\varepsilon_\mu^{\lambda}(p_1)\Big) \qquad 3.B3$$

Now we have

$$\varepsilon_\mu^{o}(p) = (|\underline{p}|;\ E\,\hat{\underline{p}})/m$$

$$\varepsilon_\mu^{\pm}(p) = (0;\ \hat{\underline{n}}^{\pm}(\underline{p})) \qquad 3.B4$$

$$\text{where} \quad \hat{\underline{n}}^{\pm}(\underline{p})\cdot\underline{p} = 0$$

and $\Sigma_\lambda\, \varepsilon_\nu^{*\lambda}(p)\, g^{\nu\mu}\, \varepsilon_\mu^{\lambda}(p) = 3$

we are also using C.M. helicity states and so, for this exercise, $\underline{p}_1 = -\underline{p}_2$ we can easily rewrite 3.B3 as $2\Delta(s,m_1^2,m_2^2)\,\sigma_{TOT}(s) =$

$$3\lambda_1 + \Big(\frac{\Delta(s,m_1^2,m_2^2)}{2m_1}\Big)^2 \lambda_2 \qquad 3.B5$$

Translated back to the notation of Chapter III the s we are using here is M_x^2. The contribution from λ_2 is enhanced by a factor of s^2 over that from λ_1 in equation 3.9. Since equation 3.B5 shows that λ_1 can only be enhanced by a factor of $(M_x^2)^2$ over λ_2 we see that the contribution of λ_1 in equation 3.9 must be suppressed with respect to that of λ_2 by a factor of $(M_x^2/s)^2$, and so in the limit $s/M_x^2 \to \infty$ we can ignore the contribution from λ_1 in 3.9.

The problem of how to decide on a reasonable form for

λ_2 persists however.

We can split the contribution to the total cross section coming from the differing polarization of the 1^- particle using 3.B4 and we have

$$2\Delta(s,m_1^2,m_2^2)\,\sigma^{o}_{TOT} = \text{Disc}_s\,\lambda_2\left(\frac{\Delta(s,m_1^2,m_2^2)}{2m_1}\right)^2 + \text{Disc}_s\,\lambda_1$$

$$2\Delta(s,m_1^2,m_2^2)\,\sigma^{+}_{TOT} = \text{Disc}_s\,\lambda_1 \qquad \text{3.B6}$$

$$2\Delta(s,m_1^2,m_2^2)\,\sigma^{-}_{TOT} = \text{Disc}_s\,\lambda_1$$

So if mass-shell $1^-\tfrac{1}{2}^+$ elastic scattering were possible we could use the differing polarization to find a reasonable expression for Disc λ_2.

Without introducing free parameters then, the simple choice seems to be that we neglect the longitudinal cross section with respect to the transverse and therefore write

$$\lambda_2 = \frac{8m^2\,\sigma_{TOT}}{\Delta(s,m_1^2,m_2^2)} \qquad \text{3.B7}$$

We also pass to the regime in which equation 3.B7 will be used, namely. $m_1^2 \to t$ without altering the threshold factors, since the simple replacement of m_1^2 by t results in nonsense, and no other replacement is obvious.

The philosophy of equation 3.B7 and 3.10 is therefore to give λ_2 a reasonable functional dependence and while the normalization is certainly not definitive it should not be ridiculous.

APPENDIX 3C

We wish to perform a partial wave analysis upon the expression

$$H^{\lambda_{\bar{1}}\ \lambda_{\bar{2}}\ \lambda_3}_{\lambda_1\ \lambda_2\ \lambda_{\bar{3}}}(p_{\bar{1}}p_{\bar{2}}p_3\ ;\ p_1p_2p_{\bar{3}})$$

$$= \sum_{s_x\ \lambda_x\ \eta_x} \langle p_{\bar{1}}\lambda_{\bar{1}}p_{\bar{2}}\lambda_{\bar{2}} \mid T \mid p_3\ 3,\ p_x s_x \lambda_x \eta_x\rangle$$

$$\langle p_{\bar{3}}\lambda_{\bar{3}},\ p_x s_x \lambda_x \eta_x \mid T \mid p_1\lambda_1 p_2\lambda_2\rangle \qquad 3.C1$$

Now in a obvious change of notation we take, for a two particle C.M. state

$$\mid \theta\ \phi\ \mu_1\ \mu_2\rangle = \sum_{JM} \left(\frac{2J+1}{4\pi}\right)^{\frac{1}{2}} D^J_{M\mu}(\phi,\theta,-\phi)\ \mid J\ M\ \mu_1\mu_2\rangle$$

where the two particles plane wave helicity state is related to two particle angular momentum helicity states [68]

Note that $\mu = \mu_2 - \mu_1$ which defines our type 1, type 2 particle convention.

Thus

$$\langle \Theta\ \Phi,\ \mu_3\ \mu_4 \mid T \mid \theta\ \phi, \mu_1\ \mu_2\rangle = \sum_{J\ M} \left\{ \frac{2J+1}{4\pi}\ D^{J*}_{M\mu_f}(\Phi,\Theta,-\Phi)\right.$$

$$\left. D^J_{M\ \mu_i}(\phi,\theta,-\phi)\ \langle \mu_3\ \mu_4 \mid T^{\,J}(s) \mid \mu_1\ \mu_2\rangle \right\} \qquad 3.C2$$

where $\mu_f = \mu_4 - \mu_3$, $\mu_i = \mu_2 - \mu_1$ and angular momentum conservation laws enforce that J and M are equal on both sides of the T-matrix, and rotational invariance gives us that the T-matrix does not depend on M.

When we define

$$\bar{\mu}_1 = \lambda_x - \lambda_3$$

$$\mu_1 = \lambda_x - \lambda_{\bar{3}}$$

$$\mu_2 = \lambda_2 - \lambda_1$$

$$\bar{\mu}_2 = \lambda_{\bar{2}} - \lambda_{\bar{1}}$$

and remember that the kinematics is such that the missing mass state is travelling along the positive z axis we can write

$$H^{\lambda_1\lambda_2\lambda_3}_{\lambda_1\lambda_2\lambda_3} = \sum_{\lambda_x} \sum_{\substack{J = \max\{|\bar{\mu}_1|,|\bar{\mu}_2|\} \\ J' = \max\{|\mu_1|,|\mu_2|\}}}^{\infty} \frac{2J+1}{4\pi} \frac{2J'+1}{4\pi}$$

$$D^{J*}_{\bar{\mu}_1\bar{\mu}_2}(\phi,\theta,-\phi)\, D^{J'}_{\mu_1\mu_2}(\phi',\theta',-\phi')$$

$$\sum_{s_x\eta_x} \langle\bar{\lambda}_1\bar{\lambda}_2|T^J(s,M_x^2)|\lambda_3\lambda_x, s_x\eta_x\rangle$$

$$\langle\bar{\lambda}_3\lambda_x s_x\eta_x|T^{J'}(s,M_x^2)|\lambda_1\lambda_2\rangle \qquad 3C.3$$

and since $D^j_{m'm}(\alpha,\beta,\gamma) = e^{-i\alpha m'}\, d^j_{m'm}(\beta)\, e^{-i\gamma m}$

we have

$$H^{\lambda_1\lambda_2\lambda_3}_{\lambda_1\lambda_2\lambda_3} = \sum_{\lambda_x} e^{-i\phi(\bar{\mu}_2-\bar{\mu}_1)}\, e^{-i\phi'(\mu_1-\mu_2)} \cdot$$

$$\sum_{\substack{J = \max\{|\bar{\mu}_1|,|\bar{\mu}_2|\} \\ J' = \max\{|\mu_1|,|\mu_2|\}}} \frac{2J+1}{4\pi} \frac{2J'+1}{4\pi}\, d^J_{\bar{\mu}_1\bar{\mu}_2}(\theta)\, d^{J'}_{\mu_1\mu_2}(\theta')$$

$$\sum_{s_x\eta_x} \langle\bar{\lambda}_1\bar{\lambda}_2|T^J(s,M_x^2)|\lambda_3\lambda_x s_x\eta_x\rangle$$

$$\langle\lambda_3\lambda_x s_x\eta_x|T^{J'}(s,M_x^2)|\lambda_1\lambda_2\rangle \cdot \qquad 3C.4$$

This in fact completes the partial wave analysis of the amplitude, but as such is in a form that is not readily usable. We wish to make the impact parameter approximation which leads to a remarkably simple form in which to make absorption type corrections.

Defining

$$h_{\lambda_x} = -\sum_{s_x,\eta_x} \langle\bar{\lambda}_1\bar{\lambda}_2|T^J(s,M_x^2)|\lambda_3\lambda_x s_x\eta_x\rangle \cdot$$

$$\langle\lambda_3\lambda_x s_x\eta_x|T^{J'}(s,M_x^2)|\lambda_1\lambda_2\rangle \qquad 3C.5$$

and

$$H_{\lambda_x} = \sum_{\substack{J = \max\{|\bar{\mu}_1|,|\bar{\mu}_2|\} \\ J' = \max\{|\mu_1|,|\mu_2|\}}} \frac{2J+1}{4\pi} \frac{2J'+1}{4\pi} d^{J}_{\bar{\mu}_1\bar{\mu}_2}(\theta).$$

$$d^{J'}_{\mu_1\mu_2}(\theta')\, h_{\lambda_x}(J, J', s, M_x^2) \qquad 3C.6$$

The first step towards the impact parameter approximation is to write H_{λ_x} in an approximate form with J and J' treated as continuous parameters and the summations over J and J' as integrals. We can justify this procedure physically if $h_{\lambda_x}(J, J', s, M_x^2)$ does not have a strong variation between contiguous values of J, J' and so the continuous function can account reasonably for the J, J' behaviour in an average sense. H_{λ_x} can then be expressed as

$$H_{\lambda_x} = \frac{1}{4\pi^2} \int_{\max\{|\bar{\mu}_1||\bar{\mu}_2|\}}^{\infty} dJ(J+\tfrac{1}{2}) \int_{\max\{|\mu_1||\mu_2|\}}^{\infty} dJ'(J'+\tfrac{1}{2})\, d^{J}_{\bar{\mu}_1\bar{\mu}_2}(\theta)\, d^{J'}_{\mu_1\mu_2}(\theta')\, h_{\lambda_x}(J, J', s, M_x^2) \qquad 3C.7$$

The next step is to approximate the d^J functions since their precise form is very complicated. A general expression is

$$d^{j}_{m'm}(\beta) = \sum_n \left\{ \frac{(-1)^n [(j+m)!(j-m)!(j+m')!(j-m')!]^{\frac{1}{2}}}{(j-m'-n)!(j+m-n)!(n+m'-m)!n!} \right.$$

$$\left. (\cos\tfrac{1}{2}\beta)^{2j+m-m'-2n} (-\sin\tfrac{1}{2}\beta)^{m'-m+2n} \right\} \qquad 3C.8$$

This can be approximated to order $(1 - \cos\beta)$ in the form

$$d^{j}_{m'm}(\beta) = (-1)^{m'-m} \left\{ \frac{\Gamma(j+m'+1)\Gamma(j-m+1)}{\Gamma(j+m+1)\,\Gamma(j-m'+1)} \right\}^{\frac{1}{2}}$$

$$\lambda(j,m',m)^{-(m'-m)/2}\, J_{m'-m}[(2(1-\cos\beta)\lambda(j,m',m))^{\frac{1}{2}}] \qquad 3C.9$$

where $\lambda(j,m',m) = j(j+1) - \frac{1}{2}m'(m'+1) - \frac{1}{2}m(m-1)$ with $j \geq |m'|, |m|$ and $m' \geq m$. J is a Bessel function of the first kind. This can be seen using the series form for the Bessel function [69]

$$J_\nu(Z) = (\tfrac{1}{2}Z)^\nu \sum_{k=0}^{\infty} \frac{(-\frac{1}{4}Z^2)^k}{k!\Gamma(\nu+k+1)}$$

This approximate form will be valid for small angles β whatever values m and m' take on, but is still difficult to apply because of the complex form for the λ factor and the Γ functions. At high energies and for small angle scattering it can be argued that the region of interest will be the higher partial waves, i.e. integration over regions where $j >> 1$. Also in two body scattering clearly m and m' will be of the order of 1, and in this case a further level of approximation can be made. We will have $\lambda(j,m',m) \approx (j + \frac{1}{2})^2$ and, for $m' = m$ or for both around a value of 1 we will have

$$\left[\frac{\Gamma(j+m'+1)\Gamma(j-m+1)}{\Gamma(j+m+1)\Gamma(j-m'+1)}\right]^{\frac{1}{2}} \cdot \quad \lambda(j,m',m)^{-(m'-m)/2} \approx 1$$

and thus

$$d^j_{m'm}(\beta) \equiv (-1)^{m'-m} J_{m'-m}[2(j+\tfrac{1}{2})\ \mathrm{Sin}\tfrac{1}{2}\beta] \qquad 3C.10$$

This extremely elegant approximation to the d^j function has been widely used in two body scattering, however in the present case there is a difficulty in using this form. It will be perfectly adequate for small values of the mssing mass helicity, λ_X, but theoretically λ_X can become very large as greater helicity flip into the missing mass state takes place. We remark here that for $\beta = 0$ no helicity flip into the missing mass state can take place, and helicity flip will be suppressed for small values of β.

Setting these problems aside we can say at least for small values of λ_X that

$$H_{\lambda_X} = \frac{1}{4\pi^2} \int dJ\ (J + \tfrac{1}{2}) \int dJ'(J' + \tfrac{1}{2})$$

$$J=\max\{|\bar{\mu}_1||\bar{\mu}_2|\}\ J'=\max\{|\mu_1||\mu_2|\}$$

$$\bar{J}^{-\bar{\mu}_1-\bar{\mu}_2}_{\mu_1-\mu_2}(2(J+\tfrac{1}{2})\mathrm{Sin}\tfrac{1}{2}\theta)\ J_{\mu_1-\mu_2}(2(J'+\tfrac{1}{2})\mathrm{Sin}\tfrac{1}{2}\theta')$$

$$h_{\lambda_X}(J, J', s, M_X^2). \qquad 3C.11$$

If we now define

$$b = (J + \tfrac{1}{2})/k \qquad \tau = 2k\mathrm{Sin}\tfrac{1}{2}\theta$$

$$b' = (J' + \tfrac{1}{2})/k \qquad \tau' = 2k\mathrm{Sin}\tfrac{1}{2}\theta'$$

where k is the modulus of the three momentum of the initial particles then

$$H_{\lambda_x} = \frac{1}{4\pi^2} \int_{b_o}^{\infty} dbb\, J_{\bar{\mu}_1 - \bar{\mu}_2}(b\tau) \int_{b'_o}^{\infty} db'b'\, J_{\mu_1 \bar{\mu}_2}(b'\tau')$$

$$h_{\lambda_x}(b, b', s, M_x^2) \qquad 3C.12$$

where

$$kb_o = \max\{|\bar{\mu}_1|, |\bar{\mu}_2|\}$$

$$kb'_o = \max\{|\mu_1|, |\mu_2|\} \qquad 3C.13$$

For high energy interactions k goes as $\sqrt{s}$ and so, if λ_x is small we can set b_o and b'_o to zero. As the missing mass increases, so should the available spin states, thus in our previous notation the s_x sum extends to larger values, and with s_x the possible values of λ_x that can be attained. If the maximum s_x that we need consider increases as M_x^2 then in a kinematic region with M_x^2/s fixed we have b_o increasing as $\sqrt{s}$ for the largest possible values of λ_x we need consider. If s_x increases only as $(M_x^2)^{\frac{1}{2}}$ then b_o will behave as a constant for large λ_x, and for s_x increasing less rapidly with M_x^2 we will be able to set b_o to zero for all values of λ_x encountered.

Assuming that this is the case, or at least for small values of λ_x we can invert 3C.12 using the orthogonality properties of the Bessel function, namely

$$\int_0^{\infty} xJ_\nu(ax)\, J_\nu(a'x)dx = \frac{1}{a}\,\delta(a' - a') \,. \qquad 3C.14$$

Thus

$$h_{\lambda_x}(b', b, s, M_x^2) = 4\pi^2 \int_0^{\infty} d\tau\tau\; J_{\bar{\mu}_1 - \bar{\mu}_2}(b\tau)$$

$$\int_0^{\infty} d\tau'\tau'\, J_{\mu_1 - \mu_2}(b'\tau')\, H_{\lambda_x}(\tau, \tau', s, M_x^2) \qquad 3C.15$$

CHAPTER IV

A Closed Regge-Eikonal Formula For Multiple Exchange Contributions to the Inclusive Six Point Function

INTRODUCTION

In the previous chapter we formulated a fairly simple model for applying absorption type corrections to inclusive spectra, more on a phenomenological level then theoretical, but were forced at the end to conclude that it could not account, in the given form, for the physics of the situation. The choice is to persevere with the basic framework of this simple model and add some complexity and refinement to the structure, or to attempt to derive a completely new formula which will not contain any of the basic defects of the old.

There have been by now, many attempts at the problem of introducing corrections of the re-scattering or multiple exchange type. Several [36,46]concentrate on the initial channel as we did in the previous chapter. Pumplin [40] argues that rescattering between the final particle and the non-dissociating particle in the fragmentation region should be the important mechanism. Paige and Trueman[38] analyse the situation from the standpoint of Gribov calculus, but are unable to present a phenomenologically useful formula due to the generality of their method.

We wish to produce a closed formula that will be of greater generality than the approaches which take one or other of the possible rescattering channels into account. To this end we will work with the Regge-Eikonal Approximation, first proposed by Frautschi and Margolis [70] and subsequently given a certain amount of respectability when it was derived by summing nested ladder diagrams in a ϕ^3 theory, with certain extra assumptions

[71]It must be emphasised here that one of the primary purposes of this derivation will be to determine precisely which assumptions must be made in order to extend this concept from the two body case where kinematical considerations dictate that the exchanged momentum become transverse, to the inclusive or 3-body case where more complex considerations come into force.

The technique we use in order to arrive at our eikonal approximation will be a simple generalisation of that of Abarbaniel and Itzykson[72] . They use the technique of functional derivation to sum up all multi-meson exchanges in a two body case. In Appendix 4A we present this technique in slightly more detail than that found in the reference.

The generalisation we use involves partly the exchange of four point Green's functions whose legs we composed of spinless mesons. We use this form since it is suggestive of exchanging sums of ϕ^3 ladders which, in a leading logarithm calculation add up to a Regge pole behaved exchange[73] which is the behaviour we require finally.

DERIVATION IN THE THREE BODY CASE

In this section we wish to proceed with the derivation of a Regge-Eikonal correction to the one-particle inclusive reaction. We start by considering the three body "amplitude" shown in figure 4.1. For simplicity we consider the equal masses case. We do this by exchanging four point Greens functions between various of the legs of the six point functions. Since we will finally wish to go to the Regge limit of these four point functions, we exchange them only between legs that will have a large channel energy in the limit that interests us namely $s\to\infty$, $s/M_X^2\to\infty$. Bearing in mind that we wish to take a discontinuity in M_X^2 we need only consider exchanges between a, c and b legs and $\bar{a}$, $\bar{c}$ and $\bar{b}$ legs. All other exchanges will either not Reggerize or, in the eikonal approximation to be taken later, will disappear when the M_X^2 discontinuity is taken.

We must then, write the analogue of equation 4A.1 for the three body case which interests us. This is complicated by the fact that we must attach not only four point Green's function in all combinations, but also a six-point Green's function which we will take to account for the,possibly,large momentum changes between particle a and particle c in the fragmentation region.

One expression we could use for this would be

$$(2\pi)^4\delta^4(p_a+p_b-p_c-p_{\bar{a}}-p_{\bar{b}}+p_{\bar{c}})\;H(p_a,p_b,p_c;p_{\bar{a}},p_{\bar{b}},p_{\bar{c}})$$

$$= D^*D_Y D\;\mathrm{Lt}_{p_\alpha^2\to m^2}\;\Pi(p_\alpha^2-m^2)\langle p_c|GC\,)G_o^{-1}G(A)|p_a\rangle$$

$$\langle p_{\bar{b}}|G(B)G_o^{-1}G(B)|p_b\rangle\langle p_{\bar{a}}|G(A)G_o^{-1}G(C)|p_c\rangle\Big|_{\substack{A=B=C=0\\ \bar{A}=\bar{B}=\bar{C}=0}} \qquad 4.1$$

where the D,D* operators would account for the exchange of the four point functions in all possible combinations and the term D_Y would have the form

$$D_Y = \int \prod_{i=1}^{6} d^4y_i G^6(y_1 \ldots y_6) \frac{\delta}{\delta A(y_1)} \frac{\delta}{\delta G(y_2)} \frac{\delta}{\delta \bar{C}(y_3)}$$

$$\frac{\delta}{\delta \bar{A}(y_4)} \frac{\delta}{\delta \bar{B}(y_5)} \frac{\delta}{\delta B(y_6)} \qquad 4.2$$

which could account for, say, a charge exchange reaction between particles a and c. The formulation of equation 4.1 would lead to diagrams of the form shown in figure 4.4, where the attachments of the legs deriving from the D_s and D_Y are intermingled. Only in the case where no large momentum need travel through the various Green's functions i.e. the case where M_x^2 is small, could this formulation possibly eikonalise in its entirety. For M_x^2 large, at some stage large components of longitudinal momentum must flow away from the momentum of particle a to form the large missing mass.

Since our task is not to consider in detail these complex momentum effects we accordingly assume that our four-point Green's functions G^4 are strongly suppressed not merely for large $|q^2|$ (see figure 4.2) but also for large components of momentum travelling down any of the legs. This assumption of $k/\sqrt{s} \to o$ is after all the main content of the eikonal approximation. We also however, insist that the large components of momentum do flow down the legs of the six-point Green's function, G^6. This treats two objects, which might seem superficially similar, in a completely different manner. The main justification for this is that it allows us to achieve our stated end.

We can then, either discard completely those terms which are represented by that of figure 4.4, or, since time ordering becomes unimportant in the eikonal approximation, we could consider gathering together the legs of the G^4 that intersperse those of the G^6 and separate them from the G^4's, that will eikonalise. This amounts to a redefinition for the input G^6.

Whichever of these courses is adopted we utilise the completeness relation

$$\int \frac{d^4p}{(2\pi)^4} \; 2\pi\delta^+(p^2-m^2)\,|p><p| \; = 1 \qquad 4.3$$

since the scources act only on single particle states and can then write

$$(2\pi)^4\delta^4(p_a+p_b-p_c-p_{\bar{a}}-p_{\bar{b}}+p_{\bar{c}})\; H(p_a,p_b,p_c;p_{\bar{a}},p_{\bar{b}},p_{\bar{c}})$$

$$= D^*D \int \prod_{\alpha,\bar{\alpha}} \frac{d^4p'_\alpha}{(2\pi)^4} \frac{d^4p'_{\bar{\alpha}}}{(2\pi)^4} \; 2\pi\delta^+(p'^2_\alpha-m^2)\,2\pi\delta^+(p'^2_{\bar{\alpha}}-m^2)$$

$$(2\pi)^4\delta^4(p'_a+p'_b-p'_c-p'_{\bar{a}}-p'_{\bar{b}}+p'_{\bar{c}})$$

$$\tau^*(p_{\bar{a}},p'_{\bar{a}};\bar{A})\;\tau^*(p_{\bar{b}},p'_{\bar{b}};B)\;\tau^*(p_{\bar{c}},p'_{\bar{c}};C)$$

$$Y(p'_a,p'_b,p'_c;p'_{\bar{a}},p'_{\bar{b}},p'_{\bar{c}})$$

$$\tau(p_c,p'_c;C)\;\tau(p_b,p'_b;B)\;\tau(p_a,p'_a;A)\Big|_{\substack{A=B=C=0\\ \bar{A}=\bar{B}=\bar{C}=0}} \qquad 4.4$$

where

$$\tau(p_\alpha, p_\alpha'; A) = \langle p_\alpha' | T\exp\{-i\int_0^\infty d\tau A(X-2P\tau)\}A(X)|p_\alpha\rangle \qquad 4.5$$

whose derivation can be found in Appendix 4A.

We can now define the two operators D and D^*.

We say

$$D = D_{ab}\left(\frac{\delta}{\delta A}, \frac{\delta}{\delta B}\right) D_{ac,b}\left(\frac{\delta}{\delta A}, \frac{\delta}{\delta C}, \frac{\delta}{\delta B}\right) D_{cb}\left(\frac{\delta}{\delta C}, \frac{\delta}{\delta B}\right)$$

$$D_{ab} = \exp\left[i\int\prod_{i=1}^{4} d^4y_i \frac{\delta}{\delta A(y_1)} \frac{\delta}{\delta A(y_2)} G^4(y_1, y_2, y_3, y_4) \frac{\delta}{\delta B(y_3)} \frac{\delta}{\delta B(y_4)}\right]$$

$$D_{ac,b} = \exp\left[i\int\prod_{i=1}^{4} d^4y_i \frac{\delta}{\delta A(y_1)} \frac{\delta}{\delta C(y_2)} G^4(y_1, y_2, y_3, y_4) \frac{\delta}{\delta B(y_3)} \frac{\delta}{\delta B(y_4)}\right] \qquad 4.6$$

The eikonal approximation can be made in equation 4.5 in a similar manner to that in Appendix 4A exvept that instead of the symmetric approximation used there we replace the operator P in each τ by the external momentum. This should not lead to extreme errors and simplifies the calculations.

Thus

$$\tau_\alpha(p', p; A) = \int d^4x e^{i(p-p')\cdot x} \frac{\partial}{i\partial\alpha} \exp\left[-i\int_\alpha^\infty d\tau A(x-2p\tau)\right] \qquad 4.7$$

We can also carry out the functional differentiation by noticing that it acts as a shift operator as in Appendix 4A and we find the lengthy expression arises

$$(2\pi)^4\delta^4(p_a+p_b-p_c-p_{\bar{a}}-p_{\bar{b}}+p_{\bar{c}})H(p_a,p_b,p_c;p_{\bar{a}},p_{\bar{b}},p_{\bar{c}})$$

$$=\int\prod_{\gamma\,\bar{\gamma}}\frac{d^4p'_\gamma}{(2\pi)^4}\frac{d^4p'_{\bar{\gamma}}}{(2\pi)^4}\,2\pi\delta^+(p'^2_\gamma-m^2)\,2\pi\delta^+(p'^2_{\bar{\gamma}}-m^2)$$

$$\int\prod_{\beta\,\bar{\beta}}d^4x_\beta\,d^4x_{\bar{\beta}}\,e^{i(p_a-p'_a)\cdot x_a+i(p_b-p'_b)\cdot x_b+i(p'_c-p_c)\cdot x_c}$$

$$e^{i(p_{\bar{a}}-p_{\bar{a}})\cdot x_a+i(p_{\bar{b}}-p_{\bar{b}})\cdot x_b+i(p_{\bar{c}}-p_{\bar{c}})\cdot x_c}\,\frac{\partial}{i\partial\alpha_a}\,\frac{\partial}{i\partial\alpha_b}\,\frac{\partial}{i\partial\alpha_c}$$

$$\exp\Big[i\int_{\alpha_a}^{\infty}d\tau_a d\tau_a\int_{\alpha_b}^{\infty}d\tau_b d\tau_b\,G^4_{ab}$$

$$+i\int_{\alpha_a}^{\infty}d\tau_a\int_{\alpha_c}^{\infty}d\tau_c\int_{\alpha_b}^{\infty}d\tau_b d\tau'_b G^4_{ac,b}+i\int_{\alpha_c}^{\infty}d\tau_c d\tau'_c\int_{\alpha_b}^{\infty}d\tau_b d\tau'_b G^4_{cb}\Big]$$

$$(2\pi)^4\delta^4(p'_a+p'_b-p'_c-p'_{\bar{a}}-p'_{\bar{b}}+p'_{\bar{c}})\;Y(Q'_{ac},Q'_{\bar{a}\bar{c}},Q'_{b\bar{b}},s_{ab},M_x^2)$$

$$\frac{\partial}{-i\partial\alpha_{\bar{a}}}\,\frac{\partial}{-i\partial\alpha_{\bar{b}}}\,\frac{\partial}{-i\partial\alpha_{\bar{c}}}\exp\Big[i\int_{\alpha_{\bar{a}}}^{\infty}d\tau_{\bar{a}}d\tau'_{\bar{a}}\int_{\alpha_{\bar{b}}}^{\infty}d\tau_{\bar{b}}d\tau'_{\bar{b}}\,G^{4*}_{\bar{a}\bar{b}}$$

$$+i\int_{\alpha_{\bar{a}}}^{\infty}d\tau_{\bar{a}}\int_{\alpha_{\bar{c}}}^{\infty}d\tau_{\bar{c}}\int_{\alpha_{\bar{b}}}^{\infty}d\tau_{\bar{b}}\,d\tau'_{\bar{b}}\;G^{4*}_{\bar{a}\bar{c},\bar{b}}+i\int_{\alpha_{\bar{c}}}^{\infty}d\tau_{\bar{c}}\,d\tau'_{\bar{c}}\int_{\alpha_{\bar{b}}}^{\infty}d\tau_{\bar{b}}\;\;d\tau'_{\bar{b}}\,G^{4*}_{\bar{c}\bar{b}}\Big]\quad 4.8$$

where

$$Q'_{ac}=(p'_a-p'_c),\;Q'_{\bar{a}\bar{c}}=(p'_{\bar{a}}-p'_{\bar{c}}),\;Q'_{b\bar{b}}=(p'_b-p'_{\bar{b}})$$

and

$$G^4_{ab}=G(2p_a(\tau_a-\tau'_a),x_a-x_b-p_a(\tau_a+\tau'_a)+p_b(\tau_b+\tau'_b),2p_b(\tau'_b-\tau_b))$$

$$G^4_{cb}=G(2p_c(\tau_c-\tau'_c),x_c-x_b-p_c(\tau_c+\tau'_c)+p_b(\tau_b+\tau'_b),2p_b(\tau'_b-\tau_b))$$

$$G^4_{ac,b}=G(x_a-2p_a\tau_a-x_c+2p_c\tau_c,\tfrac{1}{2}(x_a+x_c)-x_b-p_a\tau_a-p_c\tau_c+$$

$$p_b(\tau_b+\tau'_b),2p_b(\tau_b-\tau'_b))\qquad 4.9$$

Before we continue further there are two points of interest to note about the form of equation 4.8. The first is that, as will shortly become clear, we can define two independant impact parameters Bab, Bcb. In the case of $M_x^2 \to 0$ where we have quasi-two-body scattering we would not expect these impact paramters to be independant. However, for large M_x^2 we would expect such independance from naive physical arguments. Secondly we must realise that equation 4.8 does not give the whole story - it forms the most complicated part but does not allow for diagrams where some of the possible elastic scatterings do not occur, and most transparently does not allow for the case where no intermediate scattering takes place. These unconnected, or partially unconnected pieces could be allowed for at this stage, but the resulting expression would be considerably longer than 4.8. The analysis for these pieces would also be simpler than for the expression of 4.8. We therefore carry this analysis through and remark at a later stage what effect the inclusion of these pieces would be.

We simplify the expression of equation 4.8 by making various transformations of variables. The first will be

$$y_{ab} = x_a - x_b, y_{cb} = x_c - x_b, \; X = \frac{1}{3}(x_a + x_b + x_c)$$

$$y_{\overline{ab}} = x_{\overline{a}} - x_{\overline{b}}, \; y_{\overline{cb}} = x_{\overline{c}} - x_{\overline{b}}, \; \overline{X} = \frac{1}{3}(x_{\overline{a}} + x_{\overline{b}} + x_{\overline{c}}) \qquad 4.10$$

The Jacobeans of these transformations are unity.

Equation 4.9 tells us that there is no dependance on X or $\overline{X}$ in either of the exponential factors and of course Y is defined as translationally invariant so we immediately perform the d^4X, $d^4\overline{X}$ integrations which produce the factors

$$(2\pi)^4\delta^4(p_a+p_b-p_c-p_a'-p_b'+p_c')(2\pi)^4\delta^4(p_{\bar{a}}+p_{\bar{b}}-p_{\bar{c}}-p_{\bar{a}}'-p_{\bar{b}}'+p_{\bar{c}}')$$

These two δ-functions allow us, in combination with that already existing, both to factor of the overall conservation of momentum δ-function and also to perform the d^4p_b and $d^4p_{\bar{b}}$ integration. If we also notice that, having performed these integrations we have

$$e^{i(\frac{2}{3}(p_a-p_a')-\frac{1}{3}(p_b-p_c-p_b'+p_c'))\cdot y_{ab}} = e^{i(p_a-p_a')\cdot y_{ab}}$$

$$e^{i(\frac{2}{3}(p_c'-p_c)-\frac{1}{3}(p_a+p_b-p_a'-p_b'))\cdot y_{ab}} = e^{i(p_c'-p_c)\cdot y_{ab}}$$

We can write

$$H(Q_{ac}^2, s_{ab}, M_x^2) = \int \frac{d^4p_a'}{(2\pi)^4}\frac{d^4p_c'}{(2\pi)^4}\, 2\pi\delta^+(p_a'^2-m^2)$$

$$2\pi\delta^+(p_c'^2-m^2)\; 2\pi\delta^+(p_b'^2-m^2)$$

$$\int \frac{d^4p_{\bar{a}}'}{(2\pi)^4}\frac{d^4p_{\bar{c}}'}{(2\pi)^4}\, 2\pi\delta^+(p_{\bar{a}}'^2-m^2)\,2\pi\delta^+(p_{\bar{b}}'^2-m^2)\,2\pi\delta^+(p_{\bar{c}}'^2-m^2)$$

$$\int d^4y_{ab}\,d^4y_{cb}\,d^4y_{\bar{a}\bar{b}}\,d^4y_{\bar{c}\bar{b}}\; e^{i(p_a-p_a')\cdot y_{ab}}\; e^{i(p_c'-p_c)\cdot y_{cb}}$$

$$e^{i(p_{\bar{a}}'-p_{\bar{a}})\cdot y_{\bar{a}\bar{b}}}\; e^{i(p_{\bar{c}}-p_{\bar{c}}')\cdot y_{\bar{c}\bar{b}}}\; \frac{\partial}{i\partial\alpha_a}\,\frac{\partial}{i\partial\alpha_b}\,\frac{\partial}{i\partial\alpha_c}\,\frac{\partial}{-i\partial\alpha_{\bar{a}}}$$

$$\frac{\partial}{-i\partial\alpha_{\bar{b}}}\,\frac{\partial}{-i\partial\alpha_{\bar{c}}}\; \exp[iV_{ab}+iV_{ac,b}+iV_{cb}]\quad Y(Q_{ac}',Q_{\bar{a}\bar{c}}',Q_{\bar{b}\bar{b}}',s_{ab},M_x^2)$$

$$\exp[-iV_{\bar{a}\bar{b}}^* - iV_{\bar{a}\bar{c},\bar{b}}^* - iV_{\bar{c}\bar{b}}^*]$$

where

$$V_{ab} = \int_{\alpha_a}^{\infty} d\tau_a d\tau_a' \int_{\alpha_b}^{\infty} d\tau_b d\tau_b' G^4_{ab}$$

$$V_{ac,b} = \int_{\alpha_a}^{\infty} d\tau_a \int_{\alpha_c}^{\infty} d\tau_c \int_{\alpha_b}^{\infty} d\tau_b d\tau_b' G^4_{ac,b}$$

$$V_{cb} = \int_{\alpha_c}^{\infty} d\tau_c d\tau_c' \int_{\alpha_b}^{\infty} d\tau_b d\tau_b' G^4_{cb}$$

$$V^*_{\bar{a}\bar{b}} = \int_{\alpha_{\bar{a}}}^{\infty} d\tau_{\bar{a}} d\tau_{\bar{a}}' \int_{\alpha_{\bar{b}}}^{\infty} d\tau_{\bar{b}} d\tau_{\bar{b}}' G^{4*}_{\bar{a}\bar{b}}$$

$$V^*_{\bar{a}c,\bar{b}} = \int_{\alpha_{\bar{a}}}^{\infty} d\tau_{\bar{a}} \int_{\alpha_{\bar{c}}}^{\infty} d\tau_{\bar{c}} \int_{\alpha_{\bar{b}}}^{\infty} d\tau_{\bar{b}} d\tau_{\bar{b}}' G^{4*}_{\bar{a}c,\bar{b}}$$

$$V_{\bar{c}b} = \int_{\alpha_{\bar{c}}}^{\infty} d\tau_{\bar{c}} d\tau_{\bar{c}}' \int_{\alpha_{\bar{b}}}^{\infty} d\tau_{\bar{b}} d\tau_{\bar{b}}' G_{\bar{c}b} \qquad 4.11$$

The next changes of variables we make are the Sudakov decompositions

$$y_{ab} = B_{ab} - 2\,\sigma_{ab}\,p_a + 2\,\sigma_{ab}'\,p_b$$

$$y_{cb} = B_{cb} - 2\,\sigma_{cb}\,p_c + 2\,\sigma_{cb}'\,p_b \qquad 4.12$$

where $B_{ab}\cdot p_a = B_{ab}\cdot p_b = B_{cb}\cdot p_c = B_{cb}\cdot p_b = 0$

with a similar decomposition for the barred variables.

We also define the momentum transfer variables

$Q_a = (p_a - p_a')$, $Q_c = (p_c' - p_c)$ and similarly for the barred variables.

In a completely analogous manner to the shift of integration variables we found in 4A19 and 20 in Appendix A we can now shift the τ-integration variables. In the two-body case this accounts for all the σ integrations eventually, bit in this case we account only for six out of the eight. We also rewrite the d^4p_α' integrations in terms of the Q_α s, which is a simple shift of origin and we find

$$H = (2\pi)^{-8} \int d^4Q_a d^4Q_c d^4\bar{Q}_a d^4\bar{Q}_c \delta^+(p_a'^2 - m^2)\delta^+(p_b'^2 - m^2)$$

$$\delta^+(p_c'^2 - m^2)\ \delta^+(p_a'^2 - m^2)\ \delta^+(p_b'^2 - m^2)\ \delta^+(p_c'^2 - m^2) J_{ab}\ J_{cb} J_{\bar{a}\bar{b}}\ J_{\bar{c}\bar{b}}$$

$$\int d\ B_{ab} d\ B_{cb} e^{iQ_a \cdot B_{ab}}\ e^{iQ_c \cdot B_{cb}} \int d\ B_{\bar{a}\bar{b}} d\ B_{\bar{c}\bar{b}}\ e^{-i\bar{Q}_a \cdot B_{\bar{a}\bar{b}}}\ e^{-i\bar{Q}_c \cdot B_{\bar{c}\bar{b}}}$$

$$\int d\sigma_{ab} d\sigma_{ab}' d\sigma_{cb} d\sigma_{\bar{a}\bar{b}} d\sigma_{\bar{a}\bar{b}}' d\sigma_{\bar{c}\bar{b}}\ \ \frac{d\sigma}{2\pi}\ e^{2i\sigma(Q_c \cdot p_b)}\ \ \frac{d\bar{\sigma}}{2\pi}\ e^{2i\bar{\sigma}(\bar{Q}_c \cdot \bar{p}_b)}$$

$$\frac{\partial}{\partial \sigma_{ab}}\ \frac{\partial}{\partial \sigma_{ab}'}\ \frac{\partial}{\partial \sigma_{cb}}\ \exp[iV_{ab} + iV^{\sigma}_{ac,b} + iV^{\sigma}_{cb}]$$

$$Y(Q_{ac}', \bar{Q}_{\bar{a}\bar{c}}', \bar{Q}_{\bar{b}\bar{b}}', s_{ab}', M_x^2)$$

$$\frac{\partial}{\partial \sigma_{ab}} \frac{\partial}{\partial \sigma_{ab}'} \frac{\partial}{\partial \sigma_{cb}} \exp[-iV^{*}_{ab} - iV^{\bar{\sigma}*}_{ac,b} - iV^{\bar{\sigma}*}_{cb}] \qquad 4.13$$

where $\sigma = \sigma_{ab}' - \sigma_{cb}'$, $\bar{\sigma} = \sigma_{\bar{a}\bar{b}}' - \sigma_{\bar{c}\bar{b}}'$

and $J_{\alpha\beta} = 4\ (p_\alpha \cdot p_\beta - p_\alpha^2\ p_\beta^2)^{\frac{1}{2}}$

We further define

$$Q_{ac'} = p_a' - p_c' = Q_{ac} - Q_a + Q_c;\ Q_{ac} = p_a - p_c$$

$$Q_{\overline{ac}'} = p_{\overline{a}}' - p_{\overline{c}}' = Q_{\overline{ac}} - Q_{\overline{a}} + Q_{\overline{c}};\ Q_{\overline{ac}} = p_{\overline{a}} - p_{\overline{c}}$$

$$Q_{b\overline{b}'} = p_{\overline{b}}' - p_b' = Q_{\overline{a}} + Q_{\overline{c}} - Q_a - Q_c$$

$$V_{ab} = \int_{\alpha_a}^{\infty} d\tau_a\, d\tau_a' \int_{\alpha_b}^{\infty} d\tau_b d\tau_b' G^4 (2p_a(\tau_a'-\tau_a),$$

$$B_{ab} - p_a(\tau_a+\tau_a') + p_b(\tau_b+\tau_b'),\ 2p_b(\tau_b'-\tau_b)$$

$$V^{\sigma}_{ac,b} = \int_{\alpha_a}^{\infty} d\tau_a \int_{\alpha_c}^{\infty} d\tau_c \int_{\alpha_b}^{\infty} d\tau_b d\tau_b' G^4 (B_{ab} - B_{cb} - 2p_a\tau_a + 2p_c\tau_c - 2\sigma p_b$$

$$\tfrac{1}{2}(B_{ab}+B_{cb}) - p_a\tau_a - p_c\tau_c + p_b(\tau_b+\tau_b') + 2\sigma p_b, 2p_b(\tau_b'-\tau_b))$$

$$V^{\sigma}_{cb} = \int_{\alpha_c}^{\infty} d\tau_c d\tau_c' \int_{\alpha_b}^{\infty} d\tau_b d\tau_b' G^4 (2p_c(\tau_c'-\tau_c),$$

$$B_{cb} - p_c(\tau_c+\tau_c') + p_b(\tau_b+\tau_b') + 2p_b\sigma, 2p_b(\tau_b'-\tau_b))$$

and similarly for the barred quantities.

It is now possible to carry out the integration of the total derivatives implied in equation 4.13. If we consider one half (the unbarred half) the result contains the term

$$\exp[i\chi_{ab} + i\chi_{ac,b} + i\chi_{cb}]$$

where χ_{ab} represents V_{ab} with the lower limits of integration $(-\sigma_{ab}, -\sigma_{ab}')$ taken to $-\infty$. This is the only term we would expect, however, we also obtain terms

$$\exp[i\chi_{ab}] + \exp[i\chi_{cb}] - 1$$

that these terms are included arises from the formulation of equation 4.4 which only accounts for diagrams where all possible types of interaction are connected. Clearly the term 1 would be cancelled if no intermediate scattering took place and similarly the terms exp $[i\chi_{ab}]$ and exp$[i\chi_{cb}]$ are cancelled by the terms where only a-b or c-b rescattering takes place. The term which does survive is then

$$S(B_{ab},B_{cb},\sigma) = \int_{-\infty}^{\infty} d^2B_{ab}d^2B_{cb}\; e^{iQ_a\cdot B_{ab}}\; e^{iQ_c\cdot B_{cb}}$$

$$\exp[i\chi_{ab} + i\chi^{\sigma}_{ac,b} + i\chi^{\sigma}_{cb}] \qquad 4.14$$

The final transformation to be made is to decompose Q_a and Q_c into their transverse and longitudinal parts according to

$$Q_a = \frac{2p_b\cdot Q_a}{2p_a\cdot p_b}\; p_a + \frac{2p_a\cdot Q_a}{2p_a\cdot p_b}\; p_b + \vec{Q}_a$$

$$Q_c = \frac{2p_b\cdot Q_c}{2p_c\cdot p_b}\; p_c + \frac{2p_c\cdot Q_c}{2p_c\cdot p_b}\; p_b + \vec{Q}_c$$

where $\vec{Q}_a\cdot p_a = \vec{Q}_a\cdot p_b = 0$

$$\vec{Q}_c\cdot p_c = \vec{Q}_c\cdot p_b = 0 \qquad 4.15$$

We have in equation 4.15 neglected terms of order Q_a^2/S and so on.

Also we consider the mass-shell delta functions, for example

$$\delta^{+}(p_a'^2 m^2) = \delta((p_a - Q_a)^2 - m^2)$$

$$= \delta(2p_a \cdot Q_a - Q_a^2)$$

and so on.

Having done this we arrive at the expression

$$H = (2\pi)^{-8} \int_{-\infty}^{\infty} d^2\vec{Q}_a d^2\vec{Q}_c d^2\vec{Q}_{\bar{a}} d^2\vec{Q}_{\bar{c}}\; e^{i\vec{Q}_a \cdot B_{ab} + i\vec{Q}_c \cdot B_{cb} - i\vec{Q}_{\bar{a}} \cdot B_{\bar{a}\bar{b}} - i\vec{Q}_c \cdot B_{cb}}$$

$$\int_{-\infty}^{\infty} d\alpha d\bar{\alpha} \int_{-\infty}^{\infty} d(p_a \cdot Q_a)\, d(p_b \cdot Q_a)\, 2\delta(2Q_a \cdot p_a - Q_a^2)\, \delta(2Q_a \cdot p_b + \alpha - (Q_a + Q_c)^2)$$

$$\int_{-\infty}^{\infty} d(p_c \cdot Q_c)\, d(p_b \cdot Q_c)\, 2\delta(2p_c \cdot Q_c + Q_c^2)\, \delta(2p_b \cdot Q_c - \alpha)$$

$$\int_{-\infty}^{\infty} d(p_{\bar{a}} \cdot Q_{\bar{a}})\, d(p_{\bar{b}} \cdot Q_{\bar{a}})\, 2\delta(2p_{\bar{a}} \cdot Q_{\bar{a}} - Q_{\bar{a}}^2)\, \delta(2p_{\bar{b}} \cdot Q_{\bar{a}} + \bar{\alpha} + (Q_{\bar{a}} + Q_{\bar{c}})^2)$$

$$\int_{-\infty}^{\infty} d(p_{\bar{c}} \cdot Q_{\bar{c}})\, d(p_{\bar{b}} \cdot Q_{\bar{c}})\, 2\delta(2p_{\bar{c}} \cdot Q_{\bar{c}} + Q_{\bar{c}}^2)\, \delta(2p_b \cdot Q_{\bar{c}} - \bar{\alpha})$$

$$\int_{-\infty}^{\infty} \frac{d\sigma}{2\pi} e^{i\alpha\sigma} \int_{-\infty}^{\infty} \frac{d\bar{\sigma}}{2\pi} e^{-i\bar{\alpha}\bar{\sigma}}\, S(Q_a, Q_c, \sigma)$$

$$Y(Q_{ac}', Q_{\bar{a}\bar{c}}', Q_{b\bar{b}}', s_{ab}, M_X^2)\, S^*(Q_{\bar{a}}, Q_{\bar{c}}, \bar{\sigma}) \qquad 4.16$$

In equation 4.16 we note that the Jacobeans of this most recent calculation cancel with the Jacobeans $J_{ab}, J_{cb}, J_{ab}, J_{cb}$ of a previous transformation to order 1/s and also we have introduced the variables α and $\bar{\alpha}$ via the insertion of

$$\int_{-\infty}^{\infty} d\alpha\ \delta(2p_b.Q_c-\alpha)\int_{-\infty}^{\infty} d\bar{\alpha}\,\delta(2p_{\bar{b}}.Q_{\bar{c}} - \bar{\alpha})$$

which clarifies some of the forthcoming manipulations.

It is possible to immediately perform eight of the integrations in equation 4.16 and we can of course note that since B_{ab} is orthogonal to both P_a and P_b etc, so remembering that $\alpha = 2p_b.Q_c$

$\bar{\alpha} = 2p_{\bar{b}}.Q_{\bar{c}}$

we can rewrite equation 4.16 in the slightly simpler form

$$H = \int_{-\infty}^{\infty} \frac{d^2\vec{Q}_a}{(2\pi)^2}\frac{d^2\vec{Q}_c}{(2\pi)^2}\frac{d^2\vec{Q}_{\bar{a}}}{(2\pi)^2}\frac{d^2\vec{Q}_{\bar{c}}}{(2\pi)^2}\, e^{i\vec{Q}_a.B_{ab}+i\vec{Q}_c.B_{cb}-i\vec{Q}_{\bar{a}}.B_{\bar{a}\bar{b}}-i\vec{Q}_{\bar{c}}.B_{\bar{c}\bar{b}}}$$

$$\int_{-\infty}^{\infty} d\sigma d\sigma S(\vec{Q}_a,\vec{Q}_c,\sigma)\ S^*(\vec{Q}_{\bar{a}},\vec{Q}_{\bar{c}},\sigma)$$

$$\int_{-\infty}^{\infty}\frac{d\alpha}{2\pi}\, e^{i\alpha\sigma}\int_{-\infty}^{\infty}\frac{d\alpha}{2\pi}\ e^{i\alpha\sigma}\, Y(Q'_{ac},Q'_{\bar{a}\bar{c}},Q'_{\bar{b}\bar{b}},s_{ab},M_x^2) \qquad 4.17$$

This formula is as far as we can proceed without detailed considerations of the dependances of the variables of the Y function. In fact the spirit of the eikonal approximations is present in the choice of variables made.

The full dependance of the Y function could be shown, after taking the forward M_x^2 discontinuity, as

$$Y(Q'^2_{ac},\ Q'^2_{\bar{a}\bar{c}},\ Q'^2_{\bar{b}\bar{b}},\ s'_{ab},\ s'_{\bar{a}\bar{b}},\ M_x^2)$$

M_x^2 cannot be affected by the intermediate rescatterings because of overall conservation of momentum, but if we define

$$s'_{ab} = (p'_a + p'_b)^2$$

$$s'_{\bar{a}\bar{b}} = (p'_{\bar{a}} + p'_{\bar{b}})^2$$

Then these quantities will not be identically equal to s_{ab}. It is not reasonable, in the light of all the other assumptions made, that we would expect the region where these quantities are severely deviated from the original value to be of any importance in our calculation. The expressions for s'_{ab} and $s'_{\bar{a}\bar{b}}$ thus tell us which quantities it is perfectly safe to ignore with respect to s. It turns out that α and $\bar{\alpha}$ are among these and also that Q'^2_{ac} and $Q'^2_{\bar{a}\bar{c}}$ depend only on α/s and $\bar{\alpha}/s$ at worst. These facts are briefly demonstrated in Appendix 4B.

That we can ignore the α and $\bar{\alpha}$ dependance of the Y-function clearly leads to a great simplification of equation 4.17 since we are able to perform the α and $\bar{\alpha}$ integrations and these yield two delta functions of the form $\delta(\sigma)$ and $\delta(\bar{\sigma})$. We then use these δ-functions to perform the σ and $\bar{\sigma}$ integrations, effectively setting $\sigma = \bar{\sigma} = 0$.

If we now take the forward M_x^2 discontinuity and make the definitions

$$t_{ac} = (Q_{ac} - Q_a + Q_c)^2$$

$$t_{\bar{a}\bar{c}} = (Q_{\bar{a}\bar{c}} - Q_{\bar{a}} + Q_{\bar{c}})^2$$

$$t_o = (Q_a + Q_c - Q_{\bar{a}} - Q_{\bar{c}})^2$$

$$t = Q_{ac}^2 = Q_{\bar{a}\bar{c}}^2 \qquad 4.18$$

We have the final form of our expression, namely

$$H(t, s_{ab}, M_x^2) = \int \frac{d^2\vec{Q}_a}{(2\pi)^2} \frac{d^2\vec{Q}_c}{(2\pi)^2} \frac{d^2\vec{Q}_{\bar{a}}}{(2\pi)^2} \frac{d^2\vec{Q}_{\bar{c}}}{(2\pi)^2}$$

$$S(\vec{Q}_a, \vec{Q}_c)\, Y(t_{ac}, t_{\bar{a}\bar{c}}, t_o, s_{ab}, M_x^2)\, S^*(\vec{Q}_{\bar{a}}, \vec{Q}_{\bar{c}})$$

where

$$S = \int d^2B_{ab} d^2B_{cb} e^{i\vec{Q}_a.B_{ab} + i\vec{Q}_c.B_{cb}} e^{i(\chi_{ab}(B_{ab}) + \chi_{ac,b}(B_{ab},B_{cb}) + \chi_{cb}(B_{cb}))}$$

and

$$S^* = d^2B_{ab} d^2B_{\overline{cb}} e^{-i\bar{Q}_a.i\bar{Q}_c.B_{\overline{cb}}} e^{-i(\chi^*_{\overline{ab}}(B_{\overline{ab}}) + \chi^*_{\overline{ac},\overline{b}}(B_{\overline{ab}},B_{\overline{cb}}) + \chi^*_{\overline{cb}}(B_{\overline{cb}}))}$$

4.19

We also use Appendix 4B to show the following

If $p_c = xp_a + yp_b + \vec{p}_{c\perp}$

with $y = \frac{m^2 + \vec{p}^2_{c\perp}}{xs} - \frac{xm^2}{s}$

Then

$$s_{cb} = xs_{ab}, \quad M_x^2 = (1-x)s_{ab}$$

to order 1/s, and also

$$t_{ac} = (2-x)m^2 - \frac{m^2 - (\vec{p}^{\mu}_{c\perp} + x\vec{Q}^{\mu}_a + \vec{Q}^{\mu}_c)^2}{x}$$

$$t_{\overline{ac}} = (2-x)m^2 - \frac{m^2 - (\vec{p}^{\mu}_{c\perp} + x\vec{\bar{Q}}^{\mu}_a + \vec{\bar{Q}}^{\mu}_c)^2}{x}$$

$$t = (2-x)m^2 - \frac{m^2 - \vec{p}^2_{c\perp}}{x}$$

$$t_o = (\vec{Q}^{\mu}_a + \vec{Q}^{\mu}_c - \vec{\bar{Q}}^{\mu}_a - \vec{\bar{Q}}^{\mu}_c)^2$$

4.20

where we note that $\vec{\Gamma}^{\mu}$ is a four vector with only two independant components and that $p^2_{c\perp}$ is a positive quantity.

Our next task is to account for the eikonal phases of equations 4.19 [74].

The expression for χ_{ab} is

$$\chi_{ab} = \int_{-\infty}^{\infty} d\tau_a d\tau_a' \int_{-\infty}^{\infty} d\tau_b d\tau_b' G^4(2p_a(\tau_a'-\tau_a), B_{ab}+p_b(\tau_b'+\tau_b)-p_a(\tau_a+\tau_a'), 2p_b(\tau_b'-\tau_b)) \quad 4.21$$

We can make the change of variable

$$\eta = (\tau_a' - \tau_a),\ \tau = (\tau_a + \tau_a')/2$$

$$\eta' = (\tau_b' - \tau_b),\ \tau' = (\tau_b + \tau_b')/2$$

and this has Jacobean unity. Taking the fourier transform of $G^4(x, y, x')$, and its inverse we have,

$$G^4(x,y,x') = \int \frac{d^4k}{(2\pi)^4} \int \frac{d^4q}{(2\pi)^4} \int \frac{d^4k}{(2\pi)^4}\ \tilde{G}^4(k,q,k') \exp[i(k.x + q.y + k'.x')] \quad 4.22$$

Substituting equation 4.22 into equation 4.21 we have

$$\chi_{ab} = \int \frac{d^4q}{(2\pi)^4} e^{iq.B_{ab}} \int \frac{d^4k}{(2\pi)^4}\ \frac{d^4k'}{(2\pi)^4}\ \tilde{G}^4(k,q,k') \int_{-\infty}^{\infty} d\eta d\tau d\eta' d\tau' \exp(i2p_a.k\tau + i2p_b.k'\tau' - i2p_a.q\eta - i2p_b.q\eta') \quad 4.23$$

Performing the η, η' τ and τ integrations we find

$$\chi_{ab} = \int \frac{d^4q}{(2\pi)^4}\ 2\pi\delta(2p_a.q)\ 2\pi\delta(2p_b.q) e^{iq.B_{ab}} \int \frac{d^4k}{(2\pi)^4}\ \frac{d^4k'}{(2\pi)^4}\ 2\pi\delta(2p_a.k)\ 2\pi\delta(2p_b.k')\ \tilde{G}^4(k,q,k')$$

We make the transformation of variables

$d^4q \to d(2p_a.q)\,d(2p_b.q)\,d^2\vec{Q}$ where $p_a.\vec{Q}^\mu = p_b.\vec{Q}^\mu = 0$, and this has Jacobean $1/2\ s_{ab}$ (see Appendix 4A).

We can therefore write

$$\chi_{ab} = \frac{1}{2\ s_{ab}} \int \frac{d^2Q}{(2\pi)^2}\, e^{iQ.B_{ab}} \int \frac{d^4k}{(2\pi)^4}\, 2\pi\delta(2p_a.k)$$

$$\int \frac{d^4k'}{(2\pi)^4}\ 2\pi\delta(2p_b.k')\ \ \tilde{G}^4(k,q,k') \qquad 4.24$$

We use the relation

$$\underset{\varepsilon\to 0}{Lt} + \left[\frac{1}{-2p.k+i\varepsilon} + \frac{1}{2p.k+i\varepsilon}\right] = 2\pi\delta(2p.k)$$

and also note that for $s\to\infty$; $k^2/\sqrt{s}$, $t/\sqrt{s}\to 0$ we have

$$\frac{1}{(p-k)^2-m^2+i\varepsilon} + \frac{1}{(p+k)^2-m^2+i\varepsilon} \simeq \frac{1}{-2p.k+i\varepsilon} + \frac{1}{2p.k+i\varepsilon}$$

Thus the expression

$$\int \frac{d^4k}{(2\pi)^4}\ 2\pi\delta(2p_a.k) \int \frac{d^4k'}{(2\pi)^4}\ 2\pi\delta(2p_b.k)\ \tilde{G}^4(k,q,k') \qquad 4.25$$

represents the four diagrams shown in figure 4.5 in a high energy limit. In a ladder approximation these diagrams sum up to a signatured Regge pole, allowing for overcounting and so equation 4.24 is the Fourier Bessel transform for this expression and can be written as

$$\chi_{ab} = \frac{1}{s_{ab}} \int \frac{d^2\vec{Q}}{(2\pi)^2}\, e^{i\vec{Q}.B_{ab}}\, \beta_a(-\vec{Q}^2)\beta_b(-\vec{Q}^2)\xi(-\vec{Q}^2)\ s_{ab}^{\alpha(-\vec{Q}^2)} \qquad 4.26$$

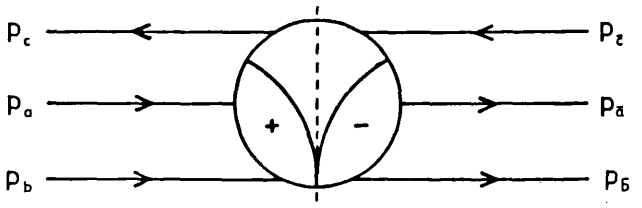

Figure 4·1.The three-body "amplitude" used for considering single particle inclusive reactions.

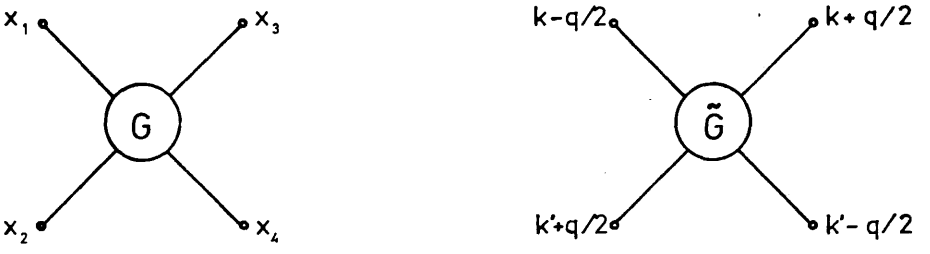

Figure 4·2.The four-point Green's function used as a basic exchange.

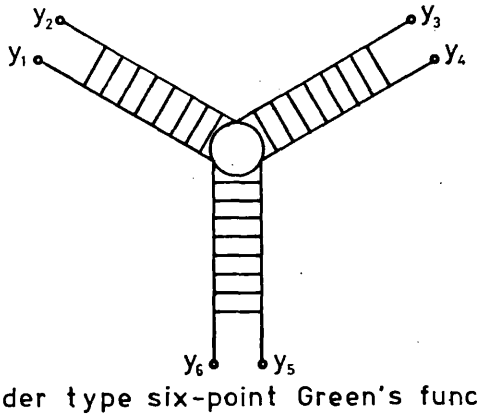

Figure 4·3.A triple ladder type six-point Green's function.

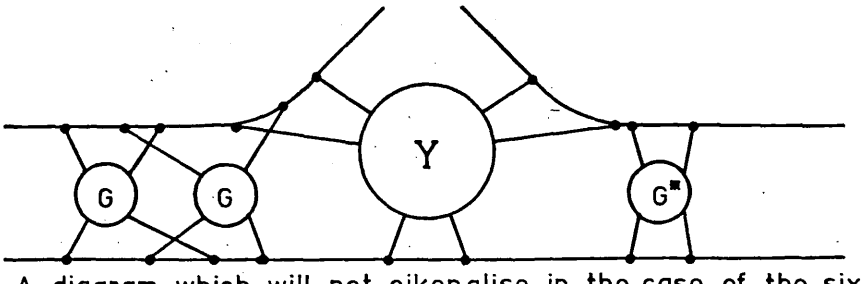

Figure 4·4.A diagram which will not eikonalise in the case of the six-point function.

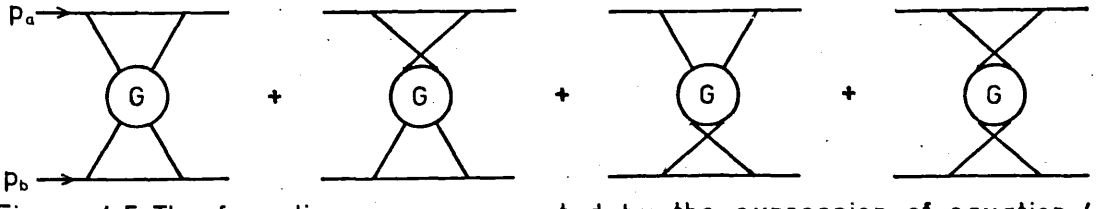

Figure 4·5.The four diagrams represented by the expression of equation 4·25

where ξ is the signature factor, α is the trajectory of the Regge pole and the quantities β_a and β_b are the vertex residues which arise from the integration

$$\int \frac{d^4k}{(2\pi)^4} \; 2\pi\delta(2p_a.k) \int \frac{d^4k'}{(2\pi)^4} \; 2\pi\delta(2p_b.k')$$

The δ-functions have the effect of keeping the interacting particle roughly on mass shell as it passes through the interaction.

The expression 4.26 also holds for χ_{cb}, $\chi_{\overline{ab}}$ and $\chi_{\overline{cb}}$ with suitable changes.

We now turn to the trickier problem of $\chi_{ac,b}$. The initial expression is given by

$$\chi_{ac,b} = \int d\tau_a d\tau_c d\tau_b d\tau_b' G^4(B_{ab}-B_{cb}-2p_a\tau_a+2p_c\tau_c,$$

$$\tfrac{1}{2}(B_{ab}+B_{cb})-p_a\tau_a-p_c\tau_c+p_b(\tau_b+\tau_b'),\ 2p_b(\tau_b-\tau_b')) \qquad 4.27$$

We again use the fourier transform to find

$$\chi_{ac,b} = \int \frac{d^4k}{(2\pi)^4} \; \frac{d^4q}{(2\pi)^4} \; \frac{d^4k'}{(2\pi)^4} \; G^4(k,q,k')\exp(iq.(B_{ab}+B_{cb})/2)$$

$$\exp(ik.(B_{ab}-B_{cb})) \int d\tau_a d\tau_c d\tau_b d\tau_b' \exp(ik.(-2p_a\tau_a+2p_c\tau_c))$$

$$\exp(iq.(-p_a\tau_a-p_c\tau_c+p_b(\tau_b+\tau_b')+ik'.2p_b(\tau_b-\tau_b')) \qquad 4.28$$

We refer to figure 4.6 for the definition of some momenta.

We can perform the τ_a, τ_c, τ_b and τ_b integration to yield δ-functions and we also make the transformation.

$$k = \frac{Q_a + Q_c}{2}, \qquad q = Q_a - Q_c$$

which has Jacobean unity. We can therefore say, after some re-arrangement

$$\chi_{ac,b} = \int \frac{d^4Q_a}{(2\pi)^4} \frac{d^4Q_c}{(2\pi)^4} 2\pi\delta(2p_a.Q_a)\ 2\pi\delta(2p_c.Q_c)$$

$$2\pi\delta(2p_b.(Q_a-Q_c))\ \exp(iB_{ab}.Q_a + iB_{\ b}\ Q_c)$$

$$\int \frac{d^4k'}{(2\pi)^4}\ 2\pi\delta(2p_b.k')\ \tilde{G}^4((Q_a+Q_c)/2, Q_a-Q_c, k') \qquad 4.29$$

Next we insert a specialisation for the form of

$$\int \frac{d^4k'}{(2\pi)^4}\ 2\pi\delta(2p_b.k)\ \tilde{G}^4\left(\frac{Q_a+Q_c}{2}, Q_a-Q_c, k'\right)$$

Which we take as

$$\Delta_F(Q_a^{\,2})\Delta_F(Q_c^{\,2})\beta(q^2)((Q_a+Q_c).p_b)^{\alpha(q^2)} \qquad 4.30$$

Where an appropriate form for $\Delta_F(k^2)$ might be

$$\int d\alpha\rho(\alpha)[k^2-\alpha^2+i\varepsilon]^{-1}$$

We also make a further transformation namely

$$Q_a = 2\sigma_a p_a + 2\tau_a p_b + \vec{Q}_a^{\mu}$$

$$Q_c = 2\sigma_c p_c + 2\tau_c p_b + \vec{Q}_c^{\mu} \qquad 4.31$$

which effectively have the Jacobeans $4p_a.p_b$ and $4p_c.p_b$
We therefore acquire the form

$$\chi_{ac,b} = \int \frac{d^2\vec{Q}_a}{(2\pi)^2} \frac{d^2\vec{Q}_c}{(2\pi)^2} \exp\,(iB_{ab}.\vec{Q}_a+iB_{cb}.\vec{Q}_c)$$

$$4p_a.p_b\ 4p_c.p_b\ \frac{1}{2\pi}\int_{-\infty}^{\infty} d\sigma_a d\tau_a d\sigma_c d\tau_c \delta(4p_a.p_b\tau_a)$$

$$\delta(4p_c.p_b\tau_c)\,\delta(4(p_a.p_b\sigma_a-p_c.p_b\sigma_c))\,\Delta_F(Q_a^2)\,\Delta_F(Q_c^2)$$

$$\beta(q^2)\,(2p_a.p_b\sigma_a+2p_c.p_b\sigma_c)^{\alpha(q^2)} \qquad 4.32$$

We can now do three of the σ/τ integrations, say τ_a, τ_c, σ_c, which pull down Jacobean factors and if we have $x\sigma_c = x\sigma = \sigma_a$ from the third of these integrations then

$$\chi_{ac,b} = \frac{1}{s_{cb}} \int \frac{d^2Q_a}{(2\pi)^2} \frac{d^2Q_c}{(2\pi)^2} \exp(iB_{ab}.Q_a+iB_{cb}.Q_c)$$

$$\beta(q^2)\,(s_{cb})^{\alpha(q^2)}\ \frac{1}{4\pi}\int d\sigma \Delta_F(Q_a{}^2)\,\Delta_F(Q_c^2)\,\sigma^{\alpha(q^2)}$$

where $Q_a{}^2$ and $Q_c{}^2$ can be expected to be functions of σ but q^2 is not.
It is perfectly possible to make explicit the σ dependance of $Q_a{}^2$ and $Q_c{}^2$ and thereby perform the $d\sigma$ integrations.
However we must always remember that our calculation has been performed throughout in the eikonal approximation and we therefore expect the region of integration of importance to be that where all components of $Q_a/\sqrt{s}$ are small with respect to 1.

If we consider equation 4.31 this indicates that we expect the region of integration of interest to be where σ is small with respect to 1. If we consider the specialised form 4.30 used, the propagators $\Delta_F(Q_a^2)$, $\Delta_F(Q_c^2)$ will only enforce a peaking for σ small with respect to s and therefore 4.30 does not explicitly conform to the eikonal approximation. We can insert the desired peaking very crudely by hand by considering the integral

$$\frac{1}{4\pi}\int_{-\infty}^{\infty} d\sigma \Delta_F(Q_a^2)\Delta_F(Q_c^2)\delta(\sigma)\sigma^{\alpha(q^2)} \qquad 4.33$$

which is zero.

We can only conclude from this that in the eikonal approximation we would expect $\chi_{ac,b}$ to be small.

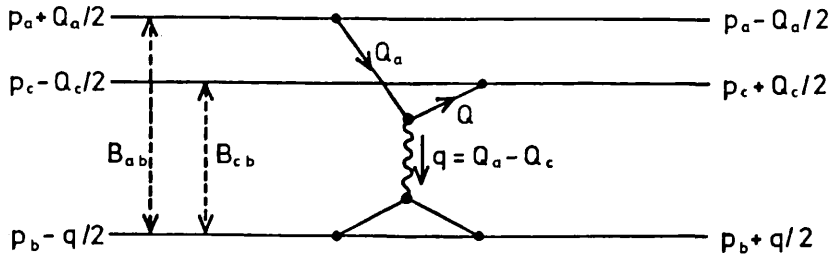

Figure 4.6. The diagram for the mixed eikonal phase.

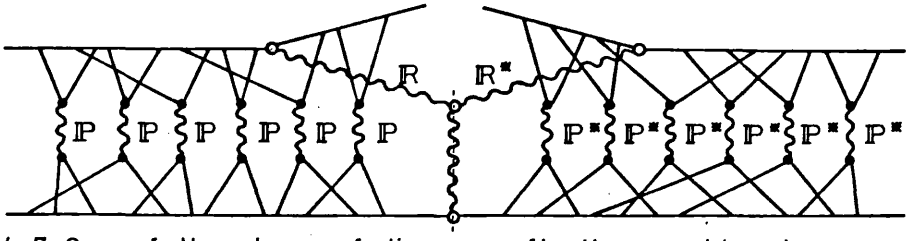

Figure 4.7. One of the class of diagrams finally considered.

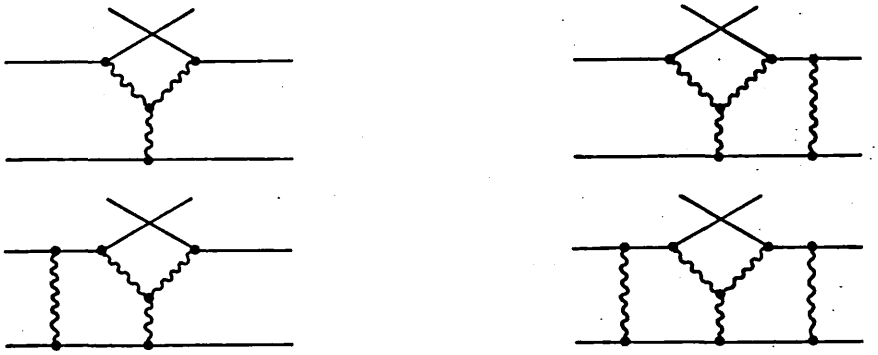

Figure 4.8. The re-scattering correction diagrams of ref.36.

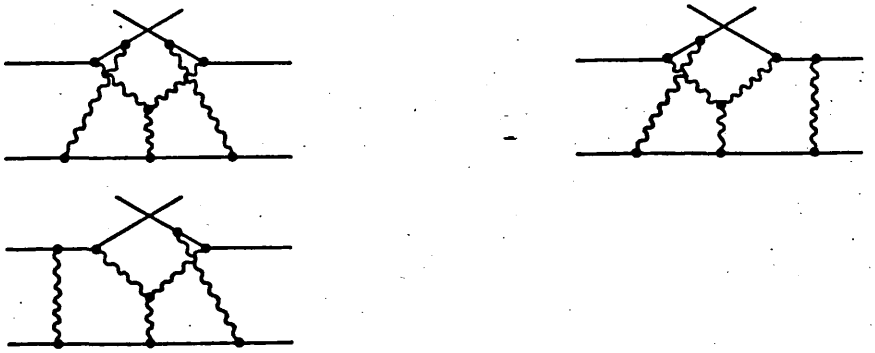

Figure 4.9. Extra diagrams considered by the present model which would contribute to the filling of a naturality dip.

DISCUSSION

In equation 4.19 we have derived a formula which accounts for, in the eikonal approximation, all corrections to a Regge-pole only graph of the class of which the diagram shown in figure 4.7 is a member. We see that there are three distinct types of correction namely rescattering between particles a and b rescattering between particles c and b, and a mixed rescattering which we do not believe to be important in the eikonal approximation. In this way we fully overcome one of the objections raised about the formula of Chapter III. We are also in a position to calculate target assymetries since we have no need to reglect $Sin\theta_{CM}$ in the present formula and we would not expect spurious zeros to occur via use of the formula of equation 4.19.

We need to discuss two further points concerning this formula. Because we include two independant impact parameters and eikonal phases we might easily expect the absorption corrections that we derive to be considerably stronger than those found from a calculation where only one phase is present [40,36], however, our formula would contain many more second order diagrams, if cut off at this level, than would the model of Craigie et al [36] which contains only those shown in figure 4.8. The absorption corrections of Ref.36 were introduced principally to remove a forward dip which was dictated via naturality considerations in the pole only diagram and not seen in the $\gamma p \to \pi^{\pm} X$ data. This calculation, when fitted to the data, produced an opacity C, which was considerably larger than unity.

One reason for this large size was that only one of the diagrams shown in figure 4.8, namely the second order diagram, can contribute to filling in the naturality dip. The other three all have these dips.
We can now see the reason for the inordinately large value of C found. The one second order diagram must dominate over the sum of the other three at small $k_\perp^2$ which can only happen for values of C larger than 1.

In the present model, there are several diagrams at the second order level which would contribute to filling in such a naturality dip and so we could expect that values of C much closer to unity would suffice in fitting the $\gamma p \to \pi^{\pm} x$ data. We will see later that the present model, for values of the opacity similar to those used in Chapter III, does not produce large absorption effects compared to those of the model used in the previous chapter. This is also due to the extra second order diagrams considered and so while we would not expect the present model to give rise to extremely strong absorption corrections we would expect the naturaltiy dips of Ref. 36 to be much better filled in.

The second point we wish to make, almost in passing, is that if a full ϕ^3 calculation were attempted we would expect only a contribution from the phase $\chi_{ac,b}$ in analogy with AFS/Mandlestam cuts in two body reactions.[74] The eikonal calculation we have made, while borrowing some of the features of ϕ^3 ladders does in fact require extra mechanism which are not made explicit in order to enforce the $k^2/\sqrt{s}$ conditions necessary for the eikonal approximation to be valid.

APPENDIX 4A

Abarbanel and Itzykson [72] wish to sum the class of graphs shown in fig.4A.1 in the eikonal approximation their starting point is Schwinger's [75]expression for this set of graphs namely

$$\frac{-i}{(2\pi)} T(p'_2, p_2; p'_1, p_1)\,\delta(p_2+p'_2-p_1-p'_1)$$

$$= \mathrm{Lt}_{p_i^2\to m^2} (p_1^2-m^2)(p_2^2-m^2)(p_1'^2-m^2)(p_2'^2-m^2)$$
$$K(A,A')\langle p_2|G(A)|p_1\rangle\langle p'_2|G(A')|p'_1\rangle|_{A,A=0} \qquad 4A.1$$

which is for equal mass spinless scattering. $|p\rangle$ is a one particle plane wave state, G(A) is the Greens function for the interaction of a spinless particle in an external scalar source A i.e.

$$G^{-1}(A) = P^2-m^2-A(X)+i\varepsilon \qquad 4A.2$$

P and X are four dimensional momentum and space operators which satisfy

$$[X_\mu, P_\nu] = ig_{\mu\nu} \qquad 4A.3$$

The term K(A,A') is a functional derivative operator and determines the type of interaction which takes place between the two spinless particles and can account for many sorts of interaction, with the proviso that they attach to the interacting particle via a spinless intermediary. The form chosen is

$$K = \exp\int d^4y\, d^4y' \frac{\delta}{\delta A(y)} D(y-y') \delta A'(y')$$

$$\text{with } D(x) = \frac{ig^2}{(2\pi)^4}\int \frac{d^4k\, e^{-ik.x}}{k^2-\mu^2+i\varepsilon} \qquad 4A.4$$

which is the form for exchanging spinless particles of mass μ between the two particles.

It is important to note, as will become clear later, that this form already has the non-interacting part subtracted from it. This part is not required for this two body case, but we must take care to include it when considering the 3 body case later.

We must now cast this equation into a form in which the introduction of the eikonal approximation is more transparent.

We will use the operator identities [76]

$$(A+B)^{-1} = \int_0^\infty dt \exp(i(A+B)t)$$

$$\exp(i(A+B)) = \exp(iA)\,T\exp\int_0^1 dt\, e^{-iAt}\, iB e^{iAt}$$

and the formal solution of $G(A)$,

$$G(A) = \frac{1}{P^2-m^2+i\varepsilon} + G(A)A(X)\frac{1}{P^2-m^2+i\varepsilon} \qquad 4A.5$$

when we consider

$$\lim_{p_i^2\to m^2} (p_1^2-m^2)(p_2^2-m^2)\langle p_2|\frac{1}{P^2-m^2+i\varepsilon}|p_1\rangle$$

$$= \lim_{p_2^2\to m^2}(p_2^2-m^2)\delta^4(p_1-p_2) = 0 \qquad 4A.6$$

we see that the first term of the expansion for $G(A)$ does not contribute. This is the mechanism for subtracting off the non-interacting part.

Thus using 4A.5 and 4A.6 we have

$$\langle p_2|G(A)|p_1\rangle = \langle p_2|\int_0^\infty dt\, \exp i(P^2-m^2+i\varepsilon)t$$

$$T\exp\{-i\int_0^t d\tau A(X-2P\tau)\}A(X)\frac{1}{P^2-m^2+i\varepsilon}|p_1\rangle \qquad 4A.7$$

where use has been made of the fact that, with the stated commutation relations

$$\exp(-iP^2\tau)A(X)\exp(iP^2\tau) = A(X-2P\tau) \qquad 4A.8$$

Thus

$$\begin{aligned}&\underset{p_i^2\to m^2}{\text{Lt}}\ (p_1^2-m^2)(p_2^2-m^2)\langle p_2|G(A)|p_1\rangle \\ &= \underset{p_i^2\to m^2}{\text{Lt}}\ \frac{(p_1^2-m^2)}{(p_1^2-m^2+i\varepsilon)}\ \frac{(p_2^2-m^2)}{(p_2^2-m^2+i\varepsilon)} \\ &\langle p_2|\int_o^\infty d\text{t}\, i(P^2-m^2+i\varepsilon)\ \exp\{i(P^2-m^2+i\varepsilon)t\} \\ &\text{Texp}\{-i\int_o^t d\tau A(X-2P\tau)\}\,A(X)|p_1\rangle \qquad 4A.9\end{aligned}$$

Performing a formal integration by parts and then taking the limits $\varepsilon \to o^+$, $p_i \to m^2$ in that order we have

$$\begin{aligned}&\underset{p_i^2\to m^2}{\text{Lt}}\ (p_1^2-m^2)(p_2^2-m^2)\langle p_2|G(A)|p_1\rangle \\ &= \langle p_2|i\ \text{Texp}\{-i\int_o^\infty d\tau A(X-2P\tau)\}\,A(X)|p_1\rangle \qquad 4A.10\end{aligned}$$

We can therefore rewrite equation 4A.1 as

$$\begin{aligned}&\frac{-i}{(2\pi)^4}\ T(p_2',p_2;p_1',p_1)\,\delta^4(p_2'+p_2-p_1'-p_1) \\ &= K(A,A')\langle p_2|T(A)|p_1\rangle\langle p_2'|T(A')|p_1'\rangle|_{A,A'} = 0 \qquad 4A.11\end{aligned}$$

where

$$T(A) = i\ \text{Texp}\{-i\int_o^\infty d\tau A(X-2P\tau)\}\,A(X) \qquad 4A.12$$

We can implement the eikonal approximation in this formulation simply by replacing the operators P and P' by the c - vectors $p = \frac{1}{2}(p_1+p_2), p' = \frac{1}{2}(p_1'+p_2)$. The time ordering is no longer important since the anticommutation properties of P and X are no longer in force and so we can write

$$\langle p_2 | T_E(A) | p_1 \rangle = \int \frac{d^4x}{(2\pi)^4} \exp[\, i(p_1-p_2).x \,]$$

$$\exp[-i\int_0^\infty A(x-2p\tau)d\tau]A(x)$$

$$= \int \frac{d^4x}{(2\pi)^4} \exp[\, i(p_1-p_2).x \,] \frac{\partial}{\partial\alpha} \exp[-i\int_\alpha^\infty A(x-2p\tau)d\tau\,]\Big|_{\alpha=0} \qquad 4A.13$$

The task is now to carry out the functional differentiation contained in K. We must evaluate the expression

$$\exp\left\{\int d^4y\, d^4y'\, D(y-y') \frac{\delta}{\delta A(y)} \frac{\delta}{\delta A'(y')}\right\} \cdot$$

$$\exp\left\{-i\left[\int_\alpha^\infty d\tau A(x-2p\tau) + \int_{\alpha'}^\infty d\tau' A'(x'-2p\tau')\right]\right\}\Big|_{A=A'=0} \qquad 4A.14$$

where we have

$$\frac{\delta A(x)}{\delta A(y)} = \delta^4(x-y) \qquad 4A.15$$

This evaluation is necessarily formal and the technique used is quite tedious. Since the answer can clearly be seen to be

$$\exp\left\{-\int_\alpha^\infty d\tau \int_{\alpha'}^\infty d\tau' D(x-x'-2p\tau+2p'\tau')\right\} \qquad 4A.16$$

we omit the detailed working.

Equations 4A.13 to 4A.16 contain most of the ideas which will be of use to us in the derivation of the 3-body case, however, we continue to a conclusion for the sake of completeness.

We can now re-write 4A.11 in the eikonal approximation as

$$\frac{-i}{(2\pi)^4} T_E(p_2', p_2; p_1', p_1)\, \delta^4(p_2+p_2'-p_1-p_1')$$

$$= \int \frac{d^4x\, d^4x'}{(2\pi)^8} \exp[\, i(p_1-p_2).x + i(p_1'-p_2').x' \,]$$

$$\frac{\partial}{\partial\alpha} \frac{\partial}{\partial\alpha'} \exp[-\int_\alpha^\infty d\tau \int_{\alpha'}^\infty d\tau' D(x-x'-2p\tau+2p'\tau')] \Big|_{\substack{\alpha=0 \\ \alpha'=0}} \qquad 4A.17$$

We can integrate over $x + x'$ directly which effects the cancellation of the overall momentum δ-function.

Next we make the transformation

$$x - x' = b - 2p\sigma + 2p'\sigma' \qquad 4A.18$$

where b is orthogonal to both p and p'. This has the Jacobean $2\tilde{s}$ where $\tilde{s} = s[1-(t+4m^2)/s]^{\frac{1}{2}}$. We leave the derivation of this Jacobean until later.

We also have

$p_1 - p_2 = -(p_1' - p_2')$ with both orthogonal to p and p'.

Whence

$$T_E(s,t) = 2i\tilde{s}\int d^2b \exp[-i(\vec{p}_1-\vec{p}_2).b] \int_{-\infty}^{\infty} d\sigma d\sigma' \frac{\partial}{\partial\alpha}\frac{\partial}{\partial\alpha'} \exp\left[-\int_{\alpha}^{\infty} d\tau \int_{\alpha'}^{\infty} d\tau' D(b-2p(\tau+\gamma)+2p'(\tau'+\sigma'))\right] \Big| \qquad 4A.19$$

$$\alpha = \alpha' = 0$$

If we now make the shifts

$\tau \to \tau+\sigma, \tau' \to \tau'+\sigma'$

we can also shift the derivatives so that

$$\frac{\partial}{\partial\alpha} \to \frac{\partial}{\partial(\alpha-\sigma)}, \quad \frac{\partial}{\partial\alpha'} \to \frac{\partial}{\partial(\alpha'-\sigma')}$$

and so taking α, α' to zero we are able to perform the two σ integrations directly, to obtain

$$T_E(s,t) = 2i\tilde{s}\int d^2b \exp[-i(\vec{p}_1-\vec{p}_2).b] \exp\left[-\int_{-\infty}^{\infty} d\tau d\tau' D(b-2p\tau+2p'\tau')\right] \qquad 4A.20$$

If we now consider the detailed form of D we need to consider the integral

$$\int_{-\infty}^{\infty} d\tau \int_{-\infty}^{\infty} d\tau' ig^2 \int \frac{d^4q}{(2\pi)^4} \frac{\exp\left[-iq.(b-2p\tau+2p'\tau')\right]}{(q^2-\mu^2+i\varepsilon)} \qquad 4A.21$$

We can perform the two τ integrations to form δ-functions to yield

$$ig^2 \int \frac{d^4q}{(2\pi)^2} \frac{\exp[-i\vec{q}.b]}{(q^2-\mu^2+i\varepsilon)} \delta(2p.q)\delta(2p'.q) \qquad 4A.22$$

We can make the transformation of variables

$$q = \vec{q} + \eta p + \eta' p' \qquad 4A.23$$

where forms for η and η' in terms of $2p.q$ and $2p'.q$ are given later. This results in the form

$$\frac{-ig^2}{2\tilde{s}} \int \frac{d^2\vec{q}}{(2\pi)^2} \frac{\exp[-i\vec{q}.b]}{(|\vec{q}|^2+\mu^2)} \qquad 4A.24$$

and inserting this into equation 4A.20 we have

$$T_E(s,t) = 2i\tilde{s} \int d^2b \exp[-(\vec{p}_1-\vec{p}_2).b]$$

$$\left\{ \exp\left[\frac{ig^2}{2\tilde{s}} \int \frac{d^2\vec{q}}{(2\pi)^2} \frac{\exp[-i\vec{q}.b]}{|\vec{q}|^2 \mu^2} \right] -1 \right\} \qquad 4A.25$$

where $(\vec{p}_1-\vec{p}_2)^2 = t$

This is the final form. All that remains is to evaluate the Jacobeans which have been left until now.

For the transformation of 4A.18 we go to the frame where

$$p_1 = (E,-q/2,0,k)$$
$$p_2 = (E,q/2,0,k)$$
$$p_1' = (E,q/2,0,-k)$$
$$p_2' = (E,-q/2,0,k) \qquad 4A.26$$

with

$$E - q^2/4 - k^2 = m^2$$
$$s = 4E^2 = (p_1 + p_1')^2$$
$$t = -q^2 = (p_1 - p_2)^2$$

In this frame

$$p = (p_1 + p_2)/2 = (E,0,0,k)$$
$$p' = (p_1' + p_2')/2 = (E,0,0,-k)$$

then if $x = b - 2p\sigma + 2p'\sigma'$

$$= (p2E(\sigma-\sigma'),b_1,b_2,-2k(\sigma+\sigma')) \qquad 4A.27$$

the Jacobean is

$$\begin{vmatrix} -2E & 0 & 0 & -2k \\ 0 & 1 & 0 & 0 \\ 0 & 0 & 1 & 0 \\ 2E & 0 & 0 & -2k \end{vmatrix} = 8Ek$$

$$= 2s\left[\frac{k^2}{E^2}\right]^{\frac{1}{2}} = 2s\left[1 - \frac{4m^2-t}{s}\right]^{\frac{1}{2}} \qquad 4A.28$$

For the transformation of 4A.23 we consider

$$\sigma = 2p.q, \sigma' = 2p'.q$$

and we wish for the transformation.

$$d^4q \to d\sigma d\sigma' d^2\vec{q}$$

We take

$$q = \vec{q} + \eta p + \eta' p' \quad \text{where } \vec{q}.p = \vec{q}.p' = 0$$

Then

$$2p.q = 2\eta p^2 + 2\eta' p.p' = \sigma$$

$$2p'.q = 2\eta p.p' + 2\eta' p'^2 = \sigma' \qquad \text{4A.29}$$

Thus

$$q = \vec{q} + \frac{p(p.p'\sigma' - p^2\sigma)}{2((p.p')^2 - p^2p'^2)} + \frac{p'(p.p'\sigma - p'^2\sigma')}{2((p.p')^2 - p^2p'^2)} \qquad \text{4A.30}$$

We go again to the frame given in 4A.26

Then

$$p^2 = m^2 - t/4 = p'^2$$

$$p.p' = s/2 + (t/4 - m^2)$$

Thus

$$2((p.p')^2 - p^2p'^2) = \frac{s^2}{2}\left(1 - \frac{4m^2 - t}{s}\right) = \frac{\tilde{s}^2}{2}$$

So

$$q = \frac{2E}{\tilde{s}^2}(p.p' - p^2)(\sigma + \sigma'), q_1, q_2, \frac{2k}{\tilde{s}^2}(p.p' + p^2)(\sigma' - \sigma) \qquad \text{4A.31}$$

And the Jacobean is

$$\begin{vmatrix} \frac{2E}{\tilde{s}^2}(p.p' - p^2) & 0 & 0 & \frac{2E}{\tilde{s}^2}(p.p' - p^2) \\ 0 & 1 & 0 & 0 \\ 0 & 0 & 1 & 0 \\ \frac{2k}{\tilde{s}^2}(p.p' + p^2) & 0 & 0 & \frac{2k}{\tilde{s}^2}(p.p' + p^2) \end{vmatrix}$$

$$= \frac{8\,Ek(p.p'^{-2})(p.p' + p^2)}{\tilde{s}^4} \qquad \text{4A.32}$$

Now

$$(p.p' - p'^2)(p.p' + p^2) = \tilde{s}^2/4$$

$$Ek = \tilde{s}/4$$

Thus the Jacobean is $\dfrac{1}{2\tilde{s}}$

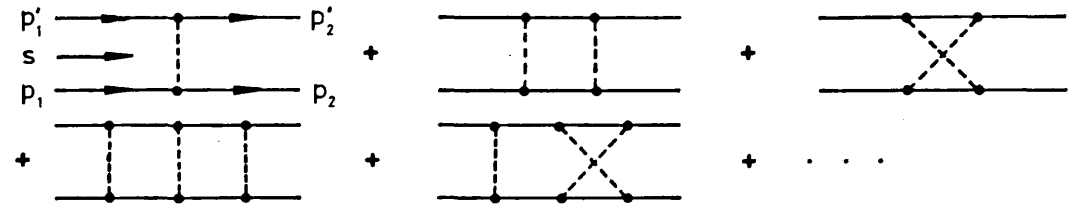

Figure 4A1. The class of diagrams to be summed in the eikonal approximation.

APPENDIX 4B

In this appendix we present calculations of various variables in slightly more detail than in the main body of the chapter.

If we take

$$p_c = xp_a + yp_b + \vec{p}_{c\perp}$$

where

$$\vec{p}_{c\perp} \cdot p_a = \vec{p}_{c\perp} \cdot p_b = 0 \qquad 4B.1$$

Then

$$p_c^2 = x^2m^2 + y^2m^2 - p_{c\perp}^2 + 2xyp_a \cdot p_b \qquad 4B.2$$

Neglecting quantities of order y^2 we find

$$y = \frac{1}{s_{ab}} \left(\frac{m^2+p_{c\perp}^2}{x} - xm^2 \right) \qquad 4B.3$$

We now consider

$$(p_a-p_c)^2 = ((1-x)p_a - yp_b - p_c)^2$$

$$\text{so } t = (1-x)^2m^2 + y^2m^2 - 2p_a \cdot p_b(1-x)y - p_{c\perp}^2$$

$$= -ys(1-x) + (1-x)^2m^2 - p_{c\perp}^2$$

$$= (2-x)m^2 - \left(\frac{m^2+p_{c\perp}^2}{x}\right) \qquad 4B.4$$

Where $p_{c\perp}^2$ is taken as a positive quantity.

If we consider $s_{cb} = (p_c+p_b)^2 = 2p_c \cdot p_b$

Then $s_{cb} = 2\,xp_a \cdot p_b + ym^2$

$$\simeq x\, s_{ab} \qquad 4B.5$$

Also $M_x^2 = (p_a + p_b - p_c)^2$

$$M_x^2 = (p_a + p_b - p_c)^2$$
$$= ((1-x)p_a + (1-y)p_b - \vec{p}_{c\perp})^2$$
$$= 2p_a.p_b(1-x) + O(1)$$
$$\simeq (1-x)s_{ab} \qquad 4B.6$$

It is now necessary to examine the variable $s'_{ab} = (p'_a+p'_b)^2$. We note that with the definition implicit in equation 4.17 and precursors

that $\alpha = 2p_b.Q_c = -2p_a.Q_a$

Thus $s'_{ab} = (p_a - Q_a + p_b + Q_a + Q_c)^2$

$$= (p_a + p_b)^2 + 2(p_a + p_b).Q_c + Q_c^2$$

We recall the decomposition of Q_c in 4.15 to write

$$s'_{ab} = s_{ab} + \alpha + 2p_a.\left(\frac{\alpha}{xs_{ab}}(x2p_a + yp_b + \vec{p}_{c\perp}) + \vec{Q}_c\right) + Q_c^2$$

$$= s_{ab} + \alpha + O\left(\frac{\alpha}{s_{ab}}\right) + O(1) \qquad 4B.7$$

Equation 4B.7 then shows us that we are perfectly entitled to neglect α/s_{ab} with respect to 1, since an eikonal approximation should not deviate the energy s'_{ab} far from s_{ab}.

We are now in a position to consider Q_a^2 and Q_c^2. We refer back to the δ-function found in equation 4.16, and also the decomposition of equation 4.15

Thus $Q_c^\mu = \frac{\alpha}{xs} p_c^\mu - \frac{Q_c^2}{xs} p_b^\mu + \vec{Q}_c^\mu$

$$Q_c^2 = \left(\frac{\alpha^2}{x^2s^2} + \left(\frac{Q_c^2}{xs}\right)^2\right)m^2 - \frac{2p_c.p_b}{x^2s^2}\alpha Q_c^2 - \vec{Q}_c^2$$

Neglecting Q_c^2/s and α/s we have

$$Q_c^2\left(1 + \frac{\alpha}{xs}\right) = -\vec{Q}_c^2$$

Thus $Q_c^2 = -\vec{Q}_c^2$ 4B.8

where $\vec{Q}_c^2$ is a positive quantity.

In a similar fashion we also have

$Q_a^2 = -\vec{Q}_a^2$ 4B.9

and also for the barred quantities.

The next variable we need to consider is

$$Q'_{ac} = (p'_a - p'_c)$$
$$= (p_a - p_c) - (Q_a + Q_c)$$

Thus $Q'^2_{ac} = t'_{ac} = Q^2_{ac} - 2(p_a-p_c).(Q_a+Q_c)+(Q_a+Q_c)^2$

$$= t - 2p_a.Q_a + 2p_c.Q_c - 2p_a.Q_c + 2p_c.Q_a + Q_a^2 + Q_c^2 + 2Q_a.Q_c$$

Using the form of the delta functions in equation 4.16 we have $2p_a.Q_a = Q_a^2$ and $2p_c.Q_c = -Q_c^2$, thus

$t'_{ac} = t - 2p_a.Q_c + 2p_c.Q_a + 2Q_a.Q_c$ 4B.10

We have from equation 4B.4

$t = (2 - x)m^2 - \frac{m^2}{x} - \frac{p_{c\perp}^2}{x}$

We now proceed to calculate the other three quantities on the R.H.S. of equation 4B.10

$$2p_a.Q_c = \frac{2\alpha}{xs}(p_a.p_c) - \frac{Q_c^2}{xs}2p_a.p_b + 2p_a.\vec{Q}_c^{\mu}$$

$$= \frac{2\alpha}{xs}(xm^2 + yp_a.p_b) - \frac{Q_c^2}{x} + 2p_a.\vec{Q}_c^{\mu}$$

We neglect the first term since it is of order $\frac{\alpha}{s}$

Also $p_c.\vec{Q}_c^{\mu} = p_b.\vec{Q}_c^{\mu} = 0$

Thus $(xp_a + yp_b + \vec{p}_c^{\mu}).\vec{Q}_c^{\mu} = 0$

and $2p_a.\vec{Q}_c^{\mu} = -\frac{2p_{c\perp}^{\mu}.\vec{Q}_c^{\mu}}{x}$, Thus $2p_a.Q_a = -\frac{Q_c^2}{x} - \frac{2p_{c\perp}^{\mu}.\vec{Q}_c^{\mu}}{x}$ 4B.11

$$2p_c\cdot Q_a = 2(xp_a+yp_b+p_{c\perp}^{\mu})\cdot\left(\frac{(-\alpha+(Q_a+Q_c)^2)}{s}\,p_a + \frac{Q_a^2}{s}\,p_b + Q_a^{\mu}\right)$$

$$= \frac{2x(-\alpha+(Q_a+Q_c)^2)m^2}{s} + \frac{2xp_a\cdot p_bQ_a^2}{s}$$

$$+ \frac{2y(-\alpha+(Q_a+Q_c)^2)}{s}\,p_a\cdot p_b + \frac{2yQ_a^2m^2}{s} + 2p_c^{\mu}\cdot\vec{Q}_a^{\mu}$$

Neglecting terms of order α/s or Q_a^2/s we have

$$2p_c\cdot Q_a = x\,Q_a^2 + 2p_c^{\mu}\cdot\vec{Q}_a^{\mu} \qquad 4B.12$$

$$2Q_a\cdot Q_c = 2\left(\frac{(-\alpha+(Q_a+Q_c)^2}{s}\,p_a + \frac{Q_a^2p_b}{s} + Q_a^{\mu}\right)\cdot$$

$$\left(\frac{\alpha}{xs}\,p_c - \frac{Q_c^2}{xs}\,p_b + Q_c^{\mu}\right)$$

$$= 2\left(\frac{-\alpha+(Q_a+Q_c)^2}{s}\,\frac{\alpha}{xs}\,p_a\cdot p_c - \frac{-\alpha+(Q_a+Q_c)^2}{s}\,\frac{Q_c^2}{xs}\,p_a\cdot p_b\right.$$

$$+ \frac{-\alpha+(Q_a+Q_c)^2}{s}\,p_a\cdot\vec{Q}_c^{\mu} + \frac{\alpha}{xs}\,\frac{Q_a^2}{s}\,p_b\cdot p_c - \frac{Q_a^2Q_c^2m^2}{xs^2}$$

$$\left. + \frac{Q_a^2}{s}\,p_b\cdot\vec{Q}_c^{\mu} + \frac{\alpha}{xs}\,p_c\cdot\vec{Q}_a^{\mu} + \vec{Q}_c\cdot\vec{Q}_a\right)$$

Neglecting all terms of order α/s or Q_a^2/s we are left with

$$2Q_a\cdot Q_c = 2\vec{Q}_c^{\mu}\cdot\vec{Q}_a^{\mu} \qquad 4B.13$$

Putting together 4B.4, 4B.11, 4B.12 and 4b.13 and substituting them into 4B.10 we finally arrive at

$$t_{ac}' = (2-x)m^2 - \frac{m^2}{x} + \frac{(p_{c\perp}^{\mu}+x\vec{Q}_a^{\mu}+\vec{Q}_c^{\mu})^2}{x}$$

and of course

$$t'_{\overline{ac}} = (2-x)m^2 - \frac{m^2}{x} + \frac{(p_{c\perp}{}^{\mu} + x\vec{Q}_{\overline{a}}{}^{\mu} + \vec{Q}_{\overline{c}}{}^{\mu})^2}{x} \qquad 4B.14$$

Finally we note that

$$t_o = (p'_b - p'_{\overline{b}})^2$$

$$= (Q_a + Q_c - Q_{\overline{a}} - Q_{\overline{c}})^2$$

and using equations 4B.8, 9 and 11 we can write

$$t_o = (\vec{Q}_a{}^{\mu} + \vec{Q}_a{}^{\mu} - \vec{Q}_{\overline{a}}{}^{\mu} - \vec{Q}_{\overline{c}}{}^{\mu})^2 \qquad 4B.15$$

CHAPTER V

An Application Of The Closed Regge-Eikonal Formula for Multiple Exchange Contributions To the Inclusive Six Point Function

INTRODUCTION

We are now in possession of a formula for absorption type corrections to the inclusive six-point function which overcomes many of the heuristic defects of the model proposed in chapter III and we therefore wish to perform certain calculations with the new model in order to examine it, both in its own right and also in comparison with the old model. To do this it is natural to choose the same family of reactions for the reasons stated previously - namely the simplicity in the Regge-pole picture. Accordingly we will make calculations of the cross-sections for the reactions

$$\pi^{\pm} + p \to \pi^{o} + X$$
$$\pi^{\pm} + p \to \eta + X$$
$$K^{+} + p \to K^{o} + X$$
$$K^{-} + p \to \bar{K}^{o} + X$$

We will also calculate target asymettries for all these interactions, which was not possible using the model of chapter III. We also note here that it is possible to extend the formula of chapter IV to cover the case where two of the scalar legs of the Green's functions (Pomerons) attach to a spin ½ particle as is seen in Appendix 5A. Also the formula is derived for the case of the coupling of two scalar mesons to a third scalar, however the use of the formula for the case of a pseudo scalar mesons should be quite acceptable.

The input triple-Regge type expression we will use will be similar to that used in Chapter III although there are some differences which will be made clear later. It is also necessary to relate various unmeasured cross-sections (such as $\pi^o p$ elastic scattering) to measured ones. This is done via the simple application of isospin, and results in all absorption parameters being fully predicted. Simple isospin ideas are also used to relate the sign of the flip amplitude to that of the non flip amplitude in order that the target asymettry be calculated.

The use of these ideas again leads to a model, as in Chapter III where no arbitrary parameters must be introduced.

FORMALISM

From the derivations of Chapter IV [74] and the extension of appendix 5A we can write down the following formula which will be sufficient for the purposes of calculating corrections to the reactions $0^- \tfrac{1}{2}^+ \to 0^- X$ via charge exchange.

We have

$$H(t,s_{ab},M_x^2) = \int_{-\infty}^{\infty} \frac{d^2\vec{Q}_a}{(2\pi)^2}\frac{d^2\vec{Q}_c}{(2\pi)^2}\frac{d^2\vec{Q}_{\bar{a}}}{(2\pi)^2}\frac{d^2\vec{Q}_{\bar{c}}}{(2\pi)^2} S(\vec{Q}_a,\vec{Q}_c)Y(t_{ac},t_{\bar{a}\bar{c}},t_o,s_{ab},M_x^2)S^*(\vec{Q}_{\bar{a}}\vec{Q}_{\bar{c}}) \quad - 5.1$$

where

$$S = \int d^2B_{ab}d^2B_{cb}\exp[i(\vec{Q}_a.B_{ab}+\vec{Q}_c.B_{cb}) + i(\chi_{ab}(B_{ab})+\chi_{ac,b}(B_{ab},B_{cb})+\chi_{cb}(B_{cb}))]$$

and

$$S^* = \int d^2B_{\bar{a}\bar{b}} d^2B_{\bar{c}\bar{b}} \exp[-i(\vec{Q}_{\bar{a}}.B_{\bar{a}\bar{b}} + \vec{Q}_{\bar{c}}.B_{\bar{c}\bar{b}}) - i(\chi_{\bar{a}\bar{b}}^*(B_{\bar{a}\bar{b}}) + \chi_{\bar{a}\bar{c},\bar{b}}^*(B_{\bar{a}\bar{b}}, B_{\bar{c}\bar{b}}) + \chi_{\bar{c}\bar{b}}^*(B_{\bar{c}\bar{b}}))] \quad - 5.2$$

The mixed eikonal phases $\chi_{ac,b}$ and $\chi_{\bar{a}\bar{c},\bar{b}}$ can be expected to be small because of the basic assumptions of the eikonal approximation, and the other phases are given by

$$\chi_{ab} = \frac{1}{s_{ab}} \int \frac{d^2\vec{Q}_a}{(2\pi)^2} \exp(-i\vec{Q}_a.B_{ab}) \beta_a(-\vec{Q}_a^2) \beta_b(-\vec{Q}_a^2) \xi_{\alpha(-\vec{Q}_a^2)} s_{ab}^{\alpha(-\vec{Q}_a^2)}$$

$$\chi_{cb} = \frac{1}{s_{cb}} \int \frac{d^2\vec{Q}}{(2\pi)^2} \exp(-i\vec{Q}_c.B_{cb}) \beta_c(-\vec{Q}_c^2) \beta_b(-\vec{Q}_c^2) \xi_{\alpha(-\vec{Q}_c^2)} s_{cb}^{\alpha(-\vec{Q}_c^2)} \quad - 5.3$$

where the notation is as for chapter IV.

To summarise this dependance of the internal momentum transfers on the Q variables we have

$$t_{ac} = t_{min} - \frac{1}{x}(\vec{p}_{c\perp} + x\vec{Q}_a + \vec{Q}_c)^2$$

$$t_{\bar{a}\bar{c}} = t_{min} - \frac{1}{x}(\vec{p}_{c\perp} + x\vec{Q}_{\bar{a}} + \vec{Q}_{\bar{c}})^2$$

$$t_o = -(\vec{Q}_a + \vec{Q}_c - \vec{Q}_{\bar{a}} - \vec{Q}_{\bar{c}})^2 \quad - 5.4$$

Here we have made a change of notation in that we now regard $p_{c\perp}, Q_a$ and Q_c as purely two dimensional vectors and the inclusion of the minus sign reflects the change of metric. The justification for this change is given in the first part of Appendix 5B.

For the parameters of the elastic scattering symbolised by the χs we take

$$\alpha(t) = 1 + \alpha'_p t$$

where α'_p is taken henceforth as 0.25

and $\xi\alpha(t) = -\exp(-i\pi\alpha(t)/2)$ - 5.5

We also use $\beta_a(t)\beta_b(t) = De^{at}$, $\beta_c(t)\beta_b(t) = D\acute{e}^{a't}$

Comparison with the absorption model allows us to relate the Ds and as to the quantities normally used namely [57]

$$D = 4\pi Ca, \quad a = 1/4\lambda \qquad - 5.6$$

where C is the opacity and would be expected to take on a value between 0 and 1, and λ is the inverse of the square of the radius of interaction . This correspondance can be seen in another way. Pumplin [40] indicates that $\int d^2B_{ab} d^2B_{cb} S \gtrsim 0$ is the condition for almost total absorption of the S-wave which a value of C such that $0<C<1$ brings about. With this parametrisation the eikonal phases of equation 5.3 become the fourier transforms of Gaussians and as such can be performed [61] to yield

$$\chi_{ab} = \frac{iD}{4\pi A} \exp\left[-B_{ab}^2/4A\right]$$

$$\chi_{cb} = \frac{iD'}{4\pi A'} \exp\left[-B_{cb}^2/4A'\right] \qquad - 5.7$$

where $A = a + \alpha'_p \log_e(s_{ab}) - i\pi\alpha'_p/2$

$$A' = a' + \alpha'_p \log_e(s_{cb}) - i\pi\alpha'_p/2$$

The traditional absorption model can be recovered if α'_p is set to zero.

The form for the S factors in equation 5.2 is therefore the fourier transform of the exponential of a sum of Gaussians i.e.

$$S = \int d^2B_{ab} \exp[i\vec{Q}_a.B_{ab}] \exp\left[-\frac{D}{4\pi A} \exp\left\{-\frac{B_{ab}^2}{4A}\right\}\right]$$
$$\int d^2B_{cb} \exp[i\vec{Q}_c.B_{cb}] \exp\left[-\frac{D}{4\pi A} \exp\left\{-\frac{B_{cb}^2}{4A}\right\}\right] \quad - 5.8$$

and when the second exponential is expanded as a sum of powers, we can exchange the order of the summation and integral operations leaving a sum of Gaussian Fourier transforms. These are similarly easily performed and using a substitution from equation 5.6 we can rewrite

$$H(t,s_{ab},M_x^2) = \int \frac{d^2\vec{Q}_a}{(2\pi)^2} \frac{d^2\vec{Q}_c}{(2\pi)^2} \frac{d^2\vec{Q}_a}{(2\pi)^2} \frac{d^2\vec{Q}_c}{(2\pi)^2}$$
$$\{(2\pi)^2\delta^2(\vec{Q}_a) + 4\pi \sum_{k=1}^{\infty} \frac{(-Ca)^k}{kk!A^{k-1}} \exp[-\vec{Q}_a^2 A/k]\}$$
$$\{(2\pi)^2\delta^2(\vec{Q}_c) + 4\pi \sum_{\ell=1}^{\infty} \frac{(-C'a')^\ell}{\ell\ell!A'^{\ell-1}} \exp[-\vec{Q}_c^2 A'/\ell]\}$$
$$Y(t_{ac},t_{\bar{a}\bar{c}},t_o,s_{ab},M_x^2)$$
$$\{(2\pi)^2\delta^2(\vec{Q}_{\bar{a}}) + 4\pi \sum_{m=1}^{\infty} \frac{(-Ca)^m}{mm!A^{*m-1}} \exp[-\vec{Q}_{\bar{a}}^2 A^*/m]\}$$
$$\{(2\pi)^2\delta^2(\vec{Q}_{\bar{c}}) + 4\pi \sum_{n=1}^{\infty} \frac{(-C'a')^n}{nn!A'^{*n-1}} \exp[-\vec{Q}_{\bar{c}}^2 A'^*/n]\} \quad - 5.9$$

It is equation 5.9 with an input Y term of the form shown diagrammatically in figure 5.1 that we use to evaluate our form of absorption correction.

The detailed form of the off-forward 3 body amplitude we will use is mentioned later and given in the second part of appendix 5B, and because of this form it is possible to perform any of the integrals implied by equation 5.9 analytically, as is indicated in appendix 5C.

The performed integrals in this appendix show that as successively more external legs become connected by intermediate Pomerons the integral becomes suppressed not only by the expected factors of C or C′ (always less than one) and reciprocals of factorials but also by factors (essentially) of 1/A or 1/A′ ; in the present case A and A′ have, approximately, the numerical value of 5. Since the infinite series of possible diagrams must be truncated at some point for a numerical calculation, and because of this suppression of the higher diagrams we feel justified in carrying through the practical calculation for diagrams arising from the exchange of not more than two extra, intermediate Pomerons. All the diagrams included in this calculation are shown in figure 5.2(a). It must also be noted that the eikonal approximation treats all the diagrams of, say, figure 5.2(b) similarly. The next step would be to include diagrams up to 4 intermediate Pomerons. There would be very many such diagrams , with the third and fourth orders at least partially mutually cancelling, and with many of them heavily suppressed by factorials. It was felt that the increase in programming complexity

and computer time used in the evaluation of the theoretical curve would not be justified by the expected small change - most of the salient features of the model should be included by the second order.

The reaction $o^-\frac{1}{2}^+ - o^-X$ is fully determined by the measurement of not only the differential cross section but also requires measurement of the target asymmetry for polarised protons. This quantity, Σ, is given by [16] .

$$\Sigma = \frac{\text{Disc}_{M_x^2}\langle - |T| + \rangle}{\text{Disc}_{M_x^2}\langle + |T| + \rangle} \qquad 5.10$$

where $\langle\lambda|T|\lambda\rangle$ represents the forward 3-body amplitude for $\frac{1}{2}^+o^-o^- \to \frac{1}{2}^+o^-o^-$ and the 'incoming' proton has helicity λ. The differential cross-section is, of course, proportional to $\sum_\lambda \langle\lambda|T|\lambda\rangle$.

Appendix 5A gives us the clue as to how we must implement the inclusion of helicity flip, and equation 5A.11 indicates just how flip and non flip amplitudes can be formed, where the quantity $\tilde{Y}(t_{ac}, t_{\bar{a}\bar{c}}, t_o, M_x^2)$ is a matrix formed from available vectors and γ-matrices.

It will be possible to use a less general formulation than equation 5A.11 which is still sufficient for our purposes, as will be seen later, and to motivate the choice for this and our choice of Regge exchanges for

the two quantities, differential cross-section and target asymmetry, we first consider an M-function decomposition for the three-body amplitude, where we use the kinematics of figure 5.3 which depicts the initial a-b cm. frame. (a is the incoming O^-, b the incoming proton and c the "outgoing" O^-).

The decomposition can be given in its most general form as [77] $H_{\lambda\lambda}(t,s,M_x^2)$

$$= \frac{1}{2m}\bar{u}^{\lambda}(p_b)[A+B\gamma\cdot p_a+C\gamma\cdot p_c+D\gamma\cdot p_a\gamma\cdot p_a\gamma\cdot p_c]\,u^{\lambda}(p_b) \qquad 5.11$$

where m is here the proton mass and

$$p_b = (E_b,-\underline{p}),\ p_a = (E_a,\underline{p}),\ p_c = (E_c,\underline{q})$$

Then

$$H_{++}=A-(m^2-E_b(E_b+E_a))B/m+(E_aE_b+pq\cos\theta)C/m + (E_aE_c-pq\cos\theta)D/m \qquad 5.12$$

and

$$H = (E_a+E_b)pq\sin\theta e^{-i\phi}D$$

where p and q are the moduli of $\underline{p}$ and $\underline{q}$, three vectors.

Since the different spin states must have the same energy dependance and $(E_a+E_b)p\sim\frac{s}{2}$

and for $\cos\theta = 1-O(\frac{1}{s})$ i.e. small t,

$$E_aE_c-pq\cos\theta\sim O(m^2)$$

we see that the term in D in H_{++} is kinematically suppressed with respect to the other terms and therefore effectively decouples in the triple-Regge region. It is this behaviour that motivates our choice of exchanges for the third or t_o leg of the triple-Regge diagram (figure 5.4).

Thus for the differential cross-section we include the Pomeron, f-Reggeon for the t_o exchanges. These exchanges could be expected to dominate and will not couple strongly to a helicity flip proton. These terms are shown diagrammatically in figure 5.4(a). The O^-O^--Reggeon vertex admits only ρ, A_2 or ρ and A_2 exchanges for all the different processes. Since the Pomeron and f-Reggeon have the same signature and isospin properties [78] there will be no sign changes between the ppf, A_2A_2f and ppP and A_2A_2P triple Regge couplings.

The flip amplitude, to which the target asymmetry is proportional, is mediated by the ρ-Reggeon (shown in figure 5.4(b)) since the helicity flip coupling of the ρ to nucleons is large, and would certainly be expected to dominate the non flip coupling for small t_o.

Having decided upon the possible third exchanges we must incorporate the t_o threshold effects into the flip-coupling ρ-exchanges. To rewrite 5A.11 in a

slightly different notation we require

$$Y_\rho(t_{ac}, t_{\bar{a}\bar{c}}, t_o, s_{ab}, M_x^2)$$
$$= \bar{u}^{-}(p_{\bar{b}})(\not{p}_{\bar{b}}'+m)\,\Gamma^{+-}_{b\bar{b}}(\not{p}_b'+m)\,u^{+}(p_b)$$
$$\tilde{Y}(t_{ac}, t_{\bar{a}\bar{c}}, t_o, s_{ab}, M_x^2) \qquad 5.13$$

where $\tilde{Y}(t_{ac}, t_{\bar{a}\bar{c}}, t_o, s_{ab}, M_x^2)$ is to be given by a sum of exponentials and is the quantity discussed in appendix 5B. The quantity $\Gamma^{+-}_{b\bar{b}}$ is some gamma matrix, and all the threshold behaviour is taken to reside in this spinor/γ-matrix factor.

We can identify two facets of this behaviour. Firstly, consistent with our formulation of the model in the eikonal approximation we treat the proton-proton-Reggeon vertex as factorisable, and since the vertex functions of spin flip Regge-vertex are required to go to zero as $-\sqrt{t_o}$ as $t_o \to 0$ [29] we wish this factor to exhibit a $\sqrt{-t_o}$ behaviour of some form. Secondly we insist that, after insertion into equation 5.9, and after all the integrals have been performed this factor produces behaviour of the form indicated in equation 5.12 i.e. the integrals call down a factor of

$$q\mathrm{Sin}\theta e^{i\phi}$$

We thus replace the spinor factors by a multiplicative factor which is sufficiently general to produce the behaviour we require. Such a factor is [32]

$$p_{c\perp}\cos\phi + Q_{a1} + Q_{c1} + i(p_{c\perp}\sin\phi + Q_{a2} + Q_{c2})$$
$$- [p_{c\perp}\cos\phi + Q_{\bar{a}1} + Q_{\bar{c}1} + i(p_{c\perp}\sin\phi + Q_{\bar{a}2} + Q_{\bar{c}2})] \qquad 5.14$$

since it produces both the correct ϕ and $p_{c\perp}$ dependances as shown in appendix 5C and also goes to zero if and only if $\sqrt{-t_o}$ goes to zero. The ordering of the barred and un-barred variables corresponds to the +- ordering in the definition of the target asymmetry as can be seen using a simple form for the pp-ρ coupling and the vector p_b and $p_{\bar{b}}$.

We now have sufficient calculation machinery to evaluate the required contributions to the model, once we have derived forms for the three quantities Yp, Yf and $\tilde{Y}p$ and also the absorption coefficients required i.e. C, C', a and a', which we now proceed to do. A detailed consideration of the $\pi\pi p \to \pi\pi p$ off forward triple-Regge terms is given in appendix 5B, and the generalisation to the other reactions is straight forward. We use simple isospin ideas to relate unknown absorption parameters to known ones and also to determine the relative signs of the flip (ρ) to non-flip (P and f) amplitudes. Strong exchange degeneracy is assumed between ρ and A_2 in order to relate the various different reactions together. The detailed way in which this is done and also tables of the various coefficients are given in appendix 5B.

The forms presented in this appendix are then sufficient to allow the integrals presented in appendix 5C to be combined in the correct forms for the calculation and plotting of differential cross-sections and target asymmetries as presented in the next section.

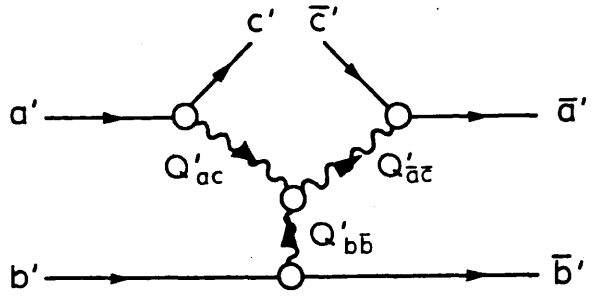

Figure 5.1 The input triple Regge expression used for correction in the formula of this chapter.

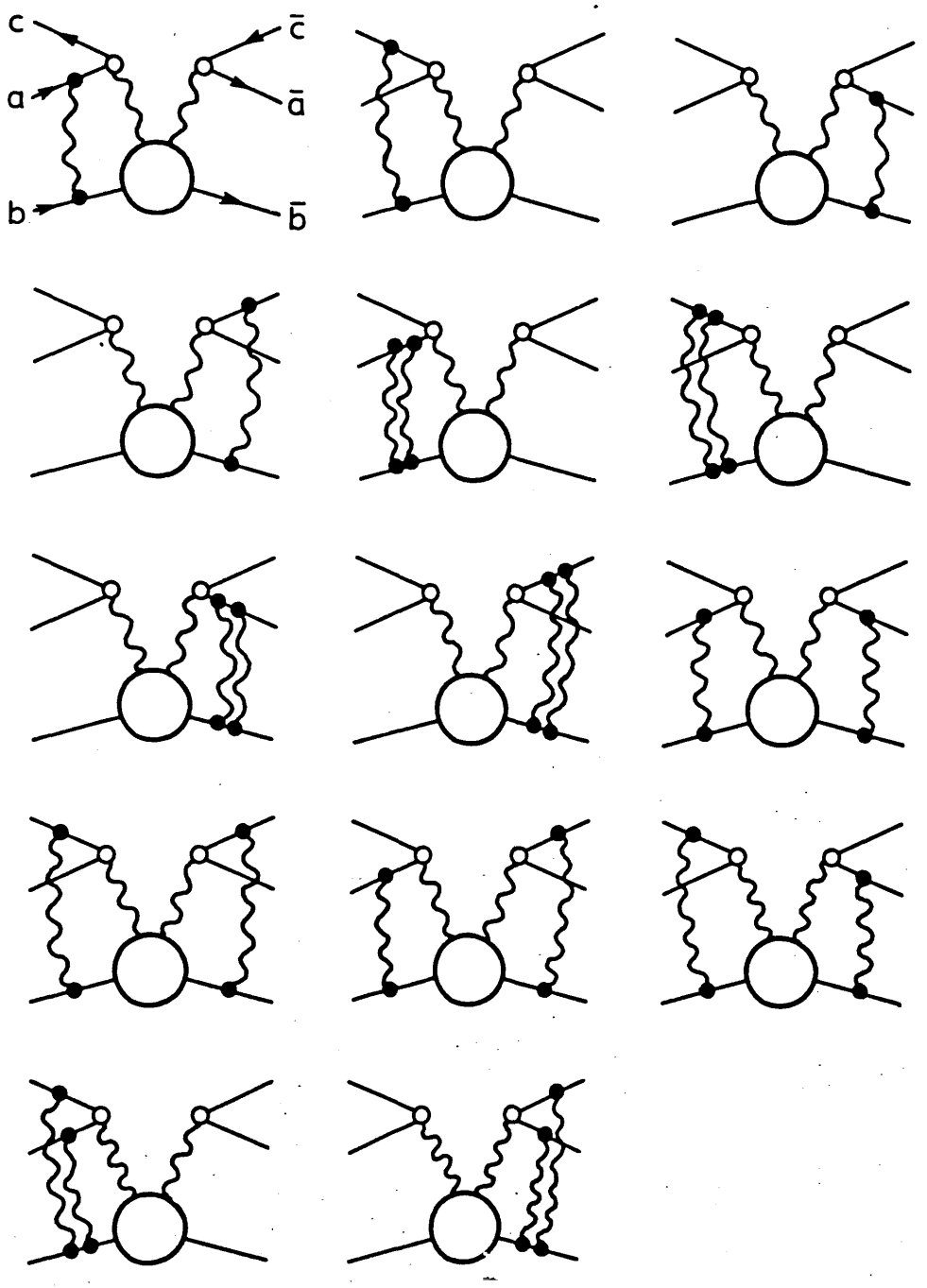

Figure 5.2(a) The classes of correction diagram actually used in the calculation of this chapter

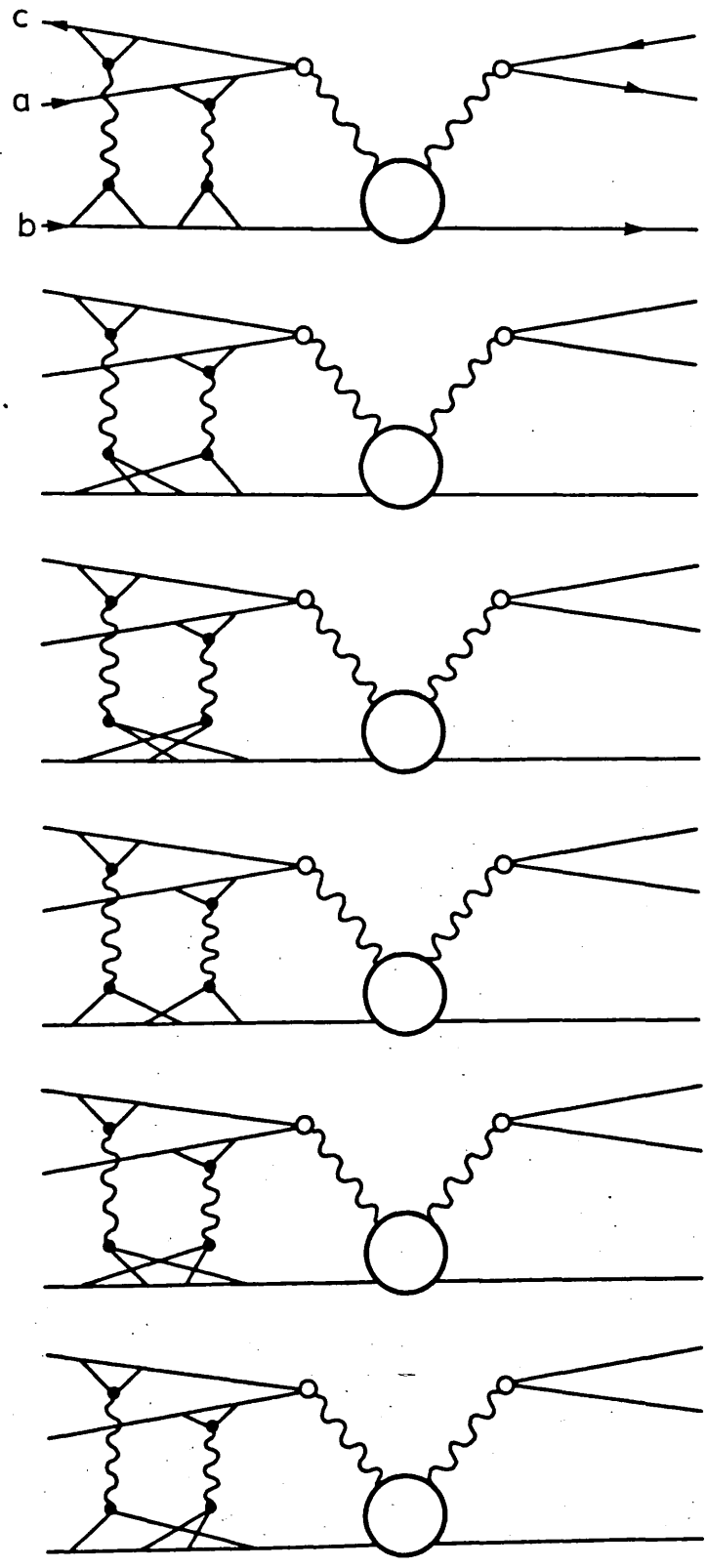

Figure 5.2(b) A class of diagrams treated similarly by the eikonal approximation used.

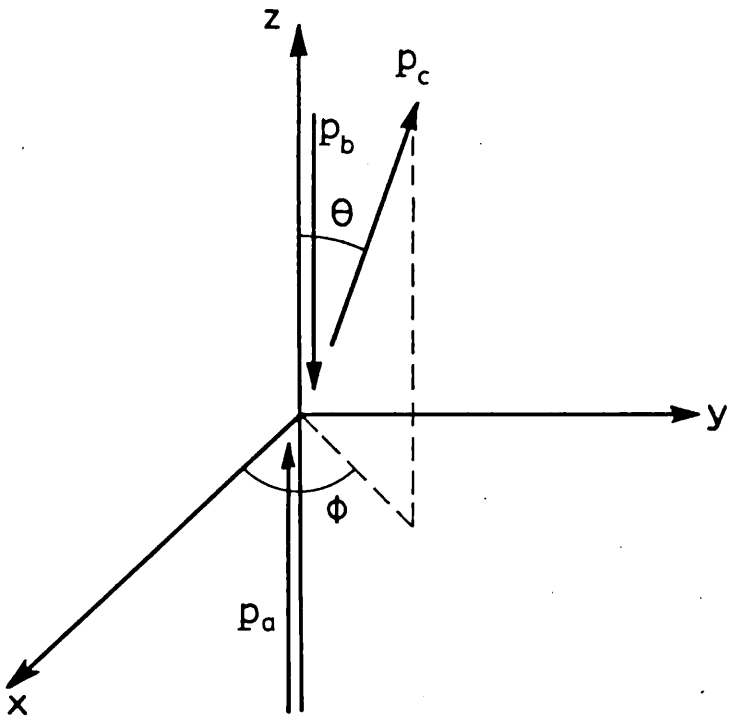

Figure 5.3. The kinematics employed for the calculation. b is the incoming proton, a is the incoming O^- particle and c is the outgoing O^- particle.

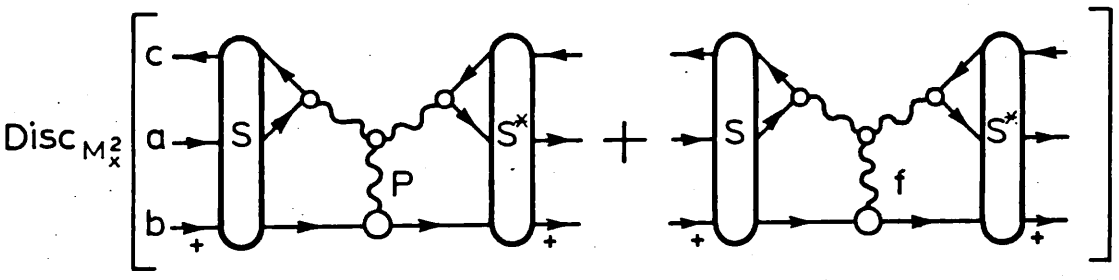

Figure 5.4(a) The two exchanges for the t_o or third leg giving rise to the differential cross-section.

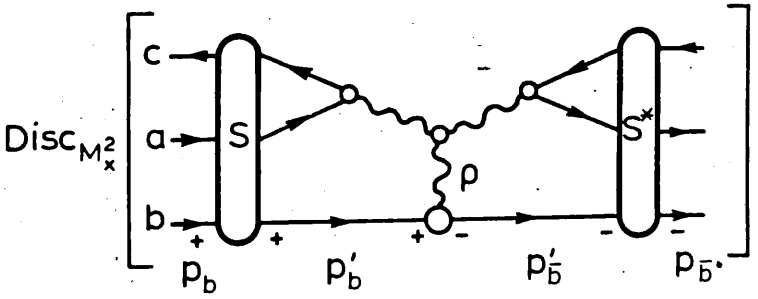

Figure 5.4 (b) The single third leg exchange which contributes to the target asymmetry

RESULTS

In figures 5.5 to 5.10 we present the results of applying the new scheme for absorption corrections, both for differential cross sections and target asymmetries, to the reactions

$$\pi^{\pm}p \to \pi^{o}+X^{o}$$
$$\pi^{+}+p \to \pi^{o}+X^{++}$$
$$\pi^{-}+p \to \eta+X^{o}$$
$$\pi^{+}+p \to \eta+X^{++}$$
$$K^{+}+p \to K^{o}+X^{++}$$
$$K^{-}+p \to \bar{K}^{o}+X^{o}$$

at $s = 100\ GeV/c^2$ for both t and M^2/s distributions as shown in the figures. In all cases allowance for the edge of phase space has been made, and for the case of the η, no allowance has been made for the branching ratio into $\gamma\gamma$; the likely experimental detection node.

Figure 5.11 gives results for the reaction $K^{-}+p \to R^{o}+X^{o}$ at the lower energy of $p_{lab} = 14.3\ GeV/c$ for which experimental data exists. In all cases for the differential cross-sections, the solid curve represents the prediction of the Regge pole only model given above and the long dashes represent the prediction of the absorption method Chapter III which is drawn here for comparison purposes. The short dashed curve is the prediction of the present model for the target asymmetry the short dash curve represents the prediction of the

present model - the two other models predict an identically zero target asymmetry.

Turning now to detailed consideration of the figures, the most striking prediction of figure 5.5(a) for the reaction $\pi^- p \to \pi^o X^o$ is that the signature dip, si prominant in the pole only curves, and merely shifted in toward t=0 in the model of chapter III is now completely obliterated for low M^2/s although it does reappear for $M^2_x/s = 0.5$. It would be difficult to maintain that full Reggeization had taken place at this point, and so less than full weight can be placed on the predictions at this value of M^2_x/s. The final curves we produce in fact bear a fairly close resemblance in shape to those of Pumplin [40] even though our starting points, and methods of carrying through absorption corrections are dissimilar.

The plots for target asymmetry for this reaction show quite a lot of detailed structure, showing the required zero as $p_{c\perp} \to 0$ and also a reduction as M^2_x/s increases, mainly due to the fact that a Reggeon with intercept $\simeq \frac{1}{2}$ is used to account for the proton flip amplitude. However since all target asymmetries, not just those for this reaction remain below two percent it seems unlikely that any of the structure would be experimentally measurable except in an extremely high statistics experiment. All that these curves predict is that

target asymmetry should be "small". Figure 5.5(b) shows the same reaction for various fixed t-bins. Any normalisation dsicrepancy between these curves and those for fixed M^2_x/s is accounted for by the fact that the curves for fixed t are found from integrating the theoretical expression over the t-bin using an 8-point Gauss Legendre quadrature. This effect is particularly noticeable for t = -0.5 GeV/c^2 where the actual pole value is below 10^{-3}, shown by figure 5.5(a), and the integration across the bin raises it above this value. From figure 5.5(b) we see that for small t, the absorbed curves show very little difference in slope from the pole only curves, although a decrease in normalisation is indicated. At t = -0.5 GeV/c^2 the dip structure plays a strong part and for still higher |t| the slopes of pole and absorption model begin to separate. We note that the present model has a greater slope in log (M^2_x/s) than does the model of Chapter III.

Figure 5.6(a) shows a very similar picture to that of 5.5(a) mainly because we predict no differences between ρ^+-Reggeon-proton scattering and that for ρ^--Reggeon and proton even though we do take account of some differences in the absorption parameters. The target asymmetries follow the same general slope and are the negative of those for $\pi^- p \to \pi^o X$ purely because we take the $G\rho^+\rho^+\rho^o$ coupling as the negative of the $G\rho^-\rho^-\rho^o$ coupling, as predicted by isospin. Figure 5.6(b) again shows the same similarity for the same reasons. Turning to figure 5.7(a) for the reactions $\pi^- p \to \eta X^o$, no signature dip is predicted in the range of $|t|$ of interest here for the pole only graph, and the present model follows the pole-only profile fairly closely, although at a slightly reduced slope and normalisation at small values of $|t|$. The present model shows less structure than that of chapter III which predicts shallow dips at $-t = 0.7$ GeV/c^2 for small M_x^2/s, and for this reaction the target asymmetries do not reach above 1%. Figure 5.7(b) shows the same reaction for fixed values of $|t|$ and for small $|t|$ we see that the present model differs from the pole only graph only in normalisation, not greatly in slope, with a slight slope change introduced for $-t > 0.5$ GeV/c^2.

Target asymmetries show the same steady fall off in M_x^2/s.

Figures 5.8(a) and (b) show the reaction $\pi^+ + p \to \eta X^{++}$, and again the graphs are extremely similar to those of $\pi^- + p \to \eta X^o$ with the difference in sign of the target asymmetry.

Figure 5.9(a) gives the results for the reaction $K^+ p \to K^o X^{++}$. We note that the present model differs in no great extent from the pole only model throughout, as usual. There is a great difference however between it and the model of chapter III which predicted zeros for small M_x^2/s. These zeros are nowhere to be seen for the present model which we believe is as it should be. Target asymmetries again fall short of great significance. Figure 5.9(b) again shows very similar slopes in M_x^2/s for the pole only and present model for small $|t|$, and slight deviations in slope as M_x^2/s gets larger.

Figure 5.10(a) and (b) show the reaction $K^- + p \to \bar{K}^o + X$. This is the line-reversed reaction to that of 5.9(a) and (b) and so the pole-only graphs are identical. The model of chapter III showed up great differences between them because of its simplicity in dealing with phases. The present model however, only gives differences in detail (viz. the two plots for $M_x^2/s = 0.10$ and the point where pole only and absorved curves cross) while the basic shape is very much the same. The target asymmetries are of course similar to those for

$K^+p \to K^oX^{++}$ except with a sign reversal. Figures 5.11(a) and (b) show the same reaction at the lower energy of p_{lab} = 14.3GeV/c for which there is data for the differential cross-section, although not for the target asymmetry [62]. Considering the fixed M_x^2/s plots first we see that, in general, the model of chapter III gives curves that seem to exhibit too much curvature for the data, and that the pole only curves exhibit too great a slope in -t for the data. The present model lies somewhere between the two. It does not exhibit curvature and structure not really called for in the data, and because of the strongest change in normalisation occuring for small |t| it shows a lesser slope in t that of the pole only curve. The change is not really sufficiently great however since in all cases the short dashed line passes through the error base of only one or two data points, the rest being taken out of range by the slope differences. There is consolation to be had, however, from the fact that better agreement is obtained at the values of M_x^2/s of 0.125 and 0.175 than larger values since for M_x^2/s = 0.375 it is possible that the upper legs (see figure 5.1) are not fully Reggeized.

A further point to note is that for small M_x^2/s the data points for large |t| are accounted for, while for larger M_x^2/s the points at smaller |t| have the error

bars interpolated by the present model. This effect is seen better in figure 5 5.11(b) where we see the general trend that all three models do not have sufficient slope in M_x^2/s, although the present model is a slight improvement on that of chapter III, and not greatly worse than that of pole only. Experience with the parameter fitting process of chapter III might suggest that the present model could be made to fit the data with less of an adjustment of Regge-Parameters because of its good behaviour in t.

It can be said, however, that agreement in both normalisation and form is surprisingly good for a model in which all parameters are predicted beforehand.

All the calculations of differential cross-sections and target asymmetries were carried out using the program ONCPLT [65] , and all the figures were initially computer plotted [49] .

CONCLUSIONS

The strongest conclusions that we can draw from this calculation are that our model does not predict large values for the target asymmetry, the largest value calculated being about 2%. Secondly we do not expect to see the signature dips seen in the exclusive case in the inclusive reaction at about $t = -0.5$ GeV/c^2. In our case they are absolutely filled in by the absorption contributions.

To return to these conclusions in more detail it is well known that either a factorisable Regge pole [77,11] or a fixed naturality exchange [77,13] for the t_o leg will give rise to zero target asymmetry. Equally well known is the kinematical angular behaviour of any asymmetry present [77,11,13,14] which our model properly reproduces. This kinematical behaviour includes a p_c suppression, and this fact that any asymmetry must vanish as $p_{c\perp}$ plus the lack of contribution from factorisable poles has led to the belief that any target asymmetry in the inclusive case will be small, and therefore difficult to measure. The present model then concurs with this view.

If large ($\sim$10%) target asymmetries are seen experimentally, then our simple prescription for an off-forward, but factorisable, Regge-pole exchange for the t_o leg would have to be abandoned in favour

of some other mechanism. One such mechanism would be the exchange of a ρP cut down the t_o leg. This entity is neither factorisable, nor of fixed naturality and so would not be constrained to give zero helicity flip contribution for $t_o = 0$, and therefore could be considered without any absorption corrections of the type considered here. Soffer and Wray [79] have considered just such a mechanism in a way that leaves the upper Reggeon-particle vertices free. They were thus able to factor off these vertices for both flip contributions and non flip contributions. This approach limited them in calculating kinematical dependancies and they were forced to insert the factor $\sqrt{-t}$ by hand. Their model is compared with data by Dick et al. [31] . This data was obtained in a $\pi^{\pm}p \rightarrow \pi^{\pm}X$ experiment at $p_{lab} = 8$ GeV/c. For $0.5<x<0.8$ the model of Soffer and Wray gives a target asymmetry fairly constant at about 7%, rising to about 10% at $x = 0.95$. On the other hand, the data presented give an asymmetry for the elastic reaction ($x = 1.0$) of about 17%, and when M_x has risen to 2 GeV/c ($x \simeq 0.75$) the target asymmetry cannot be said to be significantly above zero. This could be an indication that when Regge pole exchange is expected to dominate (i.e. $M_x^2 > 4.0$ GeV/c^2) in the t_o leg then the target asymmetry does become small, as predicted by a factorisable pole, and our model.

If we consider the signature dips, and lack of them, in $\pi^{\pm}p\rightarrow\pi^{o}X$ there is some high energy data available, as was mentioned in chapter III. O'Neill et al are able to present a ρ-pole effective trajectory which is significantly different from that predicted by either elastic data or a Chew-Frautschi plot, indicating that some form of absorption correction would seem to be indicated, although the data does not extend to large enough values of $|t|$ to resolve the questions about dip structure. Our model normalisation and theirs at $t = 0$ certainly agree to an order of magnitude. An experiment performed at the much lower energy of 5 GeV/c [64] . Here the $|t|$ behaviour is presented out to 1.9 GeV/c^2. For $M_x^2<2$ GeV/c^2 the cross-section shows a substantial dep. However this cross section would almost certainly be dominated by the reactions $\pi^-p\rightarrow\pi^o n$ and $\pi^-p\rightarrow\pi^o\Delta^o$ which could both be expected to exhibit dip structures. For $2<M_x^2<4$ the dip structure is much less apparent. For $4<M_x^2<6$ the t_{min} effect extends to obscure the region of interest. It does seem likely though, that the dip structure will not extend to higher energies, and higher values of M_x^2.

Our last comment is on the failure of our model to reproduce exactly the data of ref. 77 . For lower values of M_x^2 and for a reaction mediated by π exchange

instead of the present ρ exchange an attempt to fit the data using πρ elastic cross-sections [59] met with some success in fitting various dips and humps in the M_x^2/s spectrum. There is possibly some structure in the M_x^2/s data spectra, and were data, where high values of s/M_x^2 and M_x^2 were possible simultaneously, available we might find better agreement, due to more complete Reggeization. This argument may seem a trifle naive when the data for $t = -0.3$ GeV/c^2 are seen to hold to a very straight line in the log - plot of M_x^2/s, but the effective ρ trajectory given by O'Neill et al and that given for the ρ in chapter III indicates that a simple Regge-pole picture, exchanging poles with physical meaning, does not hold up.

Several questions therefore seem to require data at a much higher energy to resolve than satisfactory.

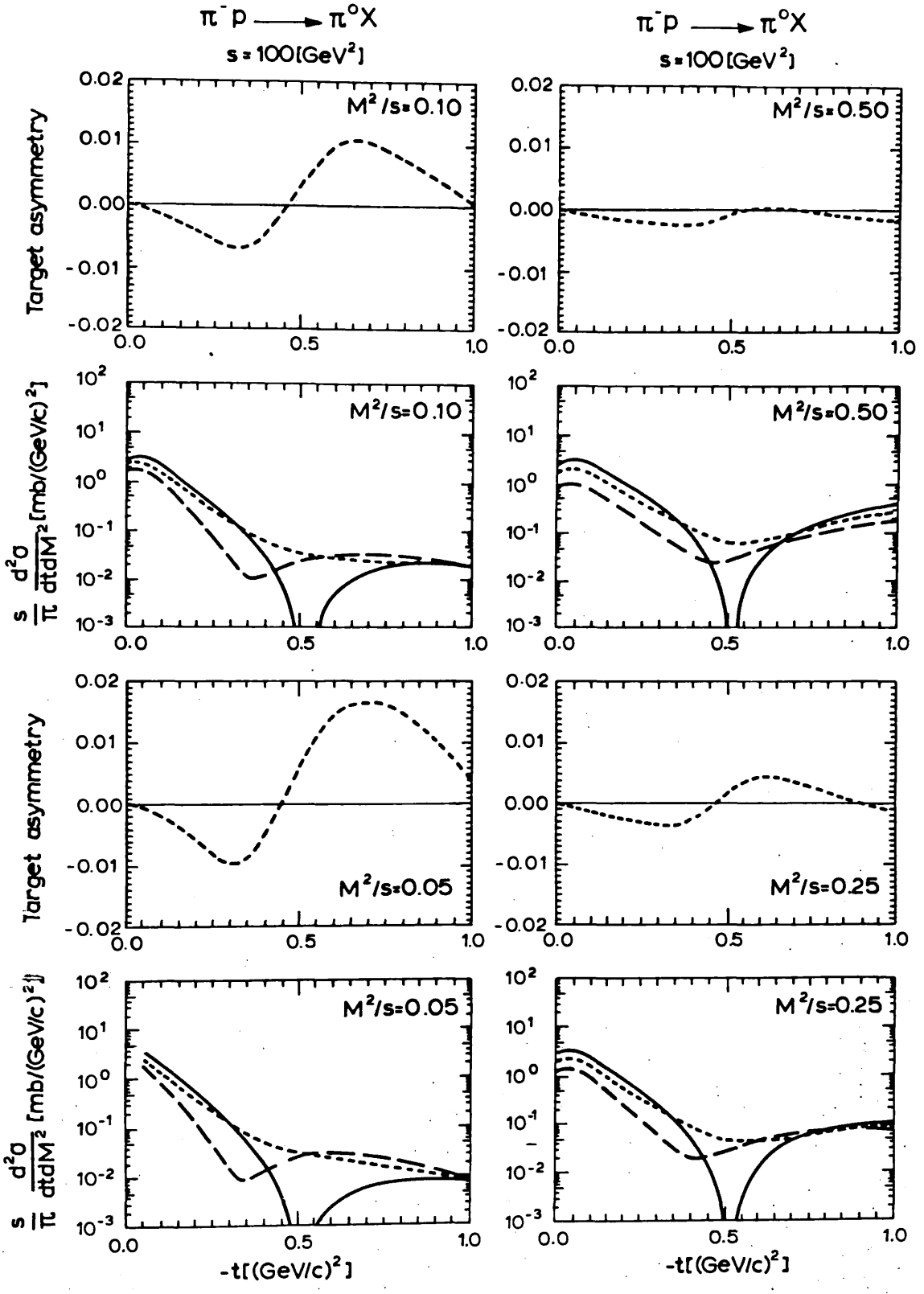

Figure 5.5(a) Differential cross-sections and target asymmetries for the reaction $\pi^- + p \to \pi^0 + X$ at s = 100 GeV/c^2 for various fixed value of M_x^2/s.

In figures 5.5 to 5.11 the solid curve represents a pole only calculation, the long dashed curve the absorption model of Chapter III and the short dashed curve the present model.

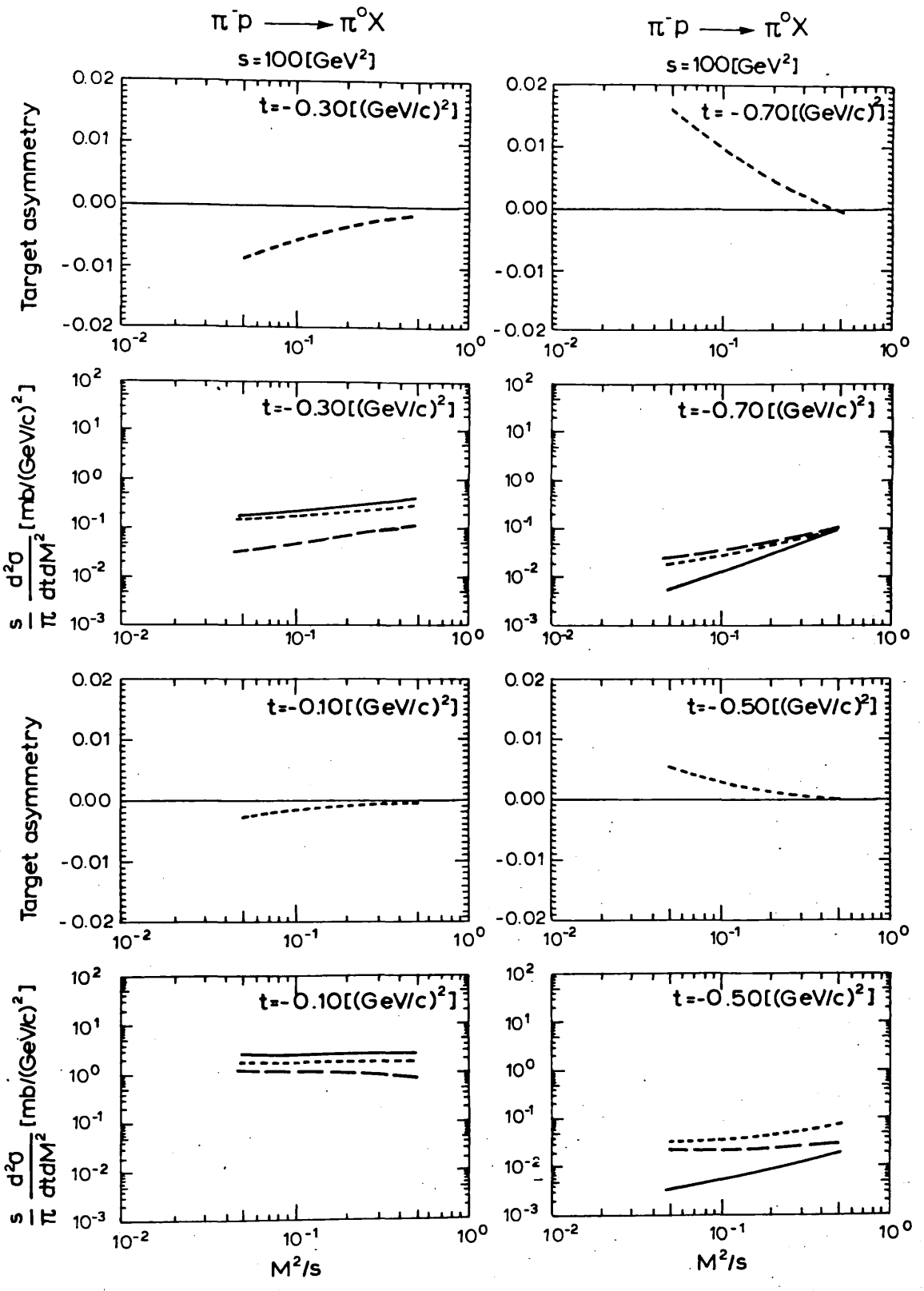

Figure 5.5 (b) Differential cross sections and target asymmetries for the reaction $\pi^- + p \rightarrow \pi^0 + X$ at s = 100 GeV/c^2 for various fixed values of t.

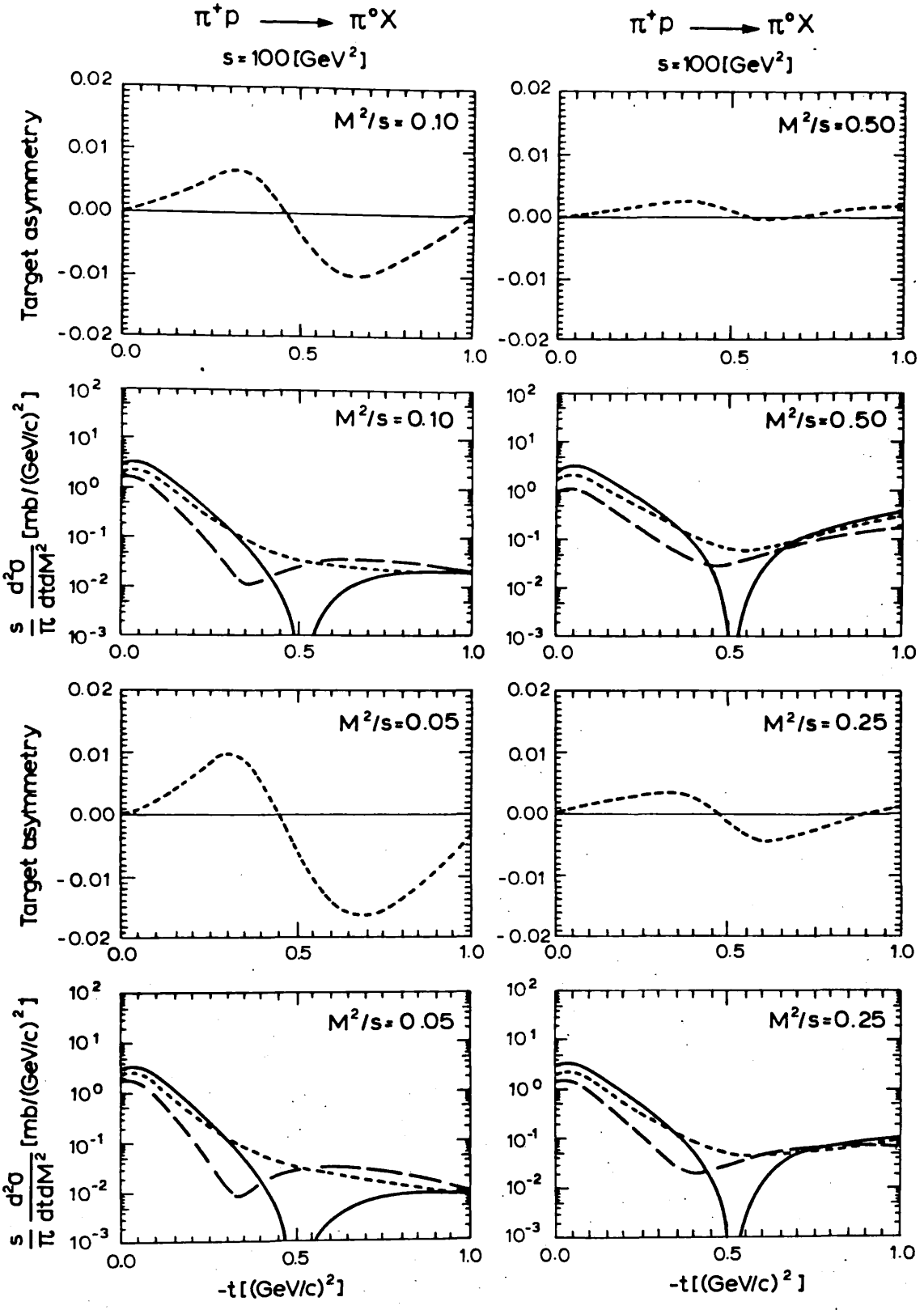

Figure 5.6(a) Differential cross-sections and target asymmetries of the reaction $\pi^+ + p \rightarrow \pi^0 + X$ at s = 100 GeV/c^2 for various fixed values of M_x^2/s.

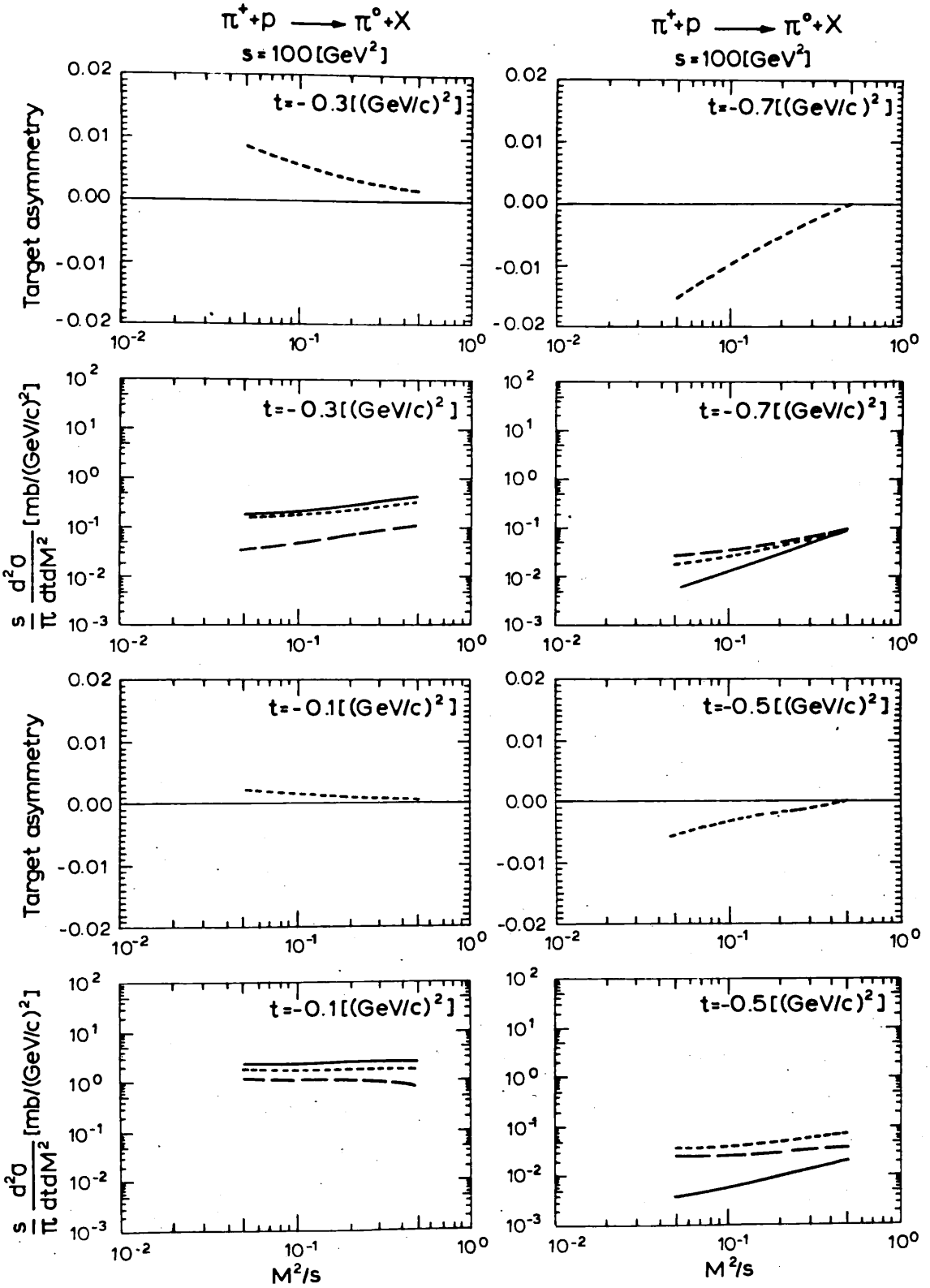

Figure 5.6(b) Differential cross-sections and target asymmetries of the reaction $\pi^+ + p \rightarrow \pi^0 + X^+$ at s = 100 GeV/c^2 for various fixed values of t.

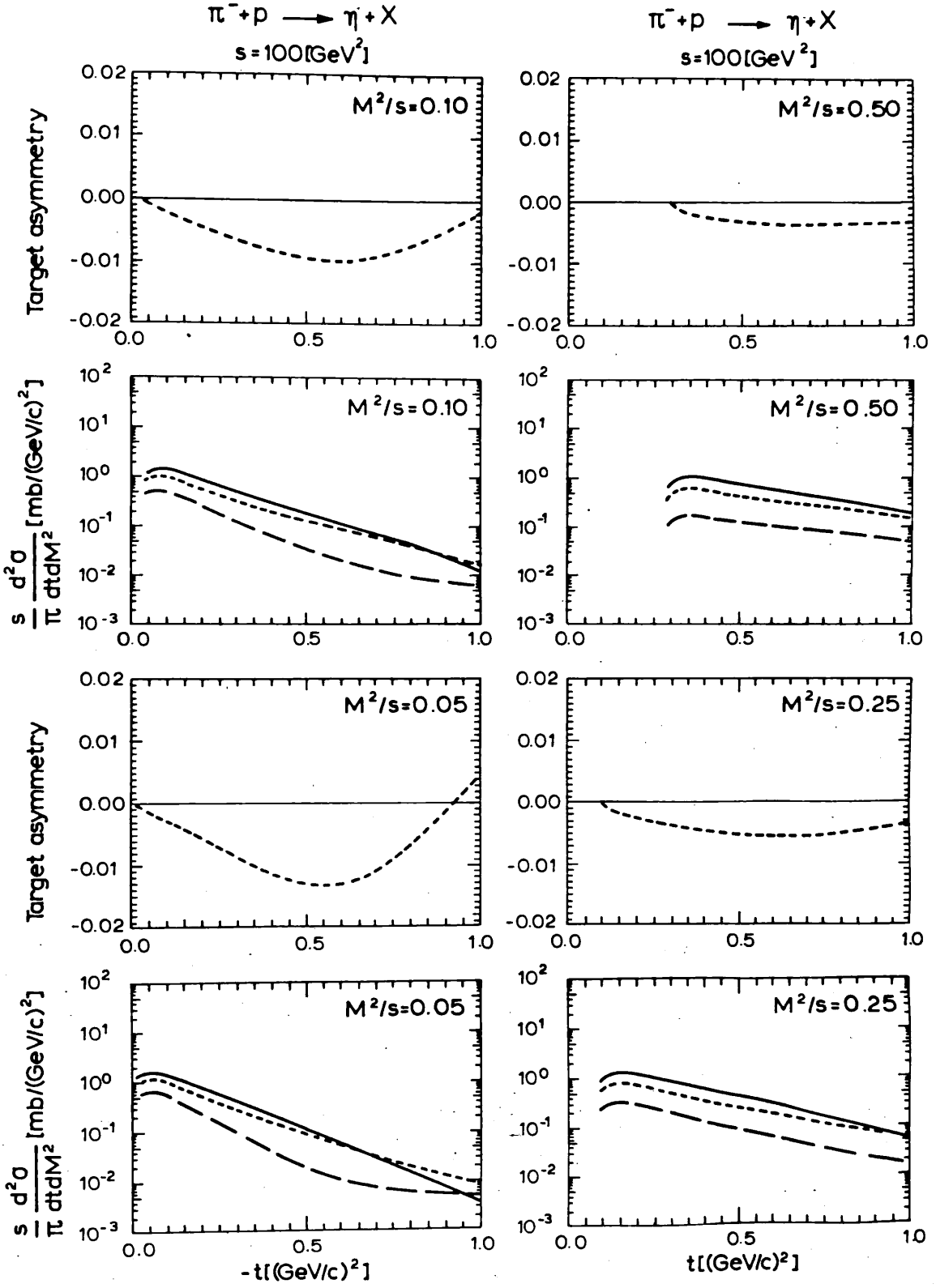

Figure 5.7(a) Differential cross-sections and target asymmetries of the reactions $\pi^- + p \to \eta + X^0$ at s = 100 GeV/c^2 for various fixed values of M_x^2/s.

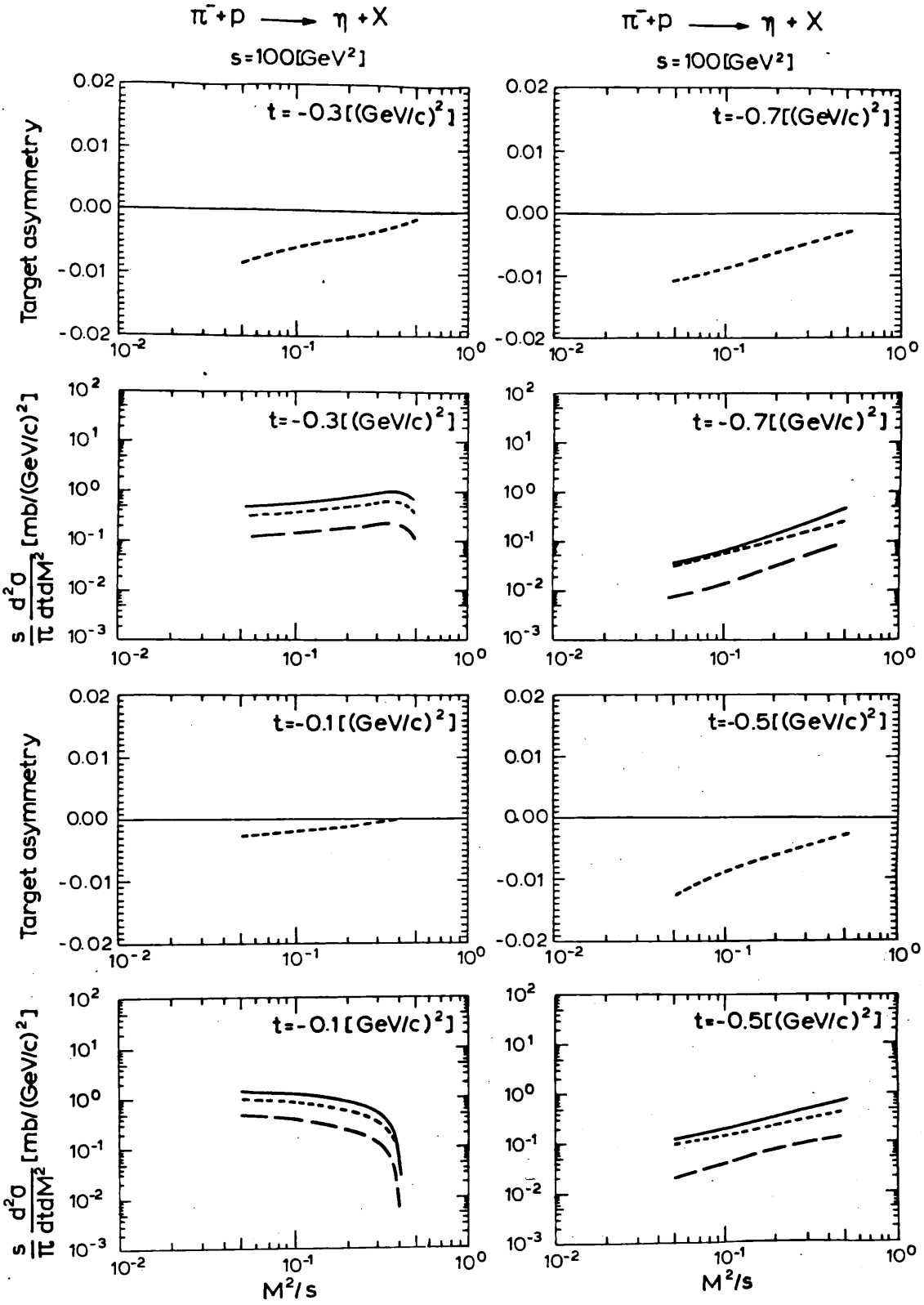

Figure 5.7(b) Differential cross-sections and target asymmetries of the reaction $\pi^-+p\rightarrow\eta+X^o$ at s = 100 GeV/c^2 for various fixed values of t.

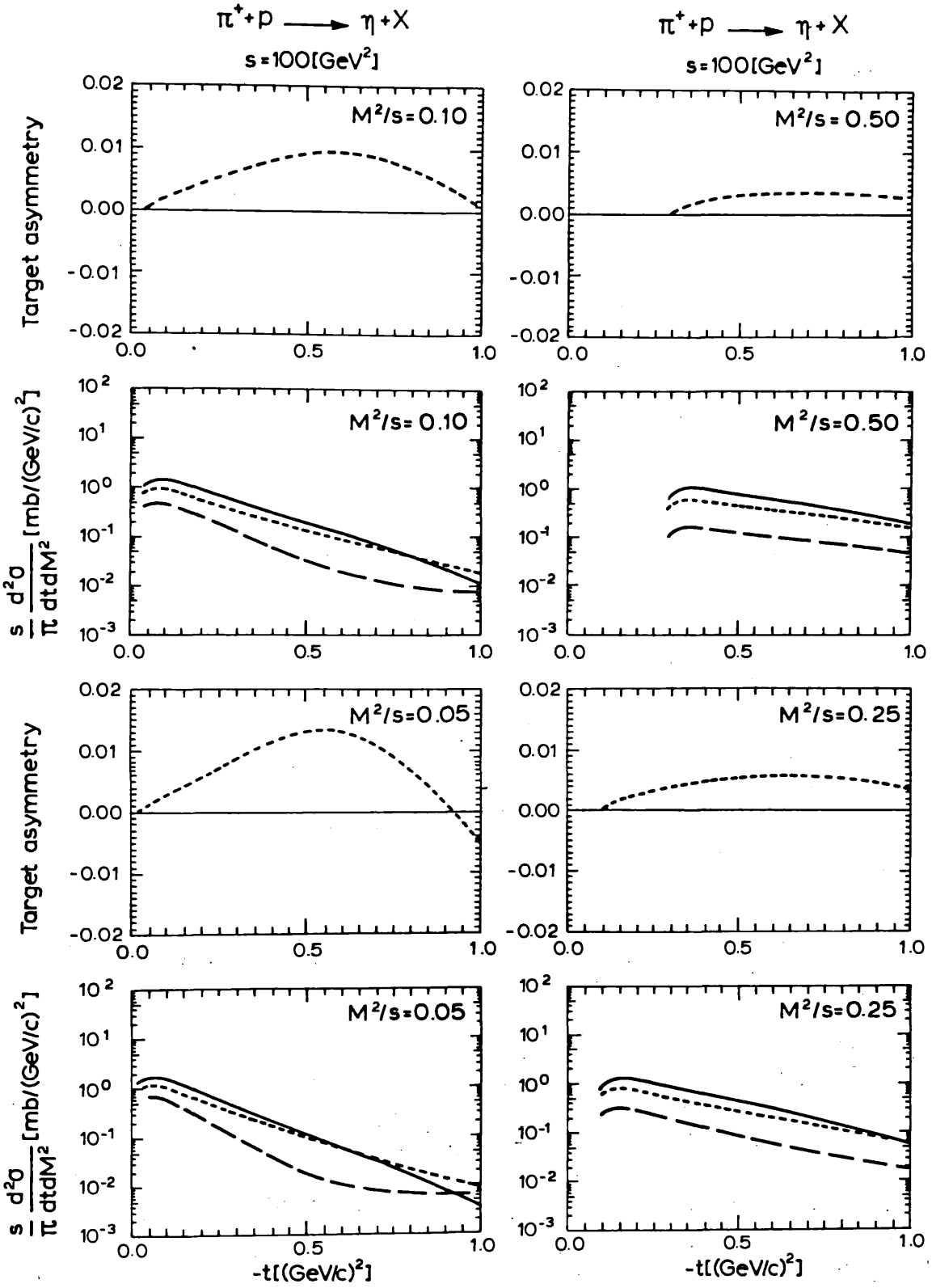

Figure 5.8(a) Differential cross-sections and target asymmetries of the reaction $\pi^+ + p \rightarrow \eta + X$ at s = 100 GeV/c^2 for various fixed values of M_x^2/s.

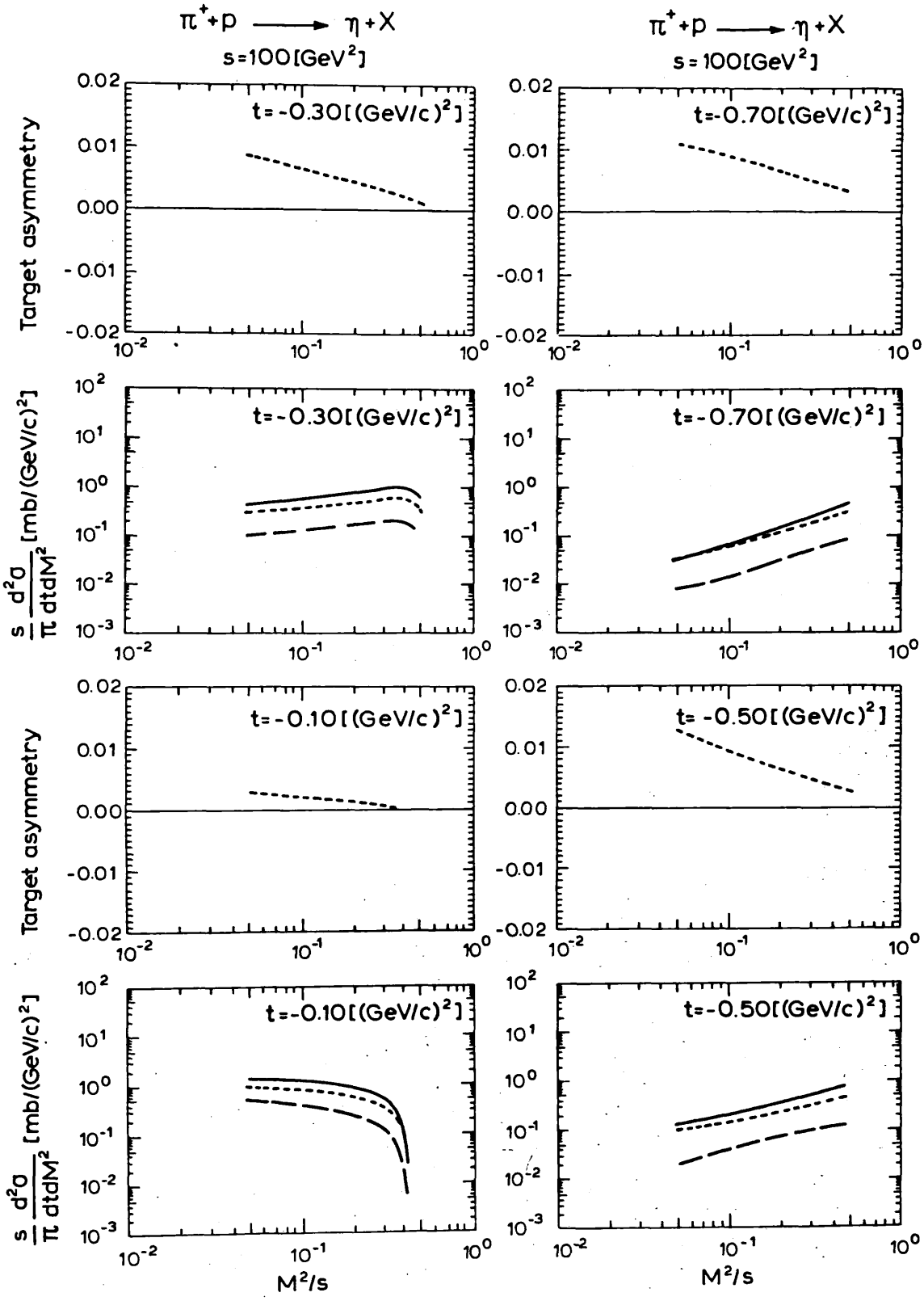

Figure 5.8(b) Differential cross-sections and target asymmetries for the reaction $\pi^+ + p \rightarrow \eta + X^{++}$

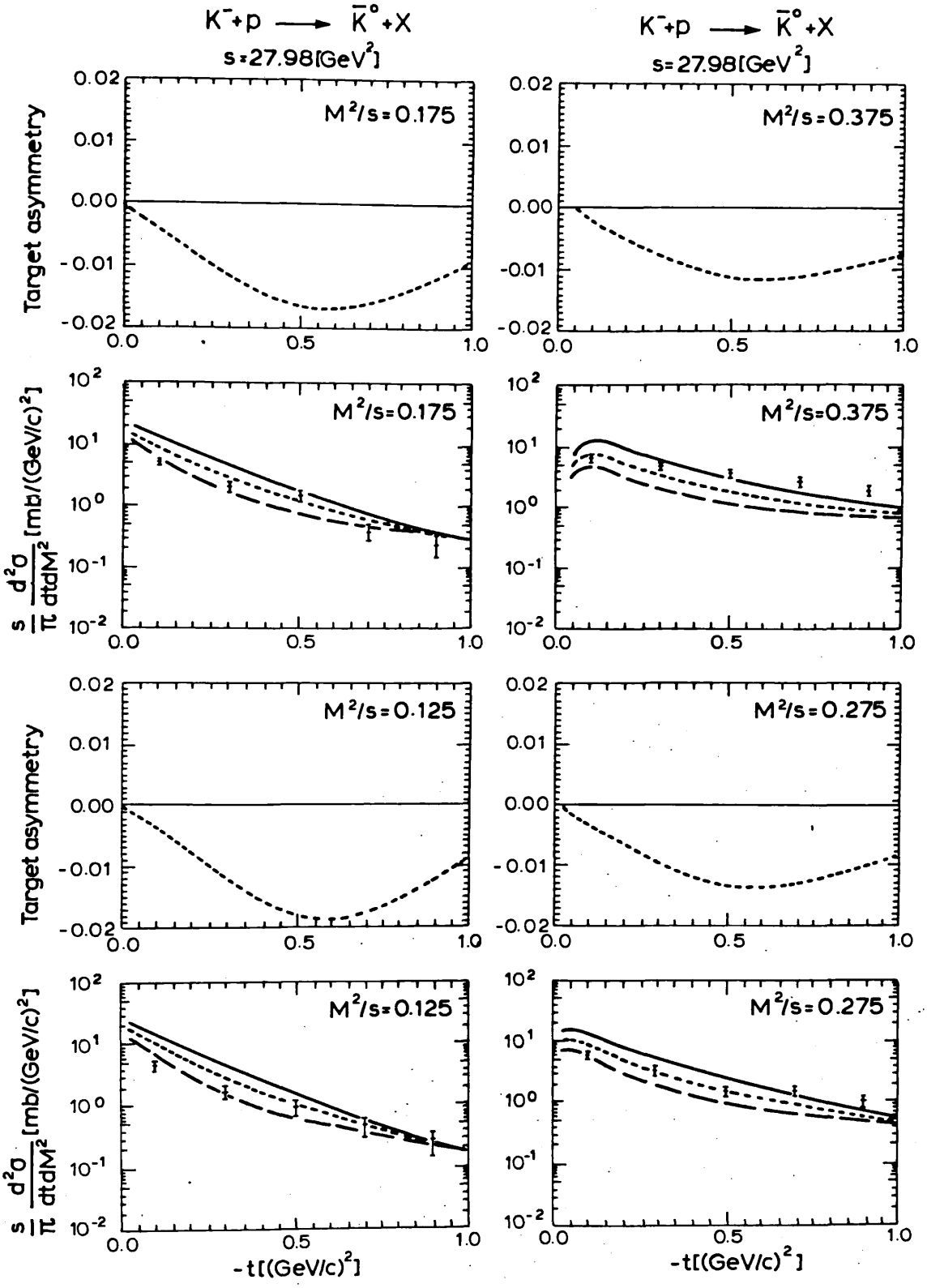

Figure 5.9(a) Differential cross-sections and target asymmetries for the reaction $K^+p \to K^o + X^{++}$ at s = 100 GeV/c^2 for various fixed values of M_X^2/s.

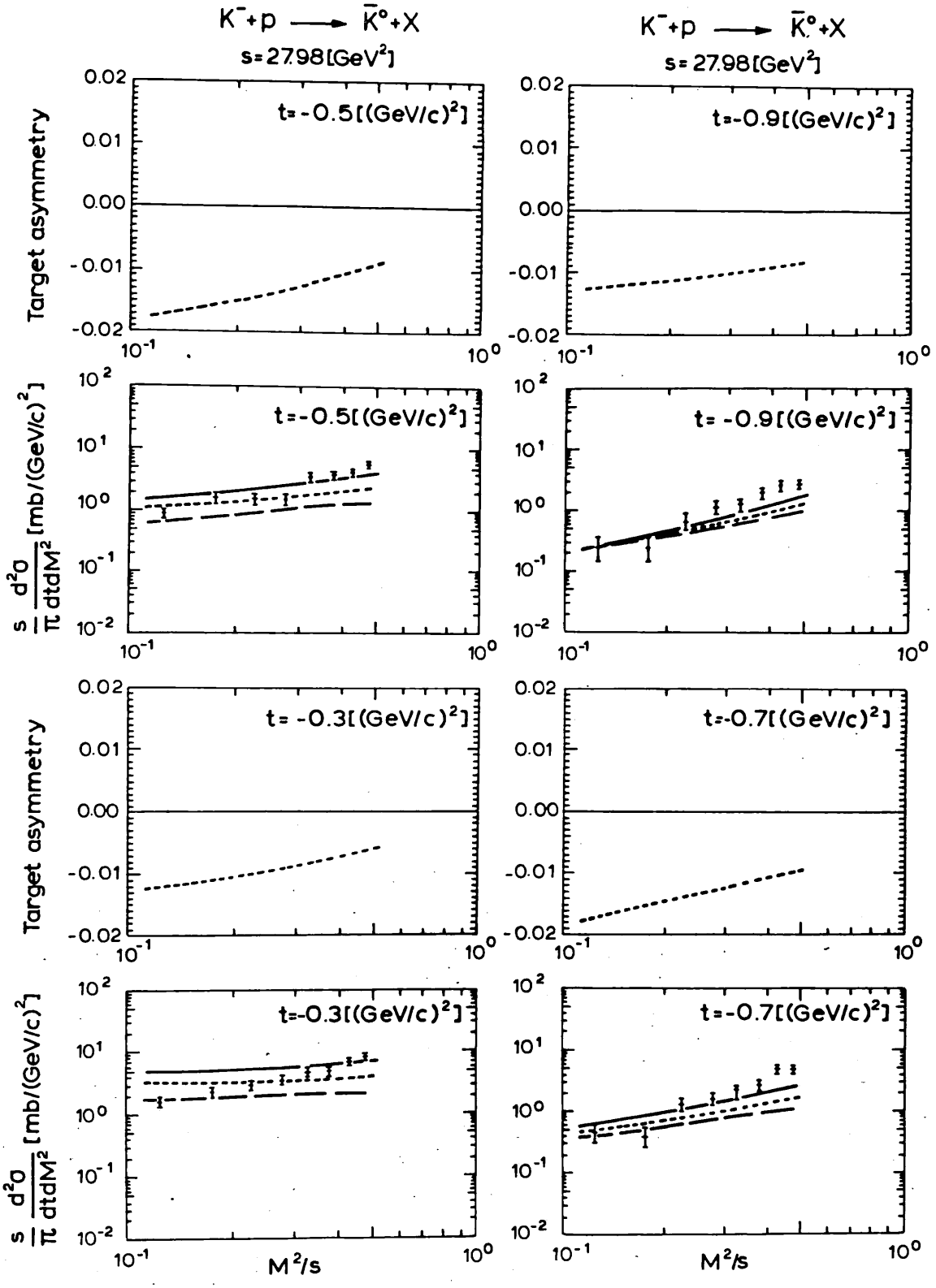

Figure 5.9(b) Differential cross-sections and target asymmetries for the reaction $K^+ + p \rightarrow K^0 + X^{++}$ at s = 100 GeV/c^2 for various fixed values of t.

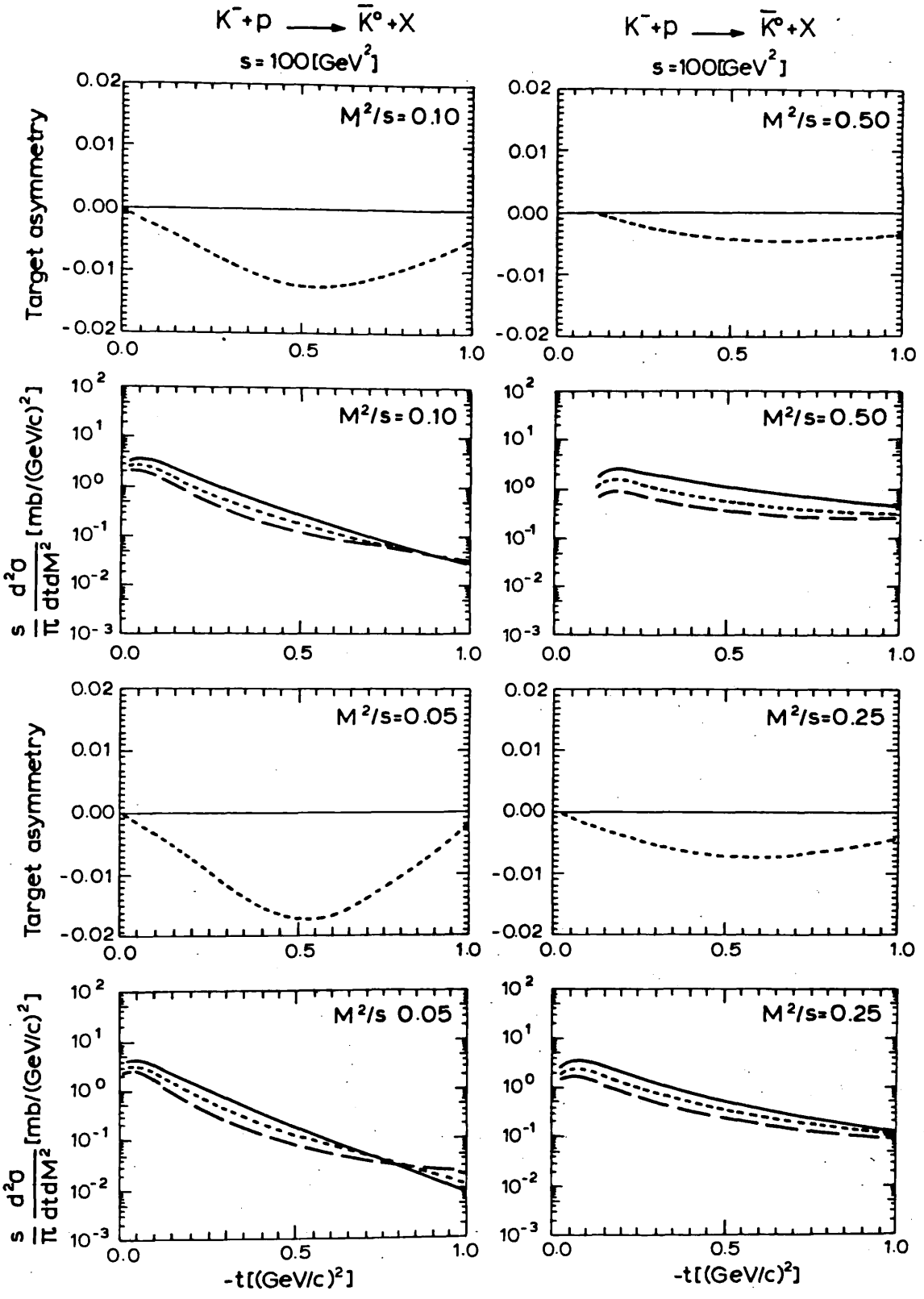

Figure 5.10(a) Differential cross-sections and target asymmetries for the reaction $K^- + p \to \bar{K}^0 + X^0$ at s = 100 GeV/c^2 for various fixed values of M_x^2/s.

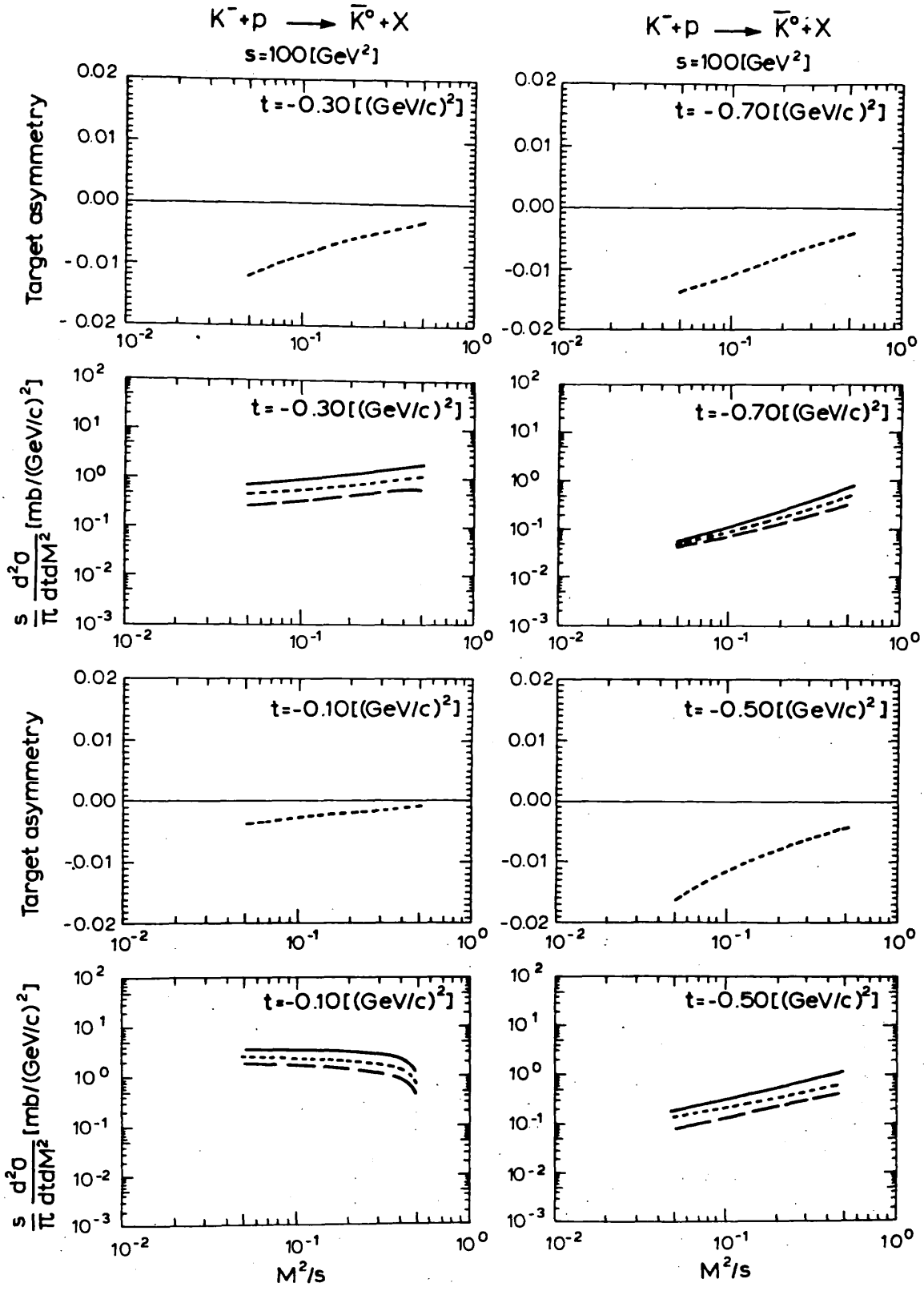

Figure 5.10(b) Differential cross-sections and target asymmetries for the reactions $K^- + p \to K^0_+ X$ at s = 100 GeV/c^2 for various fixed values of t.

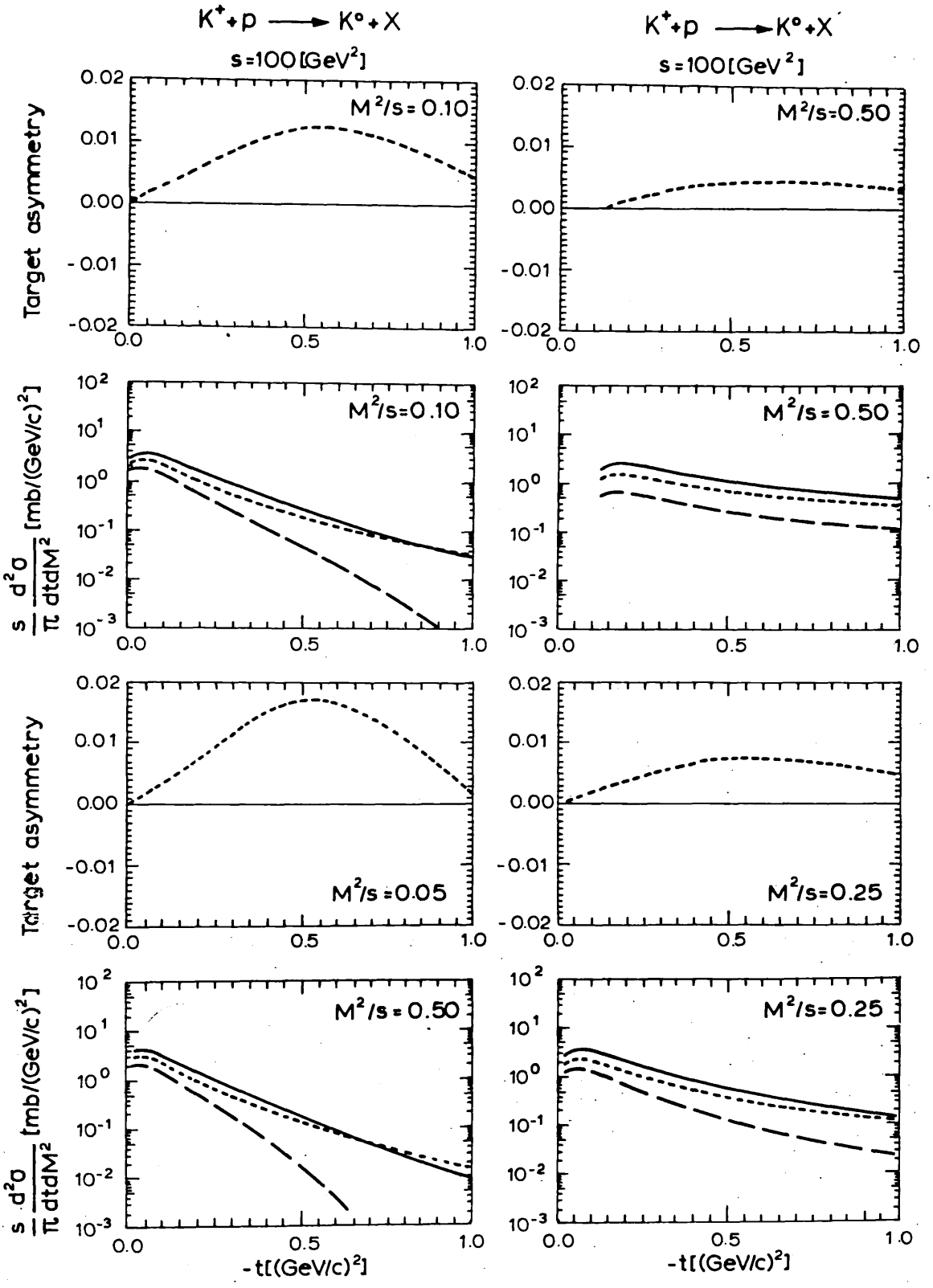

Figure 5.11(a) Differential cross-sections and target asymmetries for the reaction $K^- + p \to \bar{K}^0 + X^0$ at p_{lab} = 14.3 GeV/c for various fixed values of M_x^2/s.

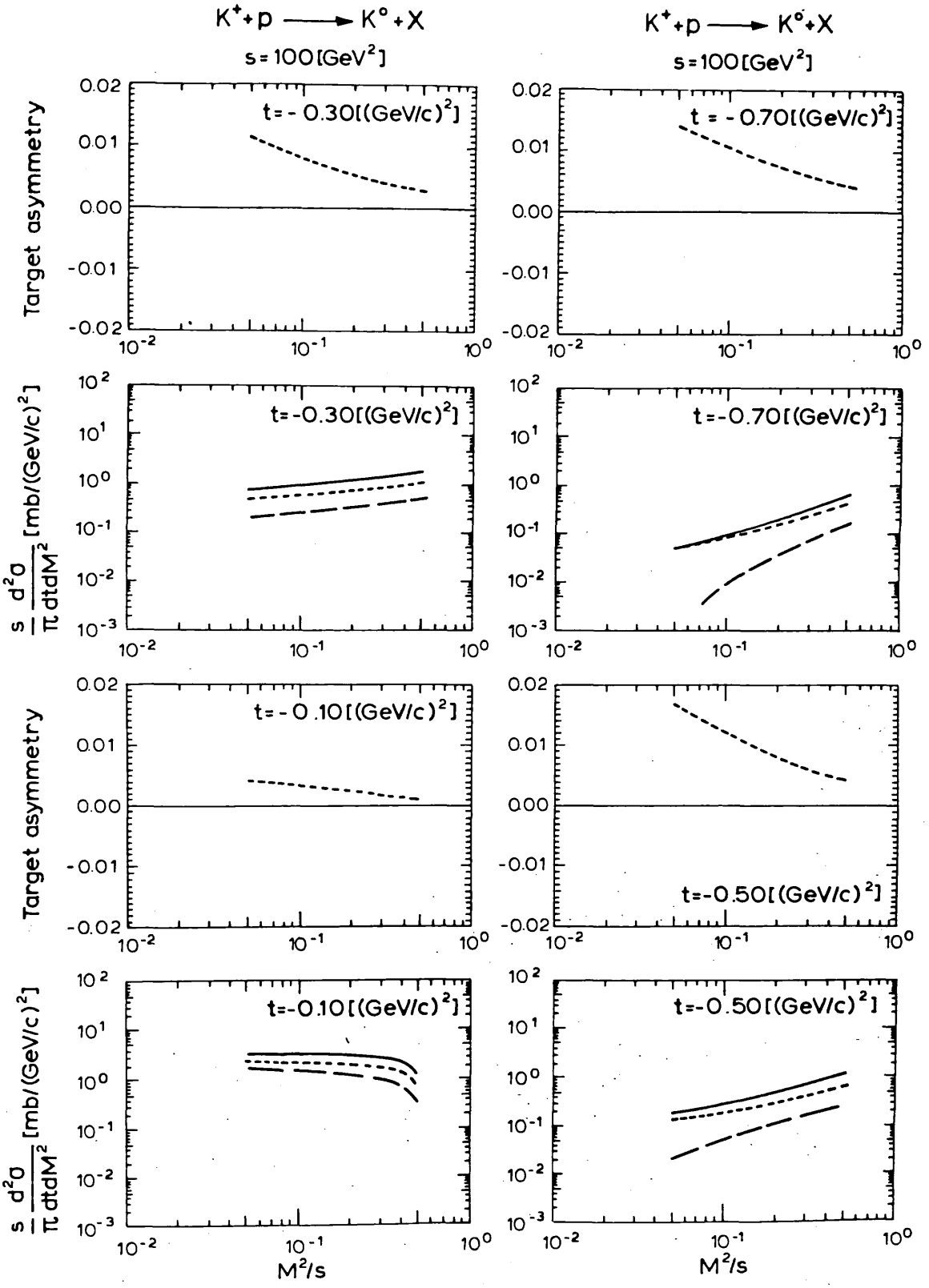

Figure 5.11(b) Differential cross-sections and target asymmetries for the reactions $K^- + p \to K^0 + X^0$ at p_{lab} = 14.3 GeV/c for various fixed values of t.

APPENDIX 5A

In this appendix we show that the eikonal approximation of Chapter IV can be extended to the case where the spinless intermediate exchanges depend from a spin $\frac{1}{2}$ particle.

We must first consider the form

$$\tau(B)=\lim_{\varepsilon\to 0^+} \lim_{p_b^2\to M^2} \lim_{p_b'^2\to M^2} (p_b^2-M^2)(p_b'^2-M^2)\langle p_b'|G(B)|p_b\rangle \qquad 5A1$$

in analogy with equation 4A1, but in this case

$$G(B) = (\not p - M - gB(X) + i\varepsilon)^{-1} \qquad 5A2$$

or alternatively

$$G(B) = \frac{\not P+M}{P^2-M^2} + \frac{g(\not P+M)\, B(x)(\not P+M)}{(P^2-M^2-(\not P+M)gB(x)+i\varepsilon(\not P+M))(P^2-M^2)} \qquad 5A3$$

where

$$\lim_{\substack{\varepsilon\to 0^+ \\ p_b'^2\to M^2 \\ p_b^2\to M^2}} \langle p_b'|\frac{\not P+M}{P^2-M^2}|p_b\rangle\,(p_b'^2-M^2)(p_b^2-M^2) = 0 \qquad 5A4$$

Using again the formal integral representation and operator identity of equation 4A5 we can write

$$(P^2-M^2-g(\not P+M)B(x)+i\varepsilon(\not P+M))^{-1}$$

$$= \int_0^\infty dt\; e^{i(P^2-M^2+i\varepsilon(\not P+M))t}\; T\exp\Big[\int_0^t d\tau$$

$$e^{-i(P^2-M^2+i\varepsilon(\not P+M))\tau}(-ig(\not P+M)B(x))e^{i(P^2-M^2+i\varepsilon(\not P+M))\tau}\Big] \qquad 5A5$$

In a completely analogous fashion to the analysis performed from equation 4A6 to equation 4A12, we can insert equation 5A5 into equation 5A1 and simplify to obtain

$$\tau(p_b,p_b';B) = \langle p_b'|i\ \mathrm{Texp}\{-i\int_0^\infty d\tau\ (\not{P}+M)gB(X-2P\tau)\}\quad g(\not{P}+M)B(X)2M|P_b\rangle. \qquad 5A6$$

It is at this stage that we eikonalize by replacing the operator P^μ by the C-number vector $p_b{}^\mu$, and thus making allowance for the spin character of the particles we can write

$$\tau_\varepsilon(p_b,p_b';B) = 2M\int\frac{d^4x_b}{(2\pi)^4}\,\bar{u}^{\lambda'}(p_b')e^{i(p_b-p_b').x_b}$$

$$\frac{\partial}{\partial\alpha_b}\exp[-ig\int_{\alpha_b}^\infty(\not{p}+M)B(x-2p_b\tau)d\tau]\Big|_{\alpha_b\to 0}u^\lambda(p_b) \qquad 5A7$$

If we make one further approximation which is consistent with the eikonal formulation namely [80]

$$\bar{u}^{\lambda'}(p_b')(\not{p}_b+M)^n u^\lambda(p_b) \simeq \bar{u}^{\lambda'}(p_b')(2M)^n u^\lambda(p_b) \qquad 5A8$$

we can provide the final formulation for

$\tau_\varepsilon(p_b,p_b';B)$ ie

$$\tau_\varepsilon(p_b,p_b';B) = \bar{u}^{\lambda'}(p_b')\{\int d^4x e^{i(p_b-p_b').x_b}$$

$$\frac{\partial}{\partial\alpha_b}\exp[-i.2Mg\int_{\alpha_b}^\infty B(x-2p_b\tau)d\tau]\Big|_{\alpha_b=0}\}2Mu^\lambda(p_b) \qquad 5A9$$

This form is the analogue of equation 4A13 and can be inserted in equation 4.4 to yield

$$(2\pi)^4\delta^4(p_a+p_b-p_c-p_{\bar{a}}-p_{\bar{b}}+p_{\bar{c}})\ H(p_a,p_b,p_c;p_{\bar{a}}p_{\bar{b}}p_{\bar{c}})$$

$$= D^*D\int \pi_{\alpha\bar{\alpha}}\ \frac{d^4p'_\alpha}{(2\pi)^4}\ \frac{d^4p'_{\bar{\alpha}}}{(2\pi)^4}\ .2\pi\delta^+(p_\alpha'^2-m_\alpha^2)2\pi\delta^+(p_{\bar{\alpha}}'^2-m_{\bar{\alpha}}^2)$$

$$(2\pi)^4\delta^4(p'_a+p'_b-p'_c-p'_{\bar{a}}-p'_{\bar{b}}+p'_{\bar{c}})$$

$$\tau_\varepsilon{}^*(p_{\bar{a}}p'_{\bar{a}};\bar{A})\tau^*(p_{\bar{c}}p'_{\bar{c}};\bar{})\tau_\varepsilon(p_a,p'_a;A)\tau_\varepsilon(p_cp'_c;C)$$

$$\bar{u}^{\lambda_{\bar{b}}}(p_{\bar{b}})\{\int \frac{d^4x}{(2\pi)^4}\ e^{i(p_{\bar{b}}-p'_{\bar{b}}).x_{\bar{b}}}\ \frac{\partial}{\partial\alpha_{\bar{b}}}\ \exp[+i2Mg\int_{\alpha_{\bar{b}}}^{\infty}\bar{B}(x.2p_{\bar{b}}\ \tau)d\tau]\Big|_{\alpha_{\bar{b}}=0}\ \}$$

$$u^{\lambda'_{\bar{b}}}(p'_{\bar{b}})\{\bar{u}^{\lambda'_{\bar{b}}}(p'_{\bar{b}})Y(p'_ap'_bp'_c;p'_{\bar{a}}p'_{\bar{b}},p'_{\bar{c}})u^{\lambda'_b}(p'_b)\}$$

$$\bar{u}^{\lambda'_b}(p'_b)\{\int \frac{d^4x}{(2\pi)^4}\ e^{i(p_b-p'_b).x_b}\ \frac{\partial}{\partial\alpha_b}\ \exp[-i2Mg\int_{\alpha_b}^{\infty}B(x-2p_b\tau)d\tau\Big|_{\alpha_b=0}\ \}\quad u^{\lambda_b}(p_b)$$

5A10

where we use the generalization of equation 4.3 to spin $\frac{1}{2}$ particles to insert the spinors around the Y function, which now has the character of a Dirac γ-matrix of some general form.

So to effect the transition to one spin $\frac{1}{2}$ leg we have only to make the replacement

$$Y(t_{ac},t_{\bar{a}\bar{c}},t_o,s_{ab},M_x^2) \rightarrow$$

$$\bar{u}^{\lambda_{\bar{b}}}(p_{\bar{b}})(\not{p}'_{\bar{b}}+M)\gamma Y(t_{ac},t_{\bar{a}\bar{c}},t_o,s_{ab},M_x^2)$$

$$(\not{p}'_b+M)u^{\lambda_b}(p_b).$$

5A11

in equation 4.19.

APPENDIX 5B

The first section of this appendix deals with the detailed representations of the vectors $\vec{Q}_a$ and $\vec{Q}_c$. If we take

$$p_a = (\sqrt{s_{ab}}/2,\ 0,\ 0,\ k)$$

$$p_b = (\sqrt{s_{ab}}/2,\ 0,\ 0,\ -k)$$

$$p_c = ((x+y)\sqrt{s_{ab}}/2,\ p_{c\perp}\mathrm{Cos}\phi,\ p_{c\perp}\mathrm{Sin}\phi,\ (x-y)k)$$

where $y = \frac{1}{s}\left(\frac{m^2+p_{c\perp}^2}{x} - xm^2\right)$ - 5.B.1

Then since $p_a.\vec{Q}_a = p_b.\vec{Q}_a = 0$ so we can take without any loss of generality

$$\vec{Q}_a = (0,\ Q_{a1},\ Q_{a2},\ 0) \qquad \text{- 5.B.2}$$

If we now take

$$\vec{Q}_c = (Q_{co},\ Q_{c1},\ Q_{c2},\ Q_{c3}) \qquad \text{- 5.B.3}$$

Then we can use the two conditions

$$p_c.\vec{Q}_c = p_b.\vec{Q}_c = 0$$

to eliminate the components Q_{co} and Q_{c3}.

So, $p_b.\vec{Q}_c = 0$ gives

$$Q_{c3} = -\frac{\sqrt{s_{ab}}}{2k}\ Q_{co} \qquad \text{- 5.B.4}$$

and $p_c.\vec{Q}_c = 0$ gives

$$0 = (x+y)\frac{\sqrt{s}}{2}\ Q_{co} - Q_{c2}p_{c\perp}\mathrm{Sin}\phi - Q_{c1}p_{c\perp}\mathrm{Cos}\phi - (x-y)kQ_{c3} \qquad \text{- 5.B.5}$$

Substituting for Q_c from equation 5.B.4 we have

$$x\sqrt{s_{ab}}Q_{co} = p_{c\perp}(Q_{c1}\mathrm{Cos}\phi + Q_{c2}\mathrm{Sin}\phi) \qquad \text{- 5.B.6}$$

For the region that interests us x is of the order of 1 and so equation 5.B.6 shows that the Q_{co} and Q_{c3} components are down on the Q_{c1} and Q_{c2} by a factor of $\sqrt{s_{ab}}$. Since the eikonal approximation assumes that the region of importance occurs when Q_{c1} and Q_{c2} (also Q_{a1} and Q_{a2} for that matter) are small with respect to $\sqrt{s_{ab}}$ we are justified in neglecting the contributions from the Q_{co} and Q_{c3} components in the expression for t_{ac} and t_o which is what we have effectively done in equation 5.4.

The next section of this appendix deals with the representation of the off forward triple-Regge expression for $\pi\pi p \to \pi\pi p$ scattering. This has the general form [81]

$$Y_R(t_{ac}, t_{\bar{a}\bar{c}}, t_o, s_{ab}, M_x^2) = \beta_{\pi\pi\rho}(t_{ac})\,\xi_\rho(t_{ac})$$

$$\left(\frac{s_{ab}}{M_x^2}\right)^{\alpha_\rho(t_{ac})} \beta_{\pi\pi\rho}(t_{\bar{a}\bar{c}}) \left(\frac{s_{ab}}{M_x^2}\right)^{\alpha_\rho(t_{ac})} \xi^*_\rho(t_{\bar{a}\bar{c}})$$

$$G_{\rho\rho R}(t_{ac}, t_{\bar{a}\bar{c}}, t_o)\,\xi_R(t_o)\,(M_x)^{\alpha_R(t_o)}\,\beta^{\lambda\lambda}_{ppR}(t_o) \qquad 5.B.7$$

Where R stands for the Pomeron or the f- or ρ-Reggeon, and the λ_s are the proton helicities and the ξs represent the appropriate signature factors. Notice that for $\lambda \neq \lambda$ for the Pomeron and f-Reggeon that $\beta^{\lambda\lambda}_{\rho\rho P}, t = 0$. Also for the ρ-Reggeon $\beta^{\lambda\lambda}_{pp\rho} = 0$. The ρ-vertex factor, however, does not take cary of any threshold effects. These are left to be dealt with by the factor of equation 5.14 and $\beta^{+-}_{pp\rho}(t_o)$ is taken to be a simple exponential in t_o, after approximations have been made.

In order to decide on the precise functional form of the various quantities in 5.B.7 we return to the form of equation 3.12.

Thus we can make the identification

$$\beta_{\pi\pi\rho}(t) = g_{\rho\pi\pi}((\bar{\phi}_5)_c(\phi_5)_a)_F \alpha'_\rho \Gamma(1-\alpha_\rho(t))/2 \qquad 5.B.8$$

and $2\mathrm{Im}\{ G_{\rho\rho P}(t,t,o)\xi_P(o)\beta^{++}_{\rho\rho P}(o) +$

$$G_{\rho\rho f}(t,t,o)\xi_f(o)\beta^{++}_{\rho\rho f}(o)/M_x^{\alpha_f(o)} \}$$

$$= 1.404(m^2_\rho)^3(98.6 + 64.9/(M_x^2)^{\frac{1}{2}} \qquad 5.B.9$$

We take [57]

$$\beta^{++}_{\rho\rho f}(t_o) = g_{\rho\rho f}\alpha'_f \Gamma(1-\alpha_f(t_o)) \qquad 5.B.10$$

and $\beta^{++}_{\rho\rho P}(t_o) = \beta^{++}_{\rho\rho P}(o)e^{\tilde{a}t_o}$

where $\tilde{a}$ is determined by considering πp and pp elastic scattering [82]

There remains the functional dependence of $G_{\rho\rho}R(t_{ac}, t_{\bar{a}\bar{c}}, t_o)$. This could in general be expected to exhibit an extremely complicated behaviour [17] . However, at this level of approximation we take the behaviour of $G_{\rho\rho}R$ to be a constant.

Separating out the two M_x^2 dependencies of the R.H.S. in equation 5.B.9 and assigning the two terms to Pomeron and f-Reggeon resepctively we can acquire the normalisations at $t_o = 0$ for the Pomeron and f-Reggeon exchanges; having assumed the functional form, we can then write down the terms

$$Y_P^{++}(t_{ac}, t_{\bar{a}\bar{c}}, t_o, s_{ab}, M_x^2) = \frac{g_{\rho\pi\pi}}{2}((\bar{\phi}_s)_c(\phi_s)_a)_F \alpha'_\rho$$

$$\Gamma(1-\alpha_\rho(t_{ac})) \left(\frac{s_{ab}}{M_x^2}\right)^{\alpha_\rho(t_{ac})} \xi_\rho(t_{ac})$$

$$\frac{g_{\rho\pi\pi}}{2} ((\bar{\phi}_5)_c(\phi_5)_a)_F \alpha'_\rho \Gamma(1-\alpha_\rho(t_{\bar{a}\bar{c}})) \left(\frac{s_{ab}}{M_x^2}\right)^{\alpha_\rho(t_{\bar{a}\bar{c}})} \xi_\rho(t_{\bar{a}\bar{c}})$$

$$.69.22(m^2\rho)^3 e^{\tilde{a}t_o(M_x^2)\alpha_P(t_o)} \qquad - 5.B.11$$

$$Y_f^{++}(t_{ac}, t_{\bar{a}\bar{c}}, t_o, s_{ab}, M_x^2) = \frac{g_{\rho\pi\pi}}{2} ((\bar{\phi}_5)_c(\phi_5)_a)_F \alpha'_\rho$$

$$\Gamma(1-\alpha_\rho(t_{ac}))\quad \left(\frac{s_{ab}}{M_x^2}\right)^{\alpha_\rho(t_{ac})}\ \xi_\rho(t_{ac})$$

$$\frac{g_{\rho\pi\pi}}{2}\quad ((\bar{\phi})_5(\phi_5)_a)_F\alpha'_\rho\ \Gamma(1-\alpha_\rho(t_{\bar{a}\bar{c}}))\quad \left(\frac{s_{ab}}{M_x}\right)^{\alpha_\rho(t_{\bar{a}\bar{c}})}\ \xi^*_\rho(t_{\bar{a}\bar{c}})$$

$$81.12(m^2_\rho)^3\ \frac{\Gamma(1-\alpha_f(t_o))}{\Gamma(1-\alpha_f(o))}\quad (M_x^2)^{\alpha_f(t_o)} \qquad - 5.B.12$$

For want of better information we take

$$Y_\rho(t_{ac},t_{\bar{a}\bar{c}},t_o,s_{ab},M_x^2) = \left(\frac{g_{\rho\pi\pi}}{2}((\bar{\phi}_5)_c(\phi_5)_a)_F\alpha'_\rho\right.$$

$$\left.\Gamma(1-\alpha_\rho)t_{ac}))\right)\left(\frac{s_{ab}}{M_x^2}\right)^{\alpha_\rho(t_{ac})}\quad \xi_\rho(t_{ac})$$

$$\left(\frac{g_{\rho\pi\pi}}{2}\ ((\bar{\phi}_5)_c(\phi_5)_a)_F\ \alpha'_\rho\ \Gamma(1-\alpha_\rho(t_{\bar{a}\bar{c}}))\right)\left(\frac{s_{ab}}{M_x^2}\right)^{\alpha_\rho(t_{\bar{a}\bar{c}})}\ \xi_\rho\ (t_{\bar{a}\bar{c}})$$

$$\tau_{ac}\ \sqrt{\frac{2}{3}}\ 81.12(m_\rho^2)^3\ \frac{\Gamma(1-\alpha_\rho(t_o))}{\Gamma(1-\alpha_\rho(0))}\ (M_x^2)^{\alpha_\rho(t_o)} \quad - 5.B.13$$

where the overall normalisation derives from that of the f-Reggeon exchange. The numerical factor $\sqrt{\frac{2}{3}}$ and the quantity τ_{ac}, which takes on the values ± 1, come from the differing isospin between the ρ and f, and is the ratio of the SU(2) Clebsch Gordan coefficients for each.

We note here that the gamma functions arise from the Gell Mann ghost eliminating mechanism and are only want for use at small values of t; accordingly we will approximate them by exponentials in t.

Also, by using ideas of SU(3) symmetry and strong exchange degeneracy between ρ and A_2, we need only alter the quantity $((\bar{\phi}_5)_c(\phi_5)_a)_F$ to $((\bar{\phi}_5)_c(\phi_5)_a)_D$ for A_2 exchange, or for the various different particles a and c.

Thus, table 5.B.I gives the Regge parameters for the four exchanges considered here, table 5.B.II gives the exponential approximations used for the gamma functions and table 5.B.III gives the quantities $((\bar{\phi}_5)_c(\phi_5)_a)_{F,D}$ and τ_{ac} for all the different reactions considered. The numbers in these tables allow calculation of all the off forward triple-Regge terms that are necessary for evaluation of the selected integrals in appendix 5.C. Consideration of equations 5.B.11, 12, 13 show that the quantities Y_P, Y_f and $\hat{Y}_\rho$ are indeed sums of exponentials of the required form.

The last, short, section to this appendix deals with the calculation of the various absorption parameters C, C', a and a' for the various particles and interactions.

We have

$$C = \sigma_{tot}/(2\pi R^2)$$

where R is the radius of interaction which seems fairly constant over the range of energies that we have taken, and are given in table 5.B.IV.

For our purposes we relate the unknown total cross-sections of π^o, η, $\bar{K}^o$ and K^o on protons to the known ones of π^+, π^-, K^+ and K^- on protons using very simple isospin ideas.

As M_x^2/s_{ab} changes so does s_{cb}, for which we need absorption parameters. To make this calculation easy we assume that total cross-sections of the four known reactions are piecewise linear between the points in energy given in table 5.B.IV. We can then calculate a value of C at any energy assuming this linearity.

TABLE 5.B.I. - REGGE PARAMETERS FOR THE FOUR EXCHANGES THAT WE CONSIDER

Trajectory	Intercept	Slope	Signature	Isospin
P	1.0	0.25	+1	0
ρ	0.47	0.905	-1	1
A_2	0.47	0.905	+1	1
f	0.4	1.0	+1	0

TABLE 5.B.II - EXPONENTIAL APPROXIMATIONS TO GAMMA FUNCTIONS

Function	Approximation
$\Gamma(1-\alpha_\rho(t))$	1.475605 exp (.6118244t)
$\Gamma(1-\alpha_f(t))$	1.307707 exp (.4856229t)

TABLE 5.B.III - SU(3) FACTORS AND RELATIVE SIGNS OF THE ρ TRIPLE REGGE COUPLING TO THAT FOR POMERON AND f

Reaction	SU(3) factor ρ	SU(3) factor A_2	Relative Sign
$\pi^- p \to \pi^o X$	2	0	-
$\pi^- p \to \eta X$	0	$2/\sqrt{3}$	-
$\pi^+ p \to \pi^o X$	2	0	+
$\pi^+ p \to \eta X$	0	$2/\sqrt{3}$	+
$K^+ p \to K^o X$	$\sqrt{2}$	$\sqrt{2}$	+
$K^- p \to \bar{K}^o X$	$-\sqrt{2}$	$\sqrt{2}$	-

TABLE 5.B.IV - ABSORPTION PARAMETERS

Reaction	Energy $(GeV/c)^2$	C	$\lambda (GeV/c)^{-2}$
$\pi^- p$	100.0	0.669	0.0676
	25.0	0.691	0.0676
$\pi^+ p$	100.0	0.694	0.0729
	25.0	0.694	0.0729
$K^- p$	100.0	0.553	0.0676
	25.0	0.572	0.0676
	14.0	0.586	0.0676
$K^+ p$	100.0	0.551	0.0729
	14.0	0.516	0.0729
	7.0	0.516	0.0729

APPENDIX 5C

This appendix is concerned with performing the integrals arising from equation 5.9 analytically. To reiterate we have

$$H = \int \frac{d^2\vec{Q}_a}{(2\pi)^2}\ \frac{d^2\vec{Q}_c}{(2\pi)^2}\ \frac{d^2\vec{Q}_{\bar{a}}}{(2\pi)^2}\ \frac{d^2\vec{Q}_{\bar{c}}}{(2\pi)^2}\ \cdot$$

$$\{(2\pi)^2\delta^2(\vec{Q}_a)+4\pi \sum_{k=1}^{\infty} \frac{(-1)^k C^k a^k}{k.k!(A)^{k-1}} \exp(-\frac{\vec{Q}_a^2 A}{k})\}$$

$$\{(2\pi)^2\delta^2(\vec{Q}_c)+4\pi \sum_{\ell=1}^{\infty} \frac{(-1)^\ell C'^\ell a'^\ell}{\ell.\ell!(A')^{\ell-1}} \exp(-\frac{\vec{Q}_c^2 A'}{\ell})\}$$

$$\{(2\pi)^2\delta^2(\vec{Q}_{\bar{a}})+4\pi \sum_{m=1}^{\infty} \frac{(-1)^m C^m a^m}{m.m'(A^*)^{m-1}} \exp(-\frac{\vec{Q}_{\bar{a}}^2 A^*}{m})\}$$

$$\{(2\pi)^2\delta^2(\vec{Q}_{\bar{c}})+4\pi \sum_{n=1}^{\infty} \frac{(-1)^n C'^n a'^n}{n.n!(A'^*)^{n-1}} \exp(-\frac{\vec{Q}_{\bar{c}}^2 A'^*}{n})\}$$

$$Y(t_{ac},t_{\bar{a}\bar{c}},t_o,s_{ab},M_x^2).f(\vec{Q}_a,\vec{Q}_c,\vec{Q}_{\bar{a}},\vec{Q}_{\bar{c}},p_{c_\perp}). \qquad 5C1$$

where

$$f = (p_{c_\perp} \mathrm{Cos}\phi + Q_{a_1} + Q_{c_1} - ip_{c_\perp} \sin\phi - iQ_{a_2} - iQ_{c_2})$$

$$-(p_{c_\perp} \mathrm{Cos}\phi + Q_{\bar{a}_1} + Q_{\bar{c}_2} - ip_{c_\perp} \sin\phi - iQ_{\bar{a}_2} - iQ_{\bar{c}_2}) \qquad 5C2$$

for integrals arising from the helicity flip 3-body discontinuity and

$$f = 1$$

for integrals arising from the helicity nonflip 3-body discontinuity.

The notation is as for the previously mentioned equations. Because of the form chosen for Y i.e. a sum of exponential terms, we need only consider integrals containing

$$e^{E\,tac}\ e^{Ft\bar{a}\bar{c}}\ e^{Gto} \qquad 5C3$$

where E, F and G can have small imaginary parts. Also because the functions we are integrating are uniformly continuous we will be able to exchange summation and integration symbols where necessary.

Therefore, the integrals that must be performed in order to be able to construct all the possible contributions to 5C1 can be listed as:-

1. $$\frac{1}{\pi}\int d^2\vec{Q}_a \exp\{-\frac{\vec{Q}_a^2 A}{k}\}\ f(\vec{Q}_a)e^{Etac}e^{Ft\bar{a}\bar{c}}e^{Gto}$$

2. $$\frac{1}{\pi}\int d^2\vec{Q}_c \exp\{-\frac{\vec{Q}_c^2 A'}{\ell}\}\ f(\vec{Q}_c)e^{Etac}e^{Ft\bar{a}\bar{c}}e^{Gto}$$

3. $$\frac{1}{\pi}\int d^2\vec{Q}_{\bar{a}} \exp\{-\frac{\vec{Q}_{\bar{a}}^2 A^*}{m}\}\ f(\vec{Q}_{\bar{a}})e^{Etac}e^{Ft\bar{a}\bar{c}}e^{Gto}$$

4. $$\frac{1}{\pi}\int d^2\vec{Q}_{\bar{c}} \exp\{-\frac{\vec{Q}_{\bar{c}}^2 A'^*}{n}\}\ f(\vec{Q}_{\bar{c}})e^{Etac}e^{Ft\bar{a}\bar{c}}e^{Gto}$$

5. $$\frac{1}{\pi^2}\int d^2\vec{Q}_a d^2\vec{Q}_c \exp\{-\frac{\vec{Q}_a^2 A}{k}-\frac{\vec{Q}_c^2 A'}{\ell}\}\ f(\vec{Q}_a,\vec{Q}_c)\quad e^{Etac}e^{Ft\bar{a}\bar{c}}e^{Gto}$$

6. $$\frac{1}{\pi^2}\int d^2\vec{Q}_{\bar{a}} d^2\vec{Q}_c \exp\{-\frac{\vec{Q}_{\bar{a}}^2 A^*}{m}-\frac{\vec{Q}_c^2 A'}{n}\}\ f(\vec{Q}_{\bar{a}},\vec{Q}_c)e^{Etac}e^{Ft\bar{a}\bar{c}}e^{Gto}$$

7. $$\frac{1}{\pi^2}\int d^2\vec{Q}_a d^2\vec{Q}_{\bar{a}} \exp\{-\frac{\vec{Q}_a^2 A}{k}-\frac{\vec{Q}_{\bar{a}}^2 A^*}{m}\}\ f(\vec{Q}_a,\vec{Q}_{\bar{a}})e^{Etac}e^{Ft\bar{a}\bar{c}}e^{Gto}$$

8. $$\frac{1}{\pi^2}\int d^2\vec{Q}_a d^2\vec{Q}_{\bar{c}} \exp\{-\frac{\vec{Q}_a^2 A}{k}-\frac{\vec{Q}_{\bar{c}}^2 A'^*}{n}\}\ f(\vec{Q}_a,\vec{Q}_{\bar{c}})e^{Etac}e^{Ft\bar{a}\bar{c}}e^{Gto}$$

9. $$\frac{1}{\pi^2}\int d^2\vec{Q}_c d^2\vec{Q}_{\bar{a}} \exp\{-\frac{\vec{Q}_c^2 A'}{\ell}-\frac{\vec{Q}_{\bar{a}}^2 A^*}{m}\}\ f(\vec{Q}_c,\vec{Q}_{\bar{a}})e^{Etac}e^{Ft\bar{a}\bar{c}}e^{Gto}$$

10. $$\frac{1}{\pi^2}\int d^2\vec{Q}_c d^2\vec{Q}_{\bar{c}}\ \exp\{-\frac{\vec{Q}_c^2 A'}{\ell}-\frac{\vec{Q}_{\bar{c}}^2 A'^*}{n}\}\ f(\vec{Q}_c,\vec{Q}_{\bar{c}})e^{Etac_e Ft\bar{a}\bar{c}_e Gto}$$

11. $$\frac{1}{\pi^3}\int d^2\vec{Q}_c d^2\vec{Q}_{\bar{a}} d^2\vec{Q}_{\bar{c}}\ \exp\{-\frac{\vec{Q}_c^2 A'}{\ell}-\frac{\vec{Q}_{\bar{a}}^2 A^*}{m}-\frac{\vec{Q}_{\bar{c}}^2 A'^*}{n}\}\ f(\vec{Q}_c,\vec{Q}_{\bar{a}},\vec{Q}_{\bar{c}})e^{Etac_e Ft\bar{a}\bar{c}_e Gto}$$

12. $$\frac{1}{\pi^3}\int d^2\vec{Q}_a d^2\vec{Q}_{\bar{a}} d^2\vec{Q}_{\bar{c}}\ \exp\{-\frac{\vec{Q}_a^2 A}{k}\frac{\vec{Q}_{\bar{a}}^2 A^*}{m}-\frac{\vec{Q}_{\bar{c}}^2 A'^*}{n}\}\ f(\vec{Q}_a,\vec{Q}_{\bar{a}},\vec{Q}_{\bar{c}})e^{Etac_e Ft\bar{a}\bar{c}_e Gto}$$

13. $$\frac{1}{\pi^3}\int d^2\vec{Q}_a d^2\vec{Q}_c d^2\vec{Q}_{\bar{c}}\ \exp\{-\frac{\vec{Q}_a^2 A}{k}-\frac{\vec{Q}_c^2 A'}{\ell}-\frac{\vec{Q}_{\bar{c}}^2 A'^*}{n}\}\ f(\vec{Q}_a,\vec{Q}_c,\vec{Q}_{\bar{c}})e^{Etac_e Ft\bar{a}\bar{c}_e Gto}$$

14. $$\frac{1}{\pi^3}\int d^2\vec{Q}_a d^2\vec{Q}_c d^2\vec{Q}_{\bar{a}}\ \exp\{-\frac{\vec{Q}_a^2 A}{k}-\frac{\vec{Q}_c^2 A'}{\ell}-\frac{\vec{Q}_{\bar{a}}^2 A^*}{n}\}\ f(\vec{Q}_a,\vec{Q}_c,\vec{Q}_{\bar{a}})e^{Etac_e Ft\bar{a}\bar{c}_e Gto}$$

15. $$\frac{1}{\pi^4}\int d^2\vec{Q}_a d^2\vec{Q}_c d^2\vec{Q}_{\bar{a}} d^2\vec{Q}_{\bar{c}}\ \exp\{-\frac{\vec{Q}_a^2 A}{k}-\frac{\vec{Q}_c^2 A'}{\ell}-\frac{\vec{Q}_{\bar{a}}^2 A^*}{m}-\frac{\vec{Q}_{\bar{c}}^2 A'^*}{n}\}$$

$$f(\vec{Q}_a,\vec{Q}_c,\vec{Q}_{\bar{a}},\vec{Q}_{\bar{c}})e^{Etac_e Ft\bar{a}\bar{c}_e Gto}. \qquad 5C4$$

The order of these integrals are, of course 2, 4, 6 and 8 but since the dependence on the 1-components (say Q_{a_1}) decouples from all the 2-components, these integrals are made up of products of 1st, 2nd, 3rd and 4th order integrals.

Once the integrals listed 1 to 15 are written out the full Q-component dependence shown it will be seen that there are just eight separate integrals which must be performed, and that all the integrals of interest are formed from sums of products of these eight, with possibly different arguments. These integrals can be listed as:-

a) $$\frac{1}{\pi^{\frac{1}{2}}}\int dz\ \exp\{-M_z z^2 - 2\beta_z z\}.$$

b) $$\frac{1}{\pi^{\frac{1}{2}}}\int dz\ z\ \exp\{-M_z z^2 - 2\beta_z z\}$$

c) $$\frac{1}{\pi}\int dydz\ \exp\{-M_y y^2 - M_z z^2 - 2\beta_y y - 2\beta_z z + 2\gamma_{yz} yz\}$$

d) $$\frac{1}{\pi}\int dyydz\ \exp\{-M_y y^2 - M_z z^2 - 2\beta_y y - 2\beta_z z + 2\gamma_{yz} yz\}$$

e) $$\frac{1}{\pi^{3/2}}\int dxdydz\ \exp\{-M_x x^2 - M_y y^2 - M_z z^2 - 2\beta_x x - 2\beta_y y - 2\beta_z z$$

$$+ 2\gamma_{xy} xy + 2\gamma_{xz} xz + 2\gamma_{yz} yz\}$$

f) $$\frac{1}{\pi^{3/2}}\int dxxdydz\ \exp\{-M_x x^2 - M_y y^2 - M_z z^2 - 2\beta_x x - 2\beta_y y - 2\beta_z z$$

$$+ 2\gamma_{xy} xy + 2\gamma_{xz} xz + 2\gamma_{yz} yz\}$$

g) $$\frac{1}{\pi^2}\int dwdxdydz\ \exp\{-M_w w^2 - M_x x^2 - M_y y^2 - M_z z^2 - 2\beta_w w - 2\beta_x x - 2\beta_y y - 2\beta_z z$$

$$+ 2\gamma_{wx} wx + 2\gamma_{wy} wy + 2\gamma_{wz} wz + 2\gamma_{xy} xy + 2\gamma_{xz} xz + 2\gamma_{yz} yz\}$$

h) $$\frac{1}{\pi^2}\int dwwdxdydz\ \exp\{-M_w w^2 - M_x x^2 - M_y y^2 - M_z z^2 - 2\beta_w w - 2\beta_x x - 2\beta_y y$$

$$+ 2\beta_z z + 2\gamma_{wx} wx + 2\gamma_{wy} wy + 2\gamma_{wz} wz + 2\gamma_{xy} xy + 2\gamma_{xz} xz + 2\gamma_{yz} yz\}$$

5C5

Now Gradsteyn and Rhyzik [61] give us that

$$\int_{-\infty}^{\infty} du\ e^{-\{\alpha u^2 + 2\beta u\}} = \sqrt{\frac{\pi}{\alpha}}\ \exp\{\frac{\beta^2}{\alpha}\} \quad \text{for} \quad \text{Re}\ \alpha > 0 \qquad 5C6$$

and

$$\int_{-\infty}^{\infty} du\ u\ e^{-\{\alpha u^2 + 2\beta u\}} = -\frac{\beta}{\alpha}\sqrt{\frac{\pi}{\alpha}}\ \exp\{\frac{\beta^2}{\alpha}\} \quad \text{for} \quad \text{Re}\ \alpha > 0$$

and repeated use of these two integrals is all that is necessary to evaluate the multiple integrals of equations 5C4.

We list the forms of the integrals of 5C5 as

a) $$\frac{1}{\sqrt{M_z}} \exp\{\frac{\beta_z^2}{M_z}\}$$

b) $$-\frac{\beta_z}{M_z^{3/2}} \exp\{\frac{\beta_z^2}{M_z}\}$$

c) $$\frac{1}{A_{yz}^{1/2}} \exp\{\frac{B_{yz}}{A_{yz}}\}$$

where $$A_{yz} = M_y M_z - \gamma_{yz}^2$$

$$B_{yz} = M_y\beta_z^2 + M_z\beta_y^2 + 2\beta_y\beta_z\gamma_{yz}$$

d) $$-\frac{[\beta_y M_z + \beta_z\gamma_{yz}]}{A_{yz}^{3/2}} \exp\{\frac{B_{yz}}{A_{yz}}\}$$

e) $$\frac{1}{A_{xyz}^{1/2}} \exp\{\frac{B_{xyz}}{A_{xyz}}\}$$

where $$A_{xyz} = M_x M_y M_z - M_x\gamma_{yz}^2 - M_y\gamma_{xz}^2 - M_z\gamma_{xy}^2 - 2\gamma_{xy}\gamma_{yz}\gamma_{xz}$$

$$B_{xyz} = A_{yz}\beta_x^2 + A_{xz}\beta_y^2 + A_{xy}\beta_z^2$$

$$+ 2M_x\beta_y\beta_z\gamma_{yz} + 2M_y\beta_x\beta_z\gamma_{xz} + 2M_z\beta_x\beta_y\gamma_{xz}$$

$$+ 2\beta_y\beta_z\gamma_{xy}\gamma_{xz} + 2\beta_x\beta_z\gamma_{xy}\gamma_{yz} + 2\beta_x\beta_y\gamma_{xz}\gamma_{yz}$$

f) $$\frac{-[\beta_x A_{yz} + \beta_z\gamma_{xz}M_y + \beta_y\gamma_{xy}M_z + \beta_z\gamma_{xy}\gamma_{yz} + \beta_y\gamma_{xz}\gamma_{zy}]}{A_{xyz}} \exp\{\frac{B_{xyz}}{A_{xyz}}\}$$

g) $$\frac{1}{A_{wxuz}^{1/2}} \exp\{\frac{B_{wxyz}}{A_{wxyz}}\}$$

where $$A_{wxyz} = M_w M_x M_y M_z + \gamma_{xy}^2\gamma_{wz}^2 + \gamma_{xz}^2\gamma_{wy}^2 + \gamma_{xw}^2\gamma_{yz}^2$$

$$- 2M_w\gamma_{xy}\gamma_{xz}\gamma_{yz} - 2M_x\gamma_{wy}\gamma_{wz}\gamma_{yz} - 2M_y\gamma_{wx}\gamma_{wz}\gamma_{xz} - 2M_z\gamma_{wx}\gamma_{wy}\gamma_{xy}$$

$$- 2\gamma_{wx}\gamma_{wy}\gamma_{xz}\gamma_{yz} - 2\gamma_{wx}\gamma_{wz}\gamma_{xy}\gamma_{yz} - 2\gamma_{wz}\gamma_{xz}\gamma_{wy}\gamma_{xy}$$

$$- M_w M_x\gamma_{yz}^2 - M_w M_y\gamma_{xz}^2 - M_w M_z\gamma_{xy}^2$$

$$- M_x M_y\gamma_{wz}^2 - M_x M_z\gamma_{wy}^2 - M_y M_z\gamma_{wz}^2$$

and $$B_{wxyz} = \beta_w^2 A_{xyz} + \beta_x^2 A_{wyz} + \beta_y^2 A_{wxz} + \beta_z^2 A_{wxy}$$

$$+ 2\beta_w\beta_x A_{wx,yz} + 2\beta_w\beta_y A_{wy,xz}$$

$$+ 2\beta_w\beta_z A_{wz,xy} + 2\beta_x\beta_y A_{xy,wz}$$

$$+ 2\beta_x\beta_z A_{xz,wy} + 2\beta_y\beta_z A_{yz,wx}$$

with $$A_{wx,yz} = M_y M_z\gamma_{wx} + M_y\gamma_{wz}\gamma_{xz} + M_z\gamma_{wy}\gamma_{zy}$$

$$- \gamma_{wx}\gamma_{yz}^2 + \gamma_{wy}\gamma_{xz}\gamma_{yz} + \gamma_{wz}\gamma_{xy}\gamma_{yz}$$

h) $$\frac{-[\beta_w A_{xyz} + \beta_x A_{wx,yz} + \beta_y A_{wy,xz} + \beta_z A_{wz,xy}]}{A_{wxyz}^{3/2}} \exp\{\frac{B_{wxyz}}{A_{wxyz}}\}$$ 5C7

The form of the integrals e - h of 5C7 might suggest that the algebra involved in determining them was almost interminable however it was possible to use the symmetry properties between the integration variables to fix the final form without full recourse to detailed algebra. Part of this is brought out by the notation where any quantity with two or more subscripts not separated by commas is symmetric under exchange of any two of the subscripts in position.

To conclude this appendix we give the expanded form of all the integrals of 5C4 to show that they can indeed be written as sums and products of the integrals of 5C5 and for integrals 1 - 10 we also give the detailed structure of the final answer. We do not do this for integrals 11 - 15 since these were not utilised in the actual calculations of this chapter, and the form would be so complex that little or no insight into the analytic properties would be gained from it.

1. $$\frac{1}{\pi} e^{(E+F)t} \int dQ_{a_1} dQ_{a_2} f(\vec{Q}_a)$$

$$\exp\{-(\frac{A}{k} + Ex + G)Q_{a_1}^2 - 2p_{c_1} \cos\phi E Q_{a_1}\}$$

$$\exp\{-(\frac{A}{k} + Ex + G)Q_{a_2}^2 - 2p_{c_1} \sin\phi E Q_{a_2}\}$$

for $f(\vec{Q}_a) = 1$

$$I_{a,k} = \frac{\exp(E+F)t}{(\frac{A}{k} + Ex + G)} \exp\{\frac{p_{c_1}^2 E^2}{\frac{A}{k} + Ex + G}\}$$

for $f(\vec{Q}_a) = Q_{a_1} + i Q_{a_2}$

$$I'_{a,k} = \frac{-p_{c_1} E e^{i\phi}}{(\frac{A}{k} + Ex + G)^2} \exp(E + F)t \exp\{\frac{p_{c_1}^2 E^2}{\frac{A}{k} + Ex + G}\}$$

2) $$\frac{1}{\pi} e^{(E+F)t} \int dQ_{c_1} dQ_{c_2} \; f(\vec{Q}_c) \cdot$$

$$\exp\{-(\frac{A'}{\ell} + \frac{E}{x} + G)Q_{c_1}^2 - 2p_{c_1} \cos\phi \frac{E}{x} Q_{c_1}\}$$

$$\exp\{-(\frac{A'}{\ell} + \frac{E}{x} + G)Q_{c_2}^2 - 2p_{c_1} \sin\phi \frac{E}{x} Q_{c_2}\}$$

for $f(\vec{Q}_c) = 1$

$$I_{c,\ell} = \frac{\exp(E+F)t}{(\frac{A'}{\ell} + \frac{E}{x} + G)} \exp\{\frac{p_{c_1}^2 E^2/x^2}{\frac{A'}{\ell} + \frac{E}{x} + G}\}$$

for $f(\vec{Q}_c) = Q_{c_1} + iQ_{c_2}$

$$I'_{c,\ell} = \frac{-p_{c_1} E/x \, e^{i\phi} \exp\{(E+F)t\}}{(\frac{A'}{\ell} + \frac{E}{x} + G)^2} \exp\{\frac{p_{c_1}^2 E^2/x^2}{\frac{A'}{\ell} + \frac{E}{x} + G}\}$$

3) $$\frac{1}{\pi} e^{(E+F)t} \int dQ_{\bar{a}_1} dQ_{\bar{a}_2} \; f(\vec{Q}_{\bar{a}})$$

$$\exp\{-(\frac{A^*}{m} + Fx + G)Q_{\bar{a}_1}^2 - 2p_{c_1} \cos\phi F Q_{\bar{a}_1}\}$$

$$\exp\{-(\frac{A^*}{m} + Fx + G)Q_{\bar{a}_2}^2 - 2p_{c_1} \sin\phi F Q_{\bar{a}_2}\}$$

for $f(\vec{Q}_{\bar{a}}) = 1$

$$I_{\bar{a},m} = \frac{\exp(E+F)t}{(\frac{A^*}{m} + Fx + G)} \exp\{\frac{p_{c_1}^2 F^2}{\frac{A^*}{m} + Fx + G}\}$$

for $f(\vec{Q}_{\bar{a}}) = -Q_{\bar{a}_1} - iQ_{\bar{a}_2}$

$$I'_{\bar{a},m} = \frac{p_{c_1} F e^{ip} \exp\{(E+F)t\}}{(\frac{A^*}{m} + Fx + G)^2} \exp\{\frac{p_{c_1}^2 F^2}{\frac{A^*}{m} + Fx + G}\}$$

4) $$\frac{1}{\pi} e^{(E+F)t} \int dQ_{\bar{c}_1} dQ_{\bar{c}_2} f(\vec{Q}_{\bar{c}})$$

$$\exp\{-(\frac{A'^*}{n} + \frac{F}{x} + G)Q^2_{\bar{c}_1} - 2p_{c_1} \cos\phi \frac{F}{x} Q_{\bar{c}_1}\}$$

$$\exp\{-(\frac{A'^*}{n} + \frac{F}{x} + G)Q^2_{\bar{c}_2} - 2p_{c_1} \sin\phi \frac{F}{x} Q_{\bar{c}_2}\}$$

for $f(\vec{Q}_{\bar{c}}) = 1$

$$I_{\bar{c},n} = \frac{\exp\{(E+F)t\}}{(\frac{A'^*}{n} + \frac{F}{x} + G)} \exp\{\frac{p^2_{c_1} F^2/x^2}{\frac{A'^*}{x} + \frac{F}{x} + G}\}$$

for $f(\vec{Q}_{\bar{c}}) = - Q_{\bar{c}_1} - iQ_{\bar{c}_2}$

$$I'_{\bar{c},n} = \frac{p_{c_1} F/x e^{i\phi} \exp\{(E+F)t\}}{(\frac{A}{n} + \frac{F}{x} + G)^2} \exp\{\frac{p^2_{c_1} F^2/x^2}{\frac{A}{n} + \frac{F}{x} + G}\}$$

5) $$\frac{1}{\pi^2} e^{(E+F)t} \int dQ_{a_1} dQ_{c_1} dQ_{a_2} dQ_{c_2} f(\vec{Q}_a, \vec{Q}_c)$$

$$\exp\{-(\frac{A}{k} + Ex + G)Q^2_{a_1} - (\frac{A'}{\ell} + \frac{E}{x} + G)Q^2_{c_1} - 2p_{c_1} \cos\phi EQ_{a_1}$$

$$- 2p_{c_1} \cos\phi \frac{E}{x} Q_{c_1} - 2(E + G)Q_{a_1} Q_{c_1}\}$$

$$\exp\{-(\frac{A}{k} + Ex + G)Q^2_{a_2} - (\frac{A'}{\ell} + \frac{E}{x} + G)Q^2_{c_2} - 2p_{c_1} \sin\phi EQ_{a_2}$$

$$- 2p_{c_1} \sin\phi \frac{E}{x} Q_{c_2} - 2(E + G)Q_{a_2} Q_{c_2}\}$$

for $f(\vec{Q}_a, \vec{Q}_c) = 1$

$$I_{ac,k\ell} = \frac{\exp\{(E+F)t\}}{(\frac{A}{k} + Fx + G)(\frac{A'}{\ell} + \frac{E}{x} + G) - (E+G)^2}$$

$$\exp\left\{\frac{p_{c_1}^2 E^2\left(\frac{A}{kx^2} + \frac{A'}{\ell} + G\left(\frac{1}{x} - 1\right)^2\right)}{\left(\frac{A}{k} + Ex + G\right)\left(\frac{A'}{\ell} + \frac{E}{x} + G\right) - (E+G)^2}\right\}$$

for $f(\vec{Q}_a, \vec{Q}_c) = Q_{a_1} + Q_{c_1} + i(Q_{a_2} + Q_{c_2})$.

$$I'_{ac,k\ell} = \frac{-p_{c_1} E\left(\frac{A'}{\ell} + \frac{A}{kx}\right) e^{i\phi} \exp\{(E+F)t\}}{\left\{\left(\frac{A}{k} + Ex + G\right)\left(\frac{A'}{\ell} + \frac{E}{x} + G\right) - (E+G)^2\right\}^2}$$

$$\exp\left\{\frac{p_{c_1}^2 E^2\left(\frac{A}{kx^2} + \frac{A'}{\ell} + G\left(\frac{1}{x} - 1\right)^2\right)}{\left(\frac{A}{k} + Ex + G\right)\left(\frac{A'}{\ell} + \frac{E}{x} + G\right) - (E+G)^2}\right\}$$

6) $$\frac{1}{\pi^2} e^{(E+F)t} \int dQ_{\bar{a}_1} dQ_{c_1} dQ_{\bar{a}_2} dQ_{c_2} f(\vec{Q}_{\bar{a}}, \vec{Q}_c)$$

$$\exp\{-(\tfrac{A^*}{m} + Fx + G)Q_{\bar{a}_1}^2 - (\tfrac{A'}{\ell} + \tfrac{E}{x} + G)Q_{c_1}^2$$

$$- 2p_{c_1} \cos\phi F Q_{\bar{a}_1} - 2p_{c_1} \cos\phi E/x Q_{c_1} + 2G Q_{\bar{a}_1} Q_{c_1}\}$$

$$\exp\{-(\tfrac{A^*}{m} + Fx + G)Q_{\bar{a}_2}^2 - (\tfrac{A'}{\ell} + \tfrac{E}{x} + G)Q_{c_2}^2$$

$$- 2p_{c_1} \sin\phi F Q_{\bar{a}_2} - 2p_{c_1} \sin\phi E/x Q_{c_2} + 2G Q_{\bar{a}_2} Q_{c_2}\}$$

for $f(\vec{Q}_{\bar{a}}, \vec{Q}_c) = 1$

$$I_{\bar{a},c,m,\ell} = \frac{\exp\{(E+F)t\}}{\left(\frac{A'}{\ell} + \frac{E}{x} + G\right)\left(\frac{A^*}{m} + Fx + G\right) - G^2}$$

$$\exp\left\{\frac{p_{c_1}^2 \left(C^2\left(\frac{A'}{\ell} + \frac{E}{x} + G\right) + \frac{E^2}{x^2}\left(\frac{A^*}{m} + Fx + G\right) - \frac{2EFG}{x}\right)}{\left(\frac{A'}{\ell} + \frac{E}{x} + G\right)\left(\frac{A^*}{m} + Fx + G\right) - G^2}\right\}$$

for $f(\vec{Q}_{\bar{a}}, \vec{Q}_c) = Q_{c_1} - Q_{\bar{a}_1} + iQ_{c_2} - iQ_{\bar{a}_2}$

$$I'_{\bar{a},c,m\ell} = \frac{p_{c_\perp}^2 \left[F\frac{A'}{\ell} - \frac{FA^*}{xm}\right] e^{i\phi} \exp\{(E+F)t\}}{\{(\frac{A'}{\ell} + \frac{E}{x} + G)(\frac{A^*}{m} + Fx + G) - G^2\}^2}$$

$$\exp\{\frac{p_{c_\perp}^2 \left[F^2(\frac{A'}{\ell} + \frac{E}{x} + G) + \frac{E^2}{x^2}(\frac{A^*}{m} + Fx + G) - \frac{2EFG}{x}\right]}{(\frac{A'}{\ell} + \frac{E}{x} + G)(\frac{A^*}{m} + Fx + G) - G^2}\}$$

7) $$\frac{1}{\pi^2} e^{(E+F)t} \int dQ_{a_1} dQ_{\bar{a}_1} dQ_{a_2} dQ_{\bar{a}_2} f(\vec{Q}_a \vec{Q}_{\bar{a}})$$

$$\exp\{-(\frac{A}{k} + Ex + G)Q_{a_1}^2 - (\frac{A^*}{m} + Fx + G)Q_{\bar{a}_1}^2$$

$$- 2p_{c_\perp} \mathrm{Cos}\phi EQ_{a_1} - 2p_{c_\perp} \mathrm{Cos}\phi FQ_{\bar{a}} + 2GQ_{a_1} Q_{\bar{a}_1}\}$$

$$\exp\{-(\frac{A}{k} + Ex + G)Q_{a_2}^2 - (\frac{A^*}{m} + Fx + G)Q_{\bar{a}_2}^2$$

$$- 2p_{c_\perp} \mathrm{Sin}\phi EQ_{a_2} - 2p_{c_\perp} \mathrm{Sin}\phi FQ_{a_1} + 2GQ_{a_2} Q_{\bar{a}_2}\}$$

for $f(\vec{Q}_a, \vec{Q}_{\bar{a}}) = 1$

$$I_{a,\bar{a},k,m} = \frac{\exp\{(E+F)t\}}{(\frac{A}{k} + Ex + G)(\frac{A^*}{m} + Fx + G) - G^2}$$

$$\exp\{\frac{p_{c_\perp}^2 \left[C^2(\frac{A}{k} + Ex + G) + B^2(\frac{A^*}{m} + Fx + G) - 2EFG\right]}{(\frac{A}{k} + Ex + G)(\frac{A^*}{m} + Fx + G) - G^2}\}$$

for $f(\vec{Q}_a, \vec{Q}_{\bar{a}}) = Q_{a_1} - Q_{\bar{a}_1} + i(Q_{a_2} - Q_{\bar{a}_2})$.

$$I'_{a,\bar{a},km} = \frac{p_{c_\perp} \left[\frac{FA}{k} - \frac{EA^*}{m}\right] e^{i\phi} \exp\{(E+F)t\}.}{\{(\frac{A}{k} + Ex + G)(\frac{A^*}{m} + Fx + G) - G^2\}}$$

$$\exp\{\frac{p_{c_\perp}^2 \left[F^2(\frac{A}{k} + Ex + G) + E^2(\frac{A^*}{m} + Ex + G) - 2EFG\right]}{(\frac{A}{k} + Ex + G)(\frac{A^*}{m} + Fx + G) - G^2}\}$$

8. $$\frac{1}{\pi^2} e^{(E+F)t} \int dQ_{a_1} dQ_{\bar{c}_1} dQ_{a_2} dQ_{\bar{c}_2} \, f(\vec{Q}_a, \vec{Q}_{\bar{c}})$$

$$\exp\{-(\frac{A}{k} + Ex + G)Q_{a_1}^2 - (\frac{A'^*}{n} + \frac{F}{x} + G)Q_{\bar{c}_1}^2$$

$$- 2p_{c_1}\cos\phi EQ_{a_1} - 2p_{c_1}\cos\phi \frac{F}{x} Q_{c_1} + 2GQ_{a_1}Q_{\bar{c}_1}\}$$

$$\exp\{-(\frac{A}{k} + Ex + G)Q_{a_2}^2 - (\frac{A'^*}{n} + \frac{F}{x} + G)Q_{\bar{c}_2}^2$$

$$- 2p_{c_1}\sin\phi EQ_{a_2} - 2p_{c_1}\sin\phi \frac{F}{x} Q_{c_2} + 2GQ_{a_2}Q_{\bar{c}_2}\}$$

for $f(\vec{Q}_a \vec{Q}_{\bar{c}}) = 1$

$$I_{a,\bar{c},kn} = \frac{\exp\{(E+F)t\}}{(\frac{A}{k} + Ex + G)(\frac{A'^*}{n} + \frac{F}{x} + G) - G^2}$$

$$\exp\{\frac{p_{c_1}^2 [\frac{F^2}{x^2}(\frac{A}{k} + Ex + G) + E^2(\frac{A'^*}{n} + \frac{F}{x} + G) - \frac{2EFG}{x}]}{(\frac{A}{k} + Ex + G)(\frac{A'^*}{n} + \frac{F}{x} + G) - G^2}\}$$

for $f(\vec{Q}_a, \vec{Q}_{\bar{c}}) = Q_{a_1} - Q_{\bar{c}_1} + i(Q_{a_2} - Q_{\bar{c}_2})$.

$$I'_{a\bar{c},kn} = \frac{p_{c_1}[\frac{FA}{xk} - \frac{EA'^*}{n}] e^{i\phi} \exp\{(E+F)t\}}{\{(\frac{A}{k} + Ex + G)(\frac{A'^*}{n} + \frac{F}{x} + G) - G^2\}^2}$$

$$\exp\{\frac{p_{c_1}^2 [\frac{F^2}{x^2}(\frac{A}{k} + Ex + G) + E^2(\frac{A'}{n} + \frac{F}{x} + G) - \frac{2EFG}{2}]}{(\frac{A}{k} + Ex + G)(\frac{A'}{n} + \frac{F}{x} + G) - G^2}\}$$

9. $\frac{1}{\pi^2} \int dQ_{\bar{a}_1}\, dQ_{\bar{c}_1}\, dQ_{\bar{a}_2}\, dQ_{\bar{c}_2}\, f(\vec{Q}_{\bar{a}}\ \vec{Q}_{\bar{c}})\cdot$

$$\exp\{-(\frac{A'^*}{n} + \frac{F}{x} + G)Q^2_{\bar{c}_1} - (\frac{A^*}{m} + Fx + G)Q^2_{\bar{a}_1}$$

$$- 2p_{c_1}\mathrm{Cos}\phi\frac{F}{x}\,Q_{\bar{c}_1} - 2p_{c_1}\mathrm{Cos}\phi F Q_{\bar{a}_1} - 2(F + G)Q_{\bar{a}_1}Q_{\bar{c}_1}\}$$

$$\exp\{-(\frac{A'^*}{n} + \frac{F}{x} + G)Q^2_{\bar{c}_2} - (\frac{A^*}{m} + Fx + G)Q^2_{\bar{a}_2}$$

$$- 2p_{c_1}\mathrm{Sin}\phi\frac{F}{x}\,Q_{\bar{c}_2} - 2p_{c_1}\mathrm{Sin}\phi F Q_{\bar{a}_2} - 2(F + G)Q_{\bar{a}_2}Q_{\bar{c}_2}\}$$

for $f(\vec{Q}_{\bar{a}}, \vec{Q}_{\bar{c}}) = 1$

$$I_{\bar{a}\bar{c},mn} = \frac{\exp\{(E + F)t\}}{(\frac{A'^*}{n} + \frac{F}{x} + G)(\frac{A^*}{m} + Fx + G) - (F + G)^2}$$

$$\exp\{\frac{p^2_{c_1}\frac{F^2}{x^2}[(\frac{A^*}{m} + Fx + G) + x^2(\frac{A'^*}{n} + \frac{F}{x} + G) - 2x(F + G)]}{(\frac{A'^*}{n} + \frac{F}{x} + G)(\frac{A^*}{m} + Fx + G) - (F + G)^2}\}$$

for $f(\vec{Q}_{\bar{a}}\ \vec{Q}_{\bar{c}}) = -(Q_{\bar{a}_1} + Q_{\bar{c}_1}) - i(Q_{\bar{a}_2} + Q_{\bar{c}_2})$

$$I'_{\bar{a}\bar{c},mn} = \frac{p_{c_1}F[\frac{A'^*}{n} + \frac{A^*}{mx}]e^{i\phi}\exp\{(E + F)t\}}{\{(\frac{A'^*}{n} + \frac{F}{x} + G)(\frac{A^*}{m} + Fx + G) - (F + G)^2\}^2}$$

$$\exp\{\frac{p^2_{c_1}\frac{F^2}{x^2}[(\frac{A^*}{m} + Fx + G) + x^2(\frac{A'^*}{n} + \frac{F}{x} + G) - 2x(F + G)]}{(\frac{A'^*}{n} + \frac{F}{x} + G)(\frac{A^*}{m} + Fx + G) - (F + G)^2}\}$$

10. $$\frac{1}{\pi^2}\int dQ_{c_1}\, dQ_{\bar{c}_1}\, dQ_{c_2}\, dQ_{\bar{c}_2}\, f(\vec{Q}_c,\vec{Q}_{\bar{c}})$$

$$\exp\{-(\frac{A'}{\ell}+\frac{E}{x}+G)Q_{c_1}^2-(\frac{A'^*}{n}+Fx+G)Q_{\bar{c}_1}^2$$

$$-2p_{c_1}\mathrm{Cos}\phi\,\frac{E}{x}\,Q_{c_1}-2p_{c_1}\mathrm{Cos}\phi\,\frac{F}{x}\,Q_{\bar{c}_1}+2GQ_{c_1}Q_{\bar{c}_1}\}$$

$$\exp\{-(\frac{A'}{\ell}+\frac{E}{x}+G)Q_{c_2}^2-(\frac{A'^*}{n}+Fx+G)Q_{\bar{c}_2}^2$$

$$-2p_{c_1}\mathrm{Sin}\phi\,\frac{E}{x}\,Q_{c_2}-2p_{c_1}\mathrm{Sin}\phi\,\frac{F}{x}\,Q_{\bar{c}_2}+2GQ_{c_2}Q_{\bar{c}_2}\}$$

for $f(\vec{Q}_c\vec{Q}_{\bar{c}})=1$

$$I_{c\bar{c},\ell n}=\frac{\exp\{(E+F)t\}}{(\frac{A'}{\ell}+\frac{E}{x}+G)(\frac{A'^*}{n}+\frac{F}{x}+G)-G^2}$$

$$\exp\{\frac{p_{c_1}^2/x^2\,[F^2(\frac{A'}{\ell}+\frac{E}{x}+G)+E^2(\frac{A'^*}{n}+\frac{F}{x}+G)-2EFG]}{(\frac{A'}{\ell}+\frac{E}{x}+G)(\frac{A'^*}{n}+\frac{E}{x}+G)-G^2}\}$$

for $f(\vec{Q}_c,\vec{Q}_{\bar{c}})=Q_{c_1}-Q_{\bar{c}_1}+i(Q_{c_2}-Q_{\bar{c}_2})$

$$I'_{c\bar{c}\ell n}=\frac{p_{c_1}\,[\frac{FA'}{x\ell}-\frac{EA'^*}{xn}]\,e^{i\phi}\exp\{(E+F)t\}}{\{(\frac{A'}{\ell}+\frac{E}{x}+G)(\frac{A'^*}{n}+\frac{F}{x}+G)-G^2\}^2}$$

$$\exp\{\frac{p_{c_1}^2/x^2\,[F^2(\frac{A'}{\ell}+\frac{E}{x}+G)+E^2(\frac{A'^*}{n}+\frac{F}{x}+G)-2EFG]}{(\frac{A'}{\ell}+\frac{E}{x}+G)(\frac{A'^*}{n}+\frac{F}{x}+G)-G^2}\}$$

11. $\frac{1}{\pi^3}\ e^{(E+F)} \int dQ_{c_1} dQ_{\bar{a}_1} dQ_{\bar{c}_1} dQ_{c_2} dQ_{\bar{a}_2} dQ_{\bar{c}_2}\ f(\vec{Q}_c,\vec{Q}_{\bar{a}}\vec{Q}_{\bar{c}})$

$$\exp\{-(\frac{A'}{\ell} + \frac{E}{x} + G)Q_{c_1}^2 - (\frac{A^*}{m} + Fx + G)Q_{\bar{a}_1}^2 - (\frac{A'^*}{n} + \frac{F}{x} + G)Q_{\bar{c}_1}^2$$

$$- 2p_{c_1}\text{Cos}\phi\ \frac{E}{x}\ Q_{c_1} - 2p_{c_1}\text{Cos}\phi FQ_{\bar{a}_1} - 2p_{c_1}\text{Cos}\ \frac{F}{x}\ Q_{\bar{c}_1}$$

$$+ 2GQ_{c_1}Q_{\bar{a}_1} + 2GQ_{c_1}Q_{\bar{c}_1} - 2(F + G)Q_{\bar{a}_1}Q_{\bar{c}_1}\}$$

$$\exp\{-(\frac{A'}{\ell} + \frac{E}{x} + G)Q_{c_2}^2 - (\frac{A^*}{m} + Fx + G)Q_{\bar{a}_2}^2 - (\frac{A^*}{n} + \frac{F}{x} + G)Q_{\bar{c}_2}^2$$

$$- 2p_{c_1}\text{Sin}\phi\ \frac{E}{x}\ Q_{c_2} - 2p_{c_1}\text{Sin}\phi FQ_{\bar{a}_2} - 2p_{c_1}\text{Sin}\phi\ \frac{F}{x}\ Q_{\bar{c}_2}$$

$$+ 2GQ_{c_2}Q_{\bar{a}_2} + 2GQ_{c_2}Q_{\bar{c}_2} - 2(F + G)Q_{\bar{a}_2}Q_{\bar{c}_2}\},$$

where $f(\vec{Q}_c,\vec{Q}_{\bar{a}}\vec{Q}_{\bar{c}}) = 1$ or $= Q_{c_1} - Q_{\bar{a}_1} - Q_{\bar{c}_1} + i(Q_{\bar{c}_2} - Q_{\bar{c}_2} - Q_{\bar{a}_2})$

12. $\frac{1}{\pi^3}\ e^{(E+F)} \int dQ_{a_1} dQ_{\bar{a}_1} dQ_{\bar{c}_1} dQ_{a_2} dQ_{\bar{a}_2} dQ_{\bar{c}_2}\ f(\vec{Q}_a,\vec{Q}_{\bar{a}}\vec{Q}_{\bar{c}})$

$$\exp\{-(\frac{A}{k} + Ex + G)Q_{a_1}^2 - (\frac{A^*}{m} + Fx + G)Q_{\bar{a}_1}^2 - (\frac{A'^*}{n} + \frac{F}{x} + G)Q_{\bar{c}_1}^2$$

$$- 2p_{c_1}\text{Cos}\phi EQ_{a_1} - 2p_{c_1}\text{Cos}\phi FQ_{\bar{a}_1} - 2p_{c_1}\text{Cos}\phi\ \frac{F}{x}\ Q_{\bar{c}_1}$$

$$+ 2GQ_{a_1}Q_{\bar{a}_1} + 2GQ_{a_1}Q_{\bar{c}_1} - 2(F+G)Q_{\bar{a}_1}Q_{\bar{c}_1}\}$$

$$\exp\{-(\frac{A}{k} + Ex + G)Q_{a_2}^2 - (\frac{A^*}{m} + Fx + G)Q_{\bar{a}_2}^2 - (\frac{A'^*}{n} + \frac{F}{x} + G)Q_{\bar{c}_2}^2$$

$$- 2p_{c_1}\text{Sin}\phi EQ_{a_2} - 2p_{c_1}\text{Sin}\phi FQ_{\bar{a}_2} - 2p_{c_1}\text{Sin}\phi\ \frac{F}{x}\ Q_{\bar{c}_2}$$

$$+ 2GQ_{a_2}Q_{\bar{a}_2} + 2GQ_{a_2}Q_{\bar{c}_2} - 2(F + G)Q_{\bar{a}_2}Q_{\bar{c}_2}\}$$

where $f(\vec{Q}_a \vec{Q}_{\bar{a}} \vec{Q}_{\bar{c}}) = 1$ or $= Q_{a_1} - Q_{\bar{a}_1} - Q_{\bar{c}_1} + i(Q_{a_2} - Q_{\bar{a}_2} - Q_{\bar{c}_2})$.

13. $$\frac{1}{\pi^3} e^{(E+F)t} \int dQ_{a_1} dQ_{c_1} dQ_{\bar{c}_1} dQ_{a_2} dQ_{c_2} dQ_{\bar{c}_2} f(\vec{Q}_a \vec{Q}_c \vec{Q}_{\bar{c}})$$

$$\exp\{-(\frac{A}{k} + Ex + G)Q_{a_1}^2 - (\frac{A'}{\ell} + \frac{E}{x} + G)Q_{c_1}^2 - (\frac{A'^*}{n} + \frac{F}{x} + G)Q_{\bar{c}_1}^2$$

$$-2p_{c_1} \cos\phi E Q_{a_1} - 2p_{c_1} \cos\phi \frac{E}{x} Q_{c_1} - 2p_{c_1} \cos\phi \frac{F}{x} Q_{\bar{c}_1}$$

$$- 2(E + G)Q_{a_1} Q_{c_1} + 2GQ_{a_1} Q_{\bar{c}_1} + 2GQ_{c_1} Q_{\bar{c}_1}\}$$

$$\exp\{-(\frac{A}{k} + Ex + G)Q_{a_2}^2 - (\frac{A'}{\ell} + \frac{E}{x} + G)Q_{c_2}^2 - (\frac{A'^*}{n} + \frac{F}{x} + G)Q_{\bar{c}_2}^2$$

$$-2p_{c_1} \sin\phi E Q_{a_2} - 2p_{c_1} \sin\phi \frac{E}{x} Q_{c_1} - 2p_{c_1} \sin\phi \frac{F}{x} Q_{\bar{c}_2}$$

$$- 2(E + G)Q_{a_2} Q_{c_2} + 2GQ_{a_2} Q_{\bar{c}_2} + 2GQ_{c_2} Q_{\bar{c}_2}\}$$

where $f(\vec{Q}_a \vec{Q}_c \vec{Q}_{\bar{c}}) = 1$ or $= Q_{a_1} + Q_{c_1} - Q_{\bar{c}_1} + i(Q_{a_2} + Q_{c_2} - Q_{\bar{c}_2})$.

14. $$\frac{1}{\pi^3} e^{(E+F)t} \int dQ_{a_1} dQ_{c_1} dQ_{\bar{a}_1} dQ_{a_2} dQ_{c_2} dQ_{\bar{a}_2} f(\vec{Q}_a \vec{Q}_c \vec{Q}_{\bar{a}})$$

$$\exp\{-(\frac{A}{k} + Ex + G)Q_{a_1}^2 - (\frac{A'}{\ell} + \frac{E}{x} + G)Q_{c_1}^2 - (\frac{A^*}{m} + Fx + G)Q_{\bar{a}_1}^2$$

$$- 2p_{c_1} \cos\phi E Q_{a_1} - 2p_{c_1} \cos\phi \frac{E}{x} Q_{c_1} - 2p_{c_1} \cos\phi F Q_{\bar{a}_1}$$

$$- 2(E + G)Q_{a_1} Q_{c_1} + 2GQ_{a_1} Q_{\bar{a}_1} + 2GQ_{c_1} Q_{\bar{a}_1}\}$$

$$\exp\{-(\frac{A}{k} + Ex + G)Q_{a_2}^2 - (\frac{A'}{\ell} + \frac{E}{x} + G)Q_{c_2}^2 - (\frac{A^*}{m} + Fx + G)Q_{\bar{a}_2}^2$$

$$- 2p_{c_1}\,\mathrm{Sin}\phi EQ_{a_2} - 2p_{c_1}\,\mathrm{Sin}\phi\,\frac{E}{x}\,Q_{c_2} - 2p_{c_1}\,\mathrm{Sin}\phi FQ_{\bar{a}_2}$$

$$- 2(E+G)Q_{a_2}Q_{c_2} + 2GQ_{a_2}Q_{\bar{a}_2} + 2GQ_{c_2}Q_{\bar{a}_2}\}$$

15. $\frac{1}{\pi^4}\,e^{(E+F)} \int dQ_{a_1}\,dQ_{c_1}\,dQ_{\bar{a}_1}\,dQ_{\bar{c}_1}\,dQ_{a_2}\,dQ_{c_2}\,dQ_{\bar{a}_2}\,dQ_{\bar{c}_2}\; f(\vec{Q}_a\vec{Q}_c\vec{Q}_{\bar{a}}\vec{Q}_{\bar{c}})$

$$\exp\{-(\tfrac{A}{k}+Ex+G)Q_{a_1}^2 - (\tfrac{A'}{\ell}+\tfrac{E}{x}+G)Q_{c_1}^2 - (\tfrac{A^*}{m}+Fx+G)Q_{\bar{a}_1}^2$$

$$- (\tfrac{A'^*}{n}+\tfrac{F}{x}+G)Q_{\bar{c}_1}^2$$

$$- 2p_{c_1}\,\mathrm{Cos}\phi EQ_{a_1} - 2p_{c_1}\,\mathrm{Cos}\phi\,\frac{E}{x}\,Q_{c_1} - 2p_{c_1}\,\mathrm{Cos}\phi FQ_{\bar{a}_1} - 2p_{c_1}\,\mathrm{Cos}\phi\,\frac{F}{x}\,Q_{\bar{c}_1}$$

$$- 2(E+G)Q_{a_1}Q_{c_1} + 2GQ_{a_1}Q_{\bar{a}_1} + 2GQ_{a_1}Q_{\bar{c}_1}$$

$$+ 2GQ_{a_1}Q_{\bar{a}_1} + 2GQ_{c_1}Q_{\bar{c}_1} - 2(F+G)Q_{\bar{a}_1}Q_{\bar{c}_1}\}$$

$$\exp\{-(\tfrac{A}{k}+Ex+G)Q_{a_2}^2 - (\tfrac{A'}{\ell}+\tfrac{E}{x}+G)Q_{c_2}^2 - (\tfrac{A^*}{m}+Fx+G)Q_{\bar{a}_2}^2$$

$$- (\tfrac{A'^*}{n}+\tfrac{F}{x}+G)Q_{\bar{c}_2}^2$$

$$- 2p_{c_2}\,\mathrm{Sin}\phi EQ_{a_2} - 2p_{c_1}\,\mathrm{Sin}\phi\,\frac{E}{x}\,Q_{c_1} - 2p_{c_1}\,\mathrm{Sin}\phi FQ_{\bar{a}_1} - 2p_{c_1}\,\mathrm{Sin}\phi\,\frac{F}{x}\,Q_{\bar{c}_1}$$

$$- 2(E+G)Q_{a_2}Q_{c_2} + 2GQ_{a_2}Q_{\bar{a}_2} + 2GQ_{a_2}Q_{\bar{c}_2}$$

$$+ 2GQ_{c_2}Q_{\bar{a}_2} + 2GQ_{a_2}Q_{\bar{c}_2} - 2(F+G)Q_{\bar{a}_2}Q_{\bar{c}_2}\}$$

where $f(\vec{Q}_a,\vec{Q}_c,\vec{Q}_{\bar{a}},\vec{Q}_{\bar{c}}) = 1$ or $= Q_{a_1} + Q_{c_1} - Q_{\bar{a}_1} - Q_{\bar{c}_1} + i(Q_{a_2} + Q_{c_2} - Q_{\bar{a}_2} - Q_{\bar{c}_2})$.

-5C8.

It is easily seen that integrals 11 - 15 of 5C8 can be performed by repeated application of the integrals e - h of equations 5C7. We also note that the correct kinematical factor namely, $p_{c_1} e^{i\phi}$, multiplies all the I' integrals which contribute to the "flip" discontinuity, i.e. the target asymmetry. This justifies the choice of the form of the factor given in 5.14.

CHAPTER VI

Reprise

In the preceding four chapters we have developed a fairly sophisticated model for the evaluation of absorptive type corrections to so called triple-Regge distributions. This has proceeded via the writing of a fairly large computer program [65] which is intended to ease the extensive data handling, calculations and, not least important, display of results, which accompany work on single particle inclusive reactions. We then went on to develop and evaluate a fairly simplistic model for incorporating absorptive corrections with the basic triple-Regge formalism. This simplistic model was however found to be too naive in concept, and was shown up as unsatisfactory, both at an heuristic and phenomenological level. The next stage was to develop a more rigorous and better motivated model. While the previous model was derived from the stand-point of considering the sums of quasi-two body reactions, the newer model was to consider absorptive type corrections to a three body amplitude, taking the discontinuity in M_X^2 to make contact with single particle inclusive reactions via the generalised optical theorem of Muller. These corrections were of a fairly general type, under the Regge-eikonal approximation, but we re-iterate that we could not hope to incorporate all possible corrections of the type we were considering, and still have been able to retrieve a reasonable, closed, eikonal form at the end of the calculations. We were, in fact, pleased and suprised at the level of approximations necessary in order to achieve the final closed form which does not come about as simply and automatically as in the two body case.

In the final chapter of these four the formula just derived was applied to the problem of charge exchange spinless meson reactions. None of the gross heuristic and phenomenological defects of the previous model were present and comparison with data was quite encouraging, although complete agreement was not found. This might possibly be put down to the relatively low energy of the experiment for a "triple-Regge" type calculation. We feel that data at a substantially higher energy are needed in order to be able to resolve questions of the detailed M_x^2/s dependance. Such data should be available in a relatively short period.[56]

Quite a lot of effort has been expended on the question of absorptive corrections to the triple-Regge spectrum, and quite a few calculations have been presented in the literature. Those, to date, that I have found most interesting have been briefly considered, separately in Chapter I. It is now possible to "compare and contrast" these formulae with that derived in Chapter IV.

Perhaps the most useful form in which to view the formula of Chapter IV is (see 4.19)

$$H(t, s_{ab}, M_x^2) = \int \frac{d^2\vec{Q}_a}{(2\pi)^2} \frac{d^2\vec{Q}_c}{(2\pi)^2} \frac{d^2\vec{Q}_{\bar{a}}}{(2\pi)^2} \frac{d^2\vec{Q}_{\bar{c}}}{(2\pi)^2}$$

$$S(\vec{Q}_a, \vec{Q}_c)\ Y\ (t_{ac}, t_{\bar{a}\bar{c}}, t_o, s_{ab}, M_x^2)\ S^*(\vec{Q}_{\bar{a}}, \vec{Q}_{\bar{c}}) \qquad 6.1$$

Our model does, in fact, make a specific, eikonal, choice for the form of the S factors, but we need not be concerned with this precise form. Equation 6.1 is enough.

When we turn to other models we see that an equation of the form

$$H(p_{c\perp}) = \int \frac{d^2k_\perp}{2\pi} \frac{d^2k'_\perp}{2\pi} S_{eff}(p_{c\perp} - k_\perp)$$

$$Y(p_{c\perp} - k_\perp, p_{c\perp} - k'_\perp) S^*_{eff}(p_{c\perp} - k'_\perp) \qquad 6.2$$

crops up repeatedly. Note that the slight change in normalisation is taken up in the S_{eff} factors. This formula is used by Craigie and Kramer [36] , Goldstein and Owens [46] and Capella, Kaplan and Tran Thanh Van [41], although this fact is not transparent in the last case. Different definitions of the impact parameter and hence $k_\perp$ are made; such details should not affect phenomenology, and also different definitions of S_{eff}, which however, always refer to rescattering in the a-b or 1-2 channels. Pumplin [40] also produces a formula of this type, but in his case the re-scattering is deemed to occur in the c-b or 3-2 channel. Since in most of the detailed models the absorption paramters will not be strongly energy dependant, even this change should not be strongly reflected in the phenomenology.

Paige and Sidhu [39] derive a formula, not too dissimilar to that given in equation 6.2, from the viewpoint of the Reggeon calculus, however, while equation 6.2 clearly allows for the possibility of rescattering in both the "incoming" and "outgoing" 1-2 or a-b channels, Paige and Sidhu discount this, and make the correction to the pole only graph with the sum of the two "singly rescattered" graphs with an extra elastic reaction in either the "incoming" or "outgoing" channel. Their derivation uses the Gribov cut coupling functions of the form $N_{\alpha_5\alpha_2}(q_\perp + k_\perp, k_\perp)$ for the upper 1,3 vertex and $N_{\alpha_4\alpha_2}(k_\perp)$ for the 2-2 vertex.

Of course in this form there is no factorization into the form

$S_{eff}\ Y\ S^{*}_{eff}$

where the Y represents the pole only expression. However, Paige and Sidhu specialise to the "absorption model" form for these functions, namely

$$N_{\alpha_5\alpha_2}(t_2,t') = \beta_{13\alpha_5}(t_2)\ \beta_{11\alpha_5}(t')$$

$$N_{\alpha_4\alpha_2}(t',t') = \beta^{2}_{22P}(t') \qquad 6.3$$

and the use of this parametrization brings their model more nearly to the form given by equation 6.2.

Bartels and Kramer [45] also derive an absorption model in the Reggeon calculus. They make similar assumptions to Paige and Sidhu, but go much further by considering more complicated diagrams, including enhanced graphs (graphs with more than one triple-Pomeron coupling) and also by deriving an eikonal-approximation which gives a similar form to that of Capella et al. Bartels and Kramer indicate that they feel at present day energies several terms in their eikonal expansion will be important while at higher energies the enhanced graphs will assume greater and greater importance.

We now return to a point made in the above authors derivation of their eikonal model; namely that in the case of charge exchange with also the exchange of several eikonal Pomerons they can see the 2 particle - n Pomeron, 1 Reggeon cut coupling function N_{n+1} in either of the forms $g_a^n\ g_a R_a$ or $g_a R_c g_c^n$. This is of course in the eikonal approximation, and from their point of view the formula derived in Chapter IV and re-stated in equation 6.1 appears to embody some over counting. We shall return to this point shortly.

The above discussion then shows us that all the available absorption or cut correction models can be obtained almost as a subset of that given in Chapter IV. Of various different S-factors and input Y expressions would need to be used, with one or other of the eikonal phases χ set to zero to regain either 1-2 or 3-2 re-scattering only, and for the approach of Bartels and Kramer, the Y graph would have to embody various enhanced graphs.

There are a few further points we wish to consider however. In the case of two body reactions the parts a) and b) of figure 6.1 represent two candidates for the two body cut. They are represented in ϕ^3 theory for simplicity. Diagram a) was first studied by Amati et.al. [20] and b) by Mandelstan [23] who showed that b) will dominate a) as $s\to\infty$. The rigorous argument is quite complicated, however a simple physical argument shows the underlying reason. Clearly figure 6.1 a) has two Reggeons emitted sequentially while b) can have the two emitted simultaneously. As $s\to\infty$ the two particles will spend less time in their mutual interaction radius and two sequential events become less favourably indicated.

This fact however, has not put a stop to an immense amount of phenomenology using figure 6.1 a) as its basis. It is the so-called absorption model, and whilemuch successful work has resulted, there are indications in the polarisation measurements in $\pi^- p\to\pi^0 n$ and the line reversal breaking of $K^+n\to K^0p$ and $K^-p\to\bar{K}^0n$, which could not be accounted for by the traditional absorption model, that the precise phase of the cut is not well accounted for. This led to the proposal of the i-factor model [84] which by a brute force adjustment of the phase of the cut was able to account for both these phenomena [84,85] .

More recent phenomenological analyses [86, 87] and a theoretical argument [88] in a simple multi-peripheral dual type model lend support to this kind of model. A corresponding calculation in the Reggeon Calculus [89], where a more complicated form than the absorption model prescription for the cut coupling functions is used, is showing encouraging results.

All this points to the fact that the traditional absorption model is likely to be unable to reproduce the precise phase of the two body amplitude. Every calculation, including our own, however, does use the traditional prescription. It is perhaps slightly more justifiable since, away from x = 1 the interaction of the particles to produce a massive M_x^2 state takes place over a relatively long time [40], unlike at x = 1 where interaction timings must be of the same sort as for two body reactions.

The reason why the traditional absorption model has received so much emphasis is, of course, because it is very easy to apply and does give some quite substantial successes. It will probably continue to be applied quite extensively where the precise, detailed phase of the cut is not of paramount importance.

One further point that we must consider is that of Bartels and Kramer where the suggestion is made of overcounting in the formula 6.1. A calculation has been performed in ϕ^3 field theory for a single particle in the M_x^2 state, i.e. at x = 1 [74] This of course gives that the eikonal phases χ_{ab} and χ_{cb} are small (this is just another AFS/Mandelstan cut question) but the mixed eikonal phase $\chi_{ac,b}$ enters with the correct weight. The question is therefore not easily resolved, however, from the standpoint of our calculation we see that the question basically hinges on whether we are justified in choosing two independant impact parameters for B_{ab} and B_{cb}. For x = 1 and small t it

would seem likely that the dynamics of the situation require B_{ab} and B_{cb} to be similar. We are after all in a quasi-two body situation. Away from $x = 1$ it is not clear that this is so.

Consider the diagram of figure 6.2. We are again using a ϕ^3 Regge coupling. If we take this sort of diagram seriously, the important point to note is that in the integration about the loop over d^4k, it need not be just the small values of k, or those where $k \simeq p_1$, that contribute to building up the residue. Near $x = 1$, these values of k in the momentum picture do not affect the co-ordinate picture since the reaction will take place over short times, and this ensures that particle 3 cannot propagate to impact parameters far removed from those of particle 1. As x comes away from 1, and the times of reaction lengthen, the integral over k will ensure that all impact parameters B_{cb} are achievable. This shows us that we can indeed take B_{ab} and B_{cb} independant. It is however clear that Bartels and Kramer's argument is sound for small M_x^2.

To finally conclude, then, we feel that phenomenology in the triple-Regge inclusive region will not be successful with a pole only formulation, in any detailed sense, but in much the same way that the absorption model in two body scattering has been able to provide good detailed agreement between experiment and theory over a wide range of processes, we feel that its counterpart in the triple Regge region could be, and to an extent has been successful. To continue we also feel that the formula derived in Chapter IV provides a very flexible formulation of the "absorption model" in the triple Regge region, which when combined with the computer program outlined in Chapter II would provide a very interesting tool for examining the phenomenology of the triple-Regge region in inclusive processes.

BIBLIOGRAPHY

REFERENCES

1 G Giacomelli, Phys Reports 23C (1976) 123

2 A H Müeller, Phys Rev D2 (1970) 2963

3 See, amongst many others, R Stroynowski, Proc.VIth Int Colloq Multiparticle Reactions, Oxford 1975,RL75-143
K Böckmann Proc 18th Int Conf on High Energy Physics, Palermo (1975)

4 See, amongst many others D Horn, Phys Report 4C (1972)1
W R Fraser et al., Rev Mod Phys 44 (1972) 284

5 P D B Collins, An Introduction to Regge Theory and High Energy Physics, Cambridge University Press 1977.

6 R P Feynman Phys Rev Lett 23 (1969) 1415.

7 C E de Tar, Phys Rev D3 (1971) 128.

8 R E Cutkosky J Math Phys 1 (1960) 429, Rev Mod Phys 33 (1961)446.

9 D R O Morrison in J R Smith (ed.) Proceedings of the 4th International Conference on High Energy Collisions (Rutherford Laboratory 1972).

10 K E Cahill and H P Stapp, Phys Rev D6 (1972) 1007
Phys Rev D8 (1973) 2714
J C Polkinghorne, Nuovo Cimento 7A (1972) 555.

11 H D I Abarbanel and D J Gross, Phys Rev Lett 26 (1971) 732
G A Ringland, R J N Phillips and R Worden, Phys Lett 40B (1972) 239.

12 J P Ader, C Meyers and Ph. Salin,Nucl Phys B47 (1972) 397, Nucl Phys B82 (1974) 237.

REFERENCES (cont.)

13 G R Goldstein and J F Owens, Nucl Phys B103 (1976) 145.

14 J Randa and A Donnachie, Nucl Phys B109 (1976) 495.

15 M Jacob and G C Wick, Ann Phys 7 (1959) 404.

16 R D Field, II Polarisation Effects in Inclusive Processes, CALT-68-459 (1974).

17 For a review on multi-Regge limits which includes the case for the six-point furnction see e.g. R C Brower, C E de Tar and J H Weis, Phys Reports 14C (1974) 257.

18 H D I Abarbanel and A Schwimmer, Phys Rev D6 (1972)3018.
C E de Tar and J H Weis, Phys Rev D4(1971)3141.
C E Jones, F E Low and J E Young, Phys Rev D4(1971)2358.
P Goddard and A R White, Nuovo Cimento, 1A (1971)645.
N S Craigie and G Kramer, Nucl Phys B82(1974)69.

19 This fact is perhaps best seen using the Su dakov parameters, and was first brought to the authors attention during the D.I.C. course (Physics Department, Imperial College, London, 1973-4).

20 D Amati, A Stanghellini and S Fubini, Nuovo Cimento 26 (1962) 896.
D Amati, S Fubini and A Stanghellini, Phys Lett 1(1962)29.

21 J Benecke, T T Chou, C N Yang and E Yen, Phys Rev 188 (1969) 2159.

22 See, for instance M Jacob in Proceedings of the 16th International Conference on High Energy Physics, Batavia (Batavia Laboratory 1972).

23 S Mandelstam, Nuovo Cimento 30 (1963) 1127, 1148.

24 See for example I Ambats et al., Phys Rev D9 (1974) 1179.

25 See for example R G Roberts, RL-73-095 (T.68) (Rutherford Laboratory, September 1973) and references contained therein.

26 H D I Abarbanel, J Bartels, J M Bronzan and D Sidhu, Phys Rev D12 (1975) 2459.
I Halliday and C T Sachrajda, Phys Rev D8 (1973) 3589.

27 For a review of this subject see e.g. A H Mueller in Proceedings of the 16th International Conference on High Energy Physics, Batavia (Batavia Laboratory 1972).

28 L Caneshi and A Schwimmer, Nucl Phys B48 (1972) 519.

29 H D I Abarbanel and D J Gross, Phys Rev Lett 26 (1971) 732.

30 G R Goldstein and J F Owens Nucl Phys B103 (1976) 145.

31 L Dick et al. Spin Effects in the Inclusive Reactions $\pi^{\pm}+p(\uparrow)\rightarrow\pi^{\pm}$ + Anything at 8 GeV/c, Phys Lett 57B (1975) 93.

32 K Ahmed, J G Körner, G Kramer and N S Craigie, Nucl Phys B106 (1976) 275.

33 N S Craigie, G Kramer and J G Körner, Nucl Phys B68 (1974) 509.

34 K C Moffeit et al. Phys Rev D5 (1972) 1603.

35 K J M Moriarty and J H Tabor, Nuovo Cim Lett 15 (1976) 17.
K J M Moriarty J H Tabor and A Ungkitchanukit, Acta Phys Aust 45 (1976) 325.
K J M Moriarty, J P Rad, J H Tabor and A Ungkitchanukit, Acta Phys Aust 46 (1977) 105.
P Choudhury, K J M Moriarty, J H Tabor and A Ungkitchanukit Acta Phys Aust 46 (1977) 229.

REFERENCES (cont.)

35 K J M Moriarty, J H Tabor and A Ungkitchanukit, Corrections to a Mueller-Regge Model of the Reactions $O^-\frac{1}{2}^+ \to O^-X$ Proceeding via Charge Exchange. To be published in J Phys G

P Choudhury, K J M Moriarty, J H Tabor and A U gkitchanukit, Acta Phys Aust 48 (1977)1.

N S Craigie, K J M Moriarty, J H Tabor and A Ungkitchanukit, Proceedings of the Rencontre de Moriond 11 (1976) 253.

K J M Moriarty, JP Rad, J H Tabor and A Ungkitchanukit, Absorptive Corrections to Single Particle Inclusive Charge Exchange Nucleon Interactions, Royal Holloway College Preprint, May (1976).

K J M Moriarty, J H Tabor and A Ungkitchanukit Phys Rev D15(1977).

K J M Moriarty, J H Tabor and J P Rad, Nuovo Cim Lett 19 (1977) 565.

K J Moriarty, J P Rad, J H Tabor and A Ungkitchanukit, Nuovo Cim Lett 17 (1976) 366.

36 N S Craigie and G Kramer Nucl Phys B75 (1974) 509.

37 L Durand and Y T Chiu, Phys Rev 139 (1965) B646.

38 F E Paige and T L Trueman, Phys Rev D12 (1975) 2422.

39 F E Paige and D P Sidhu, Phys Rev D13 (1976) 3015

F E Paige and D P Sidhu, BNL-21695 (Brookhaven National Laboratory, 1976).

REFERENCES (cont.)

40 J Pumplin, Phys Rev D13 (1976) 1249, 1261.

41 A Capella, J Kaplan and J Tran Thanh Van, Nucl Phys B105 (1976) 333.

42 A Capella, J Kaplan and J Tran Thanh Van, Nucl Phys B27 (1975) 493, A Capella and J Kaplan, Phys Lett 52B (1974) 448.

43 A Garcia Azcarate, LPTPE 77/5 (Laboratoire de Physique Théoretique et Particules Elément-aires, Orsay, France.

44 K J M Moriarty, J P Rad, J H Tabor and A Ungkitchanukit, Acta Phys Aust 46 (1977) 105
K J M Moriarty, J P Rad, J H Tabor and A Ungkitchanukit. Absorption Corrections to a Parameter-free Model for Inclusive Charge Exchange Nucleon Interactions Royal Holloway College Preprint(1977).

45 J Bartels and G Kramer, Nucl Phys B120(1977) 96.

46 G R Goldstein and J F Owens Nucl Phys B118(1977) 29.

47 F Elvekjaer and J L Petersen, Nucl Phys B94 (1975) 100
F Elvekjaer, Nucl Phys B101(1975) 112.

48 P Choudhury, K J M Moriarty, J H Tabor and A Ungkitchanukit, Acta Phys Aust 48(1977) 1.
K J M Moriarty, J H Tabor and A Ungkitchanukit, Phys Rev D16 (1977) 130.

49 J Anderson K J M Moriarty and R C Beckwith, Comp Phys Comm 9 (1975) 85.

50 F James and M Roos, Comp Phys Comm 10 (1975) 343

51 K J M Moriarty and J H Tabor, Nuovo Cimento Letters 16 (1976) 362.

52 A H Stroud and D Secrest, Gaussian Quadrature Formulas (Prentice-Hall, Inc., Englewood Cliff, N.J., 1966).

53 P Choudhury, K J M Moriarty, J H Tabor and A Ungkitchanukit. A Study of Inclusive Δ-production. Royal Holloway College Preprint 1975.

54 V Barger, Proceedings of XVIII International Conference on High Energy Physics, London, July 1974 and References therein.

55 R J N Phillips, Proceedings of the Amsterdam International Conference on Elementary Particles Amsterdam, June-July 1971.

56 A Barnes, G Fox, J Mellema, A Tolle strup, R Walker, O Dalil, R Johnson, R Kenney, A Osa a, S Shannon, G Donaldson, H Gordon and I Strummer. A proposal to study π^0 and η inclusive Production with Incident π^- in the Triple Regge Region. Cal.Tech. Preprint CALT-68-472, October 1974.

57 S A Adjei, P A Collins, B Hartley, K J M Moriarty and R W Moore, Annals of Physics 75 (1973) 405.

58 J J Sakurai and D Schildnecht, Physics Letters 40B (1972) 121.

59 A Ungkitchanukit Ph.D.Thesis, University of London 1976.

60 R J Glauber, Lectures in Theoretical Physics, ed W E Brittin Vol.1 (1959) Interscience Publishers inc.NY.

61 I S Gradsteyn and I M Ryzhik, Tables of Integrals Series and Products (1965) Academic Press N.Y.

REFERENCE (cont.)

62 K Paler, S N Tovey, T P Shah, J J Phelan, R J Miller, M Spiro, R Bartouloud, M Bardadin-Otwinowska, A Borg, B Chaurand, B Drevillon, J Gago and R A Salmeron, Nucl Phys B96 (1975) 1.

63 K J M Moriarty and J H Tabor, Nuovo Cim.Lett 15 (1976) 17.

64 G Burleson, G Hicks, C L Wilson, T Droege, P F M Koehler, T B Novey, B Sandler, H M Spinka, A Yokosawa and T Ferbel, Phys Rev D12 (1975) 2557.

65 K J M Moriarty and J H Tabor, Comp Phys Comm 12 (1976) 277, AAUR.

66 L H O'Neill, R L Ford, J F Crawford, R Hofstadter, E B Hughes, R F Schilling and R Wedemeyer. Phys Rev D14 (1976) 2878.

67 P Dennery and A Krzywicki, Mathematics for Physicists (1969) Harper and Row N.Y.

68 See e.g. A D Martin and T D Spearman. Elementary Particle Physics (1970) North Holland, Amsterdam.

69 M Abramowitz and I Stegun Handbook of Mathematical Functions, Dover Publications inc. N.Y.

70 S Frautschi and B Margolis, Nuovo Cim 56A (1968) 1158

71 S J Chang and T M Yan, Phys Rev Lett 55B (1970) 1586
C M Circuta and R L Sugar, Phys Rev D3 (1971) 970

72 H D I Abarbanel and C Itzykson, Phys Rev Lett.23 (1969) 53.

73 See H D I Abarbanel, G F Chew, M L Goldberger and L M Saunders, Ann Phys (N.Y.) 73 (1971) 156 and references therein.

74 N S Craigie, K J M Morairty and J H Tabor Th2140, CERN and Phys Rev D - to be published.

75 J Schwinger, Proc Natl Acad Sci U.S. 37 (1951) 452, C Møller, P T Matthews, J Schwinger, N Fukuda and J J Sakurai, Brandeis University, 1960 Summer Institute in Theoretical Physics, Lecture notes (unpublished) P.223-372.

76 R P Feynman, Phys Rev 84 (1951) 108; M L Goldberger and E N Adams II, J Chem Phys 20 (1952) 240.

77 Ph. Salin and J Soffer, Nucl Phys B71 (1974) 125.

78 Particle Data Group 1977.

79 J Soffer and D Wray Nucl Phys B73 (1974) 231.

80 N S Craigie private communication.

81 See almost any paper on multi-Regge ideas. Ref.16 for example.

82 K J M Moriarty,private communication

83 M Perl High Energy Hadron Physics, Wiley Interscience (1974) and references therein.

84 G A Ringland, R G Roberts D P Roy and J Tran Thanh Van Nucl Phys B44 (1972) 395.

85 D Barkai and K J M Moriarty, Nucl Phys B50 (1972) 354.

86 B Sadoulet, Nucl Phys B53 (1973) 135.

87 Chan Hong-Mo, J E Paton, Tson Sheung Tsun and Ng Sing Wai, Nucl Phys B92 (1975) 13.

88 D W Duke, Phys Lett 61 B(1976) 67.

89 R W B Ardill, P Koehler and K J M Moriarty, Lett al Nuovo Cimento 18 (1977) 161, 19 (1977) 1.